# MATH 283A Topics in Topology

*Shintaro Fushida-Hardy*
*381B Sloan Hall, Stanford University, CA*

This document contains course notes from MATH 283A (taught at Stanford, Fall 2020, by Ciprian Manolescu) transcribed by Shintaro Fushida-Hardy. Some additional thoughts and mistakes may have been added.

# Contents

# Chapter 1

# Introduction to Heegaard Floer homology

## 1.1 Admin (lecture 1)

Topics in the course will include:

1. The definition of Heegaard Floer homology for 3-manifolds using pseudo-holomorphic curves.
2. Heegaard Floer invariants for 4-manifolds.
3. Knot Floer homology and applications to concordance.
4. Methods for computing Heegaard Floer invariants.
5. Involutive Heegaard Floer homology and applications to homology cobordism.

There is no official textbook for the course; material is taken from several research articles primarily by Ozsváth and Szabó:

- P. Ozsváth and Z. Szabó, Holomorphic disks and topological invariants for closed three-manifolds, *Annals of Math.* (2) 159 (2004), no. 3, 1027-1158.
- P. Ozsváth and Z. Szabó, Holomorphic disks and three-manifold invariants: properties and applications, *Annals of Math.* (2) 159 (2004), no. 3 1159-1245.
- P. Ozsváth and Z. Szabó, Holomorphic triangles and invariants for smooth four-manifolds, *Adv. Math.* 202 (2006), no. 2, 326-400.
- P. Ozsváth and Z. Szabó, Holomorphic disks and knot invariants, *Adv. Math.* 186 (2004), no. 1, 58-116.

- P. Ozsváth and Z. Szabó, Knot Floer homology and integer surgeries, *Alg. Geo. Top.* 8 (2008) no. 1, 101-153.
- S. Sarkar and J. Wang, An algorithm for computing some Heegaard Floer homologies, *Annals of Math.* (2) 171 (2010), no. 2 1213-1236.
- C. Manolescu, P. Ozsváth, and S. Sarkar, A combinatorial description of knot Floer homology, *Annals of Math.* (2) 169 (2009), no. 2, 633-660.
- C. Manolescu, P. Ozsváth, Z. Szabó, and D. Thurston, On combinatorial link Floer homology, *Geo. Top.* 11 (2007), 2339-2412.
- K. Hendricks, C. Manolescu, Involutive Heegaard Floer homology, *Duke Math. J.* 166 (2017), no. 7, 1211-1299.

The following survery articles may be helpful:

- Ozsváth-Szabó, An introduction to Heegaard Floer homology, in *Floer homology, gauge theory, and low dimensional topology*, 3-27, AMS, 2006.
- Ozsváth-Szabó, Lectures on Heegaard Floer homology, in *Floer homology, gauge theory, and low dimensional topology*, 29-70, AMS, 2006.
- Ozsváth-Szabó, Heegaard diagrams and holomorphic disks, in *Different faces of geometry*, 301-348, Kluwer/Plenum, New York, 2004.
- C. Manolescu, An introduction to knot Floer homology, in *Physics and mathematics of link homology*, 99-135, Contemp. Math. 680, AMS, 2016.
- J. Hom, A survery on Heegaard Floer homology and concordance. *J. Knot Theory Ramifications* 26 (2017), no. 2, 1740015, 24 pp.

Prerequisites: algebraic and differential topology (such as Math 215A, 215B), including knowledge of characteristic classes and Morse theory. Symplectic geometry (Math 257A) is recommended but not required.

## 1.2 Big aims of topology and Floer homology

The primary goal of topology is to classify topological objects. The most fundamental of these are manifolds. What are all of the manifolds (of each dimension) up to homeomorphism? What are the smooth manifolds? What are the oriented, closed, connected smooth manifolds?

- Dimension 0: any connected, oriented, closed smooth manifold is a point.

- Dimension 1: any such manifold is a circle.
- Dimension 2: any such manifold is a surface of genus $g$, for some $g \in \mathbb{N}$.
- Dimension 3: connected, oriented, closed smooth manifolds are classified by the geometrisation theorem (Thurston-Hamilton-Perelman). Essentially any such 3-manifold $Y^3$ can be cut along copies of $\mathbb{S}^2$ and $\mathbb{T}^2$ into fundamental "geometric pieces" of 8 types. Of these, 7 are well understood, and the most interesting case corresponds to hyperbolic geometry - 3 dimensional hyperbolic geometry is not yet completely understood.
- Dimensions at least 5: these are understood by surgery theory for $\pi_1 = 1$, by the work of Milnor, Smale, ... in the 60s.

This leaves dimension 4, in which there are still very many questions! (This was the primary focus of the topics course from the previous quarter.) So how do we try to classify smooth manifolds in four dimensions? One approach is gauge theory! For example, Yang-Mills and Seiberg-Witten gauge theory. These give rise to invariants of 4-manifolds that can detect exotic smooth structures.

For example, we can find 4-manifolds $X$ and $X'$ which are homeomorphic, but such that $SW(X) \neq SW(X')$, where $SW(X) \in \mathbb{Z}$ is the *Seiberg-Witten invariant* of $X$. But given a 4-manifold $X$, can we typically compute $SW(X)$? This invariant is a certain count of solutions to differential equations on the manifold, and is difficult to compute in general. One approach is to use gluing formulae.

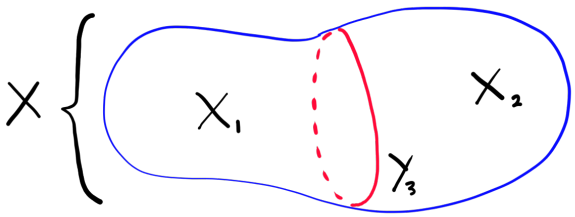


Figure 1.1: Decomposition of 4-manifold $X$.

In figure 1.1, we have decomposed a closed 4-manifold $X$ as two simpler 4-manifolds $X_1, X_2$ glued together along their boundary $Y$ (which is a 3-manifold). The gluing formulae state that

$$SW(X) = \langle SW(X_1), SW(X_2) \rangle,$$

where $SW(X_1) \in HM(Y)$, $\quad SW(X_2) \in HM(Y)^*$. Here $HM(Y)$ is something called the *monopole Floer homology* or *Seiberg-Witten Floer homology* of the 3-manifold $Y$, and is

a vector space over $\mathbb{Z}/2\mathbb{Z}$ (with some grading). This is an example of a Floer homology constructed from the Seiberg-Witten equations.

There are different versions of monopole Floer homology corresponding to different equivariant homologies, such as $\widetilde{HM}, \widehat{HM}$, and $\overline{HM}$. In fact, these fit into an exact triangle

$$\cdots \to \widehat{HM}_*(Y) \to \overline{HM}_*(Y) \to \widetilde{HM}_*(Y) \to \widehat{HM}_*(Y) \to \cdots .$$

The Seiberg-Witten equations have a symmetry given by $\mathrm{Pin}(2) = \mathbb{S}^1 \cup j\mathbb{S}^1 \subset \mathbb{C} \oplus j\mathbb{C} = \mathbb{H}$. Given any $G < \mathrm{Pin}(2)$, we can also consider $G$-equivariant Seiberg-Witten Floer homology.

This is enough about monopole Floer homology - what about Heegaard Floer homology? This is a symplectic replacement for Seiberg-Witten theory introduced by Ozsváth and Szabó in 2001. These are again $\mathbb{Z}/2\mathbb{Z}$-vector spaces defined for a closed oriented 3-manifold $Y^3$, denoted by

$$\widehat{HF}(Y), HF^+(Y), HF^-(Y), \underline{\widehat{HF}}(Y), HF^\infty(Y), \ldots .$$

(Again these are all various types of Heegaard Floer homology which we will encounter later on.) We said that they are symplectic replacements for Seiberg-Witten theory - what does this mean?

**Theorem 1.2.1.**

$$\widehat{HF}(Y) \cong \textit{“non-equivariant Seiberg-Witten Floer homology”}$$

*(Kutluhan, Lee, Taubes, circa 2011),*

$$HF^+(Y) \cong \textit{“}\mathbb{S}^1\textit{-equivariant Seiberg-Witten Floer homology”}$$

*(Colin, Ghiggini, Honda, circa 2011).*

This shows that Heegaard Floer homology recovers the same information as Seiberg-Witten Floer homology, so why do we care? What are advantages and disadvantages of Heegaard Floer homology?

**Advantages of Heegaard Floer homology.** The key advantage is that it's easier to compute than Seiberg-Witten Floer homology! In fact, we can use it to recover many results in 4-manifold theory (which were originally proven using Seiberg-Witten invariants), following this vague outline. First, Heegaard Floer homology forms a functor from the cobordism category of 3-manifolds to graded vector spaces. More concretely, given a 4-manifold $W$ with boundary $\partial W = Y_0 \sqcup (-Y_1)$, we obtain maps

$$\widehat{F}_W : \widehat{HF}(Y_0) \to \widehat{HF}(Y_1), \quad F^\pm_W : HF^\pm(Y_0) \to HF^\pm(Y_1).$$

Moreover, if $W$ is a closed 4-manifold, we can remove two copies of $\mathbb{S}^3$ as in figure 1.2 to study $W$ in terms of the induced maps above. The cobordism $W_1$ from $\mathbb{S}^3$ to $N$ induces a map $F^+_{W_1}$, and the cobordism $W_2$ from $N$ to $\mathbb{S}^3$ induces a map $F^-_{W_2}$. Mixing these together in a certain way, we obtain $F_{\mathrm{mix}}(W) \in \mathbb{Z}$, a “mixed invariant for 4-manifolds”.

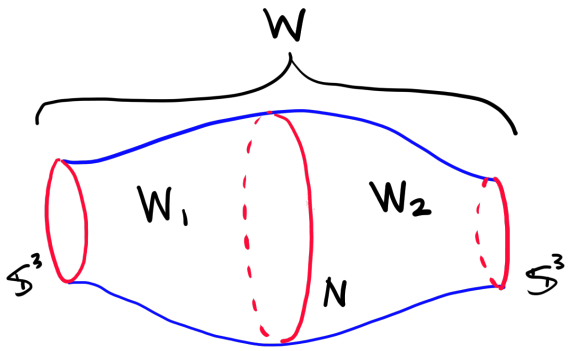


Figure 1.2: Using Heegaard Floer homology to study closed 4-manifolds.

**Conjecture.** Given a closed 4-manifold $W$, $F_{\text{mix}}(W) = SW(W)$.

Even though the above is still only a conjecture, enough properties of $F_{\text{mix}}$ are known that we can, for example, recover a proof of the existence of exotic smooth structures. While Seiberg-Witten invariants of 4-manifolds are typically difficult to compute, there are combinatorial algorithms for computing Heegaard Floer homology.

**Disadvantages of Heegaard Floer homology.** Less relation to differential geometry! For example, in Seiberg-Witten theory it is not too difficult to show that any 4-manifold admitting a positive scalar curvature metric has trivial Seiberg-Witten invariant. However, this type of result is difficult in the Heegaard picture.

## 1.3 Applications of Heegaard Floer homology: 4-manifolds

Above we mentioned applications to 4-manifold topology by comparison with Seiberg-Witten theory. Another application is the following question:

**Open question.** Let $W$ be a smooth 4-manifold with boundary a connected manifold $Y$. Given $Y$, what are the possibilities for $H_*(W)$? What are the possibilities for the intersection form $Q_W : H^2(W;\mathbb{Z}) \otimes H^2(W;\mathbb{Z}) \to \mathbb{Z}$? More specifically, when is $W$ a homology 4-ball?

For $W$ to be a homology ball, we certainly need (from the homology long exact sequence) that $Y$ is a homology 3-sphere; $H_*(Y) = H_*(\mathbb{S}^3)$. This motivates the definition of the *homology cobordism group*.

**Definition 1.3.1.** The *homology cobordism group* $\Theta^3_{\mathbb{Z}}$ consists of integral homology 3-spheres, up to homology cobordism. This means that $\Theta^3_{\mathbb{Z}} = \{Y^3 \text{oriented}, H_*(Y;\mathbb{Z}) =$

$H_*(\mathbb{S}^3;\mathbb{Z})\}/\sim$, where $Y_0 \sim Y_1$ if and only if there is a cobordism $W$ from $Y_0$ to $Y_1$ with $H_*(W, Y_i) = 0$ for both $i$. This truly forms a group:

$$[\mathbb{S}^3] = 0, \quad [-Y] = -[Y], \quad [Y_0 \# Y_1] = [Y_0] + [Y_1].$$

We care about the homology cobordism group because $[Y] = 0$ if and only if $Y$ is homology cobordant to $\mathbb{S}^3$, but this is exactly when $Y$ bounds a homology 4-ball! In summary, to understand our original question, the real task is to understand the homology cobordism group. Much work was gone into studying the homology cobordism group, and this has been helped by Heegaard Floer homology.

Before Floer Homology came into play, the first steps in understanding the homology cobordism group were carried out by Rokhlin. He defined a surjective homomorphism, now called the *Rokhlin invariant*,

$$\mu : \Theta^3_{\mathbb{Z}} \to \mathbb{Z}/2\mathbb{Z}$$

which was the first proof that the homology cobordism group is non-trivial. In particular, the 3-sphere has Rokhlin invariant 0, and the Poincaré homology sphere has Rokhlin invariant 1. In the 70s it was conjectured that the Rokhlin invariant was an isomorphism. However, this can be disproven by Donaldson's diagonalisation theorem - the homology cobordism group is infinite. More precisely, the *Casson invariant* (which is discussed in my notes on homology 3-spheres) is a surjective map $\Theta^3_{\mathbb{Z}} \to \mathbb{Z}$, so this gives another proof of the infinitude of $\Theta^3_{\mathbb{Z}}$. It turns out that the Casson invariant is some sort of Euler characteristic for Floer homology! perhaps we will touch on this eventually.

In fact, Ciprian showed (in 2013?) using his version of Seiberg-Witten Floer homology that the homology cobordism group has no elements of order 2! This is equivalent to the falsity of the triangulation conjecture for manifolds of dimension at least 5! That is, there exist topological manifolds of dimension at least five that do not admit compatible triangulations. This is also discussed in my notes on homology 3-spheres.

Where does Heegaard Floer homology come into play?

- Using $HF^+$, one can define a surjective *homomorphism*

  $$d : \Theta^3_{\mathbb{Z}} \to \mathbb{Z}.$$

  In particular, $d(P) = 2$, where $P$ is the Poincaré homology sphere. This shows that $P$ does not bound a homology 4-ball (which we of course already knew from the Rokhlin or Casson invariants). This is really telling us that the homology cobordism group has a $\mathbb{Z}$ direct summand.

- In fact, using involutive Heegaard Floer homology (Hendricks-Manolescu, 2016), we can extract even more information. involutive Heegaard Floer homology is an analogue of $\mathbb{Z}/4\mathbb{Z}$-equivariant Seiberg-Witten Floer homology, where $\mathbb{Z}/4\mathbb{Z} = \langle j \rangle$ sits inside $\mathrm{Pin}(2) \subset \mathbb{H}$. Using involutive Heegaard Floer homology, it was later shown that $\Theta^3_{\mathbb{Z}}$ actually has a $\mathbb{Z}^\infty$ direct summand! (Dai-Hom-Stoffregen-Truong, 2018).

## 1.4 Interlude: Hungarian pronunciation

A prerequisite to studying Heegaard Floer homology is to learn some Hungarian pronunciation! Much of the field was pioneered by two Hungarian mathematicians, Ozsváth and Szabó. Here is a table of some key things to keep in mind:

| Hungarian | English |
|---|---|
| s | sh (like **sh**oe) |
| sz | s (like **s**poon) |
| zs | zh (like plea**s**ure) |
| j | y (like **y**eet) |
| c | ts (like spo**ts**) |
| w | v (like **v**inyl) |

If we place consonants adjacently (e.g. "th") in Hungarian, we would not read this as **th**ought, but as a "t" followed by an "h" (so in English this is just approximated by a single t).

We can practice our pronunciation with some names that we might encounter:

Peter Ozsváth  Zoltán Szabó  András Vasy  András Stipsicz  András Juhász.

## 1.5 Applications of Heegaard Floer homology: 3-manifolds

**Question.** Let $Y^3$ be closed and oriented, and $h \in H_2(Y;\mathbb{Z})$. Then $h$ can be represented by a closed oriented (possibly disconnected) surface. What is the simplest such surface?

Suppose $\Sigma$ is a surface representing $h$. Then we can write $\Sigma = \bigcup \Sigma_i$ for each component, so that its Euler characteristic is

$$\chi(\Sigma) = \sum \chi(\Sigma_i) = \sum (2 - 2g(\Sigma_i)).$$

Given any $\Sigma$, addition of handles will decrease $\chi(\Sigma)$ by 2, while addition of contractible spheres will increase $\chi(\Sigma)$ by 2. One approach to interpreting the previous question is "what is the minimum Euler characteristic of a surface representing a given second homology class, when we account for the previous two modifications?" This is essentially the definition of the Thurston norm.

**Definition 1.5.1.** Given a surface $\Sigma$, $\chi_+(\Sigma) = \sum_i \max\{0, -\chi(\Sigma_i)\} = -\sum_{\Sigma_i \text{ not a sphere}} \chi(\Sigma_i)$. We define the *Thurston norm* of a second homology class $h$ to be the minimum $\chi_+(\Sigma)$, for $\Sigma$ representing $h$:

$$\theta(h) = \min(\chi_+(\Sigma) : [\Sigma] = h).$$

Therefore our first question can be rephrased as "given a second homology class of a 3-manifold, what is its Thurston norm?" This can be solved using Heegaard Floer homology! One can show that

$$\underline{\widehat{HF}}(Y) = \bigoplus_{s \in H^2(Y;\mathbb{Z})} \underline{\widehat{HF}}(Y;s)$$

where $\underline{\widehat{HF}}(Y;s)$ are abelian groups, non-zero only for finitely many $s$. This description of Heegaard Floer homology answers the originl question by the following theorem:

**Theorem 1.5.2** (Ozsváth-Szabó)**.**

$$\theta(h) = \max\{\langle s, h\rangle : s \in H^2(Y;\mathbb{Z}), \underline{\widehat{HF}}(Y;s) \neq 0\}.$$

Of course, one might say "hey, this doesn't answer the question! We don't necessarily know what the Heegaard Floer homology of a three manifold is! Can we compute it?" Fortunately this was solved in 2006 by Sarkar and Wang:

**Theorem 1.5.3** (Sarkar-Wang, 2006)**.** *Given any 3-manifold $Y$, there is an algorithm to compute $\underline{\widehat{HF}}(Y)$.*

## 1.6 Applications of Heegaard Floer homology: knots

Finally we look at applications to knot theory! Heegaard Floer homology has a knot-theory version, introduced independently by Ozsváth-Szabó and by Rasmussen, in 2003. Suppose $K \subset Y^3$ is null-homologous, with $K$ a knot. Then the *knot Floer homology* of $K$ is denoted by $\widehat{HFK}(Y,K)$. In particular we care about knots in $\mathbb{S}^3$, in which case we write $\widehat{HFK}(\mathbb{S}^3,K)$. Knot Floer homology decomposes as a direct sum of some smaller pieces, in a way that was analogous to Heegaard Floer homology (when we were writing a formula for the Thurston norm):

$$\widehat{HFK}(Y,K) = \bigoplus_{s \in \mathbb{Z}} \widehat{HFK}(\mathbb{S}^3,K,s).$$

This time we can use the above decomposition to describe the genus of a knot! This is generally considered to be a very difficult problem.

**Definition 1.6.1.** Let $K$ be a knot. A *Seifert surface* of $K$ is an oriented connected surface $\Sigma$ embedded in $\mathbb{S}^3$ with boundary $K$. The genus of $K$ is the minimum genus of Seifert surfaces of $K$:

$$g(K) := \min\{g(\Sigma) : \Sigma \text{ is a Seifert surface of } K\}.$$

The above definition makes it clear why the genus is generally difficult to compute: knot invariants defined in terms of maximums or minimums are typically powerful but intractible.

**Theorem 1.6.2.** *Let $K$ be a knot. Then*

$$g(K) = \max\{s : \widehat{HFK}(\mathbb{S}^3, K, s) \neq 0\}.$$

As was the case with the Thurston norm problem, to really conclude that the above theorem solves the genus problem, we must ensure that $\widehat{HFK}(\mathbb{S}^3, K, s)$ can actually be computed. This can indeed be done!

**Theorem 1.6.3** (Manolescu-Ozsváth-Sarkar, 2006)**.** *There exists a combinatorial algorithm for computing $\widehat{HFK}$.*

One of the biggest goals in knot theory was to understand the *unknotting problem*. Given a diagram of a knot, how do we decide whether or not the diagram represents the unknot? More formally, is there an algorithm to determine whether or not a given knot projection is the unknot?

- This was solved in the affirmative in 1961 by Haken, using *normal surfaces*.
- A new solution is given by the above results in terms of knot Floer homology: a knot is the unknot if and only if it has genus 0. But the genus is expressed in terms of knot Floer homology, and this can be computed algorithmically.

Of course this gives a new proof, but it would be nice to find a solution to a problem that has yet to be solved using non-knot Floer homology methods. A possible direction for this is the problem of classifying slice knots. Currently there is no known algorithm for determining whether or not a knot is *slice*.

**Definition 1.6.4.** Let $K$ be a knot in $\mathbb{S}^3$. Let $B^4$ be the 4-ball bound by $\mathbb{S}^3$, so that $K$ lies on the boundary of $B^4$. $K$ is said to be *topologically slice* if there is a locally flat topological embedding of a disk $D^2 \hookrightarrow B^4$, so that $\partial D^2 = K$. $K$ is said to be *slice* or *smoothly slice* if there is a smooth embedding $D^2 \hookrightarrow B^4$ with $\partial D^2 = K$.

While the problem of classifying slice knots is unsolved, knot Floer homology provides many obstructions! Examples include $\tau, \epsilon, \nu, \nu^+, \upsilon, \ldots$. Of course, just listing their names doesn't really mean anything, but hey - there are lots of them! To understand what the point of these obstructions are, we can recall the Rasmussen invariant $s$ obtained from Khovanov homology (which we constructed in the Spring 2020 topics course). Using the $s$ invariant, we showed for example that there are topologically slice knots which are not slice! (Moreover, we used this to show the existence of exotic $\mathbb{R}^4$s!)

- Define the *slice genus* $g_s(K)$ of a knot $K$ to be the minimum genus of a smoothly embedded surface $\Sigma$ embedded in $B^4$ whose boundary is $K \subset \partial B^4 = \mathbb{S}^3$.
- A knot is slice if and only if its slice genus is 0.

- A key property of Rasmussen's $s$ invariant is that $s(K)$ is a lower bound for $2g_s(K)$. One can show that the Whitehead double of the torus knot $T_{2,3}$ has Rasmussen invariant 2, so it is not slice.
- On the other hand, the Alexander polynomial of a Whitehead double is trivial! And a result by Freedman gives that knots with trivial Alexander polynomial are topologically slice.

This derivation shows how we can use obstructions to sliceness such as the Rasmussen invariant to begin classyfing slice knots. Later in the course we'll encounter the knot Floer theoretic obstructions to sliceness!

In our efforts to study 4-manifolds a few sections earlier, we naturally encountered the *homology cobordism group*. The analogous object in knot theory is the *concordance group*, which tells us about slice knots.

**Definition 1.6.5.** The *knot concordance group* or just *concordance group* is $\mathcal{C} = \{\text{knots}\}/\sim$, where $K_0 \sim K_1$ if $K_0$ and $K_1$ are *concordant*. That is, if there exists a smooth embedded annulus $A \subset \mathbb{S}^3 \times [0,1]$ such that $\partial A = (-K_0) \sqcup K_1$.

In particular, this means that $K$ is concordant to the unknot if and only if $K$ is slice. In much the same way that the structure of the homology cobordism group $\Theta^3_{\mathbb{Z}}$ eludes us, so does the structure of $\mathcal{C}$.

- (Classical result, using algebraic topology) $\mathcal{C}$ has a $\mathbb{Z}^\infty$ direct summand.
- (Result using knot Floer homology) $\mathcal{C}_{TS} < \mathcal{C}$, the subgroup generated by topologically slice knots, also has a $\mathbb{Z}^\infty$ direct summand.

# Chapter 2

# Preliminaries for Heegaard and Lagrangian Floer homology

This entire chapter is dedicated to the construction of Heegaard Floer homology. We introduce all necessary background concepts, most notably some symplectic geometry results.

## 2.1 Outline of the construction of Heegaard Floer homology

All of the details of this brief section will be fleshed out in the next few lectures. Heegaard Floer homology, as the name suggests, is constructed using Heegaard splittings.

- Let $Y$ be a closed oriented 3-manifold. Then $Y$ admits a *Heegaard splitting*, and moreover a representation via a *Heegaard diagram*; $\mathcal{H} = (\Sigma_g, \alpha_1, \ldots, \alpha_g, \beta_1, \ldots, \beta_g)$. (Then $Y$ is obtained by gluing disks to $\Sigma_g$ along the curves $\alpha_i$ and $\beta_i$ on each side of $\Sigma_g$, and finally filling the holes with a ball $B^3$ for each side.)

- From $\Sigma_g$ we obtain a manifold called its symmetric product, which happens to canonically be a *symplectic manifold*:

  $$\mathrm{Sym}^g(\Sigma_g) = \Sigma \times \Sigma \times \cdots \times \Sigma / S_g.$$

  This is a $2g$-dimensional manifold containing two $g$-dimensional submanifolds (tori) determined by the Heegaard diagram:

  $$\mathbb{T}_\alpha = \alpha_1 \times \cdots \times \alpha_g, \mathbb{T}_\beta = \beta_1 \times \cdots \times \beta_g \subset \mathrm{Sym}^g(\Sigma_g).$$

  These tori happen to be Lagrangian submanifolds!

- (By transversality) the intersection $\mathbb{T}_\alpha \cap \mathbb{T}_\beta$ is some finite number of points. Let $CF$ denote the free abelian group generated by $\mathbb{T}_\alpha \cap \mathbb{T}_\beta$. ($CF$ probably stands for Floer chain (complex).) $CF$ admits a grading, and there are maps $\partial : CF_n \to CF_{n-1}$ making this a chain complex. The boundary maps count *pseudo-holomorphic disks*.

- The homology $H_*(CF, \partial)$ of the Floer chain complex $(CF_n, \partial)$ is exactly the Heegaard Floer homology;
$$HF(Y) = H_*(CF, \partial).$$

## 2.2 Heegaard splittings and diagrams (lecture 2)

For the duration of this lecture, $Y = Y^3$ denotes a closed oriented 3-manifold.

**Definition 2.2.1.** A *Heegaard splitting* of $Y$ is a decomposition

$$Y = H_g \sqcup_f H'_g,$$

where $H_g, H'_g$ are handlebodies of genus $g$, and $f : \partial H_g \to \partial H'_g = \Sigma_g$ is a diffeomorphism (defining how $H_g$ is glued to $H'_g$).

Heegaard splittings are used to describe three manifolds using lower dimensional data, and are useful because they always exist!

**Theorem 2.2.2.** *Every closed oriented 3-manifold has a Heegaard splitting.*

This is often proven using Morse theory, but here we give a proof using triangulations. Recall that a triangulation is a decomposition of a manifold into simplices, and forms an intermediate tier of structure between smooth manifolds and topological manifolds.

**Definition 2.2.3.** A triangulation of a topological space $X$ is a simplicial complex $K$ together with a homeomorphism $K \to X$.

*Proof that 3-manifolds admit Heegaard splittings.* Let $M$ be a closed orientable 3-manifold, and $T$ a triangulation of $M$. Each vertex of $T$ has a neighbourhood homeomorphic to $0 \times D^3$, each edge a neighbourhood homeomorphic to $D^1 \times D^2$, each face, $D^2 \times D^1$, and each cell, $D^3 \times 0$. Taking appropriate intersections, $M$ can be expressed as a union of these pieces glued along their boundaries. Let the neighbourhoods of vertices and edges define $H_g$, and faces and cells define $H'_g$. This is a Heegaard splitting of $M$. □

This reduces the description of any closed oriented 3-manifold to descriptions of handlebodies and how they are glued together. But it turns out that any handlebody $H_g$ can be described in terms of curves on a surface $\Sigma_g$! Specifically, any $g$ linearly independent simple disjoint embedded closed curves $\alpha_1, \ldots, \alpha_g$ in $\Sigma_g$ determine a handlebody. By linearly independent, we mean in $H_1(\Sigma_g) = \mathbb{Z}^{2g}$. Then

$$H_g = \Sigma_g \cup D_{\alpha_1} \cup \cdots \cup D_{\alpha_g} \cup B^3,$$

where the disks and ball are as indicated in figure 2.1. The idea is that each closed curve

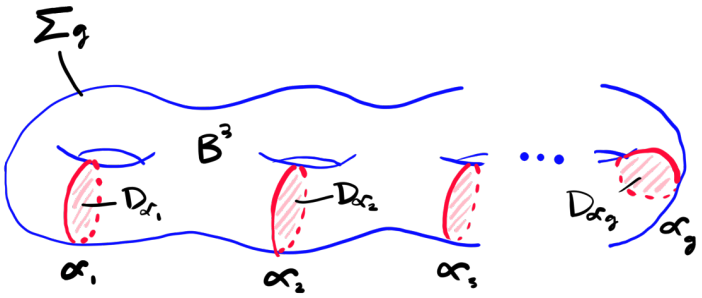


Figure 2.1: Description of a handlebody by specifying curves on a surface.

uniquely determines a disk on one side of the surface (every orientable surface is 2-sided in $\mathbb{R}^3$), and after filling in $g$ disks we're left with a cavity that can be filled with a 3-ball.

Similarly, we can specify $g$ curves $\beta_1, \ldots, \beta_g$ to describe the other handlebody, $H_g'$, of the Heegaard splitting. This constitutes the data of a *Heegaard diagram*

$$(\Sigma, \alpha_1, \ldots, \alpha_g, \beta_1, \ldots, \beta_g).$$

The overall process for specifying a closed oriented 3-manifold in terms of a Heegaard diagram (surface and embedded curves) is

$$\text{Heegaard diagram} \rightsquigarrow \text{Heegaard splitting} \rightsquigarrow \text{3-manifold}.$$

**Exercise.** Let $Y$ have Heegaard diagram $(\Sigma, \alpha_1, \ldots, \alpha_g, \beta_1, \ldots, \beta_g)$. Show that

$$H_1(Y) \cong H_1(\Sigma)/\langle \alpha_1, \ldots, \alpha_g, \beta_1, \ldots, \beta_g \rangle.$$

Hint: Mayer-Vietoris.

We now look at some examples of Heegaard diagrams. Firstly, it is a hassle to draw an actual surface all the time! Instead, we draw a flat diagram akin to a "fundamental polygon" of the surface. An example of an arbitrary Heegaard diagram in its final visual form is given in figure 2.2. The diagram on the bottom right is obtained by cutting along the holes in $\Sigma_2$. The boundary components 1 and $\overline{1}$ glue together with opposite orientations to give the first hole, and similarly for 2 and $\overline{2}$. Finally to obtain the closed surface, the bottom right diagram is compactified at a point at infinity.

The standard notation is to draw alpha curves in red, and beta curves in blue.

**Example.** The empty Heegaard diagram represents the 3-sphere. This is because it corresponds to a 2-sphere with no curves, and gluing 3-balls to each side of the 2-sphere gives $\mathbb{S}^3$.

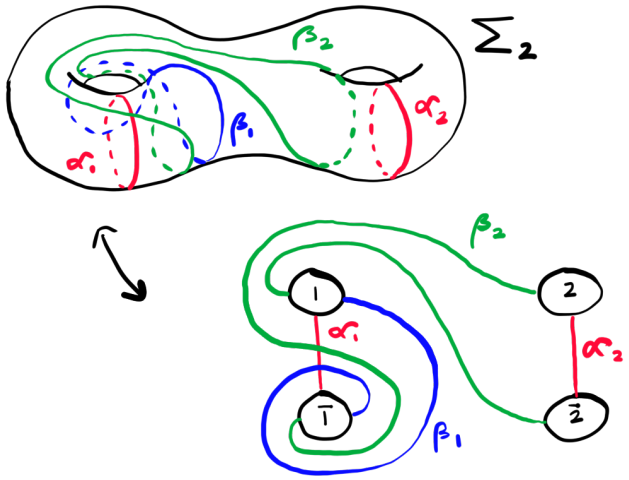


Figure 2.2: Heegaard diagram in its Super Saiyan mode.

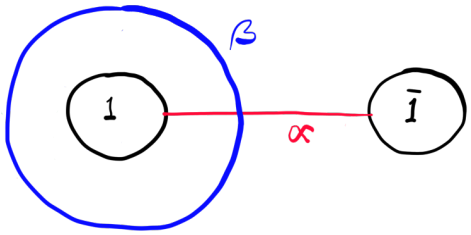


Figure 2.3: Heegaard diagram of $\mathbb{S}^3$.

**Example.** The diagram in figure 2.3 also represents a 3-sphere. This can be seen by drawing the corresponding surface and filling in disks for the given curves and so on.

**Example.** The diagram in figure 2.4 represents $\mathbb{S}^1 \times \mathbb{S}^2$. This can be seen by drawing two tori side by side with the given curves on them. Gluing these tori together corresponds to gluing the disks (from the curves) together along their boundary, so each meridian of the torus gives a copy of $\mathbb{S}^2$. The torus is foliated by $\mathbb{S}^1$ copies of meridians, so overall we have $\mathbb{S}^1 \times \mathbb{S}^2$.

**Example.** A general diagram of a genus 1 Heegaard splitting looks like 2.5. We can use a diffeomorphism of the surface to place the $\alpha$ curve in standard position, and then any $\beta$ is of the form $pm+q\alpha$ (in homology), where $\gcd(p,q) = 1$. This follows from the classification of simple closed curves on a torus.

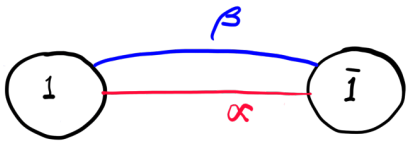


Figure 2.4: Heegaard diagram of $\mathbb{S}^1 \times \mathbb{S}^2$.

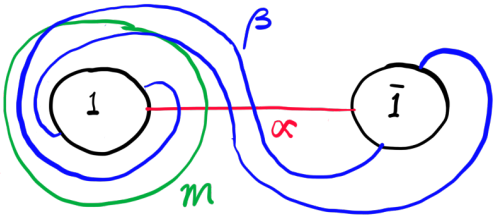


Figure 2.5: Heegaard diagram of Lens space $L(3,2)$.

For example, in this particular figure, we can count intersections and find that $\alpha \cdot \beta = 3$, while $m \cdot \beta = 2$. It follows that $p = 3$ and $q = 2$. The corresponding 3-manifold is the *Lens space* $L(p,q) = L(3,2)$. A more geometric approach to Lens spaces is $L(p,q) = \mathbb{S}^3/(\mathbb{Z}/p\mathbb{Z})$, where the group action is given by $u(z,w) = (uz, u^q w)$ for $u \in \mathbb{Z}/p\mathbb{Z}$, and $\mathbb{S}^3$ is parametrised as the unit sphere in $\mathbb{C}^2$. More explicitly,

$$L(p,q) = \{(z,w) \in \mathbb{C}^2 : |z|^2 + |w|^2 = 1\}/(z,w) \sim (uz, u^q w), u \in \mathbb{Z}/p\mathbb{Z}.$$

One can verify in each example (without having to appeal to visual intuition and simply using group presentations) that fundamental groups and homology groups are all as expected.

## 2.3 Operations on Heegaard splittings and diagrams

Consider a Heegaard diagram $(\Sigma, \alpha_1, \ldots, \alpha_g, \beta_1, \ldots, \beta_g)$ for a closed oriented 3-manifold $Y$. What are the ways we can change the diagram and for it to still represent the same Heegaard splitting? What are the ways we can change the diagram and for it to still represent the same 3-manifold?

Firstly we can isotope any curves and obtain a new Heegaard diagram for the same Heegaard splitting. A less trivial operation is that we can do *handle slides* without changing the Heegaard splitting. That is, given any two $\alpha$ loops on a surface $\Sigma$ (or any two $\beta$ loops), we can slide one over the other to obtain a new Heegaard diagram. Formally, given loops

$\alpha_1$ and $\alpha_2$, sliding $\alpha_1$ over $\alpha_2$ corresponds to replacing $\alpha_1$ with $\alpha_1'$, which is the connected sum of $\alpha_1$ with a push-off of $\alpha_2$.

On the algebraic side, let $i : \Sigma_g \to H_g$ be the inclusion map, where $H_g$ is the handlebody determined by loops $\alpha_1, \ldots, \alpha_g$ on $\Sigma_g$. The induced map $i_* : H_1(\Sigma_g) \to H_1(H_g)$ then kernel $\langle \alpha_1, \ldots, \alpha_g \rangle$. Then a *handle slide* corresponds to a change of basis of $\ker i_*$.

In fact, it turns out that isotopies and handleslides give all possible Heegaard diagrams for a given Heegaard splitting! This is formalised in the following theorem.

**Theorem 2.3.1.** *Any two collections of linearly independent simple closed curves on a surface $\Sigma$ representing the same handlebody are related by a sequence of handleslides and isotopies. In particular,*

$$\{\textit{Heegaard splittings}\} \cong \{\textit{Heegaard diagrams}\}/\textit{handle slides and isotopies.}$$

The next question is: how many Heegaard splittings does a given closed oriented 3-manifold have? It turns out that all Heegaard splittings are related by *stabilisation*. The cleanest definition of stabilisation uses Heegaard diagrams, so we first give a definition in these terms. Afterwards we will give an alternative definition which uses only the structure of the Heegaard splitting. (Spiritually, the former is a coordinate dependent definition, and the latter coordinate free.)

**Definition 2.3.2.** Let $(\Sigma, \alpha_1, \ldots, \alpha_g, \beta_1, \ldots, \beta_g)$, $(\Sigma', \alpha_1', \ldots, \alpha_h', \beta_1', \ldots, \beta_h')$ be Heegaard diagrams. The *connected sum* of these two Heegaard diagrams is

$$(\Sigma \# \Sigma', \alpha_1, \ldots, \alpha_g, \alpha_1', \ldots, \alpha_h', \beta_1, \ldots, \beta_g, \beta_1', \ldots, \beta_h').$$

Next, the *stabilisation* of $(\Sigma, \alpha_1, \ldots, \alpha_g, \beta_1, \ldots, \beta_g)$ is its connected sum with the genus 1 Heegaard diagram of a 3-sphere (seen in an earlier example).

This process really corresponds to adding a handle to each handlebody of the Heegaard splitting, in such a way that the two handles interlock to give a 3-sphere. This perspective (although messier to formalise) is more evident in the coordinate free definition.

**Definition 2.3.3.** Let $Y = H_g \cup H_g'$ be a Heegaard splitting. *Stabilisation* is the following procedure:

1. Attach an additional unknotted 1-handle $h$ to $H_g$, to obtain $H_{g+1}$. Since $H_g$ is a submanifold of $Y$, "unkotted" is formalised by saying that the core of the 1-handle bounds an embedded disk $D^2$ in $Y$.

2. Let $h'$ denote a "thickening" of the embedded disk. Then $h \cup h' \cup H_g$ is homeomorphic to $H_g$ (since $h \cup h'$ is just a boundary connected sum $D^3$ with $H_g$). Therefore $Y$ decomposes as $h \cup h' \cup H_g \cup H_g'$.

3. By studying the boundary of $h \cup h' \cup H_g$, we see that $h'$ intersects $H'_g$ along two disjoint disks. Therefore $H'_g \cup h'$ is a handlebody of genus $g+1$, which we denote by $H'_{g+1}$.

In summary we have $Y = H_{g+1} \cup H'_{g+1}$, so from our genus $g$ Heegaard splitting we can canonically obtain a genus $g+1$ Heegaard splitting. (This process is stabilisation.)

As remarked earlier, all Heegaard splittings of the same 3-manifold are in fact related by stabilisation and destabilisation!

**Theorem 2.3.4.** *(Reidemeister-Singer) Any two Heegaard splittings of the same 3-manifold are related by a sequence of stabilisations to each splitting.*

Combining this with the repvious result concering the freedom of Heegaard diagrams for a given Heegaard splitting, we have

$$\begin{aligned}\{\text{Closed oriented 3-man's}\} &\cong \{\text{Heegaard splittings}\}/\text{stab.} \\ &\cong \{\text{Heegaard diagrams}\}/\text{handle slides, isotopies, stab.}\end{aligned}$$

As a final remark before moving on to symmetric products, we introduce *based Heegaard diagrams*, which are essentially Heegaard diagrams with a distinguished base point.

**Definition 2.3.5.** A based Heegaard diagram of a 3-manifold is the data $(\Sigma, \alpha_1, \ldots, \alpha_g, \beta_1, \ldots, \beta_g, z)$ where $z$ is a point in $\Sigma$ that does not lie on any of the curves $\alpha_i, \beta_i$.

**Exercise.** Show that

$$\{\text{Based 3-manifolds}\} \cong \{\text{Based Heegaard diagrams}\}/\sim$$

where $\sim$ is stabilisation away from $z$, handle slides away from $z$, and isotopies away from $z$.

The non-trivial part of this exercise is avoiding the base point. The key is to re-write arbitrary moves in terms of those avoiding $z$.

## 2.4 Symmetric products

Recall that our goal is to construct the Heegaard Floer homology of a closed oriented 3-manifold. The first step was to understand Heegaard diagrams of 3-manifolds. Next, given a Heegaard diagram, we want to associate to it a symplectic manifold with distinguished Lagrangian submanifolds. The symplectic manifold will be obtained via a *symmetric product*.

**Definition 2.4.1.** Let $M$ be a manifold of dimension $d$. Then

$$\mathrm{Sym}^k(M) := \coprod_k M/S_k,$$

where $S_k$ acts on $\prod_k M$ be permuting $(x_1, \ldots, x_k) \in \prod_k M$. Thus $\mathrm{Sym}^k(M)$ consists of unordered $k$-tuples of points in $M$.

**Remark.** In general $S_k$ does *not* act freely on $\prod_k M$, so $\mathrm{Sym}^k(M)$ is not manifold.

**Example.**

- $\mathrm{Sym}^0(M) = \mathrm{pt}$.
- $\mathrm{Sym}^1(M) = M$.
- $\mathrm{Sym}^2(M)$ has two local models: $(m_1, m_2)$ with $m_1 \neq m_2$ determines a "smooth point", with local model $\mathbb{R}^d \times \mathbb{R}^d$. Points of the form $(m, m)$ are fixed points of $S_2 = \mathbb{Z}/2\mathbb{Z}$, so the local model is $(\mathbb{R}^d \times \mathbb{R}^d)/(\mathbb{Z}/2\mathbb{Z}) = \mathrm{Sym}^2(\mathbb{R}^d)$.

Now we wish to understand what $\mathrm{Sym}^2(\mathbb{R}^d)$ looks like. This is explicitly the space

$$\mathbb{R}^d \times \mathbb{R}^d/(x, y) \sim (y, x).$$

We can change our basis to $u = x + y, v = x - y$. Then

$$\mathrm{Sym}^2(\mathbb{R}^d) = \mathbb{R}^d \times \mathbb{R}^d/(u, v) \sim (u, -v) = \mathbb{R}^d \times (\mathbb{R}^d/(\mathbb{Z}/2\mathbb{Z})).$$

The factor on the right can equivalently be written as $C(\mathbb{S}^{d-1})/(\mathbb{Z}/2\mathbb{Z})$, where $C(X)$ denotes the cone over $X$. But now $\mathbb{S}^{d-1}/(\mathbb{Z}/2\mathbb{Z})$ is very familiar: it is the real projective space $\mathbb{RP}^{d-1}$. In summary, we have

$$\mathrm{Sym}^2(\mathbb{R}^d) = \mathbb{R}^d \times C(\mathbb{RP}^{d-1}).$$

When is this a manifold? In general it'll have a singularity. However, exactly when $d = 0, d = 2$, we have $\mathbb{RP}^{d-1} \cong \mathbb{S}^{d-1}$, so that $C(\mathbb{RP}^{d-1}) = C(\mathbb{S}^{d-1}) = \mathbb{R}^d$. In the instances $d = 0$ or $d = 2$, we have that $\mathrm{Sym}^2(\mathbb{R}^d)$ is a manifold. This suggests that for any surface $\Sigma$, $\mathrm{Sym}^2(\Sigma)$ should locally look like $\mathbb{R}^4$, and in particular be a manifold. This is indeed the case, and an even better result holds.

**Proposition 2.4.2.** Let $\Sigma_g$ be the oriented surface of genus $g$. Then $\mathrm{Sym}^k(\Sigma)$ is a $2k$-manifold.

*Proof.* We must show that the local model of $\mathrm{Sym}^k(\Sigma)$ is $\mathbb{R}^{2k} \cong \mathbb{C}^k$. First, choose any $(z_1, \ldots, z_k) \in \mathrm{Sym}^k(\Sigma)$. We group the matching coordinates, and write

$$(z_1, \ldots, z_k) = (w_1, \ldots, w_1, w_2, \ldots, w_2, \ldots),$$

where there are $\ell_1$ instances of $w_1$, $\ell_2$ instances of $w_2$, and so on, and $w_i = w_j$ if and only if $i = j$. Then the local model at $(z_1, \ldots, z_k)$ is

$$\mathrm{Sym}^{\ell_1}(\mathbb{R}^2) \times \mathrm{Sym}^{\ell_2}(\mathbb{R}^2) \times \cdots .$$

It remains to show that $\mathrm{Sym}^{\ell_i}(\mathbb{R}^2) \cong \mathrm{Sym}^{\ell_i}(\mathbb{C})$ is a manifold. We achieve this by constructing a diffeomorphism

$$\mathrm{Sym}^{\ell}(\mathbb{C}) = \prod_{\ell} \mathbb{C}/S_\ell \to \mathbb{C}^\ell$$

and its inverse map. In the forwards direction, we send the unordered tuple $\{z_1, \ldots, z_\ell\} \in \prod_\ell(\mathbb{C})$ to the ordered tuple $(s_1, \ldots, s_\ell)$, where $s_i$ is the $i$th elementary symmetric polynomial. By nature of these polynomials being symmetric, the map is well defined. The inverse map is given by sending $(s_1, \ldots, s_\ell)$ to the unordered list of roots of the polynomial $t^\ell - st^{ell-1} + \cdots + (-1)^\ell s_\ell$. □

This establishes that $\mathrm{Sym}^k(\Sigma)$ is a manifold, where in our context $\Sigma$ is the closed oriented surface obtained from a Heegaard splitting. We will show further that $\mathrm{Sym}^k(\Sigma)$ is a *symplectic* manifold with a view to constructing Heegaard Floer homology. But first, we must talk about some sympletic geometry/topology!

## 2.5 Symplectic topology crash course

Some useful references:

- McDuff-Salamon *Introduction to Symplectic Topology.*
- Weinstein *Lectures on Symplectic Manifolds.*
- Ana Cannas da Silva *Lectures on Symplectic Geometry.*

Every 2-tensor $T$ can be decomposed as $T = S + A$ with $S$ symmetric, and $A$ antisymmetric. Explicitly, this is achieved by $S(a, b) = (T(a, b) + T(b, a))/2$, and $A(a, b) = (T(a, b) - T(b, a))/2$. Since 2-tensors capture relations between two vectors on a manifold, they are the canonical structure we'd like to equip on a manifold in order to do geometry. On one hand, symmetric 2-tensors correspond to *Riemannian geometry.* The above calculation shows that all other 2-tensor structure is captured by antisymmetric 2-tensors (i.e. 2-forms) - and this is what corresponds to symplectic geometry.

**Definition 2.5.1.** Let $M^{2n}$ be a $2n$-manifold. A *symplectic form* on $M$ is a 2-tensor $\omega$ on $M$ satisfying the following properties:

- It is antisymmetric, i.e. $\omega$ is a 2-form: $\omega \in \Omega^2(M)$.
- It is closed, i.e. $d\omega = 0$.

- It is non-degenerate, i.e. $\wedge^n\omega \in \Omega^{2n}(M)$ is nowhere vanishing.

Perhaps a better motivation for symplectic structures than the one given above is to go to the original motivation: physics. The relationship between physics and sympletic geometry is described in detail in my course notes for Maths 257A (from Fall 2019).

We now look at some examples.

**Example.** If $n = 1$, the underlying manifold is a surface $\Sigma$, and $\omega$ is a closed 2-form with $\wedge^n\omega = \omega$ nowhere vanishing. This is exactly the statement that $(\Sigma, \omega)$ is a surface equipped with a volume form.

**Example.** Consider $\mathbb{R}^{2n}$ with coordinates $x_1, \ldots, x_n, y_1, \ldots, y_n$. The *canonical form* on $\mathbb{R}^{2n}$ is $\sum_{i=1}^n dx_i \wedge dy_i$. In fact, by *Darboux's theorem*, this is the local model of all symplectic manifolds!

**Example.** Let $M$ be any $n$-manifold. Then the cotangent bundle $T^*M$ is a $2n$-manifold, and can be given coordinates $x_1, \ldots, x_n, \xi_1, \ldots, \xi_n$. This is also canonically a symplectic manifold, with *canonical form* $\sum_{i=1}^n dx_i \wedge d\xi_i$. This is the most important symplectic manifold in physics - consider a physical space $M$ with position coordinates (for example $\mathbb{R}^3$). Then $T^*M$ consists of pairs $(q, p)$ where $q$ is position, and $p$ is momentum! A function $H : T^*M \to \mathbb{R}$ can then be interpreted as measuring the energy of every position-momentum pair, i.e. $H$ is a Hamiltonian! This gives a formalism which can describe all of classical mechanics.

What are some important submanifolds of a symplectic manifold? When restricting a Riemannian metric (a symmetric positive-definite bilinear form) to a submanifold, it is guaranteed to restrict as a Riemannian metric. Thus every submanifold of a Riemannian manifold is canonically a Riemannian manifold as well. However, this does not hold for symplectic manifolds! On one hand, some submanifolds are symplectic (upon restriction of the symplectic form), but on the other extreme, there are submanifolds on which the restriction of the symplectic form vanishes!

**Definition 2.5.2.** Let $N \subset (M^{2n}, \omega)$ be a submanifold.

- $N$ is said to be *symplectic* if the restriction $\omega|_N$ is itself a symplectic form (equivalently, $\omega|_N$ is non-degenerate).
- $N$ is *isotropic* if $\omega|_N = 0$.
- $N$ is *Lagrangian* if it is isotropic and $n$-dimensional.

Lagrangian submanifolds are maximal-dimensional isotropic submanifolds.

**Example.** Any curve on a surface $(\Sigma, \omega)$. This is because any one dimensional submanifold of a symplectic manifold can be shown to be isotropic, and a curve on a surface is also middle-dimensional.

**Example.** Let $s$ be a section of $T^*M$. If $s$ is closed, then $\operatorname{im} s$ is a Lagrangian submanifold of $T^*M$ (with the canonical form). In particular, the image of the zero-section is Lagrangian.

**Example.** A non-example: consider $V^n \subset (\mathbb{R}^{2n}, \omega_{\text{canonical}})$, with $V$ defined to be the tuples $(x_1, \ldots, x_n, y_1, \ldots, y_n)$ satisfying $x_1 = y_2$, but all other $y_i$ vanishing.

## 2.6 Riemannian-symplectic-complex 2-out-of-3

Loosely speaking, any two of three compatible Riemannian, almost-complex, and symplectic structures determines the third. We must explain what is meant by an almost-complex structure, but also what it means for these structures to be compatible.

**Definition 2.6.1.** Let $M$ be a $2n$-manifold.

- A *symplectic structure* is a closed nondegenerate 2-form.
- A *Riemannian structure* is a symmetric positive-definite bilinear form.
- An *almost complex structure* is a bundle map $J : TM \to TM$ covering the identity map on $M$, such that $J^2 = \mathrm{id}$.

Of course, we think of $J$ as being a generalisation of multiplication by $i$. We call $J$ an *almost complex structure*, since a complex structure should morally be the requirement that transition maps of the manifold are holomorphic, which is a stronger condition.

**Definition 2.6.2.** Let $M$ be a $2n$-manifold, equipped with a metric $g$, symplectic form $\omega$, and complex structure $J$.

- We say that $g$ and $J$ are *compatible* if $g = J^*g$.
- We say that $\omega$ and $J$ are *almost-compatible* if $\omega = J^*\omega$. $J$ is *tame* if $\omega(v, Jv) > 0$ for all $v$. Finally $\omega$ and $J$ are said to be *compatible* if they are almost-compatible and $J$ is tame.

Tameness is required to ensure that $g_J(v, w) = \omega(v, Jw)$ is positive definite, and in particular a metric. This shows that any symplectic form and almost complex form determines a canonical metric which is also compatible with the almost-complex form. Similarly, a metric and compatible almost-complex form determines a compatible symplectic form. Finally, $g$ and $\omega$ induce isomorphisms $\widetilde{g}, \widetilde{\omega} : TM \to T^*M$, and $\widetilde{g}^{-1} \circ \widetilde{\omega} : TM \to TM$ is a complex structure compatible with both $g$ and $\omega$.

**Theorem 2.6.3.** *Let $(M, g, \omega, J)$ be a manifold equipped with a metric, symplectic form, and almost-complex structure, such that $g = \omega(-, J-)$. Then any two of $g, \omega, J$ determine the third.*

*More generally, suppose $(M, \omega)$ is symplectic. Then there is a canonical map $\Theta$ admitting a canonical section $s$, giving rise to the following correspondence:*

$$\{\textit{Inner products } g \textit{ on } V.\} \underset{s}{\overset{\Theta}{\rightleftarrows}} \left\{ \begin{array}{c} \textit{Complex structures on } V, \\ \textit{compatible with } \omega. \end{array} \right\}$$

*Moreover, given any $g$, $\Theta(g)$ is compatible with $g$. As a corollary, the space of complex structures compatible with $\omega$ is contractible.*

*Conversely, suppose $(M, J)$ is almost-complex. Then there is a canonical map $\Phi$ admitting a canonical section $s$, giving rise to the following correspondence:*

$$\{\textit{Inner products } g \textit{ on } V.\} \underset{s}{\overset{\Phi}{\rightleftarrows}} \left\{ \begin{array}{c} \textit{Symplectic structures on } V, \\ \textit{compatible with } J. \end{array} \right\}$$

*The space of sympletic structures compatible with $J$ is again contractible.*

**Theorem 2.6.4.** *Let $(M, \omega, J), (M', \omega', J')$ be symplectic manifolds equipped with compatible complex structures. Then $M$ and $M'$ are isomorphic as symplectic manifolds if and only if they are isomorphic as almost-complex manifolds.*

This completes our crash course on symplectic topology! Proofs for everything in the symplectic sections of these notes can be found in my 257A Fall 2019 course notes.

## 2.7 Almost complex structures (lecture 3)

We begin by recalling some symplectic geometry definitions from the previous class.

**Definition 2.7.1.** Let $M^{2n}$ be a manifold.

- $(M, \omega)$ is *symplectic* if $\omega$ is a closed non-degenerate 2-form on $M$.
- An *almost complex structure* is a section $J$ of the endomorphism bundle of $TM$ (i.e. a bundle map $J : TM \to TM$) such that $J^2 = \mathrm{id}$.
- $J$ and $\omega$ are *compatible* if
  1. $\omega = J^*\omega$, i.e. $\omega(-,-) = \omega(J-, J-)$.
  2. $\omega(v, Tv) > 0$ for all non-zero $v$.

  In this instance, $\omega(-, J-)$ defines a metric.

At the end of the previous class, we mentioned that given a compatible triple $(M, g, \omega, J)$, any two of $g, \omega, J$ determine the third. However, we didn't really touch on a more fundamental result: the existence of compatible complex structures given a symplectic structure, and the topology of the space of compatible complex structures.

**Definition 2.7.2.** We write $\mathcal{J}(M, \omega)$ to denote the space of almost complex structures on $M$ compatible with $\omega$.

**Proposition 2.7.3.** Given any symplectic manifold $(M, \omega)$, $\mathcal{J}(M, \omega)$ is non-empty and contractible.

A proof of this result was given in class. However, a more detailed proof has been written up in my Maths 257A notes from Fall 2019, so we do not repeat the argument here.

# Chapter 3

# $J$-holomorphic curves and Lagrangian Floer homology

## 3.1 J-holomorphic curves

The $J$-holomorphic curves by Gromov revolutionised symplectic geometry. They are probably best known for leading to the Gromov-Witten invariants, but they also a key ingredient in Floer homology! They are essentially just (complex) 1-dimensional curves in almost complex manifolds.

**Definition 3.1.1.** A function $f : \mathbb{C} \to \mathbb{C}$ is complex differentiable (holomorphic) if it satisfies the *Cauchy-Riemann equations*;

$$du/dx = dv/dy, \quad du/dy = -dv/dx,$$

where $f(x, y) = (u(x, y), v(x, y))$.

We can re-write this as $f : (\mathbb{R}^2, j) \to (\mathbb{R}^2, J)$ from the "almost complex manifold" $\mathbb{C}$ to itself. Then $j$ and $J$ both have matrix representation

$$j = J = \begin{pmatrix} 0 & -1 \\ 1 & 0 \end{pmatrix}.$$

On the other hand, given that $f(x, y) = (u(x, y), v(x, y))$, we have

$$df = \begin{pmatrix} du/dx & dv/dx \\ du/dy & dv/dy \end{pmatrix}.$$

This gives

$$\begin{aligned}(df + J \circ df \circ j) &= \begin{pmatrix} du/dx & dv/dx \\ du/dy & dv/dy \end{pmatrix} + \begin{pmatrix} 0 & -1 \\ 1 & 0 \end{pmatrix} \begin{pmatrix} du/dx & dv/dx \\ du/dy & dv/dy \end{pmatrix} \begin{pmatrix} 0 & -1 \\ 1 & 0 \end{pmatrix} \\ &= \begin{pmatrix} du/dx - dv/dy & dv/dx + du/dy \\ du/dy + dv/dx & dv/dy - du/dx \end{pmatrix}.\end{aligned}$$

Therefore the Cauchy-Riemann equations are satisfied if and only if

$$df + J \circ df \circ j = 0.$$

Multiplying by $J$ (or by $j$), this is equivalently the condition that

$$df \circ j = J \circ df.$$

We observe that this is coordinate independent, and makes sense for any almost complex manifolds!

**Definition 3.1.2.** Let $(M, j), (N, J)$ be almost complex manifolds. The *Cauchy-Riemann equation* for a map $f : M \to N$ is

$$df \circ j = J \circ df.$$

If $f$ satisfies the Cauchy-Riemann equation, it is said to be *$(j, J)$-holomorphic*.

Before moving on, we introduce a little bit of notation. There is a certain calculus (Wirtinger calculus) for complex and almost complex manifolds, in which we work with *holomorphic* and *antiholomorphic* derivatives, denoted $\partial$ and $\overline{\partial}$ respectively. These give rise to a complex analogue of de Rham cohomology, known as Dolbeault cohomology (which is again explained in my Math 257A course notes from Fall 2019). What is relevant here is that we can define

$$\partial_J f = \frac{1}{2}(df - J \circ df \circ j), \quad \overline{\partial}_J f = \frac{1}{2}(df + J \circ df \circ j).$$

Notice that $\partial_J + \overline{\partial}_J = d$; the holomorphic and antiholomorphic differentials are projections of $d$ onto the space of holomorphic and antiholomorphic forms. This gives a final concise way of writing the Cauchy-Riemann equations!

**Proposition 3.1.3.** A map $f : (M, j) \to (N, J)$ satisfies the Cauchy-Riemann equation if and only if

$$\overline{\partial}_J f = 0.$$

A *$J$-holomorphic curve*, which are now ready to define, is pretty much exactly what we expect it to be!

**Definition 3.1.4.** Let $(M, \omega)$ be a symplectic manifold, and $J \in \mathcal{J}(M, \omega)$. Let $(\Sigma, j)$ be a Riemann surface. (This is equivalently an almost complex closed (real) two dimensional manifold.) A map $u : \Sigma \to M$ is a *$J$-holomorphic curve* if $\overline{\partial}_J u = 0$.

**Example.** A particular case of interest is $J$-holomorphic spheres: $u : \mathbb{S}^2 \to (M, J)$, $\overline{\partial}_J u = 0$. Notice that $\mathbb{S}^2$ admits a canonical complex structure since $\mathbb{S}^2 = \mathbb{CP}^1$.

**Definition 3.1.5.** Let $L \subset (M, \omega)$ be Lagrangian (i.e. $2 \dim L = \dim M$ and $\omega|_L = 0$). A map $u : (D^2, \partial D^2) \to (M, L)$ is a *J-holomorphic disk* if $\overline{\partial}_J u = 0$.

**Definition 3.1.6.** Let $L_0, L_1 \subset M$ be Lagrangian, and fix $x, y \in L_0 \cap L_1$. Let $u : \mathbb{R} \times [0,1] \to M$ satisfy

- $u(-, 0) \in L_0$, and $u(-, 1) \in L_1$.
- $\lim_{s \to -\infty} u(s,t) = x, \lim_{s \to \infty} u(s,t) = y$.
- $\overline{\partial}_J u = 0$.

Then $u$ is a *J-holomorphic strip*. (Sometimes these are also called $J$-holomorphic disks).

**Remark.** Why are these also called $J$-holomorphic disks? An alternative definition is to instead consider a map $u : (D, \partial D) \to (M, L_0, L_1)$ with two marked points $1, -1 \in D \subset \mathbb{C}$ mapping to marked points $x, y \in L_0 \cap L_1$, with the top half of the boundary of $D$ mapping into $L_0$ and the bottom half into $L_1$.

**Remark.** 1. The points $x$ and $y$ can coincide! 2. Many $J$-holomorphic strips can be shown to exist by the Riemann mapping theorem.

**Definition 3.1.7.** Finally we define *time-dependent J-holomorphic strips* as follows. Specify $J_t \in \mathcal{J}(M, \omega), t \in [0,1]$. A map $u : \mathbb{R} \times [0,1] \to M$ is a time-dependent $J$-holomorphic strip if it satisfies the same boundary conditions as above, but the Cauchy-Riemann condition is replaced with

$$\partial u / \partial s + J_t(u(s,t)) \partial u / \partial t = 0.$$

**Remark.** In the earlier derivation of the coordinate free Cauchy-Riemann equation from the classical Cauchy-Riemann equations, an intermediate step (which was not made explicit) is that the equations are equivalent to

$$\partial u / \partial s + J \partial u / \partial t = 0.$$

To study the space of $J$-holomorphic curves we desire some invariants. One such invariant is the *energy* of a curve.

**Definition 3.1.8.** Let $u : \Sigma \to M$ be a $J$-holomorphic curve. The *energy* of $u$ is

$$E(u) := \int_\Sigma |du|^2.$$

**Lemma 3.1.9.** $E(u) = \int_\Sigma u^* \omega$. Moreover, if $\Sigma$ is a 2-sphere, then $E(u) = [\omega][u(\Sigma)]$.

*Proof.* The second claim follows from the first. The first claim follows from this calculation:

$$\begin{aligned} |du|^2 &= g_J(du(\partial/\partial s), du(\partial/\partial s)) \\ &= g_J(du(\partial/\partial s), -du(j\partial/\partial t)) \\ &= g_J(du(\partial/\partial s), -Jdu(\partial/\partial t)) \\ &= \omega(du(\partial/\partial s), du(\partial/\partial t)). \end{aligned}$$

The first line is the definition of $|du|^2$, the second expresses the complex structure on $\Sigma$, the third is the Cauchy-Riemann equation, and the last comes from the definition of $g_J$. □

**Example.** If $\Sigma = \mathbb{S}^2$, then $E(u) = [\omega][u(\Sigma)]$. What if $\Sigma$ is a $J$-holomorphic disk? Then $[w] \in H^2(M, L)$ since $\omega|_L = 0$, and the same description as above holds using relative homology.

## 3.2 Gromov compactness theorem

Heegaard Floer homology (and more generally Lagrangian Floer homology) are defined by counting $J$-holomorphic strips (similarly to how Morse theory counts trajectories). Given any space $X$ (e.g. a space of $J$-holomorphic strips), for counting to make sense we require two basic properties:

- The space must be compact.
- The space must be 0-dimensional (i.e. discrete).

We will now investigate compactness of the space of $J$-holomorphic curves. First, an example shows that without additional premises, compactness will not be achieved:

**Example.** Let $M = \mathbb{S}^2 = \mathbb{C} \cup \{\infty\}$, equipped with the area form for its symplectic form, and $i$ for its complex structure. For each $n$, define

$$u_n : \mathbb{S}^2 \to \mathbb{S}^2, u_n(z) = z^n.$$

This has no limit as $n \to \infty$! More formally, if we compare energies, we find that

$$E(u_n) = [\omega][u_n] = 4\pi n,$$

and this has no convergent subsequences.

Here we used the energy to formally show that the space of $J$-holomorphic curves is not compact. Conversely, we might hope that energy is the only obstruction to compactness: maybe by enforcing an energy bound, we can force compactness. This is indeed the case!

**Theorem 3.2.1** (Gromov compactness theorem: spheres)**.** *Let $(M, \omega, J)$ be a symplectic manifold with a compatible almost complex structure. Let $u_n : \mathbb{S}^2 \to M$ be $J$-holomorphic spheres, and suppose there is some $K$ such that $E(u_n) < K$ for each $n$. Then there exists a subsequence $(u_{n_j})$ such that $u_{n_j}$ Gromov converges to $u$, where $u$ is a finite tree of $J$-holomorphic spheres.*

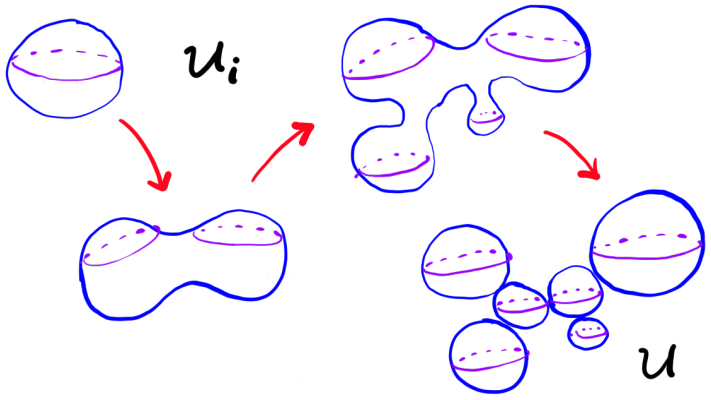


Figure 3.1: Gromov convergence of a $J$-holomorphic sphere.

This theorem also applies to disks and strips, with each generalisation giving slightly more possibilities for the "thing the sequence converges to". I.e. the boundary of the space of $J$-holomorphic things gets a bit more interesting each time.

**Theorem 3.2.2** (Gromov compactness: disks)**.** *Fix $K > 0$, and let $u_n : (D, \partial D) \to (M, L)$ be $J$-holomorphic disks. Suppose $E(u_n) < K$. Then there is a subsequence of $u_n$ that Gromov converges to some $u$, where $u$ is a finite tree of disks and spheres.*

**Theorem 3.2.3** (Gromov compactness: strips)**.** *Fix $K > 0$, and let $u_n : \mathbb{R} \times [0, 1] \to (M, L_0, L_1)$ be $J$-holomorphic strips. Suppose $E(u_n) < K$ for each $n$. Then there is a subsequence of $u_n$ that Gromov converges to some $u$, where $u$ is a broken strip, possibly with disks (in $L_0$ or $L_1$) and spheres forming a tree.*

Rather than being in the world of the abtract, we should really be looking at examples. The simplest case is to consider $M = \mathbb{C}$, and $L_0, L_1$ to be any paths in $M$.

**Example.** Figure 3.4 depicts a $J$-holomorphic strip $u_R \to M = \mathbb{C}$. By the Riemann mapping theorem, for each $R$ greater than 0 (but less than the distance from $x$ to $z$) there is a holomorphic map $u_R$ sending the strip to the image shown in the figure. As $R$ gets smaller, the sequence converges to the broken strip shown in the bottom right of the figure.

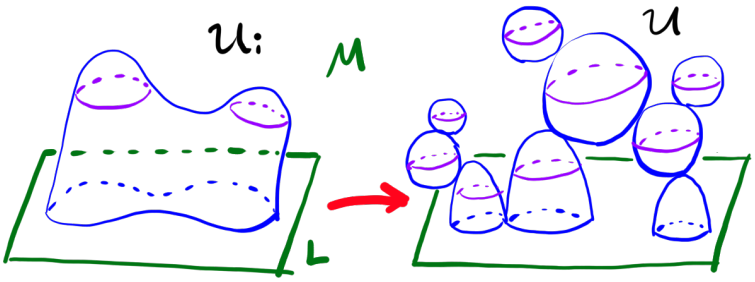


Figure 3.2: Gromov convergence of a $J$-holomorphic disk.

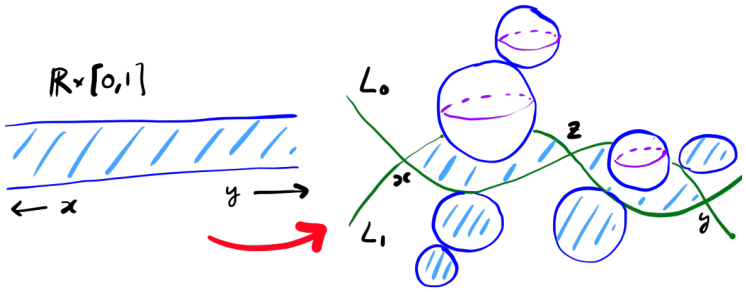


Figure 3.3: Gromov convergence of a $J$-holomorphic strip.

## 3.3 Moduli space of $J$-holomorphic curves

We've sorted out the issue of compactness via Gromov's compactness theorem. However, to count $J$-holomorphic curves, we need the space of such curves to be discrete. One characterisation of discreteness is to be a 0-dimensional manifold, so as a stepping stone we first investigate the manifold-ness of the space of $J$-holomorphic curves. We keep talking about the space of $J$-holomorphic curves, but we have yet to explicitly state what we mean by this. We now give a definition.

**Definition 3.3.1.** Let $(M,\omega)$ be a symplectic manifold, with Lagrangians $L_0, L_1$. Fix $x, y \in L_0 \cap L_1$. We write $\pi_2(x,y)$ to denote the relative homotopy classes of strips with the corresponding boundary conditions. Let $J_t$ be a path of compatible almost complex structures. The *moduli space of $J_t$-holomorphic strips* (in the class $\varphi \in \pi_2(x,y)$) is defined by

$$\mathcal{M}_{J_t}(\varphi) = \{J_t\text{-holomorphic strips } u : \mathbb{R}\times[0,1] \to (M, L_0, L_1, x, y) : [u] = \varphi\}/\sim .$$

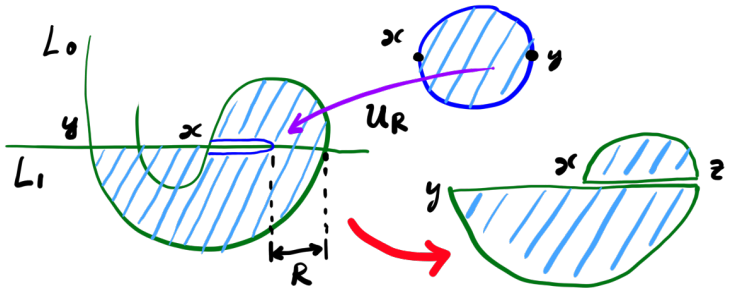


Figure 3.4: Example of a Gromov convergent sequence of $J$-holomorphic strips.

Here $\sim$ is equivalence of $J_t$-holomorphic strips, i.e. $u \sim u'$ if they are biholomorphic.

It turns out that this moduli space is indeed a manifold, given mild premises!

**Theorem 3.3.2.** *For generic $J_t$, $\mathcal{M}_{J_t}(\varphi)$ is a* smooth manifold *of dimension $\mu(\varphi)$, where $\mu(\varphi)$ is the* Maslov index *of $\varphi$ (which has yet to be defined).*

What do we mean by generic? This means there is a Baire subset $\mathcal{J}^{\text{reg}}_{[0,1]}(M,\omega) \subset \mathcal{J}_{[0,1]}(M,\omega) = \{[0,1] \to \mathcal{J}(M,\omega)\}$ for which the property holds.

**Remark.** If $M$ is a single point, and we consider $J$-holomorphic curves of a given genus $g$ and some number of marked points $m$, the corresponding moduli space is exactly the moduli space of Riemann surfaces.

In the previous theorem, we referred to the *Maslov index* which we have yet to even define! Rather than giving a formal definition, we will try to describe it in a more inutitive way. Suppose $u : \mathbb{R} \times [0,1] \to (M, L_0, L_1)$ is a $J$-holomorphic strip. We can simultaneously trivialise $u^*TM \cong \mathbb{R}^{2n}$ and $u^*TL_0 \cong \mathbb{R}^n$. But now $u^*TL_1$ cannot generally be trivialised, instead giving a loop in the space of Lagrangian subspaces of $\mathbb{R}^{2n}$.

**Exercise.** Show that

$$\pi_1(\text{Lag}(\mathbb{R}^{2n})) = \mathbb{Z}.$$

Then $[\gamma] \in \mathbb{Z}$ (from the isomorphism in the exercise) is the *Maslov index* of $u$. Intuitively the Maslov index counts how many times one Lagrangian wraps around the other. This is best seen in examples.

**Example.** Suppose $M = \mathbb{C}$. Then $\text{Lag}(\mathbb{R}^2) = \mathbb{RP}^1$. In figure 3.5 we have two examples of $J$-holomorphic strips. In the first, the tangent line of $L_0$ at $x$ is "the $y$-axis". It's also the $y$-axis at $y$! But to get from $x$ to $y$, the tangent space completes one whole rotation in $\mathbb{RP}^1$. In the second image, we have a similar situation but this time it completes two full rotations. Therefore the Maslov index of the first strip is 1, while the Maslov index of the second strip is 2.

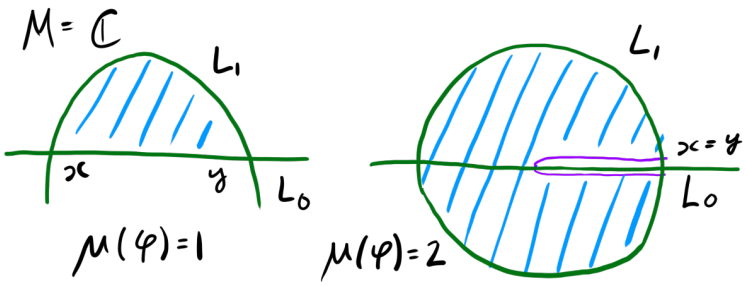


Figure 3.5: Examples of $J$-holomorphic strip Maslov indices.

## 3.4 Examples of moduli spaces of $J$-holomorphic curves (lecture 4)

In this section we will study some examples of $\mathcal{M}_J(\varphi)$, for some fixed $\varphi \in \pi_2(x, y)$.

**Example.** Figure 3.6 depicts a certain fixed choice of $u$ (which determines a class $\varphi$). We will determine $\mathcal{M}_J(\varphi)$. $u$ is required (by the definition of a $J$-holomorphic strip) to send $-1$ to $x$, and 1 to $y$. However, $u$ is also a holomorphic map. Recall from complex analysis that holomorphic maps $D^2 \to D^2$ are Möbius transformations:

$$\mathrm{Aut}(D^2) = \frac{az+b}{cz+d}, \begin{pmatrix} a & b \\ c & d \end{pmatrix} \in \mathrm{SL}(2, \mathbb{R}).$$

Therefore automorphisms of the disk are determined by three parameters. Of these, 1 and $-1$ are fixed - there is only one free parameter. Thus

$$\mathcal{M}_J(\varphi) = \mathbb{R} \cong (0, 1).$$

Visually this corresponds to the choice of "where does $-i$ get sent to?" in the "interval" from $x$ to $y$.

**Remark.** There is *always* an $\mathbb{R}$ action on $\mathcal{M}_J(\varphi)$, whatever $J$ and $\varphi$ are. This translation actions comes from viewing the holomorphic strip as having domain $\mathbb{R} \times [0, 1]$. Therefore we can instead consider $\widehat{\mathcal{M}}_J(\varphi) = \mathcal{M}_J(\varphi)/\mathbb{R}$. In our above example, $\widehat{\mathcal{M}}_J(\varphi)$ is a single point.

**Example.** Figure 3.7 depicts a more complicated example. There are qualitatively two ways that a marked disk (or strip) can be mapped into $\mathbb{C}$ to form a $J$-holomorphic strip, shown on the right of the diagram. We first consider the case of maps $u$ with image as in (a). There $\ell$ denotes the distance from $x$ to $\alpha$, travelling along first Lagrangian $L_0$. The

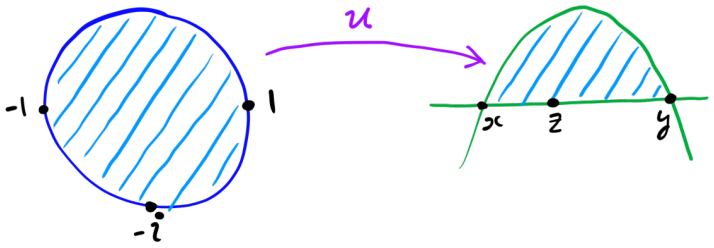


Figure 3.6: Example of $u$, for which $\mathcal{M}_J(\varphi) = \mathbb{R}$, $\varphi = [u] \in \pi_2(x, y)$.

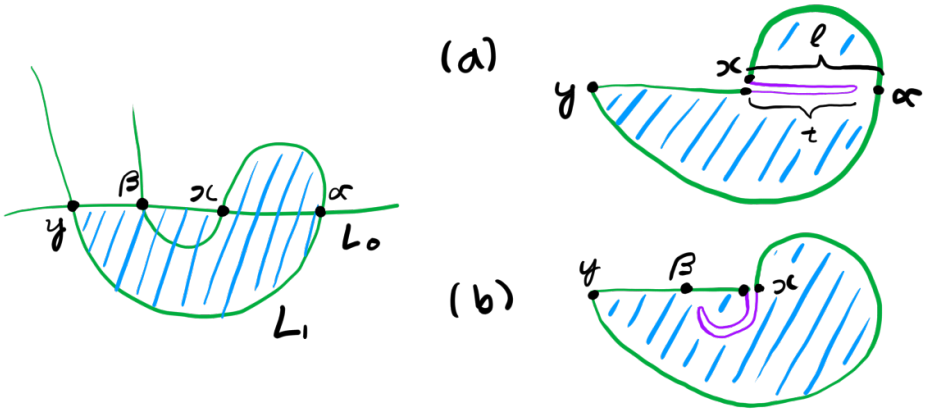


Figure 3.7: Example of $u$ for which $\widehat{\mathcal{M}}_J(\varphi) = (-\ell_2, \ell_1)$.

parameter $t$ is any real number in $[0, \ell)$. In this case, by the Riemann mapping theorem, for each such $t$ there are $\mathbb{R}$ many $J$-holomorphic strips with the designated image. (Again this $\mathbb{R}$ comes from the translation action).

In the case of (b), we have the same situation but for parameters between 0 and the length of the Lagrangian from $x$ to $\beta$. If we call these lengths $\ell_1$ and $\ell_2$, then

$$\mathcal{M}_J(\varphi) = (\mathbb{R} \times [0, \ell_1)) \cup (\mathbb{R} \times (-\ell_2, 0]) = \mathbb{R} \times (-\ell_2, \ell_1).$$

In particular, $\widehat{\mathcal{M}}_J(\varphi) = (-\ell_2, \ell_1)$.

Next we consider this example in the context of Gromov's compactness theorem. There are no bubbles, but we *do* have broken strips: while $\widehat{\mathcal{M}}_J(\varphi) = (-\ell_2, \ell_1)$, if we compatify this, we have $[-\ell_2, \ell_1]$. These correspond to the two broken strips (which arise as gluing disks together at $\alpha$ and $\beta$ respectively) as the parameter $t$ is sent to $\ell_1$ and $\ell_2$ respectively.

Notice that in the first example, $\dim \mathcal{M}_J(\varphi) = 1$, which is indeed the Maslov index of the pair of Lagrangians as shown in the example at the end of the previous lecture.

Similarly, in the second example, $\dim \mathcal{M}_J(\varphi) = 2$ as required.

## 3.5 The structure of intersections of Lagrangians

In this section we show that $L_0 \cap L_1$ has a grading induced by $J$-holomorphic strips. One ingredient we need is a binary operation on the space of relative homotopy classes of strips, $\pi_2(x, y)$.

**Definition 3.5.1.** Let $\varphi_1 \in \pi_2(x, y)$, and $\varphi_2 \in \pi_2(y, z)$. Then the *concatenation* $\varphi_1 \# \varphi_2$ of $\varphi_1$ and $\varphi_2$ is a strip in $\pi_2(x, z)$, defined as follows:

- Let $q : D^2 \to D^2 \vee D^2$ be the quotient map sending the arc $[-i, i]$ to a point, where $D^2$ is parametrised as the unit disk in $\mathbb{C}$.
- Define $\varphi$ on $D_1^2 \vee D_2^2$ as follows: On the left factor $D_1^2$, $\varphi|_{D_1^2} = \varphi_1$. Notice that $0 \in D_1^2$ maps to $y$. Similarly, $\varphi|_{D_2^2} = \varphi_2$, and $0 \in D_2^2$ maps to $y$.
- Now $\varphi \circ q$ is a (broken) strip in $\pi_2(x, z)$.

**Proposition 3.5.2.** Energy and Maslov index are additive under concatenation:

$$\mu(\varphi_1 \# \varphi_2) = \mu(\varphi_1) + \mu(\varphi_2), \quad E(\varphi_1 \# \varphi_2) = E(\varphi_1) + E(\varphi_2).$$

We are now ready to describe a grading on $L_0 \cap L_1$. We suppose $L_0$ and $L_1$ are transverse, where $L_i \in (M, \omega)$ are Lagrangian submanifolds.

**Proposition 3.5.3.** Choose $\varphi \in \pi_2(x, y)$ (assuming the latter is non-empty). Then there is a *relative grading* defined by

$$\mu(x, y) = \mu(\varphi) \in \mathbb{Z}/N\mathbb{Z}$$

for some $N$.

*Proof.* We must show that the grading is well defined in the sense that it respects the additive structure induced by concatenation. Explicitly, we want $\mu(x, y) + \mu(y, z) = \mu(x, z)$. In particular, this requires $\mu(x, x) = 0$. This is why we must mod out by $N\mathbb{Z}$, as we will see that there exists some $N$ so that $\mu(x, x) \in N\mathbb{Z}$.

Let $\varphi_1, \varphi_2 \in \pi_2(x, y)$. Then $-\varphi_i \in \pi_2(y, x)$, and

$$\varphi \#(-\varphi_1) \in \pi_2(x, x), \quad (-\varphi_2)\#\varphi \in \pi_2(y, y).$$

These define isomorphisms

$$\pi_2(x, y) \to \pi_2(x, x), \quad \psi \mapsto \psi \#(-\varphi_1),$$

and similarly for $\pi_2(x,y) \cong \pi_2(y,y)$. There exists some $N$ such that $\mathrm{im}(\mu : \pi_2(x,x) \to \mathbb{Z}) = N\mathbb{Z}$. By the above isomorphisms, $\mu(x,y)$ is defined up to $\mu(\varphi_1) - \mu(\varphi_2) \in N\mathbb{Z}$, so $\mu(x,y) \in \mathbb{Z}/N\mathbb{Z}$ is well defined.

In particular, we have the property

$$\mu(x,y) + \mu(y,z) = \mu(x,z).$$

This is a *relative grading.* □

If we fix some $x_0 \in L_0 \cap L_1$, we can define an *absolute grading* (instead of just a relative grading). This is defined by

$$\mathrm{gr}(x) = \mu(x, x_0) \in \mathbb{Z}/N\mathbb{Z}.$$

**Lemma 3.5.4.** The value $N$ above is *even.*

*Proof.* We take $L_0, L_1$ to be oriented. Then each $x \in L_0 \cap L_1$ has an induced orientation (sign) $\sigma(x)$ in $\mathbb{Z}/2\mathbb{Z}$, and $\mu(\varphi) = \sigma(x) - \sigma(y) \bmod 2$. In particular, when $x = y$, $\mu(\varphi)$ is even so $N$ is even. □

**Remark.** In general we break $L_0 \cap L_1$ into equivalence classes $x \sim y$ if and only if there exists $\varphi \in \pi_2(x,y)$. The elements of each equivalence class admit a relative grading in $\mathbb{Z}/N\mathbb{Z}$.

## 3.6 Lagrangian Floer homology

We are finally ready to define Lagrangian Floer homology (which will later be used to define Heegaard Floer homology).

**Remark.** Lagrangian Floer homology can be defined more generally than how we will define it. However, our level of generality is sufficient for the purposes of Heegaard Floer homology.

**Definition 3.6.1.** Here we number several premises (which we assume our manifold/Lagrangians satisfy) in order to define Lagrangian Floer homology. These premises will continue to appear for several lectures, with the same numbering. Let $L_0, L_1 \subset (M, \omega)$ be Lagrangians.

1. $L_0, L_1$ are compact.
2. $L_0$ and $L_1$ are transverse.
3. Either $M$ is compact, or it is "convex at infinity". These ensure that no $J$-holomorphic curves (whose boundaries are on a fixed compact subset) go off to infinity.

4. For all $A \in \pi_2(M)$ or $\pi_2(M, L_i)$, $i = 0, 1$, we have that $[\omega](A) = 0$. In other words, there can be no $J$-holomorphic disks or spheres! Only strips.

5. Let $\mu : \pi_2(x, x) \to \mathbb{Z}$ be the Maslov index. Then $E(\ker \mu)$ is bounded above, where $E$ is the *energy* of $J$-holomorphic strips. (For example, this condition is satisfied if $\mu$ is injective.)

6. $L_0, L_1$ have spin structures. (These induce orientations on the moduli space of $J$-holomorphic strips.)

**Remark.** The purpose of premise 6 is essentially so that we can make signed counts, i.e. for defining integral Floer homology. For $\mathbb{Z}/2\mathbb{Z}$ Floer homology, we can drop the last premise.

**Remark.** The previous 5 premises all work together to ensure that Gromov compactness holds, and that limits of strips (i.e. the boundary of the space of strips) consists only of broken strips, and no disk or sphere bubbles.

In particular, premise 5 controls energy. Given these premises, we can now define the Floer chain complex!

**Definition 3.6.2.** Let $(M, \omega, L_0, L_1)$ satisfy the 6 premises. The *Lagrangian Floer chain complex* consists of the (graded) ring

$$CF_*(L_0, L_1) = \mathbb{Z}\langle x : x \in L_0 \cap L_1 \rangle.$$

Note that $L_0 \cap L_1$ is 0 dimensional by transversality (premise 2), and hence a finite set by combining this with premise 1. This can be further decomposed: let $S(L_0, L_1)$ denote the set of equivalence classes of points in $L_0 \cap L_1$, where $x \sim y$ if and only if $\pi_2(x, y)$ is non-empty. Then each $s \in S(L_0, L_1)$ gives a ring $CF_*(L_0, L_1; s)$ by restricting from $L_0 \cap L_1$ to $s$. Thus

$$CF_*(L_0, L_1) = \bigoplus_{s \in S(L_0, L_1)} CF_*(L_0, L_1, s).$$

For each $s \in S(L_0, L_1)$ we can fix an element $x_s \in s$. This allows us to define an absolute grading $\mathrm{gr}(x) = \mu(x, x_s) \in \mathbb{Z}/N\mathbb{Z}$, where $N$ depends on $s$. Using the gradings, we can define a *boundary map*.

**Definition 3.6.3.** Let $(M, \omega, L_0, L_1)$ be as above. The *boundary map* of the *Lagrangian Floer chain complex* is a map $\partial : CF_*(L_0, L_1) \to CF_{*-1}(L_0, L_1)$ defined by

$$\partial x = \sum_{y \in L_0 \cap L_1, \mu(x,y)=1} \sum_{\varphi \in \pi_2(x,y), \mu(\varphi)=1} \#\mathcal{M}_{J_t}(\varphi)/\mathbb{R} \cdot y$$

where $J_t$ is generic, and $\#$ denotes a signed count of the succeeding 0-dimensional oriented manifold.

For example, the Euler characteristic of the chain complex is given by

$$\chi(CF_*(L_0, L_1)) = \pm[L_0] \cdot [L_1] = \sum_{x \in L_0 \cap L_1} (-1)^{\mathrm{gr}(x)} = \sum_{x \in L_0 \cap L_1} \sigma(x).$$

Notice that $\mathcal{M}_{J_t}/\mathbb{R}$ is finite by Gromov compactness, and $\mu(\varphi) = 1$ ensuring that the dimension is 0.

**Proposition 3.6.4.** $\partial^2 = 0$, so the Floer chain complex is really a chain complex.

*Proof.* We do not give a proof here, but this is analogous to the proof that the Morse complex is a chain complex! See for example my notes of Morse theory. □

**Definition 3.6.5.** The *Lagrangian Floer homology* of $(M, \omega, L_0, L_1)$ is

$$HF_*(L_0, L_1) = H_*(CF_*(L_0, L_1), \partial).$$

**Lemma 3.6.6.** $HF(L_0, L_1)$ is independent of the choice of generic $J_t$.

## 3.7 Examples of Lagrangian Floer homologies (lecture 5)

Let $L_0, L_1 \subset (M, \omega)$ be Lagrangian, satisfying the conditions 1 through to 6 from the previous lecture. Recall that the Lagrangian Floer complex is then well defined:

$$CF_*(L_0, L_1) = \mathbb{Z}\langle L_0 \cap L_1 \rangle, \quad \partial x = \sum_y \sum_{\varphi \in \pi_2(x,y), \mu(\varphi)=1} \#\left(\mathcal{M}(\varphi)/\mathbb{R}\right) y.$$

From here the Lagrangian Floer homology is defined to be the homology of this complex. Before moving on with more theory, we must compute some examples of Lagrangian Floer homology to make sure we know what's going on! We'll consider four examples, as shown in figure 3.8. Suppose $M$ is any closed oriented surface, and $L_0, L_1$ are transverse embedded curves. For Lagrangian Floer homology to be well defined, we require property 4 to hold, that is,

$$[\omega](B) = 0 \text{ for all } B \in \pi_2(M), \text{ or } \pi_2(M, L_i).$$

This is guaranteed provided that $M$ has positive genus and the $L_i$ are not nullhomotopic! Therefore the examples we consider all satisfy these properties.

**Example.** First we consider the top left image, example 1, from figre 3.8. The two Lagrangians intersect at a single point $x$, so the corresponding chain complex is

$$CF_*(L_0, L_1) = \mathbb{Z}\langle L_0 \cap L_1 \rangle = \mathbb{Z}\langle x \rangle.$$

Now it is necessarily the case that $\partial = 0$, since there are no relative gradings that even need to be considered when there's only a single intersection point! Therefore

$$HF = \mathbb{Z}.$$

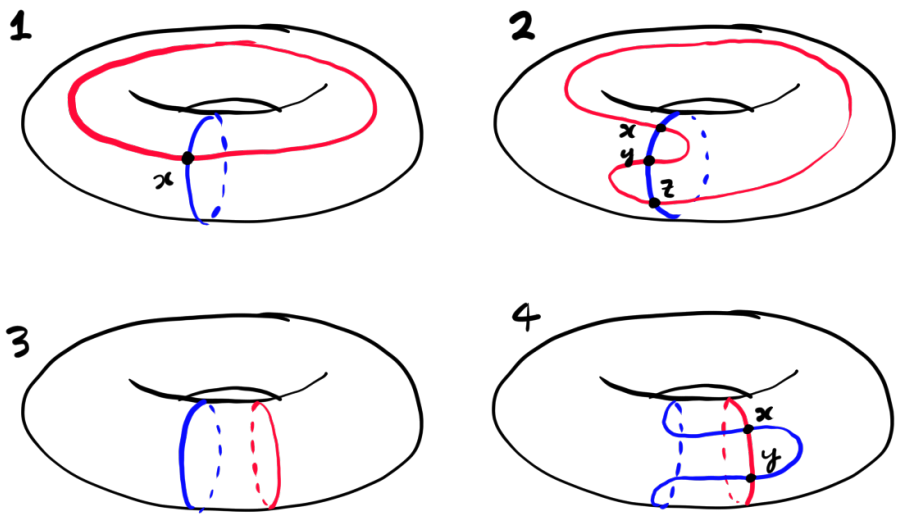


Figure 3.8: Examples for Lagrangian Floer homology.

**Example.** In example 2, the two Lagrangians intersect at three points. The corresponding chain complex is

$$CF_*(L_0, L_1) = \mathbb{Z}\langle x, y, z\rangle.$$

What are the relative gradings? We first fix orientations in order to count Maslov indices. From the figure, we see that there is a $J$-holomorphic strip realising $\varphi \in \pi_2(y, x)$. Then

$$\mu(y, x) = \mu(\varphi) = 1.$$

Similarly $\mu(y, z) = 1$. Therefore the relative grading of $y$ is 1 higher than those of $x$ and $z$ (which share the same relative grading). From here we can determine the boundary maps. The only potentially non-trivial map is

$$\partial : Z\langle y\rangle \to \mathbb{Z}\langle x, z\rangle.$$

We know by definition that

$$\partial y = \sum_{\varphi\in\pi_2(y,x),\mu(\varphi)=1} \#(\mathcal{M}(\varphi)/\mathbb{R})x + \sum_{\varphi\in\pi_2(y,z),\mu(\varphi)=1} \#(\mathcal{M}(\varphi/\mathbb{R})z.$$

Looking first at the $x$ term, there is exactly one homotopy class $\varphi$ satisfying the conditions under the sum, and from an example at the start of the previous lecture $\mathcal{M}(\varphi)/\mathbb{R}$ is a single

point. Similarly for the $z$ term. Therefore depending on the signs of the spin$^c$ structure, we have

$$\partial y = \pm x \pm z.$$

(Note that the $\pm$ for the two terms are independent). In either case, we have

$$0 \xrightarrow{\partial} \mathbb{Z}\langle y \rangle \xrightarrow{\partial'} \mathbb{Z}\langle x, z \rangle \xrightarrow{\partial''} 0,$$

with

$$\operatorname{im} \partial = 0, \ker \partial' = 0, \quad \operatorname{im} \partial' = \mathbb{Z}\langle x \pm z \rangle, \ker \partial'' = \mathbb{Z}\langle x, z \rangle.$$

Therefore the first homology group is trivial, while the second is $\mathbb{Z}$. Therefore

$$HF = \mathbb{Z}.$$

**Remark.** We see that the first two examples have isotopic Lagrangians, and the same Lagrangian Floer homologies. Perhaps $HF$ is invariant under isotopies of Lagrangians? We see that this is not quite true in the next examples.

**Example.** In the third example, there are no intersections between the Lagrangians! Therefore the Lagrangian chain complex is empty! The Floer homology is trivial:

$$HF = 0.$$

**Example.** In the final example, we have $CF = \mathbb{Z}\langle x, y \rangle$. Depending on signs, without loss of generality $y$ has a relative grading 1 above that of $x$. Therefore there is a single potentially non-trivial boundary map,

$$\partial \mathbb{Z}\langle y \rangle \to \mathbb{Z}\langle x \rangle.$$

This time there are two distinct homotopy classes of strips from $y$ to $x$: one wraps in front of the torus, the other behind. The space of such strips has size 1 (modulo the translation action of $\mathbb{R}$). Therefore depending on the spin$^c$ structures, we have

$$\partial y = x \pm x.$$

In one case, we could have $\partial y = 0$ so that all homology groups are trivial! Then $HF = \mathbb{Z}^2$. On the other hand, we could have $\partial y = 2x$. In this case, $HF = \mathbb{Z}/2\mathbb{Z}$. In either case, we see that $HF$ is non-trivial!

The key difference is that examples 1 and 2 are related by *Hamiltonian isotopies*, while examples 3 and 4 are related by isotopies which are *not* Hamiltonian.

## 3.8 Hamiltonian isotopy invariance

In this section we describe what it means for two Lagrangians to be *Hamiltonian isotopic*. More detailed exposition can be found in my notes on Symplectic geometry from Fall 2019.

**Definition 3.8.1.** Let $H_t : M \to \mathbb{R}$ be a family of smooth functions, smoothly parametrised by $t \in [0, 1]$. Suppose $\omega$ is a symplectic form on $M$. By non-degeneracy of $\omega$, there exist vector fields $X_{H_t}$ such that

$$i_{X_{H_t}}\omega = dH_t.$$

This is called a (time dependent) Hamiltonian vector field. These give rise to time dependent Hamiltonian flows:

$$\frac{d\varphi_t}{dt} = X_{H_t} \circ \varphi_t.$$

Then $\varphi_1$ is called a *Hamiltonian transformation* of $(M, \omega)$.

The idea is that $\varphi_t$ forms an isotopy from $\varphi_0$ to $\varphi_1$ which preserves the symplectic structure:

$$\varphi_t^*\omega = \omega.$$

**Theorem 3.8.2.** *Let $\psi$ be a Hamiltonian transformation of $(M, \omega)$. Then*

$$HF(L_0, L_1) \cong HF(L_0, \psi(L_1)) \cong HF(\psi(L_0), L_1).$$

*We call $\varphi_t(L)$ a* Hamiltonian isotopy *of a Lagrangian $L$.*

**Example.** Consider $\mathbb{R}^2$ equipped with the Hamiltonian $H_t(x, y) = y$. The symplectic form on $\mathbb{R}^2$ is the area form $dx \wedge dy$. Now

$$i_{X_{H_t}}(dx \wedge dy) = dy,$$

so that $X_{H_t} = \partial/\partial x$. Thus the corresponding Hamiltonian transformation $\varphi_1$ is exactly translation by 1 in the $x$ direction. Therefore *translations* are Hamiltonian.

**Example.** Again consider $(\mathbb{R}^2, dx \wedge dy)$. Consider the transformation that dilates $\mathbb{R}^2$. This is *not* Hamiltonian as it does not preserve the symplectic form $dx \wedge dy$. This is immediate because the symplectic form is the area form, and dilations literally dilate area.

More generally (even in higher dimensions) Hamiltonian transformations always preserve volumes, and there is a partial converse in which isotopies preserving volumes are in fact Hamiltonian.

# Chapter 4

# Heegaard Floer homology definition and well-definedness

## 4.1 Heegaard Floer homology definition

With the aside about Hamiltonian isotopies of Lagrangians preserving Langrangian Floer homology out of the way, we are finally ready to define Heegaard Floer homology! The definition is not too difficult to state, but the real issue is in verifying that all conditions from Lagrangian Floer homology are satisfied.

Let $Y^3$ be a closed connected oriented manifold. Choose a based Heegaard diagram

$$(\Sigma, \alpha_1, \dots, \alpha_g, \beta_1, \dots, \beta_g, z), \quad z \in \Sigma - \bigcup_i \alpha_i - \bigcup_i \beta_i.$$

The symmetric product $\mathrm{Sym}^g(\Sigma)$ is used to define the Heegaard Floer homologies $HF^{\pm}$. The space $\mathrm{Sym}^g(\Sigma - \{z\})$ is used to define $\widehat{HF}$. These are the first two types of Heegaard Floer homology we will define, but there will be more later! Next we define $L_0 = \prod_i \alpha_i \subset \Sigma^g - \{z\}$, and $L_1 = \prod_i \beta_i$. These are $g$ dimensional tori living in $\mathrm{Sym}^g(\Sigma - \{z\})$ and $\mathrm{Sym}^g(\Sigma)$. We will later see that these are Lagrangian submanifolds of the symmetric products, and the Lagrangian Floer homologies $HF(L_0, L_1)$ will be defined to be the Heegaard Floer homologies of $Y^3$.

We will also write $\mathbb{T}_\alpha$ and $\mathbb{T}_\beta$ to denote the tori.

**Theorem 4.1.1.** *We have isolated submanifolds $L_0 = \mathbb{T}_\alpha, L_1 = \mathbb{T}_\beta$ of $\mathrm{Sym}^g(\Sigma)$ and $\mathrm{Sym}^g(\Sigma - \{z\})$. The symmetric products are (canonically) symplectic manifolds, and the $L_i$ are Lagrangian submanifolds.*

Rather than giving a proof in a traditional sense, we will eventually reach the above conclusion through some more exploratory work (following the lecture).

Consider the thicc diagonal

$$\Delta \subset \mathrm{Sym}^g(\Sigma), \Delta := \{\{x_1, \ldots, x_g\} : x_i \in \Sigma, x_i = x_j \text{ for some } i \neq j\}.$$

Recall that there is an $S_g$ action on $\Sigma^g$, and the quotient by this action is the symmetric product. A key point is that $S_g$ acts freely away from $\Delta$! Moreover, our tori $\mathbb{T}_\alpha, \mathbb{T}_\beta$ are also away from $\Delta$. We want to find symplectic forms on $\mathrm{Sym}^g(\Sigma)$ and $\mathrm{Sym}^g(\Sigma - \{z\})$, but really we only care about what it's doing away from $\Delta$.

We will now find a canonical singular symplectic form on $\mathrm{Sym}^g(\Sigma)$, in the sense that it is a symplectic form away from $\Delta$ but blows up on $\Delta$. Let $j$ be a complex structure on some surface $\Sigma$. This induces a complex structure $\mathrm{Sym}^k(j)$ on $\mathrm{Sym}^k(\Sigma)$ for any $k$. Locally, we have

$$\mathrm{Sym}^k(\mathbb{C}) \cong \mathbb{C}^k$$

by symmetric polynomials (as described in an earlier lecture). This is super clean! Maybe we can do the same thing with symplectic forms? Unfortunately, this dream does quite work.

Let $dA$ be the area form (symplectic form) on a surface $\Sigma$. The hope is that $\mathrm{Sym}^k(dA)$ is a symplectic form on $\mathrm{Sym}^k(\Sigma)$. Away from $\Delta$, $\mathrm{Sym}^k(\Sigma)$ is just the product $\prod_k \Sigma$. Similarly, $\mathrm{Sym}^k(dA)$ is just the product form $\prod_k dA$. This form is $S_k$ invariant, and descends to a symplectic form on $\mathrm{Sym}^k(\Sigma) - \Delta$.

Near $\Delta$ is another matter: locally, say for $k = 2$, we have

$$\begin{aligned}\mathrm{Sym}^2(\mathbb{C}) &\cong \mathbb{C} \times \mathbb{C}/(z, w) \sim (w, z) \\ &\cong \mathbb{C} \times (\mathbb{C}/y \sim -y) \\ &\cong \mathbb{C} \times \mathbb{C}\end{aligned}$$

where we have used the change of coordinates $(w, z) \rightsquigarrow (x, y), x = w + z, y = w - z$ to parametrise $\mathbb{C} \times \mathbb{C}$ in the middle line, but then carry out a further change in coordinates to $(x, y^2)$ to parametrise $\mathbb{C} \times \mathbb{C}$ in the last line.

The area form on $\mathbb{C} \times \mathbb{C}$ (given $(x, y)$ coordinates) is $dx \wedge \overline{dx} + dy \wedge \overline{dy}$ (up to a scalar multiple). We will transform this into $(x, y^2)$ coordinates. If we write $y = re^{i\theta}$, then the area form is $rdrd\theta$ in the $y$ factor. Changing to $y^2$ then gives

$$r^2 e^{2i\theta} = \rho e^{i\tau}, \tau = 2\theta, \rho = r^2.$$

But now

$$rdrd\theta = \frac{1}{4} d(r^2) d(2\theta) = \frac{d\rho d\tau}{4} = \frac{\rho d\rho d\tau}{4\rho} = \frac{\text{area form}}{4\rho}.$$

This is singular as $\rho \to 0$, i.e. as we approach $\Delta$! In summary, $\mathrm{Sym}^k(dA)$ is generally a *singular symplectic form* on $\mathrm{Sym}^k(\Sigma)$: it is symplectic almost everywhere but blows up on $\Delta$. It turns out that this issue can be resolved, by a theorem of Perutz.

**Theorem 4.1.2.** *There exists an honest symplectic form on* $\mathrm{Sym}^k(\Sigma)$ *which agrees with* $\mathrm{Sym}^k(dA)$ *away from a neighbourhood of* $\Delta$.

In particular, the above symplectic form agrees with $\mathrm{Sym}^k(dA)$ near $\mathbb{T}_\alpha$ and $\mathbb{T}_\beta$, the tori obtained from the Heegaard diagram. It follows that the tori are Langrangian, since whenever $L_0, L_1$ are Lagrangian submanifolds of $M_0, M_1$, then their product is a Lagrangian submanifold of $M_0 \times M_1$. Finally we're ready to define Heegaard Floer homology, since we have verified that the symmetric product is really symplectic, and the tori are really Lagrangian.

**Definition 4.1.3.** The *hatted Heegaard Floer homology* $\widehat{HF}(Y)$ of a closed oriented 3-manifold $Y^3$ is defined to be the Lagrangian Floer homology $HF(\mathbb{T}_\alpha, \mathbb{T}_\beta)$ of $\mathbb{T}_\alpha$ and $\mathbb{T}_\beta$ in $\mathrm{Sym}^g(\Sigma - \{z\})$, where $(\Sigma, \alpha_i, \beta_i, z)$ is a based Heegaard diagram of $Y$. Similarly, the *signed Heegaard Floer homology* $HF^{\pm}(Y)$ of $Y$ is defined to be the Lagrangian Floer homology of the above tori in $\mathrm{Sym}^g(\Sigma)$ (as opposed to $\mathrm{Sym}^g(\Sigma - \{z\})$).

**Remark.** Largely speaking two things need to be verified to ensure that this is well defined: first, we must verify that an arbitrary Heegaard diagram of a 3-manifold as above satisfies all the conditions for Lagrangian Floer homology to be well defined. Second, we must ensure that Heegaard Floer homology is independent of the choice of Heegaard diagram for $Y$.

We will dedicate several lectures to verifying well-definedness. Recall the 6 necessary conditions to define Lagrangian Floer homology: the first two automatically hold given a Heegaard diagram of a 3-manifold. We will now verify the 3rd condition:

- Given a symplectic manifold $M$, to define Lagrangian Floer homology, we require that either $M$ is compact or "convex at infinity". In other words, no $J$-holomorphic strips escape to infinity.

For our two versions of Heegaard Floer homology, our ambient spaces are $\mathrm{Sym}^g(\Sigma)$ and $\mathrm{Sym}^g(\Sigma - \{z\})$. The former is automatically compact since it is a quotient of a product of compact spaces. However, the latter is not necessarily compact so we must do some work.

Let $R_z = \{z\} \times \mathrm{Sym}^{g-1}(\Sigma) \subset \mathrm{Sym}^g(\Sigma)$. While $\mathrm{Sym}^g(\Sigma)$ is a $2g$-dimensional manifold, the former is a codimension 2 submanifold. Observe that

$$\mathbb{T}_\alpha \cap R_z = T_\beta \cap R_z = \varnothing, \quad \mathrm{Sym}^g(\Sigma - z) = \mathrm{Sym}^g(\Sigma) - R_z.$$

Suppose $u$ is a $J$-holomorphic strip in $\mathrm{Sym}^g(\Sigma)$, with homotopy class $\varphi \in \pi_2(x, y)$. This has 2-dimensional image, so it intersects $R_z$ along a zero dimensional space! The signed intersections $[u] \cdot [R_z]$ will be denoted by $n_z(\varphi)$. Now $u$ lies in $\mathrm{Sym}^g(\Sigma - z)$ if and only if $n_z(\varphi) = 0$.

The goal is to verify that sequences of $J$-holomorphic strips don't go off to infinity. Suppose $u_n$ converges to $u$, with each $u_n$ a strip in $\mathrm{Sym}^g(\Sigma - z)$. We must verify that $u$ is

also a strip in $\mathrm{Sym}^g(\Sigma - z)$ (i.e it does not meet $z$). By the above observation, we have for each $n$ that $n_z(u_n) = 0$. It follows that $n_z(u) = 0$, and positivity of complex intersections then gives $u \in \mathrm{Sym}^g(\Sigma - z)$. This verifies property 3.

Properties 4 and 5 require us to study the topology of $\mathrm{Sym}^g(\Sigma)$. We now take a step back to develop some more machinery before tackling these conditions (for Lagrangian Floer homology to be well defined).

## 4.2 Branched covers and the tautological correspondence

In this section we will establish the *tautological correspondence* between immersions into symmetric products and bracnhed covers. This allows us to understand some properties of $J$-holomorphic strips in terms of branched covers (for which a wealth of machinery exists).

**Definition 4.2.1.** Let $p : M^m \to N^m$ be a smooth map. $p$ is an $\ell$-fold branched cover, branched over $Z^{m-2} \subset N$, if $p|_{p^{-1}(N-Z)}$ is an $\ell$-fold cover, and near $x \in M$ with $p(x) \in Z$, the local model is given by $(x_1, \ldots, x_{m-2}, z) \mapsto (x_1, \ldots, x_{m-2}, z^k$ for some $k \geqslant 1$.

Notice that the local model really determines the fact that the branch set as codimension 2.

**Example.** $\mathbb{S}^2 \to \mathbb{S}^2$, given by rotation: $z \mapsto z^k$. This is bracnhed over the north and south pole. More generally this map can be suspended to give branched covers $\mathbb{S}^n \to \mathbb{S}^n$ which are branched over $\mathbb{S}^{n-2}$.

**Example.** Next we will study double covers of the disk $D^2$, branched over $k$ points.

A double cover is precisely a principal $\mathbb{Z}/2\mathbb{Z}$-bundle. By the associated bundle construction, there is an isomorphism

$$\mathrm{Prin}_{\mathbb{Z}/2\mathbb{Z}}(X) \cong H^1(X; \mathbb{Z}/2\mathbb{Z}).$$

(See my notes of algebraic topology for more on this.) But by the universal coefficient theorem, $H^1(X; \mathbb{Z}/2\mathbb{Z}) \cong \hom(\pi_1(X); \mathbb{Z}/2\mathbb{Z})$. Thus double covers of $D^2 - \{k \text{ points}\}$ are classified by maps $\pi_1(D^2 - \{k \text{ points}\}) \to \mathbb{Z}/2\mathbb{Z}$. In particular we care about the map which is branched over the $k$ points - we want loops around each of the $k$ points to map to 1 in $\mathbb{Z}/2\mathbb{Z}$. This fixes a homomorphism, so there is a unique 2-fold branched cover of $D^2$ over the $k$ points.

What does the topology of this double cover look like? The boundary of the disk is homotopically the product of the loops around the $k$ points. Therefore under the map $\pi_1 \to \mathbb{Z}/2\mathbb{Z}$, the boundary maps to $k$. It follows that the boundary lifts to a single component (under the branched cover) when $k$ is odd, and lifts to two components when $k$ is even.

This does not yet pin down the topology of the double cover - we must know its genus as well. For this we use the *Riemann-Hurwitz formula*. Suppose we triangulate the base

space, and ensure that branch points lie on vertices. Then lifting the triangulation to the branched double cover $\Sigma$ gives that

$$\chi(\Sigma) = \widetilde{v} - \widetilde{e} + \widetilde{f} = (2v - k) - 2e + 2f = 2\chi(D^2) - k = 2 - k.$$

Therefore $\Sigma$ has genus $(k-2)/2$ for $k$ even, and $(k-1)/2$ for $k$ odd.

**Example.** The map $\Sigma \times \mathrm{Sym}^{k-1}(\Sigma) \to \mathrm{Sym}^k(\Sigma)$ is a $k$-fold branched cover, branched over $\Delta$. (The map is defined in the canonical way).

The main result of this section is the *tautological correspondence* which allows us to think about $J$-holomorphic strips as branched covers.

**Theorem 4.2.2.** *There is a correspondence (not necessarily bijective, but canonical) as follows:*

$$\left\{ \begin{array}{c} \textit{(J-holomorphic) immersions} \\ X \hookrightarrow \mathrm{Sym}^k(\Sigma). \end{array} \right\} \rightleftharpoons \left\{ \begin{array}{c} \textit{k-fold branched cover } Y \to X \\ \textit{and (J-holomorphic) map} \\ Y \to \Sigma. \end{array} \right\}$$

**Remark.** Why must the maps on the left be immersions? This insures well-behavedness at the level of the tangent space, which is required to ensure that the local model on the right corresponds to branched covers.

*Proof.* We will ignore the $J$-holomorphic part, but this is easy to verify. (In general if $X \to \mathrm{Sym}^k(\Sigma)$ satisfies property $P$, then $X \to \Sigma$ will satisfy property $P$ etc.)

For the first direction, suppose $X \to \mathrm{Sym}^k(\Sigma)$ is an immersion. There is a canonical $k$-fold branched cover $\Sigma \times \mathrm{Sym}^{k-1}(\Sigma) \to \mathrm{Sym}^k(\Sigma)$ as remarked earlier. The pullback of these two maps defines the space $Y$, along with the map $Y \to X$. On the other hand, there is a projection map $\Sigma \times \mathrm{Sym}^{k-1}(\Sigma) \to \Sigma$, and composing this with the pullback map $Y \to \Sigma \times \mathrm{Sym}^k(\Sigma)$ gives the map $Y \to \Sigma$. See the following diagram:

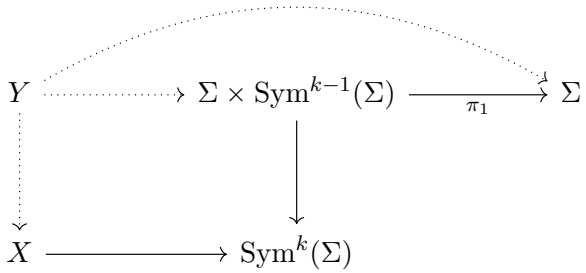


For the second direction, suppose we have a map $f : Y \to \Sigma$ and a $k$-fold branched cover $p : Y \to X$. Then $X \to \mathrm{Sym}^k(\Sigma)$ is defined by $x \mapsto f(p^{-1}(x))$. Nice and easy! $\square$

## 4.3 Topology of $\mathrm{Sym}^g(\Sigma)$; premise 4 (lecture 6)

Using the tautological correspondence, we can study the topology of $\mathrm{Sym}^g(\Sigma)$ and verify that the 4th premise for Lagrangian Floer homology is satisfied. To this end, we start with a lemma:

**Lemma 4.3.1.** $H_1(\mathrm{Sym}^g(\Sigma)) \cong H_1(\Sigma)$.

*Proof.* Fix a basepoint $z \in \Sigma$. Let $i : \Sigma \to \mathrm{Sym}^g(\Sigma)$ be defined by

$$i : x \mapsto \{z, \dots, z, x\}.$$

This induces a map $i_* : H_1(\Sigma) \to H_1(\mathrm{Sym}^g(\Sigma))$. The inverse $j_*$ is provided by the tautological correspondence: let $\mathbb{S}^1 \to \mathrm{Sym}^g(\Sigma)$ represent an element of $H_1(\mathrm{Sym}^g(\Sigma))$. This corresponds to a branched cover $Y \to \mathbb{S}^1$ and a map $Y \to \Sigma$, where $Y$ is some collection of circles. The image of this map is an element of $H_1(\Sigma)$, so the tautological corresponds *is* the map $H_1(\mathrm{Sym}^g(\Sigma)) \to H_1(\Sigma)$. This is indeed the inverse of $i_*$. □

We can now describe the topology of $\mathrm{Sym}^g(\Sigma)$: for any $g$, we have that

$$\pi_1(\mathrm{Sym}^g(\Sigma)) = H_1(\mathrm{Sym}^g(\Sigma)) = H_1(\Sigma) = \mathbb{Z}^{2g}.$$

Similarly, from the tautological correspondence, when $g > 2$

$$\{\mathbb{S}^2 \to \mathrm{Sym}^g(\Sigma)\} \leftrightsquigarrow \left\{\mathbb{S}^2 \leftarrow X^2 \to \Sigma\right\}$$

for some $X^2$ which establishes the same result but for second homology:

$$\pi_2(\mathrm{Sym}^g(\Sigma)) = H_2(\Sigma).$$

**Theorem 4.3.2.** *More generally, by the Dold-Thom theorem,*

$$\pi_i(\mathrm{Sym}^k(X)) \cong H_i(X) \text{ for } k \gg 0.$$

**Corollary 4.3.3.** *Premise 4 is satisfied by* $\mathrm{Sym}^g(\Sigma - z)$. *That is, for all* $A \in \pi_2(M)$ *or* $\pi_2(M, L_i)$, $[\omega](A) = 0$ *(which ensures that in Gromov compactness there is no disk or sphere bubbling - the boundary of the moduli space of strips consists only of broken strips). Here* $M$ *denotes* $\mathrm{Sym}^g(\Sigma - z)$.

*Proof.* We will in fact show that $\pi_2(M)$ and $\pi_2(M, \mathbb{T}_\alpha)$ are trivial. The former is automatically trivial from the above discussion. The second comes from the following long exact sequence:

$$\pi_2(M) = 0 \to \pi_2(M, \mathbb{T}_\alpha) \to \pi_1(\mathbb{T}_\alpha) = \mathbb{Z}^g \hookrightarrow \pi_1(M) = \mathbb{Z}^{2g}.$$

Since the third map is an inclusion, the middle map has trivial image. On the other hand, the first map is the zero map, so by exactness the middle map also has trivial kernel. Therefore the first isomorphism theorem, $\pi_2(M, \mathbb{T}_\alpha)$ is trivial. □

So far we have established that $(\mathrm{Sym}^g(\Sigma - z), \mathbb{T}_\alpha, \mathbb{T}_\beta)$ satisfies premises 1 through 4. To prove that $\widehat{HF}$ is well defined (given a Heegaard diagram), it remains to verify premise 5 and discuss premise 6.

## 4.4 Symplectic energy bounds for $\mathbb{Q}H\mathbb{S}^3$s; premise 5

The next goal is to prove that

$$E(\ker(\widehat{\pi}_2(x,x) \xrightarrow{\mu} \mathbb{Z}))$$

is bounded. This is the 5th premise to ensure that Lagrangian Floer homology "makes sense". In this section we will derive a topological condition which ensures that the energy is bounded - namely for $Y^3$ a rational homology sphere (a $\mathbb{Q}H\mathbb{S}^3$). Later we will study the more general case with positive first Betti number.

The careful reader will say "hey what's $\widehat{\pi}_2(x,x)$? We haven't even defined this!" In general, everything with a hat will denote the analogue of the unhatted version of a concept (from $\mathrm{Sym}^g(\Sigma)$) applied to $\mathrm{Sym}^g(\Sigma - z)$.

**Definition 4.4.1.** Let $x, y \in \mathbb{T}_\alpha \cap \mathbb{T}_\beta$. Then

$$\pi_2(x,y) = \{\text{homotopy classes of strips in } \mathrm{Sym}^g(\Sigma)\},$$

while

$$\widehat{\pi}_2(x,y) = \{\text{homotopy classes of strips in } \mathrm{Sym}^g(\Sigma - z)\}.$$

Let $S(Y)$ denote the equivalence classes

$$x \sim y \quad \Leftrightarrow \quad \widehat{\pi}_2(x,y) \neq \varnothing.$$

Recall that the Floer chain complex $CF_*$ is generated by points in $\mathbb{T}_\alpha \cap \mathbb{T}_\beta$, and by partitioning with respect to the above equivalence relation, we have a decomposition

$$CF_*(Y) = \bigoplus_{s \in S(Y)} CF_*(Y,s),$$

where $CF_*(Y,s)$ is the chain complex generated by restricting only to the points in $s$. This induces a decomposition

$$\widehat{HF}(Y) = \bigoplus_{s \in S(Y)} \widehat{HF}(Y,s).$$

To better understand $S(Y)$, we introduce the following path spaces:

- $\Omega(\mathbb{T}_\alpha, \mathbb{T}_\beta) \coloneqq \{\gamma : [0,1] \to \mathrm{Sym}^g(\Sigma) : \gamma(0) \in \mathbb{T}_\alpha, \gamma(1) \in \mathbb{T}_\beta\}$.
- $\widehat{\Omega}(\mathbb{T}_\alpha, \mathbb{T}_\beta) \coloneqq \{\gamma : [0,1] \to \mathrm{Sym}^g(\Sigma - z) : \gamma(0) \in \mathbb{T}_\alpha, \gamma(1) \in \mathbb{T}_\beta\}$.

Given this terminology, we have

$$S(Y) = \pi_0(\widehat{\Omega}(\mathbb{T}_\alpha, \mathbb{T}_\beta)), \quad \text{If } x \sim y, \text{ then } \widehat{\pi}_2(x,y) \cong \widehat{\pi}_2(x,x) \cong \pi_1(\widehat{\Omega}(\mathbb{T}_\alpha, \mathbb{T}_\beta)).$$

The question is then: what is the topology of $\widehat{\Omega}(\mathbb{T}_\alpha, \mathbb{T}_\beta)$? This can be understood from the following Serre fibrtion:

$$\Omega(\mathrm{Sym}^g(\Sigma - z)) \to \widehat{\Omega}(\mathbb{T}_\alpha, \mathbb{T}_\beta) \to \mathbb{T}_\alpha \times \mathbb{T}_\beta,$$

where the first space is the loop space (and the map an inclusion), while the second map is $\gamma \mapsto (\gamma(0), \gamma(1))$. Using this fibration, the following identities can be computed:

**Proposition 4.4.2.**

$$\begin{aligned} S(Y) &\cong \pi_0(\widehat{\Omega}(\mathbb{T}_\alpha, \mathbb{T}_\beta)) \cong H_1(Y) \cong H^2(Y) \\ &\cong \pi_0(\Omega(\mathbb{T}_\alpha, \mathbb{T}_\beta)). \\ \widehat{\pi_2}(x, y) &\cong \pi_1(\widehat{\Omega}(\mathbb{T}_\alpha, \mathbb{T}_\beta)) \cong H^1(Y) \cong H_2(Y). \\ \pi_2(x, y) &\cong \pi_1(\Omega(\mathbb{T}_\alpha, \mathbb{T}_\beta)) \cong H^1(Y) \oplus \mathbb{Z}. \end{aligned}$$

This proposition tells us how the topology of our 3-manifold $Y$ can help control the spaces $\widehat{\pi}_2(x, y)$ and $S(Y)$, which in turn affects the Maslov indices of the spaces and hence the energy. Therefore we might hope to use this knowledge to at least give some conditions for when $E(\ker(\mu))$ is bounded! This is indeed the case - we now have a small interlude to dicuss closed oriented 3-manifolds.

Let $Y$ be a closed connected oriented 3-manifold. What can we say about its homology? We automatically have that $H_0(Y) = \mathbb{Z}$ by connectedness and $H_3(Y) = \mathbb{Z}$ by orientability. By Poincaré duality, this also gives $H^0(Y) = H^3(Y) = \mathbb{Z}$. This leaves $H_1(Y) = H^2(Y) = \mathbb{Z}^{b_1} \oplus \text{Torsion}, \quad H^1(Y) = H_2(Y) = \mathbb{Z}^{b_1}$.

- Homologically, the simplest closed connected oriented 3-manifolds satisfy $H_1(Y) = 0$, and this is enough to ensure that $Y$ is an *integral homology sphere*, i.e. a $\mathbb{Z}H\mathbb{S}^3$.
- A slightly weaker condition is to assume that the first Betti number vanishes, i.e. $H^1(Y) = 0$. This does *not* ensure that $H_1(Y; \mathbb{Z})$ vanishes, as it might have torsion. However, the rational first homology vanishes. Therefore such a $Y$ is called a *rational homology sphere*, or a $\mathbb{Q}H\mathbb{S}^3$.
- Finally if we remove restrictions on the first Betti number, we get to the general case of all closed connected oriented 3-manifolds.

**Theorem 4.4.3.** *Given a Heegaard diagram for a rational homology sphere $Y$, the hatted Heegaard Floer homology $\widehat{HF}(Y)$ is well defined. (More precisely, the corresponding $(\mathrm{Sym}^g(\Sigma, \mathbb{T}_\alpha, \mathbb{T}_\beta))$ satisfy premise 5, which is the last remaining premise to ensure that Lagrangian Floer homology is well defined.)*

Note that premise 6 is required for integral Heegaard Floer homology, but everything can be carried out in $\mathbb{Z}/2\mathbb{Z}$ if we with to gloss over the 6th premise.

*Proof.* Since $Y$ is a rational homoloy sphere, $S(Y) = H_1(Y)$ is a finite group. Moreover, $\widehat{\pi_2}(x,x) \cong H^1(Y)$ which vanishes. Therefore the maps $\mu : \widehat{\pi}_2(x,x) \to \mathbb{Z}$ automatically have trivial kernel! Thus $E(\ker \mu) = 0$, and in particular the energy is bounded. It follows that premise 5 is satisfied. □

Moreover, recall that $\widehat{HF}(Y,s)$ is $\mathbb{Z}/N\mathbb{Z}$-graded, where $N\mathbb{Z}$ is the image of the Maslov grading map $\mu : \widehat{\pi}_2(x,x) \to \mathbb{Z}$. Since the domain vanishes, this has trivial image, so $N\mathbb{Z} = 0$. Thus each $\widehat{HF}(Y,s)$ is $\mathbb{Z}$-graded. It follows that $\widehat{HF}(Y) = \bigoplus_{s \in S(Y)} \widehat{HF}(Y,s)$ is $\mathbb{Z}$-graded.

Now that we know that $\widehat{HF}(Y)$ is well defined (for a fixed Heegaard diagram, and for $Y$ a rational homology sphere), we can look at some examples.

**Example.** Suppose $Y$ is an honest 3-sphere. Then the standard Heegaard diagram has a single intersection between the two Lagrangian tori, and $S(Y)$ is a single point. This gives $\widehat{HF}(\mathbb{S}^3) = \mathbb{Z}$.

**Example.** Next suppose $Y$ is the lens space $L(p,1)$. Then the standard Heegaard diagram has $|S(Y)| = |H_1(Y)| = p$, since the first homology of the lens space is $H_1(L(p,1)) = \mathbb{Z}/p\mathbb{Z}$. This gives

$$\widehat{HF}(Y) = \bigoplus_{s \in S(Y)} \widehat{HF}(Y,s),$$

but each of these summands is generated by a single intersection point! Therefore (recalling the first example from Lagrangian Floer homology), we have

$$\widehat{HF}(Y) = \bigoplus_{p} \mathbb{Z} = \mathbb{Z}^p.$$

## 4.5 Spin and Spin$^c$ structures; premise 6

The final premise that requires addressing is premise 6: spin$^c$ structures. These are used to induce orientations on the moduli space of $J$-holomorphic strips, to allow for signed counts (which gives integral Heegaard Floer homology instead of just $\mathbb{Z}/2\mathbb{Z}$ homology).

Let $M^m$ be a Riemannian manifold. The associated bundle construction gives a principal $\mathrm{SO}(m)$-bundle, called the frame bundle, over $M$:

$$\begin{array}{ccc} TM & \dashrightarrow & Fr(M) \\ & & \downarrow \\ & & M \end{array}$$

The fibre of this bundle above a point $p$ is an oriented orthonormal frame of $T_pM$. For $m \geqslant 3$, $\pi_1(\mathrm{SO}(m)) = \mathbb{Z}/2\mathbb{Z}$, so that $\mathrm{SO}(m)$ admits a 2-fold (universal) cover called $\mathrm{Spin}(m)$.

**Definition 4.5.1.** A *spin structure* is a lift of the frame bundle to a prinipal $\mathrm{Spin}(m)$-bundle.

More specifically, it's a bundle $S$ as in the following diagram:

$$\begin{array}{ccccc} \mathrm{Spin}(m) & \longrightarrow & S & & \\ \downarrow & & \downarrow & & \\ \mathrm{SO}(m) & \longrightarrow & Fr(M) & \longrightarrow & M \end{array}$$

Spin structures on Lagrangians induce orientations on the moduli space of $J$-holomorphic curves. Therefore if there is a spin structures over Lagrangians, Lagrangian Floer homology is well defined over $\mathbb{Z}$. For Heegaard Floer homology, our Lagrangians are tori. These have trivial tangent bundles! Therefore spin structures exist as required, and in fact there are $2^g$ choices. Recall that $\widehat{HF}(\mathbb{S}^1 \times \mathbb{S}^2)$ was either $\mathbb{Z}^2$ or $\mathbb{Z}/2\mathbb{Z}$ depending on the choice of orientation, i.e. the choice of spin structure on the Lagrangian tori. A convention is fixed by the following theorem due to Ozsváth and Szabó:

**Theorem 4.5.2.** *Fix $Y^3$ and choose a Heegaard diagram. There is a canonical choice of spin strucutre such that $\widehat{HF}$ is invariant under handleslides and stabilisations, such that $\widehat{HF}(\mathbb{S}^1 \times \mathbb{S}^2) = \mathbb{Z}^2$.*

Although spin structures do not always exist, a slightly less restrictive lift of the frame bundle is something called a *spin$^c$ structure*. These are explored in the 4-manifolds class from Spring 2020, as they are crucial in defining the Seiberg-Witten invariants.

**Definition 4.5.3.** A *spin$^c$ structure* is a lift of $Fr(M)$ to a principal $\mathrm{Spin}^c(m)$-bundle, where

$$\mathrm{Spin}^c(M) := \mathrm{Spin}(m) \times_{\mathbb{Z}/2\mathbb{Z}} \mathbb{S}^1 = \mathrm{Spin}(m) \times \mathbb{S}^1/(a,b) \sim (-a,-b).$$

There is a natural map $\mathrm{Spin}^c(m) \to \mathrm{Spin}(m)/(\mathbb{Z}/2\mathbb{Z}) = \mathrm{SO}(m)$.

**Theorem 4.5.4.** *We will not prove these, but the following results about spin$^c$ structures hold:*

1. *All oriented 3 and 4 manifolds admit spin$^c$ structures.*
2. *Let $\mathrm{Spin}^c(M)$ denote the space of spin$^c$ structures on a manifold $M$. If this is non-empty, then it is an* affine space *over $H^2(M;\mathbb{Z})$. (This means the* difference *of two spin$^c$ structures is a well defined element of $H^2(M;\mathbb{Z})$.*
3. *There is a map $c_1 : \mathrm{Spin}^c(M) \to H^2(M;\mathbb{Z})$ such that*

$$c_1(s+a) = c_1(s) + 2a, \quad a \in H^2(M;\mathbb{Z}).$$

*The map $c_1$ comes from the first Chern class.*

4. *If a 3-manifold has no 2-torsion in $H_1 \cong H^2$, then $c_1$ is injective. Therefore there is a canonical identification*

$$\mathrm{Spin}^c(M) \xrightarrow{c_1/2} H^2(M) \cong H_1(M).$$

Recall from earlier that

$$S(Y) = \pi_0(\Omega(\mathbb{T}_\alpha, \mathbb{T}_\beta)) = \pi_0(\widehat{\Omega}(\mathbb{T}_\alpha, \mathbb{T}_\beta)) \cong H_1(Y).$$

Combining this with the above result, we have $S(Y) \cong \mathrm{Spin}^c(Y)$.

We also showed earlier that $\widehat{HF}(Y, s)$ is $\mathbb{Z}/N\mathbb{Z}$-graded, where $N\mathbb{Z}$ is the image of $\mu : \widehat{\pi}_2(x, x) \to \mathbb{Z}$. It turns out that the image of this map can be detected without reference to the Maslov index: for $s \in S(Y)$, let $\mu_s : H^1(Y) \to \mathbb{Z}$ be defined by $\mu_s(h) = (c_1(s) \smile h)[Y]$. This map corresponds to the Maslov index via the above isomorphism! Therefore if

$$\delta(s) := \gcd(\mu_s(h) : h \in H^1(Y)),$$

then $\widehat{HF}(Y, s)$ is $\mathbb{Z}/\delta(s)\mathbb{Z} - graded$.

**Example.** Let $Y$ be a $\mathbb{Q}H\mathbb{S}^3$. Then $H^1$ vanishes, so by the above discussion $\delta(s) = 0$ and $\widehat{HF}$ is $\mathbb{Z}$-graded.

**Example.** Suppose $b_1 = 1$, so that $H^1(Y) = \mathbb{Z}$. Suppose further that there is no 2-torsion in $H_1$, so that $\mathrm{Spin}^c(M) \cong H_1(M)$. Then $s \in S(Y)$ is determined by $c_1(s) \in 2\mathbb{Z}$, and $\delta(s) = c_1(s)$. It follows that

- if $c_1(s) = 0$, then $\widehat{HF}$ is $\mathbb{Z}$-graded. (Best case scenario.)
- If $c_1(s) = \pm 2$, then the homology is $\mathbb{Z}/2\mathbb{Z}$-graded. (Worst case.)
- If $c_1(s) = \pm 4$, then the homology is $\mathbb{Z}/4\mathbb{Z}$-graded and so on.

We have now established many of the necessary results to show that Heegaard Floer homology is well defined (for a fixed Heegaard diagram). Two things remain:

1. Investigating premise 4, boundedness of energy, in the case $b_1(Y) > 0$.
2. Investigating $HF^{\pm}$, which is the other type of Heegaard Floer homology we briefly introduced.

## 4.6 Energy bounds more generally; premise 5 (lecture 7)

Recall that for the Lagrangian Floer homology $HF(L_0, L_1)$ to be well defined, we require $E(\ker \mu)$ to be bounded, where $\mu : \pi_2(x, x) \to \mathbb{Z}$ is the Maslov grading. In the context of Heegaard Floer homology, we've shown that this result trivially holds if the 3-manifold has trivial first Betti number, but we have yet to explore the general case.

We again make use of the tautological correspondence. A $J$-holomorphic strip $u : D^2 \to \mathrm{Sym}^g(\Sigma)$ corresponds to a branched cover $S \to D^2$ and some map $\widetilde{u} : S \to \Sigma$, for some $S$. (Recall that we classified branched covers over disks in an earlier lecture!)

**Definition 4.6.1.** The *domain* of $u$, $D(u)$, is defined to be the image of $\widetilde{u}$ interpreted as a 2-chain in $\Sigma$. We can further write

$$D(u) = \sum a_i R_i, a_i \in \mathbb{Z},$$

where the $R_i$ (called "regions") are connected components of $\Sigma - \bigcup_i \alpha_i - \bigcup_i \beta_i$.

One can observe that all regions of a Heegaard diagram are planar! It turns out that $D(u)$ depends only on the homotopy class of $u$, $[u] \in \pi_2(x, y)$. Therefore there is a well defined map

$$\pi_2(x, y) \to \{\mathbb{Z} - \text{linear combinations of regions}\}.$$

Precisely, the map is defined by

$$\varphi \mapsto D(u), u \in \varphi, \quad D(u) = \sum n_{z_i}(\varphi) R_i, z_i \in R_i, n_{z_i}(\varphi) \coloneqq \#(\varphi \cdot [\mathrm{Sym}^{g-1}(\Sigma) \times \{z_i\}]).$$

In the hatted version $\widehat{\pi}_2(x, y)$, the coefficient of the region containing $z$ is 0.

Each region has a boundary consisting of segments of curves from the Heegaard diagram. Under the branched cover, each region descends to a $J$-holomorphic strip. Lifts of the edges $\mathbb{T}_\alpha \cap u(D^2)$ and $\mathbb{T}_\beta \cap u(D^2)$ determine the $\alpha$ and $\beta$ edges of $D(u)$. Similarly, lifting the $x$ and $y$ vertices from the strip determines $x_i$ and $y_i$ intersections (corners) of $D(u)$.

More precisely, we can write $\partial D(\varphi) = \partial_\alpha D(\varphi) \cup \partial_\beta D(\varphi)$, decomposing the boundary into $\alpha$ and $\beta$ curves. The boundaries of these curves are exactly the "corners", and we have $\partial(\partial_\alpha D(\varphi)) = \partial(\partial_\beta D(\varphi))$. Moreover, in terms of singular homology, these are equal to $\sum y_i - \sum x_i$.

**Definition 4.6.2.** A domain is *periodic* if $\partial D(\varphi)$ is a sum of whole $\alpha$ and $\beta$ curves.

If $\partial D(\varphi)$ is a sum of whole $\alpha$ curves and $\beta$ curves, then $\partial(\partial_\alpha D(\varphi))$ and $\partial(\partial_\beta D(\varphi))$ must vanish. This happens when the $y_i$ and $x_i$ are equal, i.e. when $x = y$. That is, periodic domains are domains corresponding to $\varphi \in \pi_2(x, x)$.

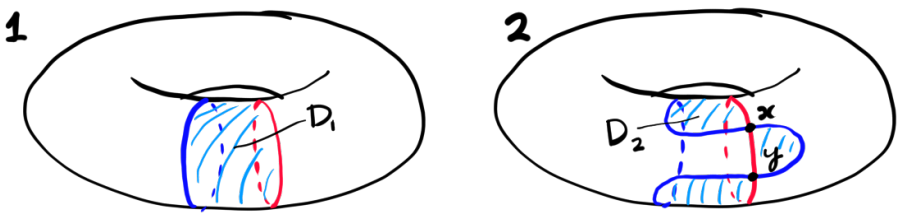


**Example.**

Figure 4.1: Examples of periodic domains.

Figure 4.1 shows two examples of periodic domains. Recall that these are Heegaard diagrams of $\mathbb{S}^1 \times \mathbb{S}^2$, and they have different Lagrangian (Heegaard) Floer homologies. In the diagram on the left, we have fixed a domain $D_1$. This is evidently a periodic domain, since it is bound by one whole $\alpha$ curve and one whole $\beta$ curve. Its boundary is $\partial D_1 = \alpha - \beta$.

In the second example, our $\alpha$ and $\beta$ curves are crossing! This gives two regions. We can give one region a positive sign and the other a negative sign. Then the resulting domain once again is periodic, with $\partial D_2 = \alpha - \beta$.

Recall that our aim is to understand when the symplectic energy is bounded, to ensure that Heegaard Floer homology is well defined. More precisely, we are interested in $\widehat{\pi}_2(x,x) \subset \pi_2(x,x)$, which consists of strips in $\mathrm{Sym}^g(\Sigma - \{z\})$, or equivalently strips $\varphi$ in $\mathrm{Sym}^g(\Sigma)$ with $n_z(\varphi) = 0$. Then we require the kernel of the Maslov grading $\mu : \widehat{\pi}_2(x,x) \to \mathbb{Z}$ to have bounded energy: $E(\ker \mu)$ must be bounded. Recall that if $u$ is a $J$-holomorphic strip in $\ker \mu$, its energy is defined by $E(u) = \int u^* \omega$. To say that $E(\ker \mu)$ is bounded, is to say that $\{E(u) : u \in \ker \mu\}$ is bounded.

Before proceeding, we again introduce some notation!

**Definition 4.6.3.** The set of periodic domains forms an abelian group (as it is a subgroup of the singular 2-chains). This is denoted by $\Pi$. The periodic domains $D$ with $n_z(D) = 0$ are denoted by $\widehat{\Pi}$.

**Proposition 4.6.4.** For any $x$, $\pi_2(x,x) \cong \Pi$ and $\widehat{\pi}_2(x,x) \cong \widehat{\Pi}$. Therefore $H^1(Y) \oplus \mathbb{Z} \cong \Pi$ and $H^1(Y) \cong \widehat{\Pi}$. (Here $Y$ is the 3-manifold for which we consider a Heegaard diagram and so on.)

*Proof.* The map $\widehat{\pi}_2(x,x) \to \widehat{\Pi}$ is given by $\varphi \mapsto D(\varphi)$. Since $\widehat{\pi}_2(x,x) = H^1(Y) = \ker\{\langle \alpha_1, \ldots, \alpha_g \rangle \oplus \langle \beta_1, \ldots, \beta_g \rangle \to H_1(\Sigma)\}$, any $\varphi \in \widehat{\pi}_2(x,x)$ arises from a linear combination of $\alpha$ and $\beta$ curves that bound a 2-chain, i.e. a periodic domain. This gives the inverse map. □

**Example.** If $Y$ is a rational homology sphere, then $\widehat{\Pi} = 0$. If $Y$ is $\mathbb{S}^1 \times \mathbb{S}^2$, then $\widehat{\Pi} = \mathbb{Z}$.

We are finally ready to talk about energy! As mentioned above, we have that

$$E(u) = \int u^*\omega, \quad \omega \text{ is an approximation to } \mathrm{Sym}^g(dA).$$

Therefore it suffices to bound $\int u^*(\mathrm{Sym}^g(dA))$, which is just the area of $D(u)$. If any of the areas of $D(u)$ are non-zero, then taking linear combinations, the set of periodic domains will have unbounded energy. Therefore for Heegaard Floer homology to be well defined, naively the best we can do is to ensure that all periodic domains have *zero* area!

**Definition 4.6.5.** A Heegaard diagram is *weakly admissible* if there exists an area form on $\Sigma$ such that all periodic domains $D$ (with $n_z(D) = 0$) have area 0.

We can make the following observations:

- If a Heegaard diagram is weakly admissible, then $\widehat{HF}$ is well defined. (In fact, this is the *only* condition we need for $\widehat{HF}$ to be well defined for a Heegaard diagram of a closed connected oriented 3-manifold, as the other premises 1 through 4 didn't have any restrictions!)
- If $\widehat{\Pi} = 0$, then any Heegaard diagram is weakly admissible. (These are exactly $\mathbb{Q}H\mathbb{S}^3$s.
- A diagram is weakly admissible if and only if every non-zero periodic domain with $n_z = 0$ admits a region with positive multiplicity and one with negative multiplicity.

**Example.** In figure 4.1, the first diagram is not weakly admissible, but the second diagram is! Notice that the weakly admissible diagram was obtained by isotoping the $\alpha$ and $\beta$ curves from an arbitrary (non-weakly admissible) diagram.

Now the important question is whether or not weakly admissible Heegaard diagrams are abundant for 3-manifolds, or if this is a significant restriction. Fortunately, they exist! And in some sense, they are all equivalent! This is captured in the following two theorems of Ozsváth and Szabó, which we will not prove. (If I recall correctly, these proofs took like a hundred pages!)

**Proposition 4.6.6.** Every Heegaard diagram can be made weakly admissible by isotopies of $\alpha$ and $\beta$ curves.

**Proposition 4.6.7.** Any two weakly admissible diagrams can be related by a sequence of Heegaard moves (i.e. isotopies, handleslides, and stabilisations), so that every intermediate diagram is also weakly admissible.

In summary we have the following huge conclusion!

**Theorem 4.6.8.** *Let $Y$ be a closed connected oriented 3-manifold. Then $\widehat{HF}(Y)$ is well defined (for a fixed weakly admissible Heegaard diagram). It remains to check invariance under weakly admissible Heegaard moves (which does turn out to hold).*

Assuming invariance under weakly admissible Heegaard moves, we are now finally ready to compute Heegaard Floer homology of an arbitrary closed connected oriented 3-manifold! As an example, we will compute the Heegaard Floer homology of $\mathbb{S}^1 \times \mathbb{S}^2$.

**Example.** Let $Y = \mathbb{S}^1 \times \mathbb{S}^2$. Consider the Heegaard diagram shown in the right, in figure 4.1. This is a weakly admissible diagram, so we can use it to compute Heegaard Floer homology. As computed in an earlier example, we have $\partial y = 0$ automatically, and $\partial x = y - y = 0$ by convention. This gives

$$\widehat{CF} = \widehat{HF} = \mathbb{Z} \oplus \mathbb{Z} = H_*(\mathbb{S}^1).$$

We will now aim to understand this a little better, by computing the summands

$$\widehat{HF}(Y) = \bigoplus_{s \in \mathrm{Spin}^c(Y)} \widehat{HF}(Y, s).$$

Recall that there is an isomorphism

$$\mathrm{Spin}^c(Y) \to H^2(Y) \cong \mathbb{Z}, \quad s \mapsto c_1(s)/2,$$

because $H_1$ has no 2-torsion. Since $x \sim y$, only one of the spin$^c$ structures is "seen" in the diagram - in general, $\widehat{HF}(Y, s) = 0$ for all but finitely many $s$ since there are only finitely many intersection points. In our case, $\widehat{HF}(Y, s)$ is non-zero for all but one $s$ - so which one is this?

Recall that $\widehat{HF}(Y, s)$ is $\mathbb{Z}/2s\mathbb{Z}$-graded, where $2s\mathbb{Z}$ is the image of $\mu : \hat{\pi}_2(x, x) \to \mathbb{Z}$. In our case, there are two regions $D_1$ and $D_2$ so that the domain shown in the diagram is $D_1 - D_2$. This gives

$$\hat{\pi}_2(x, x) = \{n(D_1 - D_2) : n \in \mathbb{Z}\},$$

but $\mu(D_1 - D_2) = \mu(D_1) - \mu(D_2) = 1 - 1 = 0$. Therefore $2s\mathbb{Z} = 0$, and hence $s = 0$. This tells us that

$$\widehat{HF}(\mathbb{S}^1 \times \mathbb{S}^2, s) = \begin{cases} H_*(\mathbb{S}^1) & s = 0 \\ 0 & \text{otherwise.} \end{cases}$$

We will outline a proof of invariance of Heegaard Floer homology under weakly admissible Heegaard moves, but before this we will investigate some other versions of Heegaard Floer homology, most notably $HF^{\pm}$.

## 4.7 Different versions of H.F. homology: $HF^\infty, HF^\pm$.

Two of the most useful versions of Heegaard Floer homology are $HF^+$ and $HF^-$. To define these, we first must define $HF^\infty$. This is similar to $\widehat{HF}$, but instead of killing everything near the basepoint of the Heegaard diagram, it keeps track of details at the basepoint.

Recall that $\widehat{HF}$ is the Lagrangian Floer homology of $\mathbb{T}_\alpha$ and $\mathbb{T}_\beta$ in $\mathrm{Sym}^g(\Sigma - z)$, i.e. the Lagrangian Floer homology of $\mathbb{T}_\alpha$ and $\mathbb{T}_\beta$ in $\mathrm{Sym}^g(\Sigma)$ restricted to strips with $n_z(\varphi) = 0$.

More generally, for an arbitrary $\varphi \in \pi_2(x, y)$, we need not have that $n_z(\varphi) = 0$, but instead $n_z(\varphi) \geqslant 0$.

**Definition 4.7.1.** $CF^\infty$ is the free $\mathbb{Z}[U, U^{-1}]$-module generated by $\mathbb{T}_\alpha \cap \mathbb{T}_\beta$. This admits a Maslov grading (in the same way as $CF$). This forms a chain complex by the boundary maps

$$\partial^\infty x = \sum_y \sum_{\varphi \in \pi_2(x,y), \mu(\varphi)=1} \#(\mathcal{M}(\varphi)/\mathbb{R}) U^{n_z(\varphi)} y.$$

The homology of this chain complex is denoted by $HF^\infty(Y)$, and is a $\mathbb{Z}[U, U^{-1}]$-module.

To make sure this is well defined, we must verify that $(\partial^\infty)^2 = 0$. This is true because additivity of $n_z$ ensures that $U^{n_z(\varphi \# \psi)} = U^{n_z(\varphi)} U^{n_z(\psi)}$. Then the result follows from the fact that $\partial^2 = 0$, where $\partial$ denotes the boundary map from $CF$ (used to define $\widehat{HF}$).

Is this really well defined? Are we satisfying the premises for Lagrangian Floer homology?

- We must check premise 4: can we prevent bubbling of $J$-holomorphic strips?
- Premise 5: is the symplectic energy bounded?

Recall that $\pi_2(x, x) = \pi_2(\mathrm{Sym}^g(\Sigma)) = H_2(\Sigma) = \mathbb{Z}$. Since this does not vanish, there could exist sphere and disk bubbles on the boundary of the moduli space of $J$-holomorphic strips! This is taken care of by a theorem of Ozsváth and Szabó:

**Theorem 4.7.2.** *$J$-holomorphic spheres appear with Maslov index at least 2 - they do not destroy $(\partial^\infty)^2 = 0$. $J$-holomorphic disks appear, but cancel out in pairs (their signed counts are zero).*

What about energy? We need $E(\ker \mu)$ to be bounded. Recall that $\Pi = \pi_2(x, x) = H^1(Y) \oplus \mathbb{Z} = \widehat{\Pi} \oplus \langle \Sigma \rangle$, where $\Sigma$ is a periodic domain with $n_z(\varphi) = 1$. Since $\mu$ on $\widehat{\pi}_2(x, x) = \widehat{\Pi}$ is bounded, it remains to see what happens on $\Sigma$. It turns out that $\mu(\Sigma) = 2$ (which we will show later). Therefore the kernel of $\mu$ on *just* $\Sigma$ is trivial (and thus has bounded energy). However, the kernel of $\mu$ on $\widehat{\Pi} \oplus \langle \Sigma \rangle$ consists of linear combinations of things that might be non-vanishing in either summand, so there is work to do.

That being said, in principle the $\Sigma$ term does not contribute to the differentials: We really only care about $\varphi$ with $\mu(\varphi) = 1$, but we have

$$\mu(\varphi + n\Sigma) = 1 + 2n \neq 1$$

for $n \neq 0$. Therefore the differentials ignore $\Sigma$ in some sense. This is a bit vague, but formally Ozsváth and Szabó deal with the problem by introducing a notion of *strongly admissible Heegaard diagrams* which ensures that $E(\ker \mu)$ is bounded.

Finally, how do we grade $HF^\infty$? It was remarked earlier that it inherits a grading from the Maslov grading akin to $\widehat{HF}$, but we must also describe how $U^k$ interacts with the grading. Suppose $\mu(\varphi) = 1$, and $\partial^\infty x$ contains $U^k y$ (i.e. $n_z(\varphi) = k$). Then

$$\mu(\varphi - k[\Sigma]) = 1 - 2k, \quad n_z(\varphi - k[\Sigma]) = 0, \varphi - k[\Sigma] \in \widehat{\pi}_2(x, y).$$

The first equality comes from $\mu(\Sigma) = 2$. We want the grading of $x$ to be equal to 1 more than the grading of $U^k y$. Therefore we set $\mathrm{gr}(U) = -2$ to cancel out the $2k$ appearing above. Now $\mathbb{T}_\alpha \cap \mathbb{T}_\beta$ will be graded by $\mathbb{Z}/\delta(s)\mathbb{Z}$ (as was $\widehat{HF}$), with $\mathrm{gr}(U^k x) = \mathrm{gr}(x) - 2k$.

In summary, we have a well defined version of Heegaard Floer homology,

$$HF^\infty(Y) = \bigoplus_{s \in \mathrm{Spin}^c(Y)} HF^\infty(Y, s),$$

where the summands on the right are $\mathbb{Z}/\delta(s)\mathbb{Z}$-graded.

**Remark.** If we ignore $U$, since $\mu(\Sigma) = 2$, (and the grading is determined by the image of the Maslov grading map), the right side would only be $\mathbb{Z}/2\mathbb{Z}$ graded.

The real question is, is this version of Heegaard Floer homology interesting? Remarkably, it's totally not interesting!

**Theorem 4.7.3** (Lidman)**.** *$HF^\infty(Y)$ is determined by (the cup product on) $H^*(Y)$.*

However, we can use it define $HF^+$ and $HF^-$, which are genuinely interesting versions of Heegaard Floer homology.

**Definition 4.7.4.** Recall that $CF^\infty$ is the free $\mathbb{Z}[U, U^{-1}]$-module generated by $x \in \mathbb{T}_\alpha \cap \mathbb{T}_\beta$. We define $CF^- \subset CF^\infty$ to be the free $\mathbb{Z}[U]$-module generated by $Ux$, $x \in \mathbb{T}_\alpha \cap \mathbb{T}_\beta$. That is, it is the subset consisting of only positive powers of $U$. We further define $CF^+ = CF^\infty/CF^-$, i.e. this consists only of the non-postive powers of $U$. The corresponding homologies are denoted by $HF^-$ and $HF^+$ respectively.

There is evidently a short exact sequence

$$0 \to CF^- \to CF^\infty \to CF^+ \to 0.$$

This means there is a long exact sequence in homology!

$$\cdots \to HF^-_*(Y) \to HF^\infty_*(Y) \to HF^+_*(Y) \to \cdots.$$

Even though $HF^\infty$ is boring in the sense that we can compute it from $H^*$, it can help us understand $HF^-$ and $HF^+$ via this exact triangle!

**Example.** Consider $\mathbb{S}^3$ with the standard genus 1 Heegaard diagram. (That is, the $\alpha$ curve is a meridian and the $\beta$ curve is a longitude of the torus.) Then $\widehat{HF} = \mathbb{Z}, HF^\infty = \mathbb{Z}[U, U^{-1}], HF^- = \mathbb{Z}[U]$, and $HF^+ = \mathbb{Z}[U, U^{-1}]/\mathbb{Z}[U]$. This can expressed in a diagram which shows the grading:

| | | $HF^-$ | $HF^\infty$ | $HF^+$ |
|---|---|---|---|---|
| Grading | 4 | | $U^{-2}x$ | $U^{-2}x$ |
| | 2 | | $U^{-1}x$ | $U^{-1}x$ |
| | 0 | | $x$ | $x$ |
| | -2 | $Ux$ | $Ux$ | |
| | -4 | $U^2x$ | $U^2x$ | |
| | -6 | $U^3x$ | $U^3x$ | |

We can make some comments:

- $\widehat{HF}$ has less information than $HF^+, HF^-$ but it suffices for most 3 dimensional applications.
- $HF^\pm$ are needed for 4-manifold invariants.
- $HF^\infty$ gives you some information about $HF^+, HF^-$.

In fact, we see that $\widehat{CF} = CF^-/U$. Therefore we have a short exact sequence

$$0 \to CF^- \xrightarrow{U} CF^- \to \widehat{CF} \to 0.$$

Therefore there is a long exact sequence

$$\cdots \to \widehat{HF} \to HF^- \xrightarrow{U} HF^- \to \cdots.$$

Similarly, there is a long exact sequence

$$\cdots \to \widehat{HF} \to HF^+ \xrightarrow{U} HF^+ \to \cdots.$$

In fact, either of these long exact sequences determines a short exact sequence

$$0 \to \operatorname{coker} U \to \widehat{HF} \to \ker U \to 0,$$

which tells us that (over a field), $\widehat{HF} = \ker U \oplus \operatorname{coker} U$.

## 4.8 The degree of $U$ in $CF^\infty$ (lecture 8)

In the previous lecture, we mentioned that

$$\mu(\Sigma) = 2$$

where $\Sigma$ is interpreted as a domain in $\pi_2(x,x)$, and $\mu$ is the Maslov index of $\Sigma$. This was used to justify that $\mathrm{gr}(U) = -2$. We will briefly re-derive that $\mathrm{gr}(U)$ should be $-2$, assuming $\mu(\Sigma) = 2$. Let $x, y \in \mathbb{T}_\alpha \cap \mathbb{T}_\beta$, and define $\mathrm{gr}(x,y) = \mu(\varphi)$ where $\varphi \in \widehat{\pi}_2(x,y)$, i.e. $\varphi \in \pi_2(x,y)$ and $n_z(\varphi) = 0$. Similarly define $\mathrm{gr}(x,Uy) = \mu(\psi)$, where $\psi \in \pi_2(x,y)$ and $n_z(\psi) = 1$. Then the corresponding domains differ by $\Sigma$:

$$D(\psi) = D(\varphi) + \Sigma \quad \Rightarrow \quad \mu(\psi) = \mu(\varphi) + \mu(\Sigma) = \mu(\varphi) + 2.$$

Therefore $\mathrm{gr}(x,y) - gr(x,Uy) = -2$. But using the induced relative gradings on $x, y$, and $Uy$, this means that $\mathrm{gr}(x) - \mathrm{gr}(y) - \mathrm{gr}(x) + \mathrm{gr}(Uy) = -2$, so $\mathrm{gr}(Uy) - \mathrm{gr}(y) = -2$. This is what we wanted to show.

So how do we determine that $\mu(\Sigma) = 2$? We will use the *Lipshitz formula*.

**Theorem 4.8.1.** *Let the ambient space be* $\mathrm{Sym}^g(\Sigma)$*, and let* $\varphi \in \pi_2(x,y)$*. Then it has a domain* $D = D(\varphi)$*, and*

$$\mu(D) = e(D) + n_x(D) + n_y(D),$$

*where* $e(D)$ *is the* Euler measure*, while* $n_x(D)$ *and* $n_y(D)$ *are* average vertex multiplicities*.*

We will not prove this theorem, but to understand the statement we must explore the Euler measure and average vertex multiplicities.

**Euler measure**: Let $D$ be a domain, and choose a metric on $\Sigma$ so that all $\alpha, \beta$ intersect at right angles *and* are geodesics. Then

$$e(D) = \frac{1}{2\pi} \int_D K dA$$

where $K$ is the Gauss curvature. Of course, we do not have to do any geometry - this quantity can be computed using the Gauss-Bonnet theorem. We now list some examples.

- A square with right angled vertices and geodesic boundary is flat: $e(\text{square}) = 0$.
- A bigon with right angled vertices has positive curvature: $e(\text{bigon}) = 1/2$.
- More generally, $e(2n\text{-gon}) = 1 - n/2$.
- If $\Sigma_g$ is the closed surface with genus $g$, then Gauss-Bonnet gives us

$$e(\Sigma_g) = \chi(\Sigma_g) = 2 - 2g.$$

- The most general case we encounter is a surface of genus $g$ with boundary. Then

$$e(D) = \chi(D) - \frac{\#\text{ angles}}{4}.$$

An important observation is that if we partition a domain as $D = D_1 \cup D_2$, then $e(D) = e(D_1) + e(D_2)$. It follows that $e(\sum a_i R_i) = \sum a_i e(R_i)$, which can aid in calculations.

**Average vertex multiplicity**: This is essentially want the name suggests: let $D$ be a domain. Recall that domains are defined in the following way: let $u : D^2 \to \mathrm{Sym}^g(\Sigma)$ be a $J$-holomorphic strip. By the tautological correspondence, this gives a $g$-fold branched cover $p : S \to D^2$ and a map $\widetilde{u} : S \to \Sigma$ (for some space $S$). Then $D(u)$ is the image of $\widetilde{u}$ interpreted as a 2-chain. But now if $D$ is a domain corresponding to $u \in \pi_2(x, y)$, then each of $x$ and $y$ lift to $g$-tuples $\{x_1, \ldots, x_g\}$ and $\{y_1, \ldots, y_g\}$ in $S$. Similarly the $\alpha$ and $\beta$ curves lift to $S$, carving out regions.

Choose some $x_i \in \{x_i\}$. This is a vertex at the intersection of a lift of an $\alpha$ and $\beta$ curve, and defines 4 neighbouring regions $R_1^i, \ldots, R_4^i$. Each of these regions appear in $D$ with some multiplicity $a_k^i$ (by writing $D = \sum a_j R_j$). The *average vertex multiplicity* at $x_i$ is then $n_{x_i}(D) = (a_1^i + \cdots + a_4^i)/4$. More generally, the *average vertex multiplicity* at $x$ is

$$n_x(D) = \sum_{i=1}^{g} n_{x_i}(D).$$

**Example.** Let $D$ be a bigon with vertices $x$ and $y$. Then $n_x(D) = 1/4$ and $n_y(D) = 1/4$, since at each vertex, exactly one of the four regions appears in a bigon. Moreover, we mentioned earlier that $e(D) = 1/2$. Therefore

$$\mu(D) = e(D) + n_x(D) + n_y(D) = 1/2 + 1/4 + 1/4 = 1.$$

**Example.** Next let $D$ be a square with vertices $x_1, x_2$, and $y_1, y_2$. Then $n_x(D) = 1/2$ and $n_y(D) = 1/2$, since each vertex once again has average multiplicity $1/4$. But from earlier, we had that $e(D) = 0$! Therefore

$$\mu(D) = e(D) + n_x(D) + n_y(D) = 0 + 1/2 + 1/2 = 1.$$

An important question in Heegaard Floer theory is: if $\mu(D) = 1$, where $D = D(\varphi), \varphi \in \pi_2(x, y)$, then what is $\#(\mathcal{M}(\varphi)/\mathbb{R})$? If we know this, we can compute Heegaard Floer homology, since this is the only difficult term appearing in the boundary map. Unfortunately this is difficult to recover from topology alone, as we will now see.

**Example.** Consider the bigon from two examples earlier, which was shown to that $\mu(D) = 1$. Several lectures ago we noted that complex automorphisms of disks have three degrees of freedom, but two of these are fixed by the restriction that $(-1, 1) \mapsto (x, y)$ in the definition of a $J$-holomorphic strip. Therefore only one degree of freedom remains, and $\mathcal{M}(\text{bigon}) = \mathbb{R}$. Therefore

$$\#(\mathcal{M}(\text{bigon})/\mathbb{R}) = \pm 1.$$

**Example.** We can also compute $\#(\mathcal{M}(\varphi)/\mathbb{R})$, where $D(\varphi)$ is a square. This time we must count the number of branched double covers from a disk with four marked boundary points to $(D^2, 1, -1)$. By complex analysis, there is a unique double cover modulo an $\mathbb{R}$ action! Once again $\#(\mathcal{M}(\varphi)/\mathbb{R}) = \pm 1$.

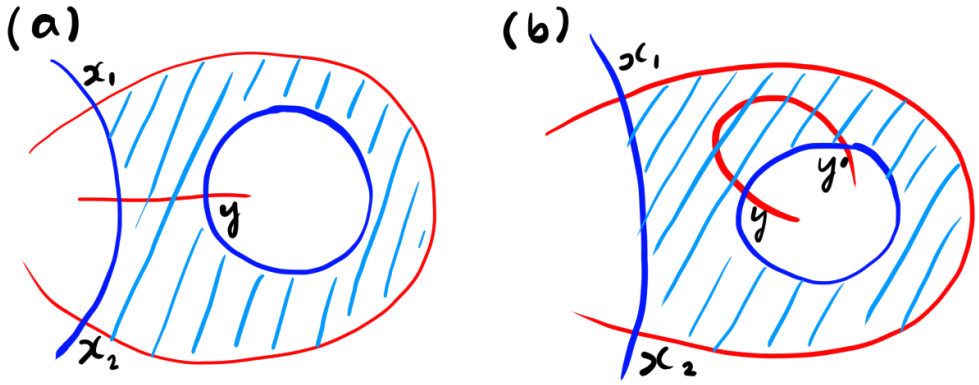


**Example.**

Figure 4.2: Example to demonstrate that $\#(\mathcal{M}(\varphi)/\mathbb{R})$ is difficult to compute.

As a final example, we consider the two images above. Since they are annuli, they have Euler characteristic 0. Since they have two vertices, their Euler measure is $-1/2$. On the other hand, the vertices $n_x(D) = 1/4 + 1/4 = 1/2$, and $n_y(D) = 1/2 + 1/2 = 1$. In summary $\mu(D) = 1$ as in the above examples. By the classification of conformal structures on annuli, one can check that $\#(\mathcal{M}(\varphi)/\mathbb{R}) = \pm 1$.

On the other hand, in the second diagram, we can have $\#(\mathcal{M}(\varphi)/\mathbb{R}) = 0$ (as well as $\pm 1$)! This is because the length of the red curve from $y$ to $y'$ can be such that it forbids the existence of any $J$-holomorphic strips. In conclusion, $\#(\mathcal{M}(\varphi)/\mathbb{R})$ is not easily determined from topology alone. This makes $HF$ difficult to compute!

**Proposition 4.8.2.** If $\Sigma$ is interpreted as a domain in itself, then $\mu(\Sigma) = 2$.

*Proof.* Suppose $\Sigma$ has genus $g$. Then $e(\Sigma) = 2 - 2g$. On the other hand,

$$n_x(\Sigma) = n_y(\Sigma) = \sum_{i=1}^{g} n_{x_i}(\Sigma) = g((1+1+1+1)/4) = g.$$

Therefore $\mu(\Sigma) = 2 - 2g + g + g = 2$. □

## 4.9 Heegaard diagram invariance

We defined $HF^\circ$ for $\circ \in \{\widehat{\ }, +, -, \infty\}$ using a fixed Heegaard diagram. However, for the invariants to really be useful, we want them to not depend on the choice of Heegaard diagram. This is indeed the case, as promised earlier!

**Theorem 4.9.1** (Ozsváth - Szabó)**.** *Heegaard Floer homology $HF^\circ(Y)$ is an invariant of the 3-manifold $Y$, where $\circ \in \{\widehat{}, +, -, \infty\}$.*

*Proof sketch.* We must verify invariance under Heegaard moves. Precisely, we must verify that Heegaard Floer homology is invariant under isotopies, handleslides, and stabilisations, where each move is going through admissible diagrams.

**Isotopy invariance.** Recall that this is true in general for Lagrangian Floer homology if we only use Hamiltonian isotopies! If we restrict ourselves to admissible diagrams, then areas between curves are zero. Moreover, isotopies can be chosen so that the intermediate diagrams are all admissible. But then areas are constantly being preserved, so the isotopy is Hamiltonian!

**Stabilisation invariance.** Suppose we use a Heegaard diagram

$$(\Sigma, \alpha_1, \dots, \alpha_g, \beta_1, \dots, \beta_g)$$

to define Heegaard Floer homology, and then stabilise it to obtain

$$(\Sigma^+, \alpha_1, \dots, \alpha_{g+1}, \beta_1, \dots, \beta_{g+1}).$$

Then $\mathbb{T}_\alpha \cap \mathbb{T}_\beta$ consists of $g$-tuples $\{x_1, \dots, x_g\}$, and $\mathbb{T}_{\alpha^+} \cap \mathbb{T}_{\beta^+}$ consists of $\{x_1, \dots, x_{g+1}\}$. Since the curves $\alpha_{g+1}$ and $\beta_{g+1}$ intersect at exactly one point, the last point $x_{g+1}$ is necessarily this one intersection point. This establishes a 1-to-1 correspondence

$$\mathbb{T}_\alpha \cap \mathbb{T}_\beta \leftrightarrow \mathbb{T}_{\alpha^+} \cap \mathbb{T}_{\beta^+}, \quad \{x_1, \dots, x_g\} \leftrightarrow \{x_1, \dots, x_{g+1}\}.$$

It follows that there is a bijective correspondence between $J$-holomorphic strips, $\varphi \in \pi_2(x, y) \leftrightarrow \varphi^+ \in \pi_2(x^+, y^+)$. Therefore the counts of $J$-holomorphic strips $\#(\mathcal{M}(\varphi)/\mathbb{R})$ also remain unchanged under stabilisation.

**Handleslide invariance.** This is what will require the most work. We use "triangle maps". Let $L_0, L_1, L_2 \subset (M, \omega)$ satisfy the usual conditions for Lagrangian Floer homology. Define $F : CF(L_0, L_1) \otimes CF(L_1, L_2) \to CF(L_0, L_2)$ by

$$F(x \otimes y) = \sum_z \sum_{\varphi \in \pi_2(x,y,z), \mu(\varphi)=0} (\#\mathcal{M}(\varphi))z.$$

Here $\varphi$ is a "$J$-holomorphic triangle", i.e. a map from a disk with three marked points into $M$, such that the boundary of the disk must map onto the Lagrangians $L_i$, and the marked points map to pairwise intersections $x, y, z$ of the Lagrangians. One can verify that $\mathcal{M}(\varphi)$ really has dimension 0. (This is essentially because maps from disks have three degrees of freedom, and here we are fixing three degrees of freedom.) In summary, the above map is well defined.

**Proposition 4.9.2.** *$F$ is a chain map. In particular, $F$ then induces a map $HF(L_0, L_1) \otimes HF(L_1, L_2) \to HF(L_0, L_2)$ which we call a triangle map.*

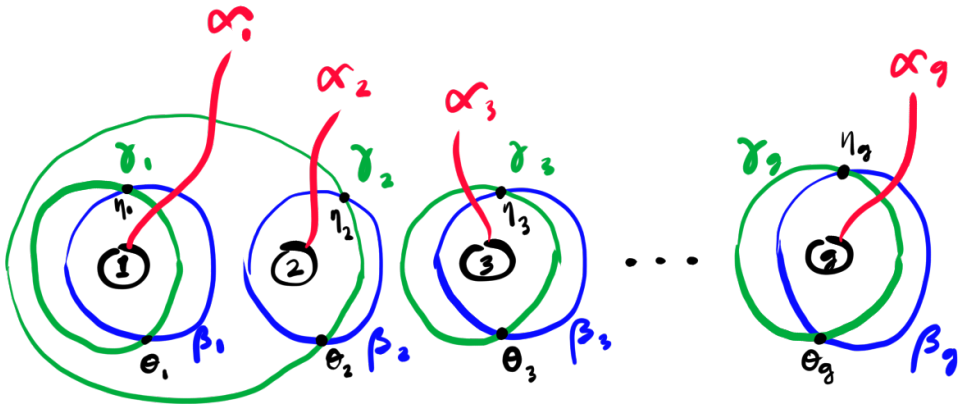


Figure 4.3: Handle slide of $\beta_2$ over $\beta_1$ to obtain new curves $\gamma_i$.

We do not give a proof of this fact, but it amounts to showing that $\partial F(x\otimes y)+F(\partial x\otimes y)+F(x\otimes\partial y)=0$. One can draw a diagram to convince oneself of this fact. We are now ready to investigate how Heegaard Floer homology is affected by handleslides! Figure 4.3 shows part of a Heegaard diagram $(\Sigma,\alpha_1,\dots,\alpha_g,\beta_1,\dots,\beta_g)$. (The $\alpha$ curves are incomplete etc.) We consider the handleslide of $\beta_2$ over $\beta_1$, which gives a new curve $\gamma_2$. Overall, we consider the new Heegaard diagram to be $(\Sigma,\alpha_1,\dots,\alpha_g,\gamma_1,\dots,\gamma_g)$. (That is, we replace the $\beta$ curves with $\gamma$ curves.)

From above, we have a triangle map

$$F_{\alpha,\beta,\gamma}:\widehat{HF}(\mathbb{T}_\alpha,\mathbb{T}_\beta)\otimes\widehat{HF}(\mathbb{T}_\beta,\mathbb{T}_\gamma)\to\widehat{HF}(\mathbb{T}_\alpha,\mathbb{T}_\gamma).$$

The first factor is $\widehat{HF}(\mathcal{H}_1)$, and the last term is $\widehat{HF}(\mathcal{H}_2)$, where our Heegaard diagram was changed from $\mathcal{H}_1$ to $\mathcal{H}_2$ via the handleslide. Our first goal is to understand the term $\widehat{HF}(\mathbb{T}_\beta,\mathbb{T}_\gamma)$. This is actually just

$$\widehat{HF}(\mathbb{T}_\beta,\mathbb{T}_\gamma)=\widehat{HF}(\#^g(\mathbb{S}^1\times\mathbb{S}^2))=(H_*(\mathbb{S}^1))^{\otimes g}=H_*(\mathbb{T}^g).$$

The last space is generated by $\{\theta_1,\eta_1\}\times\cdots\times\{\theta_g,\eta_g\}$. Define $\Theta=\{\theta_1,\dots,\theta_g\}\in\widehat{HF}(\mathbb{T}_\beta,\mathbb{T}_\gamma)$, and

$$F:\widehat{HF}(\mathcal{H}_1)\to\widehat{HF}(\mathcal{H}_2)\quad\text{by}\quad F(x)=F_{\alpha,\beta,\gamma}(x\otimes\Theta).$$

We define a map $G:\widehat{HF}(\mathcal{H}_2)\to\widehat{HF}(\mathcal{H}_1)$ similarly, by instead considering a triangle map $\widehat{HF}(\mathbb{T}_\alpha,\mathbb{T}_\gamma)\otimes\widehat{HF}(\mathbb{T}_\gamma,\mathbb{T}_\beta)\to\widehat{HF}(\mathbb{T}_\alpha,\mathbb{T}_\beta)$.

One can construct maps $H_1$ and $H_2$ which essentially count holomorphic quadrilaterals, and show that

$$FG=1+\partial H_1+H_1\partial,\quad GF=1+\partial H_2+H_2\partial.$$

It follows that $F$ is a chain homotopy equivalence, so $\widehat{HF}(\mathcal{H}_1)\cong\widehat{HF}(\mathcal{H}_2)$. □

This completes the proof (outline) that Heegaard Floer homology doesn't depend on the choice of (admissible) Heegaard diagram! It's really an invariant of closed connected oriented 3-manifolds! Next we will explore some applications in 4-dimensions.

# Chapter 5

# Heegaard Floer homology in dimension four

Heegaard Floer homology was defined earlier for closed connected oriented 3-manifolds. However, we will see in this chapter that Heegaard Floer homology is a "3+1 topological quantum field theory". This loosely means that given an oriented compact cobordism $W^4$ from $Y_0$ to $Y_1$, we obtain a homomorphism $F : HF(Y_0) \to HF(Y_1)$. This further defines an invariant for closed oriented 4-manifolds.

Applications include the existence of exotic smooth structures on 4-manifolds, which originally used gauge theory. However, this method is completely independent of gauge theory! Another important application is to the study of the homology cobordism group $\Theta^3_{\mathbb{Z}}$. Rokhlin first showed that the group was non-trivial, and Donaldson showed it was infinite. However, more precise results have been obtained using Heegaard Floer homology: Froyshov showed that $\Theta^3_{\mathbb{Z}}$ has a $\mathbb{Z}$ summand using Heegaard Floer homology! (Note that this is considered a 4 dimensional application, because the equivalence relation between homology spheres is homology cobordism, and the cobordisms are 4-dimensional. More precisely, the 4-dimensional theory of Heegaard Floer homology is used rather than just the 3-dimensional theory.)

## 5.1 Heegaard Floer homology as a 3+1 TQFT (lecture 9)

To interpret Heegaard Floer homology as a 3+1 dimensional topological quantum field theory, we must take a brief detour through some spin structure things.

**Proposition 5.1.1.** Spin$^c$-structures on a 4-manifold $X$ are in (non-canonical) one-to-one correspondence with $H^2(X;\mathbb{Z})$. (In particular, they always exist.)

Thus, if we fix any $s_0 \in \text{Spin}^c(X)$, $s - s_0$ is a well defined element of $H^2(X;\mathbb{Z})$. There

is also a map induced by the first Chern class:

$$c_1 : \mathrm{Spin}^c(X) \to H^2(X;\mathbb{Z}), \quad c_1(s+a) = c_1(s) + 2a.$$

On 3-manifolds, there exists an $s$ such that $c_1(s) = 0$. However, this need not be the case on 4-manifolds.

**Proposition 5.1.2.** If $s$ is a Spin$^c$-structure, then $\langle c_1(s), x\rangle \equiv \langle x, x\rangle \mod 2$, for all $x \in H^2(X;\mathbb{Z})$. That is, $c_1(s)$ is a *characteristic element*.

It follows that if there exists an $s$ such that $c_1(s) = 0$, then $x^2 \equiv 0 \mod 2$ for all $x \in H^2(X;\mathbb{Z})$. This is true for example in $\mathbb{S}^4$ or $\mathbb{S}^2 \times \mathbb{S}^2$, but not for $\mathbb{CP}^2$.

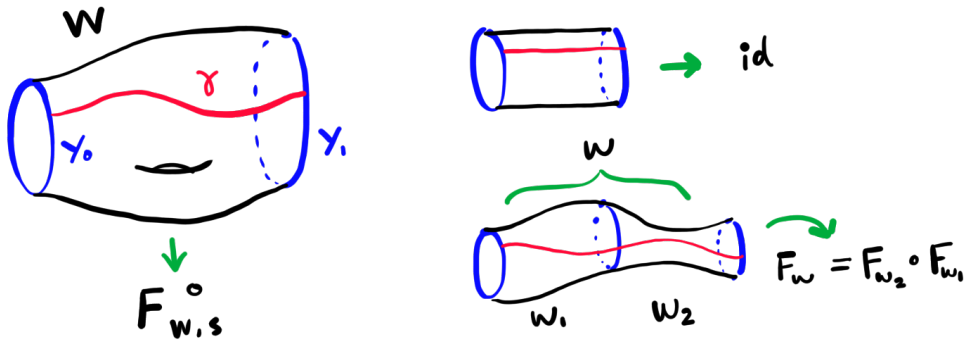


Figure 5.1: Heegaard Floer homology as TQFT.

The main theorem of this section is that Heegaard Floer homology defines a 3+1 dimensional topological quantum field theory, so it is not only an invariant of closed oriented 3-manifolds, but also for certain 4-manifolds. The precise statement is as follows:

**Theorem 5.1.3** (Ozsváth, Szabó)**.** *Let $W$ be a connected smooth oriented 4-dimensional cobordism between connected 3-manifolds $Y_0$ and $Y_1$. Fix a path $\gamma$ and $s \in \mathrm{Spin}^c(W)$. (See figure 5.1 for reference.) There is an associated map*

$$F^\circ_{W,s} : HF^\circ(Y_0, s|_{Y_0}) \to HF^\circ(Y_1, s|_{Y_1})$$

*(where $\circ \in \{\widehat{\ }, +, -, \infty\}$) satisfying the following properties.*

- *If $W = Y \times [0,1]$ and $\gamma = z \times [0,1]$, then $F^\circ_{W,s} = \mathrm{id}$.*
- *Let $W_1$ be a cobordism from $Y_0$ to $Y_1$, and $W_2$ a cobordism from $Y_1$ to $Y_2$. Let $W$ be the cobordism obtained by gluing $W_1$ to $W_2$. Then*

$$F^\circ_{W_2,s_2} \circ F^\circ_{W_1,s_1} = \sum_{s \in \mathrm{Spin}^c(W), s|_{W_i} = s_i} F^\circ_{W,s}.$$

Notice that the above two properties are just functoriality, where we view

$$(W, Y_0, Y_1, \gamma, s) \mapsto F^\circ_{W,s}$$

as a functor from the 3+1 cobordism category to $\mathbb{Z}$-mod. Therefore our theorem is really the statement that Heegaard Floer homology defines a topological quantum field theory.

**Remark.** For functoriality, we are taking a sum over "all the $s$ that restrict to $s_1$ and $s_2$. This is a bit strange - what if there are none? what if there are infinitely many? The count comes from the Mayer-Vietoris sequence:

$$\cdots \to H^1(Y_1) \xrightarrow{\delta} H^2(W) \xrightarrow{i} H^2(W_1) \oplus H^2(W_2) \to H^2(Y_1) \to \cdots .$$

The number of $s$ such that $s$ restricts to given $s_1$, $s_2$ is exactly the number of $s$ in the preimage of any given $(s_1, s_2) \in H^2(W_1) \oplus H^2(W_2)$. Thus there are $\ker i = \operatorname{im} \delta$ many such $s$. In particular, there is a unique $s$ if and only if $\delta$ is the zero map. (For example, if $Y_1$ is a rational homology sphere, in which case $H^1(Y_1) = 0$.)

We now give a sketch of the contruction of the cobordism map. (More precisely, we'll start with an outline of the sketch of the construction!)

**Outline of the construction of $F^\circ_{W,s}$.** Recall from Morse theory that every smooth manifold $M^n$ can be decomposed into handles. Precisely, an *$m$-dimensional $k$-handle* is a copy of $D^k \times D^{m-k}$ glued to the boundary of an $m$-manifold along $\partial D^k \times D^{m-k}$.

For example, suppose $X = D^3$ is the 3-ball. Then we can glue a 3-dimensional 1-handle onto $X$: this is a copy of $D^1 \times D^2$ glued to $X$ along $(\partial D^1) \times D^2 = D^2_0 \sqcup D^2_1$. The result is a solid torus.

Now suppose $W^4$ is a cobordism from $Y_0$ to $Y_1$. This can be decomposed as $W = W_1 \cup W_2 \cup W_3$, where $W_i$ consists purely of 4-dimensional $i$-handles. We will define

$$F_{W,s} = F_{W_3,s_3} \circ F_{W_2,s_2} \circ F_{W_1,s_1}.$$

Therefore the remaining steps are constructions of the cobordism map in each case where:

- the cobordism consists entirely of 1-handles,
- the cobordism consists entirely of 2-handles,
- the cobordism consists entirely of 3-handles.

**The cobordism map for 1-handles.** We start with $Y_0 \times [0,1]$ as the trivial cobordism $W$. In this context a 1-handle is a copy of $[0,1] \times D^3$. Gluing this to $W$ means we glue $[0,1] \times D^3$ via $0 \times D^3$ and $1 \times D^3$, onto $Y_0 \times \{1\}$. This is a little hard to visualise, but figure 5.2 shows that gluing a 1-handle to $W$ at $Y_0 \times \{1\}$ is equivalent to a boundary connected sum of $\mathbb{S}^1 \times D^3$ to $Y_0 \times \{1\}$, and hence the boundary component becomes $Y_0 \# (\mathbb{S}^1 \times \mathbb{S}^2)$. Thus the trivial cobordism is now replaced with a cobordism from $Y_0$ to $Y_0 \# (\mathbb{S}^1 \times \mathbb{S}^2)$.

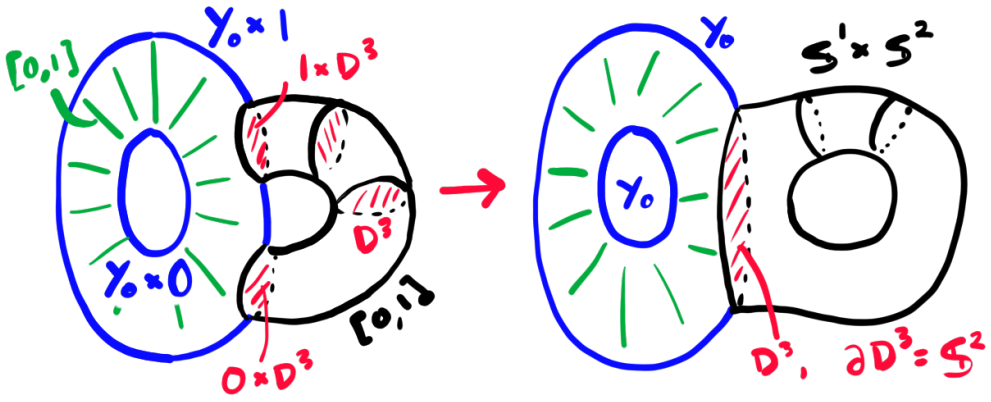


Figure 5.2: Gluing a 1-handle to a trivial cobordism.

We wish to define a map $\widehat{HF}(Y_0) \to \widehat{HF}(Y_0 \# (\mathbb{S}^1 \times \mathbb{S}^2))$. But the codomain is then just $\widehat{HF}(Y_0) \otimes \widehat{HF}(\mathbb{S}^1 \times \mathbb{S}^2) = \widehat{HF}(Y_0) \otimes \langle \theta, \eta \rangle$. Here $\langle \theta, \eta \rangle = H_*(\mathbb{S}^1)$, with $\theta$ denoting the higher graded element. We define

$$F_{W_1} : \widehat{HF}(Y_0) \to \widehat{HF}(Y_0 \# (\mathbb{S}^1 \times \mathbb{S}^2)) = \widehat{HF}(Y_0) \otimes \langle \theta, \eta \rangle, \quad x \mapsto x \otimes \theta.$$

**The cobordism map for 3-handles.** 3-handles are the opposites of 1-handles. This is very literally true - gluing a 3-handle to a trivial cobordism from $Y_1$ to $Y_1$ will change it to a cobordism from $Y_1 \# (\mathbb{S}^1 \times \mathbb{S}^2)$ to $Y_1$. Therefore we define

$$F_{W_3} : \widehat{HF}(Y_1 \# (\mathbb{S}^1 \times \mathbb{S}^2)) = \widehat{HF}(Y_1) \otimes \langle \theta, \eta \rangle \to \widehat{HF}(Y_1), \quad \begin{cases} x \otimes \eta \mapsto x \\ x \otimes \theta \mapsto 0. \end{cases}$$

**The cobordism map for 2-handles.** This case takes the most work, in the sense that most of the complexity of a 4-manifold comes from 2-handles.

In our setting, "attaching a 2-handle" means gluing $D^2 \times D^2$ to $Y \times \{1\} \subset Y \times [0,1]$ along $\mathbb{S}^1 \times D^2$. But $\mathbb{S}^1 \times D^2 \subset Y$ is a (closed) neighbourhood of a knot in $Y$! Specifically, the knot $K = \mathbb{S}^1 \times \{0\}$. Therefore attaching a 2-handle corresponds to cutting out $\mathbb{S}^1 \times D^2$, and gluing it back in via a different diffeomorphism. This is called *knot surgery*, and appeared in e.g. my notes on 4-manifolds from Spring 2020, and probably also in my notes on homology spheres or knot theory.

**Definition 5.1.4.** Let $Y$ be a 3-manifold, and $K \subset Y$ a knot. Fix a neighbourhood $\mathbb{S}^1 \times D^2$ of $K$. This has boundary $\mathbb{S}^1 \times \mathbb{S}^1$, which is parametrised by a *longitude* $\ell$ and a *meridian* $m$ respectively. The rational *$p/q$-surgery on $K$ in $Y$* is defined to be

$$(Y - \mathbb{S}^1 \times D^2) \sqcup_f (\mathbb{S}^1 \times D^2)$$

where $f$ sends a meridian $\mu$ of the second copy of $\mathbb{S}^1 \times D^2$ to a loop $c$, where $[c] = p[m]+q[\ell]$ in homotopy (with $p, q \in \mathbb{Z}$). This is denoted by $Y_{p/q}(K)$.

Observe that $p/q$-surgery occurs as the boundary of a 2-handle additional if and only if $q = \pm 1$. That is, if and only if the surgery is *integral*. (In other words, in a handle addition, we cannot "wrap around the handle" multiple times - we traverse the handle exactly once.)

In summary, the cobordism $W_2$ consisting entirely of two handles can alternatively be considered as the rest of integral surgery on a link $L$. Therefore we will define $F_{W_2,s}$ in terms of $L$. Suppose $L$ is a knot, that is, there is a single 2-handle. We will associate to the surgery cobordism $Y \to Y' = Y_p(K)$ a "triple Heegaard diagram". That is,

$$(\Sigma, \alpha_1, \dots, \alpha_g, \beta_1, \dots, \beta_g, \gamma_1, \dots, \gamma_g)$$

such that

1. $(\Sigma, \alpha_i, \beta_i)$ is a Heegaard diagram of $Y$,
2. $(\Sigma, \alpha_i, \gamma_i)$ is a Heegaard diagram of $Y'$,
3. and $\gamma_i, \beta_i$ are isotopic for $i < g$ (intersecting at two points), while $\gamma_g$ and $\beta_g$ intersect at one point.

Figure 5.3 gives an example of a triple Heegaard diagram.

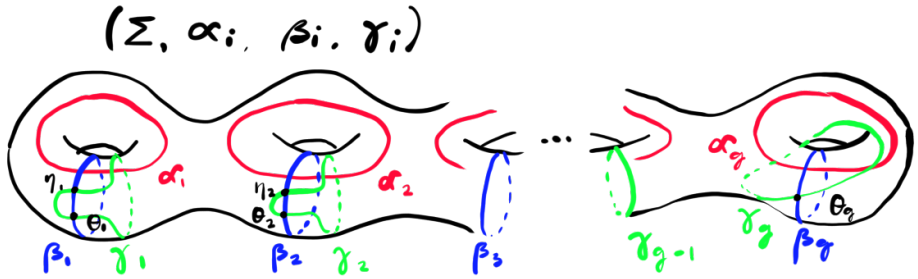


Figure 5.3: Example of triple Heegaard diagram.

From the figure, we see that $(\Sigma, \beta_i, \gamma_i)$ represents $\#^{g-1}(\mathbb{S}^1 \times \mathbb{S}^2)$. The map $F_{W_2,s_2} : HF^\circ(Y) \to HF^\circ(Y')$ is defined in a manner reminiscent to the proof of the invariance of Heegaard Floer homology with respect to handle slides: we count holomorphic triangles. More precisely we consider the triangle map

$$f : HF(\mathbb{T}_\alpha, \mathbb{T}_\beta) \otimes HF(\mathbb{T}_\beta, \mathbb{T}_\gamma) \to HF(\mathbb{T}_\alpha, \mathbb{T}_\gamma).$$

By construction $HF(\mathbb{T}_\beta, \mathbb{T}_\gamma)$ is equal to $\langle \theta_1, \eta_1 \rangle \otimes \cdots \langle \theta_{g-1}, \eta_{g-1} \rangle \otimes \langle \theta_g \rangle$. Write $\Theta = \theta_1 \otimes \cdots \otimes \theta_g$. Then the cobordism map is

$$F_{W_2,s_2} : HF^\circ(Y) \to HF^\circ(Y'), \quad x \mapsto f(x \otimes \Theta).$$

(Here we are using that $HF^\circ(Y) = HF(\mathbb{T}_\alpha, \mathbb{T}_\beta)$, and $HF^\circ(Y') = HF(\mathbb{T}_\alpha, \mathbb{T}_\gamma)$).

This completes the construction of the maps. Ozsváth and Szabó proved that the $F_{W,s}$ defined in this manner do not depend on the choice of handle decomposition of the given $W$.

**Exercise.** As an example of the fact that the maps are functorial, one can consider $\mathbb{S}^3 \times [0,1]$ as the cobordism. This can be decomposed as the union of a 1-handle and 2-handle, i.e. $W = W_1 \cup W_2$, where $W_1$ is a cobordism from $\mathbb{S}^3$ to $\mathbb{S}^1 \times \mathbb{S}^2$, and $W_2$ a cobordism from $\mathbb{S}^1 \times \mathbb{S}^2$ to $\mathbb{S}^3$. Compute $F_{W_1}$ and $F_{W_2}$, and verify that $F_{W_2} \circ F_{W_1} = \mathrm{id}$.

## 5.2 Cobordism maps on gradings

Since cobordisms $W$ between 3-manifolds $Y_0$ and $Y_1$ induce maps $HF(Y_0) \to HF(Y_1)$, an immediate question is whether or not the maps preserve the grading. If not, how does it affect the grading? We explore this question here.

**Theorem 5.2.1.** *For $c_1(s)$ torsion, there exists an absolute $\mathbb{Q}$-grading on $HF^\circ(Y,s)$ satisfying the following properties:*

- *The absolute $\mathbb{Q}$-grading lifts the relative $\mathbb{Z}/N\mathbb{Z}$-grading in the sense that* $\mathrm{gr}(x) - \mathrm{gr}(y) = \mathrm{gr}(x,y) \mod N\mathbb{Z}$ *(and* $\mathrm{gr}(x), \mathrm{gr}(y) \in \mathbb{Q}$*).*
- *Suppose $(W,s)$ is a cobordism from $(Y_0,s_0)$ to $(Y_1,s_1)$. Then the absolute $\mathbb{Q}$-gradings on $HF^\circ(Y_i,s_i)$ are related by*

$$\mathrm{gr}(F_{W,s}(\xi)) - \mathrm{gr}(\xi) = \frac{c_1(s)^2 - 2\chi(W) - 3\sigma(W)}{4}.$$

Details on the above theorem can be found in *Holomorphic triangles and four-manifold invariants* by Ozsváth and Szabó.

Recall that by a *relative $\mathbb{Z}/N\mathbb{Z}$ grading*, we mean $\mathrm{gr}(x,y) \in \mathbb{Z}/N\mathbb{Z}$ is well defined, but not $\mathrm{gr}(x)$ or $\mathrm{gr}(y)$. The relative grading satisfies the additive property $\mathrm{gr}(x,y) + \mathrm{gr}(y,z) = \mathrm{gr}(x,z)$.

**Remark.** The mysterious expression above involving the first Chern class, Euler characterstic, and signature, is equal to the expected dimension of the Seiberg-Witten moduli space of a closed 4-manifold equipped with a Spin$^c$ structure $s$.

Recall that the *signature* $\sigma(W)$ of a 4-manifold $W$ is the signature of its intersection form. That is, $\sigma(W) = p - q$ where $p$ is the number of positive eigenvalues and $q$ is the number of negative eigenvalues of $Q : H_2(W) \otimes H_2(W) \to \mathbb{Z}$.

What is $c_1(s)^2$? By Poincaré duality, $c_1(s) \in H^2(W) \cong H_2(W, \partial W)$. However, there is no intersection form on $H_2(W, \partial W; \mathbb{Z})$! This is because we can't intersect surfaces with

boundary and reasonably count intersections (or alternatively, if we view this from the cohomological perspective using the cup product, there is no fundamental class). This is where the condition that $c_1(s_i)$ is torsion comes in handy! That is, $\partial W = Y_0 \cup Y_1$, and we can write $s|_{Y_i} = s_i$.Then $c_1(s_i)$ is torsion, so $c_1(s|_{Y_0 \cup Y_1}) = c_1(s|_{\partial W})$ is also torsion. This means $c_1(s|_{\partial W}) = 0 \in H^2(\partial W; \mathbb{Q})$. The long exact sequence of cohomology reads

$$H_2(W; \mathbb{Q}) \cong H^2(W, \partial W; \mathbb{Q}) \to H^2(W; \mathbb{Q}) \to H^2(\partial W; \mathbb{Q}).$$

But now $c_1(s) \in H^2(W; \mathbb{Q})$ maps to $c_1(s)|_{\partial W} = c_1(s|_{\partial W}) = 0$ in $H^2(\partial W; \mathbb{Q})$, by exactness there exists some $x \in H^2(W, \partial W; \mathbb{Q})$ whose image is $c_1(s)$.

We now define $c_1(s)^2$ to be $\langle c_1(s) \smile x, [W] \rangle$. This makes sense because $c_1(s) \smile x \in H^4(W, \partial W; \mathbb{Q})$, while $[W] \in H_4(W, \partial W; \mathbb{Q})$.

**Proposition 5.2.2.** If $Y$ is an integral homology sphere, then the absolute $\mathbb{Q}$-grading is in fact a $\mathbb{Z}$-grading.

**Example.** In each of the following, $s$ is the unique torsion spin structure.

- $\widehat{HF}(\mathbb{S}^3, s) = \mathbb{Z}$ in grading 0.
- $\widehat{HF}(\mathbb{S}^1 \times \mathbb{S}^2, s) = \mathbb{Z} \oplus \mathbb{Z}$ in gradings $(-1/2, 1/2)$.

## 5.3 Reduced Heegaard Floer homology

If our aim is to study 4-manifolds, we would ideally like some invariants of closed 4-manifolds rather than just cobordisms of 3-manifolds. In this section we will introduce an ingredient for such an invariant (which I cannot motivate - that is, I don't see why it should have anything to do with 4-manifold invariants!)

Recall that $CF^\infty$ is generated over $\mathbb{Z}[U, U^{-1}]$ by $\mathbb{T}_\alpha \cap \mathbb{T}_\beta$. This contains a subcomplex $CF^-$ which is generated by $U^i x$ for $i \geqslant 1$, and $CF^+$ is the complex defined by $CF^\infty / CF^-$. This gives a long exact sequence

$$\dots HF^- \xrightarrow{i} HF^\infty \xrightarrow{\pi} HF^+ \xrightarrow{\delta} HF^- \to \cdots.$$

But now, from this long exact sequence, we can extract some information common to $HF^+$ and $HF^-$ which doesn't feature in $HF^\infty$! Namely, the image of $\delta$.

**Definition 5.3.1.** The *reduced Heegaard Floer homology*, denoted by $HF_{\mathrm{red}}$, is defined by any one of the following equalities:

$$HF_{\mathrm{red}} = \operatorname{coker} \pi = HF^+ / \ker \delta = \operatorname{im} \delta = \ker i.$$

**Example.** Let $Y = \mathbb{S}^3$. Recall from several lectures ago that $HF^\infty = \mathbb{Z}[U, U^{-1}], HF^- = \mathbb{Z}[U]$, and $HF^+ = \mathbb{Z}[U, U^{-1}]/\mathbb{Z}[U]$. If $x$ is a generator of $\widehat{HF} = \mathbb{Z}$, then we have the following table:

| | | $HF^-$ | $HF^\infty$ | $HF^+$ |
|---|---|---|---|---|
| Grading | 4 | | $U^{-2}x$ | $U^{-2}x$ |
| | 2 | | $U^{-1}x$ | $U^{-1}x$ |
| | 0 | | $x$ | $x$ |
| | -2 | $Ux$ | $Ux$ | |
| | -4 | $U^2x$ | $U^2x$ | |
| | -6 | $U^3x$ | $U^3x$ | |

The $\delta$ map is then necessarily trivial, so $HF_{\text{red}} = 0$.

**Example.** We will not give the details for this example, but $Y_n = \mathbb{S}^3_{1/n}(\text{trefoil})$ is an example of a 3-manifold with non-trivial $HF_{\text{red}}$. (That is, our space is the rational $1/n$-surgery on a right handed trefoil knot in the 3-sphere.) Notice that $Y_1$ is the Poincaré homology sphere. In general, we have $H_1(Y_n) = 0$, so each $Y_n$ is an integral homology sphere.

In the case of $Y_n$, the table of Heegaard Floer homology is as follows:

| | | $HF^-$ | $HF^\infty$ | $HF^+$ |
|---|---|---|---|---|
| Grading | 4 | | $U^{-2}x$ | $U^{-2}x$ |
| | 2 | | $U^{-1}x$ | $U^{-1}x$ |
| | 0 | | $x$ | $x$ |
| | -2 | | $Ux$ | $Ux, y_1, \dots, y_{n-1}$ |
| | -3 | $z_1, \dots, z_{n-1}$ | | |
| | -4 | $U^2x$ | $U^2x$ | |
| | -6 | $U^3x$ | $U^3x$ | |

The extra terms $y_1, \dots, y_{n-1}$ map to $z_1, \dots, z_{n-1}$ under $\delta$, so that $HF_{\text{red}} = \mathbb{Z}^{n-1}$. (The rest of the terms map isomorphically in the expected way, as in the case of the 3-sphere.

## 5.4 Naïve Heegaard Floer homology for closed 4-manifolds (lecture 10)

Finally we are ready to define invariants for closed 4-manifolds via Heegaard Floer homology. Before defining the "right notion", we will use the naive approach and see what goes wrong. By the naive approach, we mean taking an arbitrary closed 4-manifold, and removing two 3-balls to create a cobordism. The Heegaard Floer cobordism map would then be the associated invariant.

Let $X^4$ be a closed smooth oriented connected 4-manifold, and $s \in \text{Spin}^c(X)$. Let $W = X - (B^4 \cup B^4)$. Heegaard Floer homology induces a map

$$F^\circ_{W,s} : HF^\circ(\mathbb{S}^3) \to HF^\circ(\mathbb{S}^3),$$

where as usual $\circ \in \{\widehat{}, +, -, \infty\}$. This means we have a map $F^{\circ}_{W,s} : \mathbb{Z} \to \mathbb{Z}$, and such a map is uniquely determined by $F^{\circ}_{W,s}(1) \in \mathbb{Z}$.

However, recall that $HF^{\infty}(Y)$ is determined by $H^*(Y)$. Similarly, it turns out the cobordism maps are determined:

**Theorem 5.4.1** (Ozsváth, Szabó)**.** *Let $W$ be a cobordism from $Y_1$ to $Y_2$.*

1. *If $b_2^+(W) > 0$, then $F^{\infty}_{W,s}$ is 0.*
2. *If $b_2^+(W) = 0$, $b_1(W) = 0$, and $Q_W$ has trivial kernel, then $F^{\infty}_{W,s}$ is an isomorphism.*

Note that $Q_W : H_2(W;\mathbb{R}) \otimes H_2(W;\mathbb{R}) \to \mathbb{R}$ is the intersection form, which is a symmetric bilinear form. Over $\mathbb{R}$, such a form is equivalent to $m(1) \oplus n(-1) \oplus p(0)$, where

- $m = b_2^+$ is the dimension of the maximal subspace on which $Q_W$ is positive definite,
- $n = b_2^-$ is the dimension of the maximal subspace on which $Q_W$ is negative definite,
- and $p$ is the dimension of the kernel of $Q_W$.

In our case, $W$ is from $\mathbb{S}^3$ to itself. Closed 4-manifolds have trivial nullity, and this is preserved by cutting out two solid balls. Therefore $\text{nullity}(W) = 0$. It follows that

$$F^{\infty}_{W,s} : HF^{\infty}(\mathbb{S}^3) = \mathbb{Z}[U, U^{-1}] \to HF^{\infty}(\mathbb{S}^3) = \mathbb{Z}[U, U^{-1}]$$

satisfies

$$F^{\infty}_{W,s} \text{ is } \begin{cases} 0 & b_2^+(W) > 0 \\ \cong & b_2^+(W) = 0. \end{cases}$$

But next we have that

$$HF^{\infty} = U^{-1}HF^-, \quad HF^-(\mathbb{S}^3) = \mathbb{Z}[U].$$

The cobordism maps are related by $F^{\infty}_{W,s} = U^{-1}F^-_{W,s}$. Similarly to above, the cobordism map $F^-_{W,s}$ is determined by $b_2^+(W)$:

$$F^-_{W,s} : HF^-(\mathbb{S}^3) = \mathbb{Z}[U] \to HF^-(\mathbb{S}^3) = \mathbb{Z}[U], \quad F_i = \begin{cases} 0 & b_2^+(W) > 0 \\ \pm 1 & b_2^+(W) = 0. \end{cases}$$

Here $F_i$ is a map from $\mathbb{Z} \to \mathbb{Z}$, where we view $\mathbb{Z}[U]$ as consisting of copies of $\mathbb{Z}$ in negative gradings, and $F_i$ is the restriction of $F^-_{W,s}$ to one of these gradings ($\mathbb{Z}$). Finally $\mathbb{F}^+_{W,s}$ is determined from the exact sequence

$$\cdots \to HF^- \to HF^{\infty} \to HF^+ \to \cdots,$$

and $\widehat{F_{W,s}}$ is determined from the exact sequence

$$\cdots \widehat{HF} \to HF^- \xrightarrow{U} HF^- \to \cdots .$$

To demonstrate how the exact sequence determines, for example, $\widehat{F_{W,s}}$, consider the following diagram:

$$\begin{array}{ccccccccc}
\cdots & \longrightarrow & \widehat{HF}(\mathbb{S}^3) & \longrightarrow & HF^-(\mathbb{S}^3) & \longrightarrow & HF^-(\mathbb{S}^3) & \longrightarrow & \cdots \\
 & & \downarrow{\scriptstyle \widehat{F_{W,s}}} & & \downarrow{\scriptstyle F^-_{W,s}} & & \downarrow{\scriptstyle F^-_{W,s}} & & \\
\cdots & \longrightarrow & \widehat{HF}(\mathbb{S}^3) & \longrightarrow & HF^-(\mathbb{S}^3) & \longrightarrow & HF^-(\mathbb{S}^3) & \longrightarrow & \cdots
\end{array}$$

The map $\widehat{F_{W,s}}$ must be trivial if $F^-_{W,s}$ changes the grading, since the former has no grading change. By virtue of the diagram commuting (from everything being functorial), we have

$$\widehat{F_{W,s}} = \begin{cases} \pm 1 & 0 \text{ grading shift, } W \text{ negative definite} \\ 0 & \text{otherwise.} \end{cases}$$

In summary, our naive invariants really were quite naive! They don't contain much information at all. A more interesting 4-manifold invariant must capture the parts of $HF^+$ and $HF^-$ that don't feature in $HF^\infty$ (as losing this information was our downfall in this case). That is, we must make use of $HF_{\text{red}}$. These invariants are called *mixed invariants* and are next on our menu.

## 5.5 Mixed invariants of closed 4-manifolds

In this section, we assume $X$ is a closed oriented 4-manifold with $b_2^+(X) \geqslant 2$. We then define $W = X - (B^4 \cup B^4)$ to be our cobordism between 3-spheres. To extract more interesting information, we consider an *admissible cut* to express $W$ as a composition of two cobordisms.

**Definition 5.5.1.** An *admissible cut* $N$ (shown in figure 5.4) for $W$ is a submanifold $N^3 \subset W^4$ such that $W = W_1 \sqcup_N W_2$ with $b_2^+(W_1), b_2^+(W_2) \geqslant 1$, and $\partial H^1(N) = 0 \subset H^2(W)$.

The second condition makes it easy to glue Spin$^c$ structures together. To define mixed invariants, we start by considering the following two commutative diagrams, in which $s_i$ denotes $s|_{W_i}$, the restriction of a spin$^c$ structure on $W$ to one of the halves $W_i$:

$$\begin{array}{ccc}
HF^-(\mathbb{S}^3) & \xrightarrow{F^-_{W_1,s_1}} & HF^-(N) \\
\downarrow & & \downarrow{\scriptstyle i} \\
HF^\infty(S^3) & \xrightarrow{F^\infty_{W_1,s_1}=0} & HF^\infty(N)
\end{array}
\qquad
\begin{array}{ccc}
HF^\infty(N) & \xrightarrow{F^\infty_{W_2,s_2}=0} & HF^\infty(\mathbb{S}^3) \\
\downarrow{\scriptstyle \pi} & & \downarrow \\
HF^+(N) & \xrightarrow{F^+_{W_2,s_2}} & HF^+(\mathbb{S}^3)
\end{array}$$

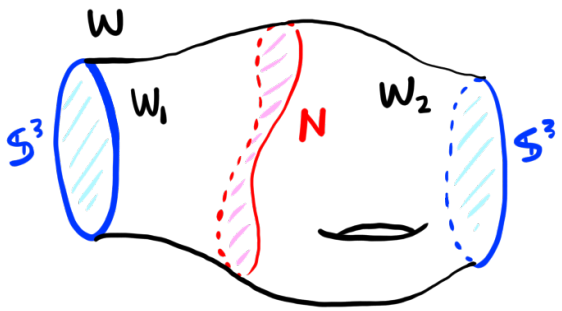


Figure 5.4: Example of an admissible cut.

All vertical maps are induced from the exact sequence

$$\cdots HF^-(Y) \to HF^\infty(Y) \to HF^+(Y) \to \cdots .$$

We first consider the diagram on the left. By the previous theorem of Ozsváth and Szabó, since $b_2^+(W_1) \geqslant 1$, we automatically know that $F^\infty_{W_1,s_1} = 0$. Therefore by commutativity of the diagram,

$$\operatorname{im} F^-_{W_1,s_1} \subset \ker i = HF_{\mathrm{red}}(N).$$

In other words, $F^-_{W_1,s_1}$ factors through $HF_{\mathrm{red}}(N)$. Similarly in the second diagram, we conclude that $F^\infty_{W_2,s_2} = 0$, and thus $\operatorname{im}\pi \subset \ker F^+_{W_2,s_2}$. By the universal property of quotients for example, we conclude that $F^+_{W_2,s_2}$ also factors through $\operatorname{coker}\pi = HF_{\mathrm{red}}(N)$. In summary, we obtain the following two diagrams:

$$\begin{array}{ccc} HF^-(\mathbb{S}^3) & \xrightarrow{F^-_{W_1,s_1}} & HF^-(N) \\ & \searrow & \uparrow \\ & & HF_{\mathrm{red}}(N) \end{array} \qquad \begin{array}{ccc} HF^+(N) & \xrightarrow{F^+_{W_2,s_2}} & HF^+(\mathbb{S}^3) \\ \downarrow & \nearrow & \\ HF_{\mathrm{red}}(N) & & \end{array}$$

The *mixed map* is now defined to be the composition

$$F^{\mathrm{mix}}_{W,s} : HF^-(\mathbb{S}^3) \to HF_{\mathrm{red}}(N) \to HF^+(\mathbb{S}^3).$$

Recall that $HF^-(\mathbb{S}^3) = \mathbb{Z}[U]$ and $HF^+(\mathbb{S}^3) = \mathbb{Z}[U^{-1}] = \mathbb{Z}[U, U^{-1}]/\mathbb{Z}[U]$. But now $\mathbb{Z} \subset \mathbb{Z}[U]$, and the image of $\mathbb{Z}$ under $F^{\mathrm{mix}}_{W,s}$ is also contained in $\mathbb{Z} \subset \mathbb{Z}[U^{-1}]$. We are finally ready to define mixed invariants!

**Definition 5.5.2.** Let $X$ be a 4-manifold as above, and $s$ a spin$^c$ structure on $X$. The *mixed invariant* of $X$ is defined to be

$$\Phi_{X,s} = F^{\text{mix}}_{W,s}(1) \in \mathbb{Z}.$$

Of course, this definition isn't well defined unless we verify the existence of admissible cuts, and admissible-cut-invariance.

**Lemma 5.5.3.** Any cobordism $W$ from $\mathbb{S}^3$ to $\mathbb{S}^3$ with $b_2^+(W) \geqslant 2$ admits an admissible cut.

*Proof.* Let $X$ be a closed 4-manifold with $b_2^+(X) \geqslant 2$. Find a surface $\Sigma \subset X$ with $[\Sigma]^2 > 0$ (by using that $b_2^+(X) \geqslant 2$). Let $N$ be the boundary of a tubular neighbourhood $N(\Sigma)$ of $\Sigma$, and write $W_1 = N(\Sigma) - B^4$, $W_2 = X - N(\Sigma) - B^4$. Now one can verify that $N$ is an admissible cut of $W = W_1 \sqcup_N W_2$:

$$\begin{aligned} H_2(N(\Sigma)) = H_2(\Sigma) = \mathbb{Z}, &\quad \Rightarrow b_2^+(W_1) = 1 \\ b_2^+(X) = b_2^+(W_1) + b_2^+(W_2), &\quad \Rightarrow b_2^+(W_2) \geqslant 1. \end{aligned}$$

The coboundary condition can also be readily checked. (Notice that $N$ is an $\mathbb{S}^1$-bundle over $\Sigma$, with Euler class $[\Sigma]^2$.) □

To complete the verification that the above definition is well defined, we simply state a theorem of Ozváth and Szabó (without proof):

**Theorem 5.5.4.** *The mixed invariant $\Phi_{X,s}$ is independent of the choice of admissible cut.*

One immediate property of mixed invariants is that if $W$ admits an admissible cut $N$ with $HF_{\text{red}}(N) = 0$, then $\Phi_{X,s} = 0$. This happens for example when $N$ is a 3-sphere, Poincaré homology sphere, or lens space.

**Corollary 5.5.5.** *If a 4-manifold $X$ can be expressed as a non-trivial connected sum (in the sense that $X = X_1 \# X_2$, with $b_2^+(X_1) \geqslant 1, b_2^+(X_2) \geqslant 1$), then $\Phi_{X,s} = 0$.*

This result can be used to prove the existence of exotic smooth structures on 4-manifolds! Finally before moving onto such applications, we state some connections with Seiberg-Witten invariants:

**Conjecture.** Let $X$ be a 4-manifold as above, and $s$ a spin$^c$ structure on $X$. Then

$$\Phi_{X,s} = SW_{X,s}$$

where the latter are Seiberg-Witten invariants.

(See for example my notes from the 4-manifolds topics class in Spring 2020 for more about Seiberg-Witten invariants.) The lower dimensional analogue has been verified, and this version is expected to hold. However, the result will take a lot of work and people are exhausted.

**Theorem 5.5.6** (Kutluhan-Lee-Taubes, Colin-Ghiggini-Honda)**.** *$HF(Y,s) = HM(Y,s)$, where the right side denotes monopole (Seiberg-Witten) Floer homology.*

## 5.6 Applications: exotic smooth structures

One of the main applications of the mixed invariant is that it gives a novel proof of the existence of exotic smooth structures on 4-manifolds. That is, there exists closed oriented 4-manifolds $X_1$ and $X_2$ which are *homeomorphic* but not *diffeomorphic*.

**Theorem 5.6.1.** *Let $X_1 = K3\#\overline{\mathbb{CP}^2}$, and $X_2 = 3\mathbb{CP}^2\#20\overline{\mathbb{CP}^2}$. Then $X_1, X_2$ are homeomorphic but not diffeomorphic.*

Recall that $K3$ denotes the *K3 surface* $\{z_0^4 + z_1^4 + z_2^4 + z_3^4 = 0\} \subset \mathbb{CP}^3$. On the other hand, $\overline{\mathbb{CP}^2}$ denotes $\mathbb{CP}^2$ endowed with the opposite orientation.

*Proof.* First we note that $X_1, X_2$ have the same intersection form on $H_2$, and they are both simply connected. Therefore by Freedman's theorem, $X_1$ and $X_2$ are homeomorphic.

Next we write

$$X_2 = (2\mathbb{CP}^2\#20\overline{\mathbb{CP}^2})\#\mathbb{CP}^2.$$

Then on the left we have $b_2^+ = 2, b_2^- = 20$. On the right, $b_2^+ = 1, b_2^- = 0$. By the obersvation about the mixed invariant factoring through $HF_{\text{red}}(\mathbb{S}^3) = 0$ (by taking the sphere from the connected sum as the admissible cut), this gives $\Phi_{X_2,s} = 0$ for every $s$.

As for $X_1$, we can consider the admissible cut given by 1/2-surgery on a trefoil knot. This is the Brieskorn sphere $\Sigma(2,3,11)$. Then $HF_{\text{red}}(\Sigma(2,3,11)) = \mathbb{Z}$, and there exists $s$ such that $\Phi_{X_1,s} = 1$. Therefore $X_1$ and $X_2$ cannot be diffeomorphic. □

**Remark.** Although we used mixed invariants (which allows us to consider just cobordisms from spheres to spheres), $\widehat{F_{W,s}}$ and $F^+_{W,s}$ can also be used on their own to detect smooth structures on some 4 dimensional cobordisms (just not those from $\mathbb{S}^3$ to $\mathbb{S}^3$).

## 5.7 Applications: homology cobordism group

Another, perhaps more important application, is to the study of the homology cobordism group $\Theta^3_{\mathbb{Z}}$. While the existence of exotic smooth structures was already known, Heegaard Floer homology has contributed new understanding to the structure of $\Theta^3_{\mathbb{Z}}$. Recall that in the first lecture, I presented some expository material on why we care about $\Theta^3_{\mathbb{Z}}$, and historical progress in its understanding.

**Definition 5.7.1.** The *homology cobordism group* $\Theta^3_{\mathbb{Z}}$ is the group of homology cobordism classes of integral homology spheres. That is,

$$\Theta^3_{\mathbb{Z}} = \{\text{oriented } \mathbb{Z}H\mathbb{S}^3\text{s}\}/\sim,$$

where $Y_0 \sim Y_1$ if and only if there is an oriented compact smooth 4-manifold $W$ such that $\partial W = (-Y_0) \sqcup Y_1$, and $H_*(W, Y_i) = 0$ for both $i$.

Observe that $\Theta^3_{\mathbb{Z}}$ is an abelian group:

$$[\mathbb{S}^3] = 0, \quad [Y_0] + [Y_1] := [Y_0 \# Y_1].$$

$[\mathbb{S}^3] = 0$ because $\mathbb{S}^3$ bounds a ball - thus $\mathbb{S}^3$ is homology cobordant to the "empty manifold". Next we note that $-[Y] = [\overline{Y}]$. This is because

$$[Y] + [\overline{Y}] = [Y \# \overline{Y}] = [\mathbb{S}^3] = 0.$$

The middle equality comes from considering $Y \times [0,1]$, which is a cobordism from $Y$ to itself. But then deleting a tubular neighbourhood of a path from $Y \times \{0\}$ to $Y \times \{1\}$ turns this into a 4-manifold bound by $Y \# \overline{Y}$. Deleting a ball from thsi manifold gives a homology cobordism from $Y \# \overline{Y}$ to $\mathbb{S}^3$ as required.

**Remark.** By definition $[Y] = 0 \in \Theta^3_{\mathbb{Z}}$ if and only if $Y$ is homology cobordant to a 3-sphere. But a 3-sphere bounds a 4-ball, so filling this in, we have that $[Y] = 0$ if and only if it bounds a homology ball!

**Remark.** We now list a few reasons why we care about the homology cobordism group.

- The homology cobordism group tells us about triangulations: fix $n \geqslant 5$. Then there exist closed orientable topological manifolds $M^n$ if and only if $\Theta^3_{\mathbb{Z}}$ contains no elements of order 2. The latter fact was proven by Manolescu using Seiberg-Witten Floer homology.

- The homology cobordism group tells us about knots: there are various homomorphisms $\mathcal{C} \to \Theta^3_{\mathbb{Z}}, \Theta^3_{\mathbb{Q}}$, where $\mathcal{C}$ denotes the knot concordance group. Understanding the structure of $\Theta^3$ helps us to understand $\mathcal{C}$ via these maps.

- Construction of smooth 4-manifolds: if a homology sphere $\Sigma$ bounds a smooth 4-manifold $X_1$ with intersection form $Q_{X_1}$, and $-\Sigma$ bounds $X_2$ with intersection form $Q_{X_2}$, then gluing along the homology sphere gives a manifold $X$ with intersection form equivalent to $Q_{X_1} \oplus Q_{X_2}$.

Of course, the question now is: what does $\Theta^3_{\mathbb{Z}}$ look like? The structure of this group is as of now unknown!

**Open question.** What is $\Theta^3_{\mathbb{Z}}$?

Here is some of the history of the understanding of this group:

1. Rokhlin: the homology cobordism group is non-trivial. Specifically, it surjects onto $\mathbb{Z}/2\mathbb{Z}$ via the *Rokhlin invariant* $\mu : \Theta^3_{\mathbb{Z}} \to \mathbb{Z}/2\mathbb{Z}$.

2. Donaldson: using Donaldson's diagonalisability theorem, one can show that the Poincaré homology sphere has infinite order in $\Theta^3_{\mathbb{Z}}$. Therefore the homology cobordism group is infinite!

3. Furuta and Fintushel-Stern: $\Theta^3_{\mathbb{Z}}$ is infinitely generated. Both proofs were gauge-theoretic, using the Chern-Simons functional. Precisely, it was shown that $\Sigma(p,q,pqk-1)$ are linearly independent over $\mathbb{Z}$ in $\Theta^3_{\mathbb{Z}}$, where $p,q \geqslant 2$ are relatively prime, and $k \geqslant 1$.

4. Frøyshov: $\Theta^3_{\mathbb{Z}}$ has a $\mathbb{Z}$ summand. This proof uses Heegaard Floer homology!

5. Dai-Hom-Stoffregen-Truong: $\Theta^3_{\mathbb{Z}}$ has a $\mathbb{Z}^\infty$ summand. This uses involutive Heegaard Floer homology.

Of course, as remarked earlier, we also have the structural result that $\Theta^3_{\mathbb{Z}}$ does *not* have any 2-torsion (whis is equivalent to the statement that in every dimension at least 5, there exist non-triangulable manifolds).

We now outline the proof that $\Theta^3_{\mathbb{Z}}$ has a $\mathbb{Z}$ summand. We must introduce the notion of *correction terms*. Let $Y$ be a $\mathbb{Q}H\mathbb{S}^3$, and $s \in \mathrm{Spin}^c(Y)$. Then $HF^\infty(Y,s) = \mathbb{Z}[U,U^{-1}]$. Tensoring with $\mathbb{Q}$, we have $HF^\infty(Y,s;\mathbb{Q}) = \mathbb{Q}[U,U^{-1}]$. Now $HF^-(Y,s;\mathbb{Q})$ decomposes as a direct sum of $\mathbb{Q}[U]$ and a torsion $\mathbb{Q}[U]$-module, i.e. $\mathbb{Q}[U] \oplus HF_{\mathrm{red}}(Y)$.

The diagram of $HF^{\infty,\pm}(Y,s;\mathbb{Q})$ is familiar, shown in figure 5.5.

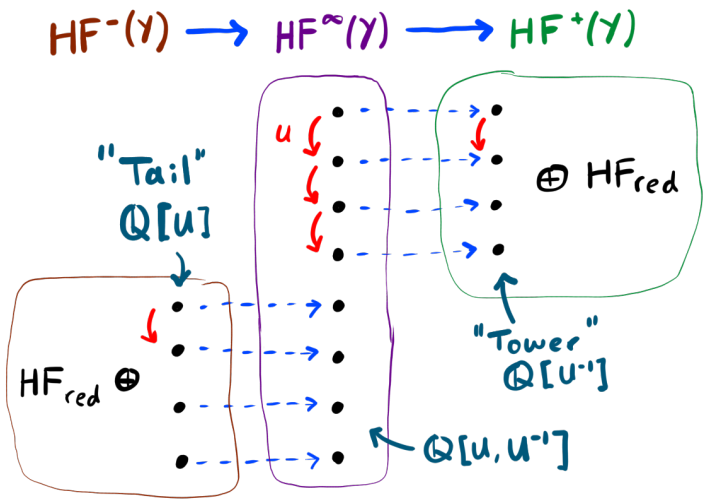


Figure 5.5: Towers and tails in Heegaard Floer homology.

**Definition 5.7.2.** Let $Y$ be a homology sphere and $s \in \mathrm{Spin}^c(Y)$. Then $HF^-(Y,s;\mathbb{Q})$ splits as $\mathbb{Q}[U] \oplus HF_{\mathrm{red}}(Y)$. The $\mathbb{Q}[U]$ summand is called the *tail* of $HF^-$, since it has a maximum grading, but continues forever in the negative-grading-direction. Similarly, $HF^+(Y,s;\mathbb{Q}) = \mathbb{Q}[U^{-1}] \oplus HF_{\mathrm{red}}$, and the $\mathbb{Q}[U^{-1}]$ summand is called the *tower* of $HF^+$.

The *correction term* $d(Y,s)$ measures the mistmatch of the absolute gradings of terms in $HF(Y)$ with that of $HF(\mathbb{S}^3)$. Precisely,

$$d(Y,s) \coloneqq \min\{\mathrm{gr}(x) : x \in \text{tower of } HF^+\} = 2 + \max\{\mathrm{gr}(x) : x \in \text{tail of } HF^-\} \in \mathbb{Q}.$$

**Proposition 5.7.3.** If $Y$ is in $\mathbb{Z}H\mathbb{S}^3$, then there is a unique spin$^c$-structure on $Y$, since $\mathrm{Spin}^c(Y) \cong H^2(Y;\mathbb{Z}) = 0$. Moreover, $d(Y) \coloneqq d(Y,s) \in 2\mathbb{Z}$.

**Proposition 5.7.4.** $d/2$ induces a surjective homomorphism

$$d/2 : \Theta^3_{\mathbb{Z}} \to \mathbb{Z}.$$

*Proof.* A few things need checking: firstly, is the map even well defined? That is, is $d/2$ constant on homology cobordism classes? Secondly, is it really a homomorphism? And finally, is it surjective?

Suppose $Y_0$ and $Y_1$ are homology cobordant integral homology spheres. We will show that $d(Y_0) = d(Y_1)$. By earlier general theory, the homology cobordism $W$ from $Y_0$ to $Y_1$ gives a morphism

$$F^+_{W,s} : HF^+(Y_0) \to HF^+(Y_1),$$

and the map necessarily has no grading shift. But now $d(Y_0) \leqslant d(Y_1)$, since $x$ in the tower of $HF^+(Y_1)$ realising the minimum grading could map to a term in $HF_{\mathrm{red}}(Y_1)$. Now by reversing $W$, we have a homology cobordism from $Y_1$ to $Y_0$ from which it follows that $d(Y_0) \geqslant d(Y_1)$. Therefore $d/2$ is constant on homology cobordism classes as required: we have established that

$$d/2 : \Theta^3_{\mathbb{Z}} \to \mathbb{Z}$$

is at least a well defined set-theoretic map. Next: is it a homomorphism? We must verfiy that

$$d([Y_0] + [Y_1]) = d(Y_0 \# Y_1) = d(Y_0) + d(Y_1).$$

This makes use of the connected sum formula

$$HF^-(Y_0 \# Y_1) = HF^-(Y_0) \otimes_{\mathbb{Z}[U]} HF^-(Y_1).$$

This formula was proven by Ozsváth and Szabó: the idea is that connected sums of 3-manifolds can be expressed as connected sums of Heegaard diagrams, then the "neck" is stretched and analysis on $J$-holomorphic curves is carried out. But now the tail of $HF^-(Y_0 \# Y_1)$ is the tensor product of the tails of each connected summand, and degrees are additive under tensor product. This completes the verification that $d/2$ is a homomorphism!

Finally, a calculation gives

$$d(P) = 2, \quad P \text{ Poincaré sphere.}$$

Therefore $d$ surjects onto $2\mathbb{Z}$, so $d/2$ is a surjective homomorphism from $\Theta^3_{\mathbb{Z}}$ onto $\mathbb{Z}$! $\square$

**Corollary 5.7.5.** *$\Theta^3_{\mathbb{Z}}$ has $\mathbb{Z}$ summand. Precisely,*

$$\Theta^3_{\mathbb{Z}} = \langle P \rangle \oplus \ker(d/2).$$

Elements in the kernel of $d/2$ can be readily constructed: given any $Y \in \Theta^3_{\mathbb{Z}}$, simply consider $Y$ connect sum $(d(Y)/2)\overline{P}$.

# Chapter 6

# Computations in Heegaard Floer homology

We've now constructed a bunch of homology nonsense, and even proven some results, but we haven't actually carried out any non-trivial calculations! Is it feasible to calculate Heegaard Floer homology? Are there any calculational tools? In this chapter we will:

- Carry out a detailed calculation of Heegaard Floer homology for lens spaces (including grading calculations).
- Introduce the *surgery exact triangle* which is the most important tool for calculations. As the name suggests, it aids in calculating Heegaard Floer homologies of manifolds obtained by surgery on knots.
- Prove that there is an algorithm for computing $\widehat{HF}$ for any 3-manifold! Given a Heegaard diagram of the 3-manifold, we can determine its Heegaard Floer homology in a combinatorial manner (without every having to reference analysis or symplectic geometry).

## 6.1 Detailed calculation of $HF$ for lens spaces (lecture 11)

In this section, the lens space $L(p,1)$ denotes $\mathbb{S}^3_p(u)$, i.e. the $p$-surgery on the unknot $u$, where $p \in \mathbb{Z}_{>0}$.

**Remark.** The above convention is used by Ozsváth and Szabó. However, other sources usually use $L(p,1) = -\mathbb{S}^3_p(u)$.

A Heegaard diagram of genus 1 for $L(p,1)$ is given in figure 6.1. In the above diagram, we see that there are $p$ intersection points in $\mathbb{T}_\alpha \cap \mathbb{T}_\beta$. Moreover, there is no topological disk between any two intersection points, bound by the curves - this means each intersection

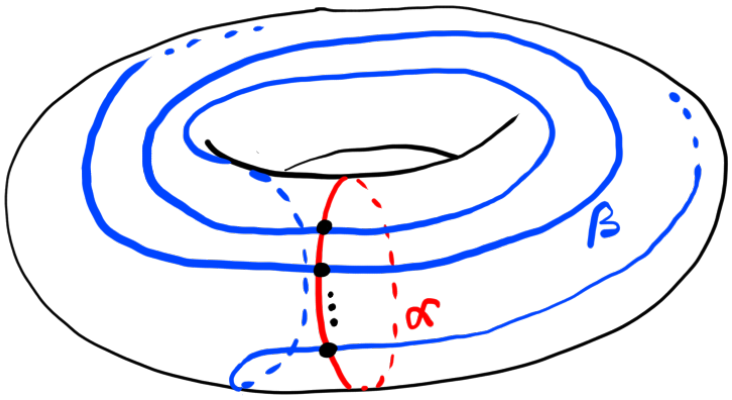


Figure 6.1: Heegaard diagram for $L(p,1)$.

point belongs a distinct equivalence class in $S(Y)$, or equivalently a distinct spin$^c$ structure. This gives

$$\mathrm{Spin}^c(L(p,1)) \cong H^2(L(p,1)) \cong H_1(L(p,1)) = \mathbb{Z}/p\mathbb{Z}$$

as expected. For each $s$, we also have

$$\widehat{HF}(L(p,1),s) = \mathbb{Z}, \quad HF^+(L(p,1),s) = \mathbb{Z}[U^{-1}], \ldots$$

as expected. The non-trivial calculations that are still required are absolute gradings: what are

$$d(L(p,1),s)$$

for each of the $p$ spin$^c$-structures? We will make use of the defining properties of the absolute grading:

- The absolute $\mathbb{Q}$-grading lifts the relative $\mathbb{Z}/N\mathbb{Z}$-grading.
- If $(W,s)$ is a cobordism from $(Y_0,s_0)$ to $(Y_1,s_1)$, then the absolute gradings of $HF^\circ(Y_i,s_i)$ are related by

$$\mathrm{gr}(F^\circ_{W,s}(\xi)) - \mathrm{gr}(\xi) = \frac{c_1(s)^2 - 2\chi(W) - 3\sigma(W)}{4}.$$

Since we know the absolute grading on $HF^\circ(\mathbb{S}^3)$, our best hope is to define a cobordism $W$ from $\mathbb{S}^3$ to $L(p,1)$. At the start of chapter 5 we introduced the cobordism map, and in its construction we explained how knot surgery corresponds to the addition of a 2-handle. That is, if we consider the cylinder $\mathbb{S}^3 \times [0,1]$, but then glue a 4 dimensional 2-handle to the second copy of $\mathbb{S}^3$ with framing $p$, trivially knotted in the cylinder, we obtain a cobordism

from $\mathbb{S}^3$ to $\mathbb{S}^3_p(u)$. This has boundary $\mathbb{S}^3 \sqcup (-\mathbb{S}^3_p(u))$, so we reverse the cobordism to ensure the cobordism is correctly oriented. (That is, we consider the cobordism as a map from $\mathbb{S}^3_p(u)$ to $\mathbb{S}^3$.

In summary, we have maps $F^\circ_{W,s} : HF^\circ(\mathbb{S}^3_p(u), s|_{\mathbb{S}^3_p(u)}) \to HF^\circ(\mathbb{S}^3)$, where $W$ is the reverse of a 2-handle addition. How does the grading change?

- What is $\chi(W)$? We have $H_0(W) = \mathbb{Z}, H_1(W) = 0, H_2(W) = \mathbb{Z}, H_3(W) = \mathbb{Z}, H_4(W) = 0$. Therefore $\chi(W) = 1 + 1 - 1 = 1$.
- What is $\sigma(W)$? The intersection form is $(-p) : H_2(W) \times H_2(W) \to \mathbb{Z}$. This is because the handle has $p$ framing, and the orientation is reversed. It follows that $\sigma = 1$.

Therefore

$$\frac{c_1(s)^2 - 2\chi(W) - 3\sigma(W)}{4} = \frac{c_1(s)^2 - 2 + 3}{4} = \frac{c_1(s)^2 + 1}{4}.$$

This tells us that

$$\mathrm{gr}(F^\circ_{W,s}(\xi)) - \mathrm{gr}(\xi) = \frac{c_1(s)^2 + 1}{4}$$

for any $\circ \in \{\widehat{\ }, +, -, \infty\}$ and any $\xi \in HF^\circ(\mathbb{S}^3_p(u), s|_{\mathbb{S}^3_p(u)})$. We are now free to choose $\circ$ and $\xi$ in ways that can be understood! For example, if we consider $HF^+$, then $1 \in HF^+(\mathbb{S}^3_p(u), s|_{\mathbb{S}^3_p(u)}) = \mathbb{Z}[U^{-1}]$ achieves the minimum grading (and hence the minumum tower grading): $\mathrm{gr}(1) = d(L(p,1), s|_{L(p,1)})$.

This becomes more useful when we recall that

$$F^\infty_{W,s} : HF^\infty(L(p,1), s|_{L(p,1)}) \to HF^\infty(\mathbb{S}^3, s|_{\mathbb{S}^3})$$

is determined by the singular cohomology on $W$: since $W$ is negative definite and $b_1(W) = 0$, the map is an isomorphism! This forces the map to be multiplication by $\pm 1$. Using the exact triangle $HF^- \to HF^\infty \to HF^+$, the cobordism map on $HF^+$ is also multiplication by $\pm 1$. Therefore $1 \in HF^+(L(p,1), s|_{L(p,1)})$ maps to $\pm 1 \in HF^+(\mathbb{S}^3, s|_{\mathbb{S}^3})$, and this is known to have grading 0! Therefore from our choice of $\circ = +$ and $\xi = 1$, we have computed

$$\mathrm{gr}(F^+_{W,s}(1)) - \mathrm{gr}(1) = 0 - d(L(p,1), s|_{L(p,1)}),$$

so that

$$d(L(p,1), s|_{L(p,1)}) = -\frac{c_1(s)^2 + 1}{4}.$$

It remains to understand the possible values of $c_1(s)^2$. To this end, recall that $\mathrm{Spin}^c(W) \cong H^2(W) = \mathbb{Z}$, and the image of $c_1 : \mathrm{Spin}^c(W) \to H^2(W)$ is precisely the space of *characteristic elements*, i.e. $\langle c_1(s), a\rangle \equiv a^2 \mod 2$ for all $a$. So what are the characteristic elements in our case? We require $c_1(s)a \equiv -a^2 p \mod 2$ for all $a \in \mathbb{Z}$. This means the characteristic elements are exactly those with parity $p$. Moreover, we know from general theory that

$c_1 : \mathrm{Spin}^c(W) \to H^2(W)$ is injective if $H^2$ has no 2-torsion. This is indeed the case, so $c_1$ defines a bijection onto the subset of $\mathbb{Z}$ with the same parity as $p$.

We describe this isomorphism by declaring that for each $j \in \mathbb{Z}$, $s_j \in \mathrm{Spin}^c(W)$ is the unique spin$^c$ structure with $c_1(s_j) = 2j - p \in \mathbb{Z} = H^2(W)$.

With this identification, we can compute $c_1(s)^2$. The intersection form is induced from Poincaré duality, in the sense that

$$PD : H_2(W; \mathbb{Q}) \to H^2(W; \mathbb{Q})$$

is given by multiplication by $-p$. Let $\xi \in H_2(W; \mathbb{Z}) \subset H_2(W; \mathbb{Q})$ be a generator. Then the Poincaré duality map sends $\xi$ to $-p\zeta$, where $\zeta$ is a generator of $H^2(W; \mathbb{Z}) \subset H^2(W; \mathbb{Q})$. Thus $\xi^2 = -p$. Now

$$\zeta^2 = (\xi/-p)^2 = \xi^2/p^2 = -p/p^2 = -1/p.$$

It follows that $a \cdot a = -a^2/p$ for $a \in H^2(W; \mathbb{Q})$. In particular,

$$c_1(s_j)^2 = -\frac{(2j-p)^2}{p}.$$

In particular, this gives

$$d(L(p,1), s_j|_{L(p,1)}) = \frac{(2j-p)^2 - p}{4p}.$$

This is currently expressed in terms of spin$^c$ structures on $W$, so it would be good to express this intrinsically in terms of spin$^c$ structures on $L(p,1)$. There is a natural map $H^2(W) \cong \mathbb{Z} \to H^2(L(p,1)) \cong \mathbb{Z}/p\mathbb{Z}$; the quotient map. Therefore there is a corresponding map

$$\mathrm{Spin}^c(W) \to \mathrm{Spin}^c(L(p,1)), \quad s_j \mapsto [s_j], s_j \sim s_j + kp, k \in \mathbb{Z}.$$

This gives an identification of $\mathrm{Spin}^c(L(p,1))$ with $\{0, \dots, p-1\}$, so that

$$d(L(p,1), s_j) = \frac{(2j-p)^2 - p}{4p}, \quad 0 \leqslant j < p.$$

This completes our example! It'll be interesting to see how things change when we consider $L(p,q)$.

## 6.2 A compuational tool: the surgery exact triangle

In our previous example, we already knew the spaces $HF$ if we ignored gradings. However, in other applications even calculating $HF^\circ(Y)$ can be tricky. The *surgery exact triangle* is a useful tool for this scenario.

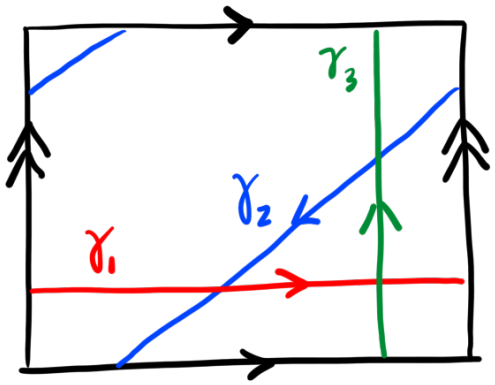


Figure 6.2: Surgery exact triangle example.

**Theorem 6.2.1.** *Let $M$ be a compact oriented 3-manifold, with $\partial M = T^2$. Let $\gamma_1, \gamma_2, \gamma_3$ be curves on $\partial M$ such that*

$$\gamma_1 \cdot \gamma_2 = \gamma_2 \cdot \gamma_3 = \gamma_3 \cdot \gamma_1 = -1.$$

*(The dot denotes signed intersections.) For each $i$, let $Y_i = M \sqcup_{\gamma_i} (\mathbb{S}^1 \times D^2)$. That is, glue $M$ to $\mathbb{S}^1 \times D^2$ along their common boundary by identifying $\gamma_i$ with the meridian $\{1\} \times \partial D^2$. Then there exists a long exact sequence (for any $\circ \in \{\widehat{\ }, +, -, \infty\}$),*

$$\cdots \to HF^\circ(Y_1) \to HF^\circ(Y_2) \to HF^\circ(Y_3) \to \cdots,$$

*where maps are induced by surgery cobordisms.*

In figure 6.2, we give examples of curves $\gamma_i$ meeting the conditions of the premise. We do not prove this theorem, but it is explained in detail in *Lectures on Heegaard Floer homology* by Ozsváth and Szabó. Instead, we now investigate an example.

**Example.** Let $M = \mathbb{S}^3 - N(K)$, where $K$ is a knot, and $N(K)$ a tubular neighbourhood of $K$. Let $m$ be the meridian of $N(K)$, and $\ell$ the longitude. That is, $[\ell] = 0$ in $H_1(M)$, $m \cdot \ell = -1$, and $m^2 = \ell^2 = 0$. We can take

$$\begin{aligned}\gamma_1 &= m \\ \gamma_2 &= pm + \ell \\ \gamma_3 &= -((p+1)m - \ell).\end{aligned}$$

These curves meet the premise for the surgery exact triangle, giving an exact sequence sequence

$$\cdots \to HF^\circ(\mathbb{S}^3) \to HF^\circ(\mathbb{S}^3_p(K)) \to HF^\circ(\mathbb{S}^3_{p+1}(K)) \to \cdots.$$

More generally, the purpose of the surgery exact triangle is the same as any long exact sequence: if we have a sufficient understanding of two of the involved spaces, we can deduce information about the third!

**Example.** Another variation of the surgery exact triangle is the following:

$$\cdots \to HF^\circ(\mathbb{S}^3) \to \bigoplus_{j \equiv i \mod p} HF^\circ(\mathbb{S}^3_0(K), j) \to HF^\circ(\mathbb{S}^3_p(K), i) \to \cdots .$$

The exact sequence holds for all $i \in \mathrm{Spin}^c(\mathbb{S}^3_p(K)) \cong \mathbb{Z}/p\mathbb{Z}$. Note that $\mathrm{Spin}^c(\mathbb{S}^3_0(K)) \cong \mathbb{Z}$, so we're summing over all the $j \in \mathbb{Z}$ congruent to a fixed $i$ mod $p$.

**Exercise.** What is the Heegaard Floer homology of $\mathbb{S}^3_p(T)$, where $T$ is the right handed trefoil knot?

A result of Moser gives that

$$\mathbb{S}^3_5(T) = L(5,4) \cong -L(5,1) = -\mathbb{S}^3_5(u).$$

We know the Heegaard Floer homology of $L(5,1)$ from our first example in class. But now a general recipe for determining the Heegaard Floer homology of $\mathbb{S}^3_p(T)$ is:

1. Determine the Heegaard Floer homology of $\mathbb{S}^3_5(T)$ by using the diffeomorphism with $-\mathbb{S}^3_5(u)$.
2. Use the version of the surgery exact triangle from the previous example to determine the Heegaard Floer homology of $\mathbb{S}^3_0(T)$.
3. Use the surgery exact triangle again to determine the Heegaard Floer homology of $\mathbb{S}^3_p(T)$ for any $p$.

In particular, $-\mathbb{S}^3_1(T)$ is the Brieskorn sphere $\Sigma(2,3,5)$, commonly referred to as the Poincaré homology sphere!

To be more explicit, the calculations to determine $HF^\circ(\mathbb{S}^3_p(T))$ can be carried out by combining two facts: firstly, the maps on $HF^\infty$ in the surgery exact triangle are all *isomorphisms*, since the cobordisms being considered are negative definite! Secondly, the

$$\cdots \to HF^- \to HF^\infty \to HF^+ \to \cdots$$

exact triangle commutes with cobordism maps. Therefore, to determine $HF^+(\mathbb{S}^3_p(K), i)$ (along with gradings), we can use the following commutative infinite grid:

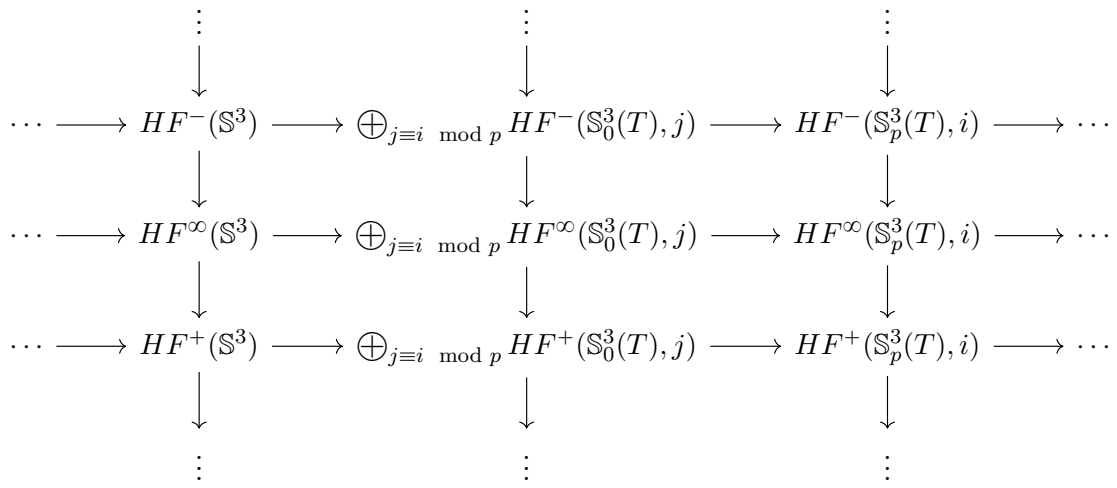

Using these exact grids, we can, for example, compute $HF^+(\Sigma(2,3,5)) = HF^+(P)$. It turns out that $HF^+(P) = \mathbb{Z}[U^{-1}]$, with $d(P) = 2$. (This is detailed in Ozsváth and Szabó's *Absolutely graded Floer homologies and intersection forms for four-manifolds with boundary.*) Recall that we used this fact earlier in our proof that $\Theta^3_{\mathbb{Z}}$ has a $\mathbb{Z}$ summand! We've just shown that $d/2 : \Theta^3_{\mathbb{Z}} \to \mathbb{Z}$ is surjective, since it sends $P$ to 1. We can also show that $HF_{\text{red}}(P) = 0$.

## 6.3 General algorithm to compute $\widehat{HF}$ (lecture 12)

As mentioned a few times prior, one of the most powerful aspects of Heegaard Floer homology is that it can theoretically be computed for any space, if we know its Heegaard decomposition! This means that any question answered in terms of Heegaard Floer homology answers the question in general. (For example, we will see in the next lecture that Heegaard Floer homology detects the Thurston norm, i.e. lower bounds on the genus of surfaces representing a class in $H^2(Y^3)$.)

**Theorem 6.3.1** (Sarkar-Wang)**.** *Let $H$ be a Heegaard diagram of a 3-manifold $Y$. There is an algorithm to compute $\widehat{HF}(Y)$ in $\mathbb{Z}/2\mathbb{Z}$-coefficients in terms of the combinatorial data of $H$.*

This theorem will take a lot of work to prove, so we'll start by explaining the goal. That is, what exactly do we need to create an algorithm for? The problem comes down to computing the differentials in the Heegaard Floer chain complex. This map cares about

$$\varphi \in \pi_2(x,y), \quad \mu(\varphi) = 1 \text{ and } D(\varphi) = \sum_i a_i R_i, a_i \geqslant 0.$$

The first condition on $\varphi$ is immediate from the definition of the map, but the second condition comes from implicit complex geometry: one can show that

$$a_i = [\varphi] \circ [\{z_i\} \times \mathrm{Sym}^{g-1}(\Sigma)], z_i \in R_i,$$

and for an arbitrary $\varphi \in \pi_2(x, y)$ this can be anything. However, for $\varphi$ to have a *holomorphic* representative, $a_i$ must be non-negative.

To understand the boundary maps, we must calculate $\#(\mathcal{M}(\varphi)/\mathbb{R})$ for $\varphi$ as above. We have discovered earlier that this is difficult in general! The idea is to change the Heegaard diagram (by Heegaard moves) to make it easy to count. Recall from earlier that we know that if a domain $D(\varphi)$ is a rectangle or bigon, then $\#(\mathcal{M}(\varphi)/\mathbb{R}) = \pm 1$. If we work in mod 2 coordinates, all signs are lost! Therefore we will aim to arrange Heegaard diagrams in this manner - then the boundary map can genuinely be computed combinatorially. The main idea of the theorem is that all Heegaard diagrams can be changed into a Heegaared diagram in which all regions (not including the basepoint) are either bigons or rectangles! Expanding and proving all of these ideas will be the goal of the rest of this section.

**Remark.** The result from this section is actually very surprising. Lagrangian Floer homology is known to require geometry and gauge theory, as well as analysis. Since $\widehat{HF}$ was modelled off Lagrangian Floer homology, it was also expected to depend on these tools. This result started a whole new direction of research.

The remainder of this section can be broken up into two subsections:

1. Proof that $\#(\mathcal{M}(\varphi)/\mathbb{R}) = \pm 1$ for $D(\varphi)$ consisting of bigons or rectangles, and $\mu(\varphi) = 1$.

2. Proof that Heegaard diagrams are equivalent to ones with just bigons and rectangles (away from the basepoint).

As mentioned above, combining these two facts leads to the desired result.

**Lemma 6.3.2.** Let $D(\varphi) = \sum_i a_i R_i$ be a domain, with $a_i \geqslant 0$ for each $i$, and $R_i$ a bigon or rectangle whenever $a_i > 0$. Suppose moreover that $\mu(\varphi) = 1$. Then $D(\varphi)$ has exactly one $J$-holomorphic representative.

*Proof.* Let $D$ be a domain for $\varphi \in \pi_2(x, y)$ as above. Recall the *Lipshitz formula*:

$$\mu(\varphi) = e(D) + n_x(D) + n_y(D),$$

where $e(D)$ is the Euler measure, and $n_x$ and $n_y$ are average vertex multiplicities. Since $x, y \in \mathbb{T}_\alpha \cap \mathbb{T}_\beta$, we can write $x = \{x_1, \ldots, x_g\}$ and $y = \{y_1, \ldots, y_g\}$, where the $x_i$ and $y_j$ are genuine intersection points of curves on $\Sigma$.

Recall that domains $D$ satisfy $\partial D = \partial_\alpha D + \partial_\beta D$, where

$$\partial(\partial_\alpha D) = \partial(\partial_\beta D) = x - y = \sum x_i - \sum y_i.$$

We now calculate some relations that must hold between the multiplies of regions meeting at a vertex. Suppose $p \in \alpha_i \cap \beta_i$ is an intersection point, with $x_i \notin x, p \notin y$. Locally $D$ looks like the left side of figure 6.3: notice that since $p$ is *not* a vertex of $D$, any multiplicity at a quadrant must be shared with neighbouring quadrants (so that no "corners" occur). Overall, the region near the quadrant must be formed by laying "strips" adjacent to $p$.

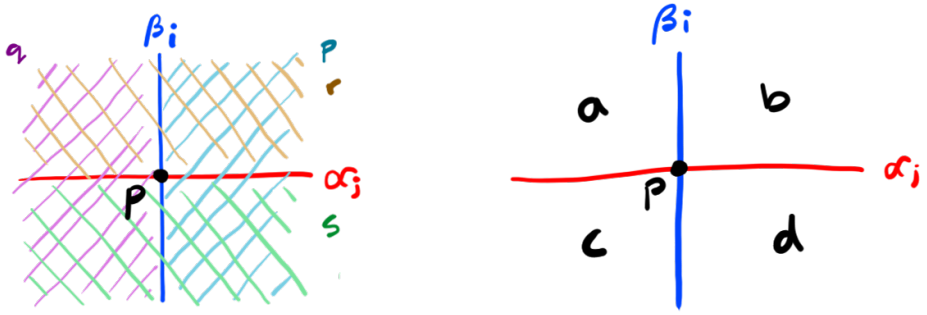


Figure 6.3: Local structure at $p$, where $p \in \alpha_j \cap \beta_i$ does not lie in $x$ nor $y$.

Using the coordinates on the right, we have

$$a = q + r, b = p + r, c = q + s, d = p + s.$$

But now $a + d = p + q + r + s = b + c$. Using similar analyses together with the local examples in figure 6.4 (to show the choice of orientation), we obtain the following identities:

- $p \notin x, p \notin y \Rightarrow a + d = b + c$
- $p \notin x, p \in y \Rightarrow a + d = b + c + 1$
- $p \in x, p \notin y \Rightarrow a + d + 1 = b + c$
- $p \in x, p \in y \Rightarrow a + d + 1 = b + c + 1 \Rightarrow a + d = b + c$.

In particular, in the first and last case, the average vertex multiplicity at $p$ is a half-integer, while in the middle cases it is an odd quarter-integer (i.e. $(a + b + c + d)/4 \in \frac{1}{2}\mathbb{Z} + \frac{1}{4}$).

We can now proceed with the main body of the proof. Let $D(\varphi) = \sum_i a_i R_i$ with $a_i \geqslant 0$, and $R_i$ a bigon or rectangle whenever $a_i > 0$. Suppose $\mu(\varphi) = 1$. Two possible types of domains satisfying these conditions are shown in figure 6.5. We know from earlier in the class that domains of the types shown in figure 6.5 have exactly one $J$-holomorphic representative. Therefore we prove that no other types of domains are possible!

By the Lipshitz formula, $\mu(\varphi) = e(D) + n_x(D) + n_y(D) = 1$. Since $e(D) = \sum_i a_i e(R_i)$, the only Euler measure contributions come from regions with $a_i > 0$. Such regions are

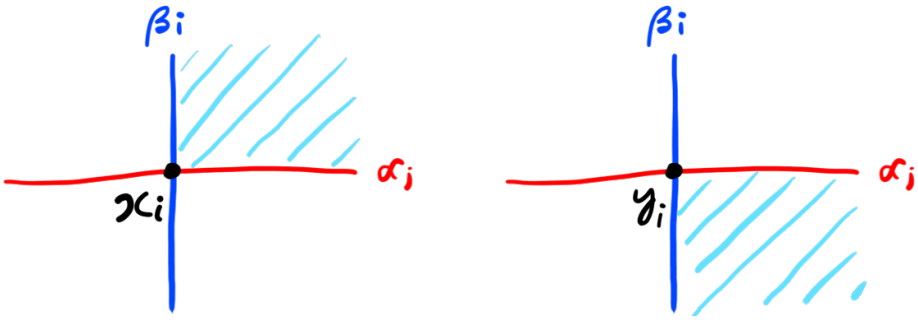


Figure 6.4: Local structure at $x_i$ and $y_i$ (example).

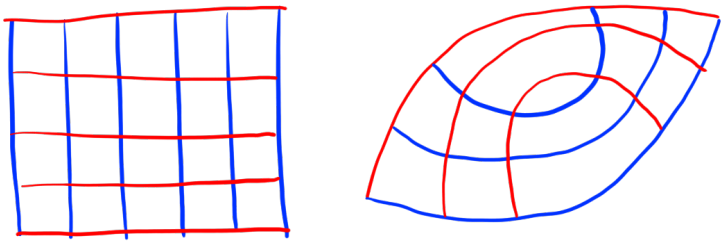

Figure 6.5: Two types of domains with one holomorphic representative.

necessarily bigons or rectangles, which have Euler measure 0 or 1/2. Recall that this comes from the formula

$$e(\Sigma) = \chi(\Sigma) - \frac{\#\text{right angles}}{4}.$$

We also have the assumption that $n_x(D), n_y(D) \geqslant 0$, from the fact that each $a_i$ is non-negative. This immediately restricts us to three cases:

1. $e(D) = 1, n_x(D) = n_y(D) = 0$.
2. $e(D) = 1/2, n_x(D) + n_y(D) = 1/2$.
3. $e(D) = 0, n_x(D) + n_y(D) = 1$.

We will now work through these cases one by one.

1. If $n_x(D) = n_y(D) = 0$, then there are no points $p \in \alpha_i \cap \beta_j \cap D$ such that $p$ lies in exactly one of $x$ or $y$. This is because of the local structure of intersection points determined at the start of this proof: the average vertex multiplicity of any such point is necessarily an odd quarter integer (which is necessarily non-zero). The sum of any number

of non-negative non-zero numbers will give a positive result, which is prohibited. Therefore all intersection points $p$ occuring in $D$ either belong to neither $x$ nor $y$, or both $x$ and $y$. This forces $x = y$ for our strip $\varphi$, so that $\varphi$ is the constant strip. Then $\mu(\varphi) = 0$. This breaks one of our premises! No domains $D$ are of the first type.

2. If $e(D) = 1/2$ and $n_x(D) + n_y(D) = 1/2$, then either $n_x(D) = n_y(D) = 1/4$, or one of them is 0 and the other is a half. We also know that the regions making up the domain must consist of exactly one bigon and many rectangles, simply by considering $e(D)$. The existence of the bigon prohibits the latter options for $n_x(D)$ and $n_y(D)$, so we must have $n_x(D) = n_y(D) = 1/4$. Now there are exactly two intersection points which are non-constant, and the rest have trivial multiplicity. Overall this tells us that $D$ must itself be a bigon, i.e. of the form described earlier.

3. In the final case, $e(D) = 0$ and $n_x(D) + n_y(D) = 1$. Since $e(D) = 0$, all regions are necessarily rectangles. The only way rectangles can be stitched together to achieve the premise is for $D$ itself to be a large rectangle, i.e. of the form described earlier.

This completes the proof that our domain $D(\varphi)$ is of a form where $\#(\mathcal{M}(\varphi)/\mathbb{R})$ is known to be plus or minus 1! □

The next question is whether or not we can take an arbitrary Heegaard diagram and turn it into a diagram where all regions are bigons or rectangles. If so, that would be our algorithm!

**Remark.** Unfortunately, this is impossible in general. Suppose the Heegaard diagram has genus $g(\Sigma) \geqslant 2$. Then

$$2 - 2g = \chi(\Sigma) = e(\Sigma) = \sum e(R_i) \geqslant 0,$$

which is absurd. Moreover, the only manifolds with Heegaard diagrams of genus at most 1 are $\mathbb{S}^3, \mathbb{S}^1 \times \mathbb{S}^2$, and lens spaces $L(p, q)$.

**Remark.** Rejoice! For $\widehat{HF}$ we only require counting regions that do not include the basepoint $z \in \Sigma$! This means we cna hopefully transform our Heegaard diagram into one for which all regions not including the basepoint are either bigons or squares. This can indeed be done.

**Theorem 6.3.3.** *Let $Y$ have based Heegaard diagram $(\Sigma, \alpha, \beta, z)$. Then one can change $\alpha, \beta$ by a sequence of handleslides and isotopies to obtain a Heegaard diagram in which all regions not containing $z$ are bigons or rectangles. (Sarkar and Wang refer to such diagrams as* nice diagrams*).*

*Proof.* Let $(\Sigma, \alpha, \beta, z)$ be the Heegaard diagram. Originally, some regions might not be polygons (that is, they might not be simply connected). By using isotopies, we can assume without loss of generality that all regions are polygons. (See figure 6.6.)

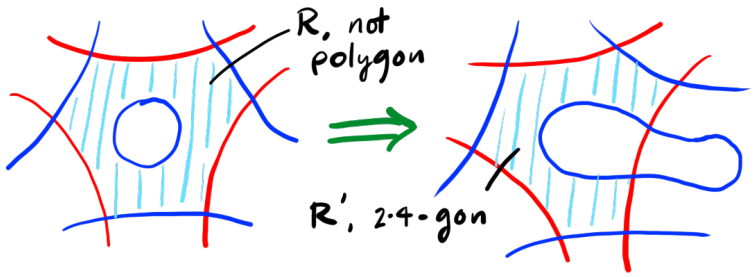


Figure 6.6: Using isotopies, all regions can be made into polygons.

Each region $R$ is now a polygon, with $2n$ edges. We say that $R$ is *good* if $n \leqslant 2$, and *bad* if $n \geqslant 3$. This is because we want our regions to eventually be bigons or rectangles, which are exactly the good polygons. We define the *badness* of a polygon to be

$$b(R) = \max(0, n-2).$$

Thus the goal of the proof is to move all of the *badness* to the region containing $z$.

Now let $D$ denote a bad region. We further define $d(D)$ to be the *minimum number of $\beta$ curves that must be crossed to get from $D$ to the region containing $z$, by a path not intersecting $\alpha$-curves.* Intuitively, $d(D)$ is the distance from $D$ to $z$ through $\beta$ curves.

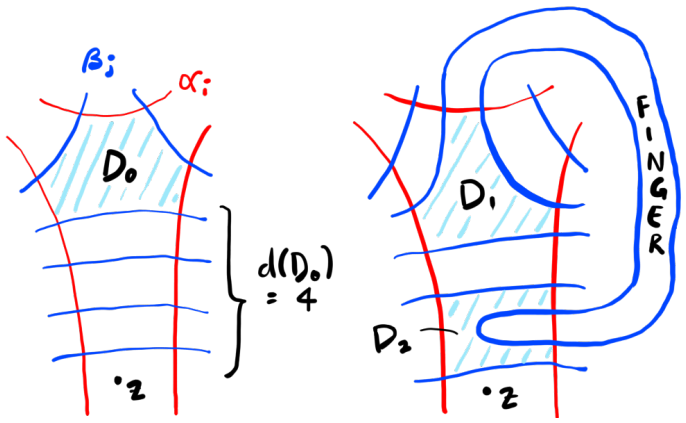


Figure 6.7: Using isotopies, all regions can be made into polygons.

In the left of figure 6.7, the region $D$ has distance $d(D) = 4$. (It also has badness $b(D) = 1$). The main idea of this proof is not to initially decrease the badness itself, but decreases the distances of the bad regions. For example, on the right of figure 6.7, we have "pushed a finger" from a $\beta$ curve through a series of $\alpha$ curves. In the resulting Heegaard

diagram, there are two bad regions instead of one; of badnesses 1 each. However, the bad regions have distance 1 and 3 from $z$, so $\max\{d(D) : b(D) \neq 0\}$ has decreased!

$$d(D_0) = 4, b(D_0) = 1 \quad \rightsquigarrow \quad \begin{cases} d(D_1) = 3, b(D_1) = 1 \\ d(D_2) = 1, b(D_2) = 1. \end{cases}$$

In our algorithm, we will aim to move all badness closer to $z$, even at the expense of the number of bad regions or individual badnesses getting worse.

More precisely, let $d = \max\{d(D) : b(D) \neq 0\}$ denote the maximum distance of any bad region from $z$. Let $D_1, \ldots, D_m$ be the bad regions at distance $d$ from $z$. We want a sequence of moves doing the following:

1. Decrease the maximum distance $d$.
2. Keep the same $d$, but decrease the total badness of the regions at distance $d$, i.e. decrease $\sum_{i=1}^{m} b(D_i)$.
3. Keep the same $d$ and $\sum_{i=1}^{m} b(D_i)$, but decrease $m$, i.e. decrease the number of regions achieving the maximum distance $d$. Formally we will decrease the *distance complexity*, which is the quantity $(b(D_1), \ldots, b(D_m))$ measured with the lexicographic norm, where $D_i$ are initially ordered so that $b(D_i) \leqslant b(D_{i+1})$. Notice that if this strictly decreases with each step, then after a finite number of steps $m$ can be made arbitrarily small.

We order these changes lexicographically - each is an improvement to the diagram, but decreasing $d$ is preferred over decreasing $\sum_{i=1}^{m} b(D_i)$ etc. Therefore if we consider the quantity

$$(d, \sum_{i=1}^{m} b(D_i), b(D_1), \ldots, b(D_m))$$

with lexicographic norm, our goal is to find a sequence of moves which continuously decreases $(d, \sum_{i=1}^{m} b(D_i), b(D_1), \ldots, b(D_m))$ until $d = 0$. We will refer to the lexicographic size of $(d, \sum_{i=1}^{m} b(D_i), b(D_1), \ldots, b(D_m))$ as the *complexity* of the diagram.

We will now describe a collection of such moves (which forms the algorithm), hence completing the proof.

1. Choose a bad region with the *least badness* amongst regions achieving the maximum distance $d$. (That is, consider the region $D_1$.)
2. Push a finger from a $\beta$ curve bounding the region through an $\alpha$ curve of the same region, and continuing pushing as follows:
   (a) If the finger enters a rectangle, keep pushing - *unless* the rectangle has a smaller distance to $z$.

(b) If the finger enters a bigon, stop.

(c) If the finger enters a bad region, stop.

(d) If the finger re-enters the original region, then it necessarily encircles a $\beta$ curve. Handleslide over the encircled $\beta$ curve, as in figure 6.8.

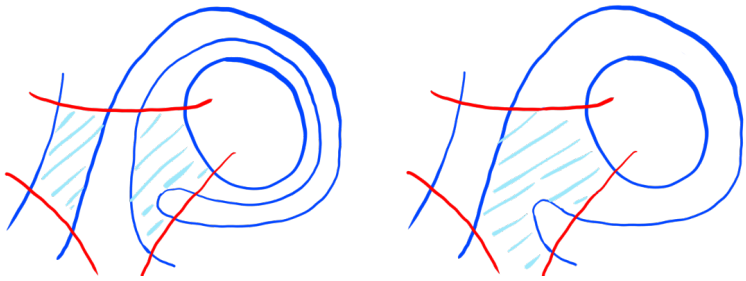

Figure 6.8: Handleslide, if a finger is pushed into its starting region.

The moves above are guaranteed to strictly decrease the completely of the Heegaard diagram with every move! Therefore it must eventually force $d = 0$, as required. It remains to verify that the moves really decrease the complexity.

- If we stop at (a), then the original region has been broken into two regions, with smaller badness. The complexity has strictly decreased because $d$ could not have increased, since the only region with increasing badness has distance less than $d$ from $z$. However, if $d$ has not decreased, then $\sum b(D_i)$ has strictly decreased, as the original region has been broken into separate regions! (One can verify that it has decreased by exactly 1.)

- If we stop at (b), the same argument as above holds.

- If we stop at (c), by the hypothesis, the region in which we've stopped has a smaller-or-equal distance to $z$. If the region has a smaller distance, the same argument as above holds. If the region has the same distance, then $d$ has not decreased, and one can verify that $\sum b(D_i)$ is also left unchanged. However, we have moved some of the badness of $D_1$ to a subsequent region, so the complexity has indeed strictly decreased.

- Finally if we stop at (d), then once against $d$ might have decreased, but if not, then $\sum b(D_i)$ has decreased!

This completes the proof! (Technically some of the details are missing in the difficult case of (d), but these can be checked in the original paper of Sarkar and Wang.) □

**Corollary 6.3.4.** *There is a combinatorial description of* $\widehat{HF}$ *over* $\mathbb{Z}/2\mathbb{Z}$.

Later we will study some other algorithms as well! In particular, Manolescu, Ozsváth and Dylan Thurston developed an algorithm for $HF^{\pm}$ and 4-manifold invariants, using surgery formulae and nice diagrams.

# Chapter 7

# Applications in three dimensions

In an earlier chapter we studied some applications of Heegaard Floer homology in four dimensions, but we have yet to see any three dimensional applications! One of the most celebrated applications is that it detects the Thurston norm. We will also study $L$-spaces, which are the "homologically simple spaces" in the setting of Heegaard Floer homology.

## 7.1 $L$-spaces (lecture 13)

**Definition 7.1.1.** A 3-manifold $Y$ is an *$L$-space* if $\widehat{HF}(Y,s) = \mathbb{Z}$ for all $s$ in $\mathrm{Spin}^c(Y)$.

This is the Heegaard Floer homology version of an integral homology sphere.

**Example.** Some $L$-spaces include $\mathbb{S}^3$, lens spaces, and the Poincaré homology sphere.

**Example.** Some spaces which are *not* $L$-spaces are $1/n$-surgeries on the trefoil knot $T$, for $n \geqslant 2$. One can also simply consider spaces with $b_1 > 0$.

**Proposition 7.1.2.** Let $Y$ be a closed oriented 3-manifold. The following are equivalent:

1. $Y$ is an $L$-space.
2. $HF^+(Y,s) = \mathbb{Z}[U^{-1}]$ for all $s$.
3. $HF^-(Y,s) = \mathbb{Z}[U]$ for all $s$.
4. $Y$ is a rational homology sphere, and $HF_{\mathrm{red}}(Y) = 0$.

**Corollary 7.1.3.** *If a closed 4-manifold $X$ admits an $L$-space as an admissible cut, then $\Phi_{X,s} = 0$ for all $s$.*

*Proof.* We now prove the previous proposition. The first three are all equivalent via the exact triangles

$$0 \to \widehat{HF} \to HF^{\pm} \xrightarrow{U} HF^{\pm} \to 0.$$

It remains to prove that $Y$ is an $L$-space if and only if $Y$ is a rational homology sphere with trivial reduced Heegaard Floer homology.

One direction is easy: suppose $Y$ is a rational homology sphere. Then

$$HF^{\infty}(Y,s) = \mathbb{Z}[U,U^{-1}],$$

from which we have that $HF^{-}(Y,s) = \mathbb{Z}[U] \oplus HF_{\mathrm{red}}$. Now if $HF_{\mathrm{red}}(Y)$ vanishes, $HF^{-}(Y,s) = \mathbb{Z}[U]$ as required.

For the converse, we require a lemma. Namely, the Euler characteristic $\chi(\widehat{HF}(Y,s))$ depends only on homology:

$$\chi(\widehat{HF}(Y,s)) = \begin{cases} \pm 1 & b_1(Y) = 0 \\ 0 & b_1(Y) > 0. \end{cases}$$

It follows that if $Y$ is an $L$-space, then it must have $\chi(\widehat{HF}(Y,s)) = \pm 1$. But then $b_1(Y) = 0$, so $Y$ is a rational homology sphere.

We now prove this lemma. Recall that

$$\widehat{HF}(Y) = \bigoplus_{s \in \mathrm{Spin}^c(Y)} \widehat{HF}(Y,s),$$

and that

$$\chi(\widehat{HF}(Y)) = [\mathbb{T}_\alpha] \cdot [\mathbb{T}_\beta] \text{ in } \mathrm{Sym}^g(\Sigma).$$

A Heegaard decomposition of genus $g$ for $Y$ consists of a CW-complex for $Y$ with one 0-cell, $g$ 1-cells, $g$ 2-cells, and one 3-cell. Therefore $H_*(Y)$ comes from the complex

$$0 \to \mathbb{Z} \xrightarrow{0} \mathbb{Z}^g \xrightarrow{D} \mathbb{Z}^g \xrightarrow{0} \mathbb{Z} \to 0,$$

where $D$ is a $g \times g$ matrix, $D_{ij} = [\alpha_i] \cdot [\beta_j]$ in $\Sigma$. Overall, we have $[\mathbb{T}_\alpha] \cdot [\mathbb{T}_\beta] = \det D$. Since $H_1(Y) = \mathbb{Z}^g / \operatorname{im} D$, if $b_1 > 0$ it must be the case that $D$ is singular ($\det D = 0$), and if $b_1 = 0$ then $|H_1(Y)| = \pm \det D$. In summary we have established that

$$\chi(\widehat{HF}(Y)) = \begin{cases} 0 & b_1 > 0 \\ \pm |H_1(Y)| & b_1 = 0. \end{cases}$$

The remaining ingredient is the fact that $\chi(\widehat{HF}(Y,s))$ is independent of $s$! This is because we can change $s$ by moving the basepoint to a different location. (That is, the bijective

correspondence of $\mathrm{Spin}^c(Y)$ with $S(Y)$ is non-canonical, depending on the choice of base point.) But we also know that $S(Y) \cong H_1(Y)$, so this implies that

$$\chi(\widehat{HF}(Y)) = \sum_{i \in |H_1(Y)|} \chi(\widehat{HF}(Y,s)) \quad \Rightarrow \quad \chi(\widehat{HF}(Y,s)) = \begin{cases} 0 & b_1 > 0 \\ \pm 1 & b_1 = 0 \end{cases}$$

as required. □

This motivates $L$-spaces in one way: understanding $L$-spaces helps us to understand 4-manifolds with trivial mixed invariant.

Another reason we care about $L$-spaces is because of the Boyer-Gordon-Watson conjecture, which we first state and then explain (since the statement will contain some unfamiliar terms).

**Conjecture.** Let $Y$ be a closed oriented 3-manifold. It is conjectured that the following are equivalent:

1. $Y$ is not an $L$-space.
2. $Y$ carries a coorientable taut foliation.
3. $\pi_1(Y)$ is left orderable.

**Remark.** This conjecture, if it holds, is truly remarkable. The first statement lies in the realm of Heegaard Floer homology, which comes from symplectic geometry (and has a combinatorial description in terms of a Heegaard decomposition). The second statement lies in the realm of differential topology, and the third statement is purely algebraic. The conjecture binds together separate mathematical realms.

We now describe what the conjecture actually means, by defining the missing terminology.

**Definition 7.1.4.** A *foliation* of an $n$-manifold $X$ is a decomposition $X = \bigcup_{t \in T} \mathcal{L}_t$ into $k$-dimensional *leaves* $\mathcal{L}_t$, so that locally $T$ satisfies

$$\mathcal{R}^n = \bigcup_{t \in \mathbb{R}^{n-k}} (\{t\} \times \mathbb{R}^k).$$

A foliation of a 3-manifold $Y^3$ by surfaces is said to be *taut* if there is an embedded circle $\gamma \in Y$ meeting every leaf transversely at least once. Finally, any foliation is said to be coorientable if the normal bundles to the leaves are orientable.

**Example.** The product $\mathbb{S}^1 \times \Sigma$ for $\Sigma$ a surface is trivially a foliation by surfaces$\{t\} \times \Sigma$. It's automatically taut, as we can take the curve $\mathbb{S}^1 \times \{\mathrm{pt}\}$ for any point in $\Sigma$.

**Example.** A non-example of a taut foliation is the Reeb foliation, which is a foliation of $\mathbb{S}^3$ by surfaces by decomposing it into two solid tori, and foliating each solid torus by spiralling "cups".

There are some cool results about taut foliations, such as the following:

**Theorem 7.1.5** (Sullivan)**.** *A foliation of $Y^3$ by surfaces is taut if and only if there exists a metric on $Y$ such that all leaves are minimal surfaces.*

**Theorem 7.1.6** (Eliashberg-Thurston)**.** *If a manifold $Y^3$ admits a taut foliation, then it admits a tight contact structure.*

We do not explain what the above theorem means, but Ozsváth and Szabó proved that if a space admits a tight contact structure then it cannot be an $L$-space! This is the only direction known to hold in the Boyer-Gordon-Watson conjecture.

Next we briefly explore the algebraic side of the conjecture.

**Definition 7.1.7.** A non-trivial group $G$ is called *left-orderable* if there exists a total order on $G$ such that $g < h$ if and only if $kg < kh$, for all $k \in G$.

**Example.** $\mathbb{Z}$, $\mathbb{R}$, and $\mathbb{Z}^n$ (lexicographical) are all left orderable.

**Example.** A non-example is any group $G$ with non-trivial torsion. Suppose $g \in G$ has order $n$. Then if $1 < g$, then $g < g^2$, and $g^2 < g^3$ and so on, until we reach $g^{n-1} < g^n = 1$. Therefore $1 < 1$, which is impossible. The same contradiction holds if $g < 1$.

The BGW conjecture has actually been verified for many classes of 3-manifolds! For example, all *graph manifolds* are known to satify the conjecture. These are manifolds that split into Seifert fibred spaces after cutting along spheres and tori.

Finally we remark that $L$-spaces are *rational* homology spheres with trivial reduced Heegaard Floer homology, so there is no clear connection with *integral* homology spheres. It turns out that the only known integral homology spheres which are $L$-spaces are obtained by gluing together the Poincaré homology sphere.

**Conjecture.** If $Y$ is a $\mathbb{Z}H\mathbb{S}^3$, then $Y$ is an $L$-space if and only if $Y$ is a connected sum

$$Y = nP\#m\overline{P}.$$

Crazy! Recall that the Poincaré homology sphere is the only non-trivial Brieskorn homology sphere with finite fundamentak group, but in principle there could be many other integral homology spheres which are $L$-spaces (as we need not restrict ourselves to Brieskorn spheres).

## 7.2 Genus bounds

Let $Y^3$ be a 3-manifold, and $a \in H_2(Y)$. To study $H_2(Y)$, one approach is to define a notion of the complexity of $a$. For this, we introduce a notion of complexity for surfaces.

Given a surface $\Sigma$, which has connected components $\Sigma_i$ (so that $\Sigma = \sqcup_i \Sigma_i$), we define

$$\chi_-(\Sigma) = \sum_i \max(0, -\chi(\Sigma_i)).$$

Then $\chi_-(\Sigma)$ is large if it has many components of high genus. Using this, we can define the *Thurston norm* for $a \in H_2(Y)$:

**Definition 7.2.1.** Given $a \in H_2(Y)$, its *Thurston norm* is defined by

$$\Theta(a) = \min\{\chi_-(\Sigma) : \Sigma \subset Y, [\Sigma] = a\}.$$

Ozsváth and Szabó proved that Heegaard Floer homology detects the Thurston norm:

**Theorem 7.2.2** (B)**.** $\underline{\widehat{HF}}(Y)$ *detects the Thurston norm, where the underline means the homology is taken with twisted coefficients.*

We will not prove this result, but we will prove a weaker result along with an example, where we use the theorem to prove a genus bound.

**Theorem 7.2.3** (A)**.** *If $Z \subset Y$ is an oriented connected surface of genus $g > 0$ and $\widehat{HF}(Y, s) \neq 0$ for some $s \in \mathrm{Spin}^c(Y)$, then*

$$|\langle c_1(s), [Z]\rangle| \leqslant 2g - 2.$$

**Example.** Let $\Sigma_g$ denote the oriented closed surface of genus $g$. Let $Y = \Sigma_g \times \mathbb{S}^1$. Let $a = [\Sigma_g \times \{\mathrm{pt}\}] \in H_2(Y)$. We will show that there is no surface $\Sigma_h \subset Y$ representing $a$ with genus lower than $g$.

This probably has a classical (algebraic topology) proof, but we can prove it using theorem A. First since $Y$ has no 2-torsion in $H_1(Y)$, we know that there is an isomorphism

$$\mathrm{Spin}^c(Y) \xrightarrow{\cong} 2H^2(Y; \mathbb{Z}) \subset H^2(Y; \mathbb{Z}).$$

Therefore we can choose $s$ such that $c_1(s) = (2g-2)PD(\{\mathrm{pt}\} \times \mathbb{S}^1)$, where $PD$ denotes the Poincaré dual.

Case 1: if $g \geqslant 2$, then $\widehat{HF}(\Sigma_g \times \mathbb{S}^1, s) \neq 0$ for our choice of $s$. Therefore the premises of theorem A are satisfied, so that if $\Sigma_h$ is any surface representing $a$, then

$$2g - 2 = |\langle c_1(s), a\rangle| = |\langle c_1(s), [\Sigma_h]\rangle| \leqslant 2h - h.$$

Therefore $g \leqslant h$, as required.

Case 2: if $g = 1$, $Y = \mathbb{T}^3$. We must show there is no embedded 2-sphere representing $a = [\mathbb{T}^2 \times \{\mathrm{pt}\}]$. But we know that $\pi_2(\mathbb{T}^3) = 0$, so all embedded spheres are trivial!

Case 3: if $g = 0$ we have nothing to prove, since spheres are already the genus minimising surface.

Now that we've seen an example application of the theorem, it's time to prove the theorem! To do this, we recall some properties of periodic domains. Let $(\Sigma, \alpha, \beta)$ be a Heegaard diagram for $Y$. A domain $D$ is said to be *periodic* if its boundary is a sum of whole $\alpha$ and $\beta$ curves. Recall that the following isomorphisms hold:

$$\widehat{\Pi} := \{\text{periodic domains, with } n_z = 0\} \cong \pi_2(x, x) \cong H^1(Y) \cong H_2(Y).$$

What exactly is the correspondence from $\widehat{\Pi}$ to $H_2(Y)$? Recall that a Heegaard diagram describes how to glue disks and an balls into surfaces to describe our given 3-manifold as a CW complex. These disks are bound by $\alpha$ and $\beta$ curves, as are periodic domains. We cap the boundaries of the periodic domains by these disks to obtain classes in $H_2$. See figure 7.1 for an example. A key fact we will make use of in the proof of theorem A is that for

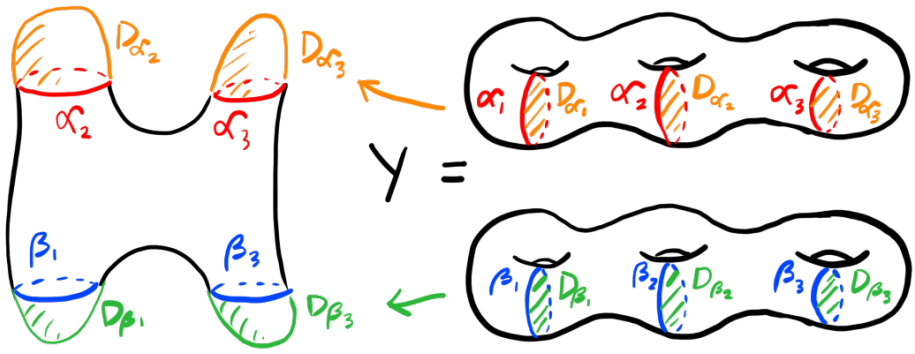


Figure 7.1: Example of the correspondence $\widehat{\Pi} \to H_2(Y)$.

any $\varphi \in \pi_2(x, x)$, if $P$ denotes the corresponding periodic domain and $\widehat{P}$ the corresponding capped surface in $H_2(Y)$, then

$$\mu(\varphi) = \langle c_1(s), [\widehat{P}] \rangle,$$

where $s$ is a spin$^c$ structure so that under the correspondence $\text{Spin}^c(Y) \cong S(Y)$, $x \in s$.

We have established all background ideas, and are now ready to proceed with the main proof.

*Proof of theorem A.* Let $Z \subset Y$ be a surface of genus $g$, and fix a tubular neighbourhood $N(Z) = Z \times [0, 1]$. Now $Y - N(Z)$ is a 3-manifold with two boundary components, each copies of $Z$. We can choose a "Heegaard decomposition" of $Y - N(Z)$:

$$(\Sigma_h, \alpha_1, \ldots, \alpha_g, \alpha_{g+1}, \ldots, \alpha_h, \beta_1, \ldots, \beta_g, \beta_{g+1}, \ldots, \beta_h).$$

Here we use quotation marks around "Heegaard decomposition", because only the curves $\alpha_{g+1}, \ldots, \alpha_h, \beta_{g+1}, \ldots, \beta_h$ mark where to fill the surface with disks $D_{\alpha_i}, D_{\beta_i}$. This is described in figure 7.2.

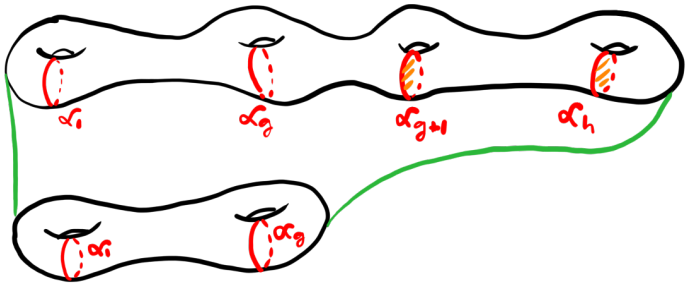


Figure 7.2: A compression body.

The disks $D_{\alpha_{g+1}}$ through to $D_{\alpha_h}$ defines a cobordism from $\Sigma_h$ to $\Sigma_g$, which we call a *compression body*. This is the natural generalisation of a handlebody which is used to construct generalisations of Heegaard decompositions for manifolds with boundary.

Figure 7.2 shows a compression body which we denote by $U_\alpha$. Similarly, there is a compression body $U_\beta$ constructed with $\beta$ curves. Gluing these together along $\Sigma_h$ gives a cobordism from $\Sigma_g$ to itself, which is exactly $Y - N(Z)$. This is decribed in figure 7.3 (ignore the blue colour for now).

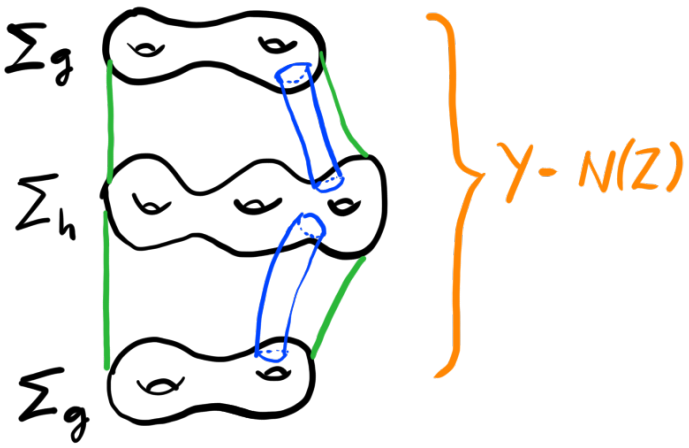


Figure 7.3: Heegaard diagram for $Y$ obtained from $Y - N(Z)$.

By gluing the two copies of $\Sigma_g$ together, we recover $Y$. Now we might think that this gives a Heegaard diagram for $Y$ - if we glue the two copies of $\Sigma_g$, we are left with an

embedded $\Sigma_h$, and perhaps cutting this gives two handlebodies. Unfortunately, if we cut along $\Sigma_h$ we only obtain one component! So it isn't a Heeegaard decomposition.

Instead, we take a sort of connected sum between each copy of $\Sigma_g$ and $\Sigma_h$, as shown by the blue tubes in figure 7.3. Now gluing the copies of $\Sigma_g$ together gives an embedded surface of genus $g + h + 1$. (See how the two tubes bend around to create the extra $+1$ genus.) That is, we have a diagram

$$(\Sigma', \alpha', \beta')$$

where the new curves $\alpha_{g+h+1}$ and $\beta_{g+h+1}$ come from tube meridians.

Now choose $s$ so that $\widehat{HF}(Y, s) \neq 0$. (We know this exists - recall the premise of the result we're proving!) Then there exists $x \in \mathbb{T}_{\alpha'} \cap \mathbb{T}_{\beta'}$ so that $x$ lies in the class of $s$. This means there is a periodic domain $P$ so that $[\widehat{P}] \in H_2(Y)$, with $[\widehat{P}] = [Z]$, and the boundary of $P$ is given by $\alpha_{g+h+1}$ and $\beta_{g+h+1}$. From our earlier fact, it follows that

$$\mu(\varphi) = \langle c_1(s), [\widehat{P}] \rangle = \langle c_1(s), [\Sigma] \rangle,$$

for any $\varphi \in \pi_2(x, x)$, with $x \in s$.

But now we apply the Lipshitz formula: we have that

$$\mu(\varphi) = e(P) + n_x(P) + n_y(P) = ((2 - 2g) - 2) + 2n_x(P).$$

Since $x = \{x_1, \ldots, x_{g+h+1}\}$ includes at least one point on $\alpha_{g+h+1}$ and one on $\beta_{g+h+1}$, we must also have $n_x(P) \geqslant 1/2 + 1/2 = 1$. It follows that

$$\mu(\varphi) \geqslant 2 - 2g.$$

Therefore

$$\langle c_1(s), [Z] \rangle \leqslant 2g - 2.$$

Finally to get the absolute value, we use the conjuagte symmetry of $\widehat{HF}$. Given any $s$, there exists $\overline{s}$ such that $c_1(\overline{s}) = -c_1(s)$, and $\widehat{HF}(Y, s) \cong \widehat{HF}(Y, \overline{s})$. Now the same inequality runs through with the minus sign, so that

$$|\langle c_1(s), [Z] \rangle| \leqslant 2g - 2$$

as required. □

# Chapter 8

# Connections to Seiberg-Witten theory

The first aim of this chapter is to explain why there seem to be four fundamental types of Heegaard Floer homology, namely $\widehat{HF}, HF^+, HF^-$, and $HF^\infty$. This comes from a deep connection between Heegaard Floer homology and Seiberg-Witten Floer homology, and the latter can expressed as four fundamental types of equivariant homology. Next we explore involutive Heegaard Floer homology, which was created through an attempt to imitate a certain construction in Seiberg-Witten Floer homology.

## 8.1 Equivariant homology overview (lecture 14)

The reason there are four types of Heegaard Floer homology and Seiberg-Witten Floer homology is because they can be interpreted as coming from four types of equivariant homology.

Let $G$ be a Lie group, acting on a finite CW complex $X$. What are the types of homology we can consider? The first type we can consider is of course

$$H_*(X),$$

the *ordinary homology of* $X$. This naïve homology theory simply ignores the group action all together!

The second type we can consider is *Borel homology*.

**Definition 8.1.1.** The *Borel equivariant homology*, also just called *equivariant homology*, is

$$H_*^G(X) := H_*(X//G),$$

where $X//G$ is the *homotopy quotient* $X \times_G EG = (X \times EG)/(x, e) \sim (gx, ge)$. Recall that $EG$ is a contractible space on which $G$ acts freely.

Recall that $BG = EG/G$ is the *classifying space* of the group $G$, which satisfies

$$\{\text{principal } G\text{-bundles over } Y\} \leftrightsquigarrow [Y, BG].$$

**Example.** If $G = \mathbb{Z}/2\mathbb{Z}$, then $EG = \mathbb{S}^\infty$ with $G$ acting via the antipodal map. $BG = \mathbb{RP}^\infty$. If $G = \mathbb{S}^1$, then $EG = \mathbb{S}^\infty$, viewed as the unit sphere in $\mathbb{C}^\infty$. $G$ acts by complex multiplication by $\mathbb{S}^1 \subset \mathbb{C}$, acting diagonally. $BG = \mathbb{CP}^\infty$.

In general there is a fibration

$$X \to X \times_G EG \to BG,$$

since $G$ acts freely on $EG$. This can be used with spectral sequences etc to compute Borel homology.

We now make a number of observations.

1. If $G$ acts freely on $X$, we also have a fibration $EG \to X \times_G EG \to X/G$. Since $EG$ has trivial homology, it follows that
$$H_*^G(X) = H_*(X/G).$$
2. If $G$ acts trivially on $X$, then $X//G = X \times BG$, so
$$H_*^G(X) = H_*(X \times BG).$$
3. In particular, $H_*^G(\{\text{pt}\}) = H_*^G(BG)$.
4. Similarly, we can define *Borel cohomology*. Then $H_G^*(\{\text{pt}\}) = H^*(BG)$. Any element of $H^*(BG)$ pulls back to $H^*(X//G) = H_G^*(X)$ via the aforementioned fibration. Therefore $H^*(BG)$ acts on $H_*^G(X)$ via the cap product. It follows that $H_*^G(X)$ is an $H^*(BG)$-module.

**Example.** Let $G = \mathbb{S}^1$. Then $H^*(BG) = H^*(\mathbb{CP}^\infty) = \mathbb{Z}[U]$, where $U$ has degree 2. Thus for any $X$, we have that $H_*^{\mathbb{S}^1}(X)$ is a $\mathbb{Z}[U]$-module, $\deg U = 2$. This looks rather similar to $HF^\pm$.

On the other hand, the ordinary homology doesn't have any structure coming from $G$ - we just ignore the action all together. That is, $H_*(X)$ is a $\mathbb{Z}$-module. This looks like $\widehat{HF}$.

We remark now that Borel homology satisfies many of the nice properties of ordinary homology, such as Mayer-Vietoris, Excision, and so on. However, we will now see that it cannot satisfy Poincaré duality:

**Example.** Observe that $H_*^{\mathbb{S}^1}(\{\text{pt}\}) = H_*(\mathbb{CP}^\infty) = Z[U^{-1}]$. (Incidentally, we notice that this is $HF^+(\mathbb{S}^3)$.) In particular this is infinite in the positive direction! (but not in the negative direction). Therefore Poincaré duality cannot hold.

So what is Poincaré dual to Borel homology? This is the *coBorel homology*. To define this, we make use of *Alexander duality*, for which we must introduce the reduced version of Borel homology.

**Proposition 8.1.2** (Alexander duality)**.** Let $X \hookrightarrow \mathbb{S}^N$ be an embedding for some large $N$. Then

$$\widetilde{H}_*(X) \cong \widetilde{H}^{N-*-1}(\mathbb{S}^N - X),$$

where $\widetilde{H}$ denotes the reduced ordinary (co)homology.

**Definition 8.1.3.** Let $x \in X$, fixed by $G$. The *reduced Borel homology* is

$$\widetilde{H}_*^G(X) \coloneqq \operatorname{coker}(H_*^G(\{x\}) \to H_*^G(X)).$$

We now have the necessary ingredients to define *coBorel homology*:

**Definition 8.1.4.** Let $G$ act on $X$, and let $X \hookrightarrow V$ where $V$ is a linear representation of $G$, $\dim V = N$. Then the *coBorel homology* of $X$ is defined by

$$c\widetilde{H}_*^G(X) \coloneqq \widetilde{H}_G^{N-*-1}(V^+ - X),$$

where $V^+$ is the one point compactification of $V$.

**Example.** $c\widetilde{H}_*^G(X)$ is usually infinite in the negative direction! For example, $\widetilde{H}_*^{\mathbb{S}^1}(\mathbb{S}^0) = \mathbb{Z}[U^{-1}]$, from which we have $c\widetilde{H}_*^{\mathbb{S}^1}(\mathbb{S}^0) = \mathbb{Z}[U]$. Notice that this is $HF^-(\mathbb{S}^3)$!

Again, the coBorel homology satisfies Mayer-Vietoris, excision, and all the other nice standard homology theory properties.

The final equivariant homology theory we consider is *Tate homology*.

**Definition 8.1.5.** Let $G$ act on $X$. The *Tate homology* of $X$ is defined by

$$t\widetilde{H}_*^G(X) = c\widetilde{H}_*^G(\widetilde{EG} \wedge X),$$

where $\widetilde{EG}$ denotes the (unreduced) suspension of $EG$.

**Example.** For example, $t\widetilde{H}_*^{\mathbb{S}^1}(\mathbb{S}^0) = \mathbb{Z}[U, U^{-1}]$. Notice that this is equal to $HF^\infty(\mathbb{S}^3)$.

- Suppose $G$ acts on $X$ freely. Then $t\widetilde{H}_*^G(X) = 0$.
- If the action is *semifree*, meaning stabilisers are 1 or $G$, then $t\widetilde{H}_*^G(X)$ depends only on $X^G$; the fixed point set of $X$ under the $G$ action. (In this case, $X = X^G \cup \{\text{free part}\}$.)

**Example.** If $\mathbb{S}^1$ acts semifreely on $X$, then

$$t\widetilde{H}_*^{\mathbb{S}^1}(X) = \widetilde{H}_*(X^{\mathbb{S}^1}) \otimes \mathbb{Z}[U, U^{-1}].$$

Finally, as one might have guessed from the development so far, there is a long exact sequence relating Borel, coBorel, and Tate homology:

**Theorem 8.1.6.** *The* Tate-Swan long exact sequence *of $H^*(BG)$-modules is*

$$\cdots \to c\widetilde{H}^G_*(X) \to t\widetilde{H}^G_*(X) \to \widetilde{H}^G_{*-1}(X) \to \cdots$$

For example, the earlier examples with $X = \mathbb{S}^0$ and $G = \mathbb{S}^1$ gives the long exact sequence induced from

$$0 \to \mathbb{Z}[U] \to \mathbb{Z}[U, U^{-1}] \to \mathbb{Z}[U^{-1}] \to 0.$$

This is the same exact sequence we see with Heegaard Floer homology for $\mathbb{S}^3$:

$$\cdots \to HF^-(\mathbb{S}^3) \to HF^\infty(\mathbb{S}^3) \to HF^+(\mathbb{S}^3) \to \cdots .$$

At this point it's very tempting to conjecture that given a 3-manifold $Y$, there is some associated space (or "spectrum") $SY$ such that

$$HF(Y) = \widetilde{H}_*(SY) \qquad HF^+(Y) = \widetilde{H}^{\mathbb{S}^1}_*(SY)$$
$$HF^-(Y) = c\widetilde{H}^{\mathbb{S}^1}_*(SY) \qquad HF^\infty(Y) = t\widetilde{H}^{\mathbb{S}^1}_*(SY).$$

In the next section, we'll see that this is indeed true.

## 8.2 Heegaard Floer vs Seiberg-Witten Floer vs equivariant homology

In Maths 283A of spring 2020, we explored the Seiberg-Witten invariants for 4-manifolds. A similar construction works for 3-manifolds as well. The Seiberg-Witten equations on a 3-manifold $Y$ are PDEs on $Y$ solving for pairs $(A, \Phi)$ where

- $A$ is a spin$^c$ connection, and
- $\Phi$ is a spinor field,

in a complex rank 2 vector bundle $S$ over $Y$. The Seiberg-Witten equations have $\Gamma(\mathrm{Aut}(S))$ gauge-symmetry. Fixing a gauge, (equivalently, modding out by gauge), we're left with a residual $U(1)$-action $e^{i\theta} : (A, \Phi) \mapsto (A, e^{i\theta}\Phi)$ under which the equations are invariant. That is, the moduli space of solutions have $U(1) = \mathbb{S}^1$ symmetry.

**Definition 8.2.1** (Kronheimer, Mrowka)**.** There are four versions of Seiberg-Witten (monopole) Floer homology, denoted

$$\widetilde{HM}, \widetilde{HM}, \widehat{HM}, \overline{HM}$$

coming from the Seiberg-Witten equations. These are read as tilde, to, from, and bar respectively.

The big result is that these can be interpreted as $\mathbb{S}^1$-equivariant homology, where the $\mathbb{S}^1$ action comes from the symmetry of the moduli space.

**Theorem 8.2.2** (Lidman, Manolescu)**.** *There is an $\mathbb{S}^1$-equivariant Seiberg-Witten Floer spectrum $SWF(Y)$ so that*

$$\widetilde{HM}(Y) = \tilde{H}_*(SWF(Y)) \qquad \widetilde{HM}(Y) = \tilde{H}_*^{\mathbb{S}^1}(SWF(Y))$$
$$\widehat{HM}(Y) = c\tilde{H}_*^{\mathbb{S}^1}(SWF(Y)) \qquad \overline{HM}(Y) = t\tilde{H}_*^{\mathbb{S}^1}(SWF(Y)).$$

Finally, everything is tied together by the following huge result of Kutluhan-Lee-Taubes and Colin-Ghiggini-Honda:

**Theorem 8.2.3.**

$$\widetilde{HM} \cong \widehat{HF}, \widetilde{HM} \cong HF^+, \widehat{HM} \cong HF^-, \overline{HM} \cong HF^\infty.$$

*The isomorphisms are on the nose; they hold for the exact same 3 manifold and spin$^c$ structure and so on.*

Notice that given the above isomorphisms, the Tate-Swan exact sequence is really

$$\cdots HF^- \to HF^\infty \to HF^+ \to \cdots .$$

**Remark.** Seiberg-Witten Floer homology could be interpreted as $\mathbb{S}^1$-equivariant homology because of the $\mathbb{S}^1$ action on the moduli space. However, there is no $\mathbb{S}^1$ action on Heegaard Floer homology! The $\mathbb{Z}[U]$-module structure comes from the basepoint of the Heegaard diagram. This is why the isomorphisms are given in the order

$$\mathbb{S}^1 - \text{equivariant hom} \leftrightsquigarrow \text{Seiberg-Witten Floer hom} \leftrightsquigarrow \text{Heegaard Floer hom}.$$

# Chapter 9

# Involutive Heegaard Floer homology

## 9.1 Construction of involutive Heegaard Floer homology

Involutive Heegaard Floer homology is a refinment of Heegaard Floer homology by using a bit more symmetry. We remarked in an earlier lecture that there is an involution on $\mathrm{Spin}^c(X)$,

$$j : s \mapsto \overline{s}, \quad c_1(\overline{s}) = -c_1(s).$$

The Seiberg-Witten equations are invariant with respect to this involution. Therefore we have

$$\mathbb{S}^1 \text{ symmetry} + j \text{ symmetry} \rightsquigarrow \mathrm{Pin}(2) \text{ symmetry}.$$

Recall that $\mathrm{Pin}(2)$ is the group

$$\mathrm{Pin}(2) = \mathbb{S}^1 \cup j\mathbb{S}^1 \subset \mathbb{C} \oplus j\mathbb{C} \cong \mathbb{H} = \mathrm{span}(1, i, j, k).$$

This group looks like two disjoint circles. In fact, if $s = \overline{s}$ in $\mathrm{Spin}^c(X)$, then $s$ comes from a spin structure! In this case $SWF(Y, s)$ is a $\mathrm{Pin}(2)$-equivariant spectrum.

**Definition 9.1.1** (Manolescu)**.** There is a $\mathrm{Pin}(2)$-equivariant Seiberg-Witten Floer homology,

$$SWFH_*^{\mathrm{Pin}(2)}(Y) = \widetilde{H}_*^{\mathrm{Pin}(2)}(SWF(Y); \mathbb{F}_2).$$

Pin(2)-equivariant Seiberg-Witten Floer homology was used to disprove the triangulation conjecture! That is, in every dimension at least 5, there exist non-triangulable manifolds.

Lin gave an alternative construction of this, in the spirit of Kronheimer and Mrowka. This is referred to as Pin(2) monopole Floer homology.

**Remark.** Recall that in general Seiberg-Witten Floer homology is more difficult to compute than Heegaard Floer homology, so we desire analogues in the Heegaard Floer setting.

Due to technical reasons, currently there is no analogue of Pin(2)-equivariant Seiberg-Witten Floer homology for Heegaard Floer homology. Instead, we have *involutive Heegaard Floer homology* due to Hendricks and Manolescu, which uses conjugation symmetry in $HF$ to construct $HFI^\circ(Y)$, for $\circ \in \{\widehat{\ }, +, -, \infty\}$.

**Conjecture.**

$$HFI^+(y,s) \cong \widetilde{H}_*^{\mathbb{Z}/4\mathbb{Z}}(SWF(Y);\mathbb{F}_2),$$

where $\mathbb{Z}/4\mathbb{Z} \cong \langle j \rangle < \mathrm{Pin}(2)$. Notice that both sides of the conjectured isomorphism are modules over $H^*_{\mathbb{Z}/4\mathbb{Z}}(\{\mathrm{pt}\};\mathbb{F}_2) = \mathbb{F}[U,Q]/Q^2$, where $U$ has degree -2 and $Q$ has degree $-1$.

We now describe the construction of involutive Heegaard Floer homology.

**Definition 9.1.2.** Let $Y$ be a 3-manifold, and $\mathcal{H} = (\Sigma, \alpha, \beta, z)$ a based Heegaard diagram of $Y$. The *conjugate diagram* of $Y$ is $\overline{\mathcal{H}} = (\overline{\Sigma}, \beta, \alpha, z)$.

Notice that swapping $\Sigma$ for $\overline{\Sigma}$ swaps $Y$ for $\overline{Y}$, but swapping $\alpha$ and $\beta$ curves also swaps orientation. Therefore $\overline{\mathcal{H}}$ is truly a diagram for $Y$. It follows that there is a sequence of Heegaard moves relating $\mathcal{H}$ to $\overline{\mathcal{H}}$.

Recall that Ozsváth and Szabo proved the invariance of $HF^\circ$ under changes Heegaard diagrams. Formally, a sequence $m$ of moves from $\mathcal{H}_1$ to $\mathcal{H}_2$ induces a chain map

$$\Phi(m) : CF^\circ(\mathcal{H}_1) \to CF^\circ(\mathcal{H}_2)$$

that induces an isomorphism on homology. Hence $HF^\circ(\mathcal{H}_1) \cong HF^\circ(\mathcal{H}_2)$, and it makes sense to talk about the Heegaard Floer homology of the manifold.

**Theorem 9.1.3** (Juhász, D. Thurston, Zemke)**.** *Heegaard Floer homology is natural. More precisely, given two sequences of moves $m_1, m_2$ from $\mathcal{H}_1$ to $\mathcal{H}_2$, the maps $\Phi(m_1)$ and $\Phi(m_2)$ are chain homotopic. Therefore the isomorphism $HF^\circ(\mathcal{H}_1) \to HF^\circ(\mathcal{H}_2)$ is well defined.*

**Remark.** This is actually important for defining the cobordism map $F_{W,s} : HF^\circ(M_1) \to HF^\circ(M_2)$ (for four manifold invariants coming from Heegaard Floer). However, Ozsváth and Szabó forgot to check this! It took five years before anyone realised there was a hole that needed filling.

In our case, we consider diagrams $\mathcal{H}, \overline{\mathcal{H}}$ for $Y$. This induces a chain map

$$\Phi : CF^\circ(\overline{\mathcal{H}}) \to CF^\circ(\mathcal{H}),$$

induced by a sequence of Heegaard moves from $\mathcal{H}$ to $\overline{\mathcal{H}}$. In particular, this map preserves spin$^c$ structures. On the other hand, there is another map we can consider as well! There is a (conjugation symmetry) map

$$\eta : CF^\circ(\mathcal{H}) \to CF^\circ(\overline{\mathcal{H}})$$

induced by the bijection of points between $\mathbb{T}_\alpha \cap \mathbb{T}_\beta$ and $\mathbb{T}_\beta \cap \mathbb{T}_\alpha$. (The $J$-holomorphic strips map bijectively.) Moreover, this map conjugates the spin$^c$ structure: it induces isomorphisms

$$CF^\circ(\mathcal{H}, s) \to CF^\circ(\overline{\mathcal{H}}, \overline{s}).$$

In summary, $CF^\circ(\mathcal{H})$ and $CF^\circ(\overline{\mathcal{H}})$ are isomorphic in *two different ways*. Composing the two maps, we have an isomorphism

$$\iota = \Phi \circ \eta : CF^\circ(\mathcal{H}, s) \to CF^\circ(\mathcal{H}, \overline{s}).$$

In particular, in the case $s = \overline{s}$, this gives a chain homotopy equivalence from $CF^\circ(\mathcal{H}, s)$ to itself. We are finally ready to define involutive Heegaard Floer homology!

**Definition 9.1.4.** The *involutive Heegaard Floer complex* is defined by

$$CFI^\circ(Y, s) = \mathrm{Cone}(CF^\circ(Y) \xrightarrow{Q(1+\iota)} Q \cdot CF^\circ(Y)),$$

where $Q$ is a formal variable of degree $-1$ such that $Q^2 = 0$. Here Cone denotes the *homological mapping cone*:

$$\mathrm{Cone}(C_* \xrightarrow{f} D_*) \coloneqq \left( C_* \oplus D_*, \begin{pmatrix} \partial & f \\ 0 & \partial \end{pmatrix} \right).$$

Therefore we can write

$$CFI^\circ(Y) \coloneqq \left( CF^\circ(Y)[-1] \otimes_{\mathbb{F}_2} \mathbb{F}_2[Q]/Q^2, \partial + Q(1+\iota) \right).$$

**Theorem 9.1.5** (Hendricks, Manolescu)**.** *$HFI^\circ(Y, s) = H_*(CFI^\circ(Y, s))$ is an invariant of $(Y, s)$.*

We do not give a proof - but it uses the Juhász, Thurston, Zemke naturality result from earlier in the lecture.

## 9.2 Properties of $HFI$ (lecture 15)

In the previous lecture we defined *involutive Floer homology* $HFI^\circ(Y, s)$ to be the homology of the *involutive Floer complex* $CFI^\circ(Y, s)$. (We are under the assumption that $s = \overline{s}$.) This complex is obtained as the cone over

$$CF^\circ(Y) \xrightarrow{Q(1+\iota)} Q \cdot CF^\circ(Y),$$

where $Q$ is a formal variable of degree $-1$. The idea is to capture the extra structure $CF^\circ(\mathcal{H})$ that isn't captured by ordinary Heegaard Floer homology: namely the map $\iota : CF^\circ(\mathcal{H}, s) \to CF^\circ(\mathcal{H}, s)$.

To justify the name *involutive Heegaard Floer homology* we now prove that $\iota$ is a homotopy involution on the Heegaard Floer chain complex.

**Proposition 9.2.1.** Let $\iota : CF^\circ(\mathcal{H}, s) \to CF^\circ(\mathcal{H}, s)$ be as defined in the previous lecture. Then $\iota^2 \sim \mathrm{id}$.

**Corollary 9.2.2.** *$\iota_* : HF^\circ(Y, s) \to HF^\circ(Y, s)$ is an involution.*

*Proof.* A calculation gives

$$\iota^2 = \Phi \circ \eta \circ \Phi \circ \eta = \Phi \circ (\eta^{-1} \circ \Phi \circ \eta),$$

using the fact that $\eta^2 = \mathrm{id}$. (This is true because $\eta$ is the map induced by the bijection $\mathbb{T}_\alpha \cap \mathbb{T}_\beta = \mathbb{T}_\beta \cap \mathbb{T}_\alpha$). On the other hand, $\Phi : CF^\circ(\overline{\mathcal{H}}) \to CF^\circ(\mathcal{H})$ is induced by a sequence of Heegaard moves. The conjugation $\eta^{-1} \circ \Phi \circ \eta$ is now a map from $CF^\circ(\mathcal{H}) \to CF^\circ(\overline{\mathcal{H}})$ also induced by Heegaard moves. But now, overall,

$$\Phi \circ (\eta^{-1} \circ \Phi \circ \eta^{-1}) : CF^\circ(\mathcal{H}) \to CF^\circ(\mathcal{H})$$

is a composition of two maps induced by Heegaard moves. On the other hand, the empty sequence of moves from $\mathcal{H} \to \mathcal{H}$ induces the identity. By Juhász, Thurston, Zemke naturality, $\iota^2 \sim \mathrm{id}$. □

The involutive Heegaard Floer homology $HFI^\circ(Y, s)$ is defined for $s$ self-conjugate, i.e. $s = \overline{s}$. Which $s$ satisfies this?

- Such an $s$ always exists, since we can take $s$ corresponding to 0 in $H^2$.
- Moreover, if $H^2$ has no torsion, then

$$s = \overline{s} \quad \Rightarrow \quad c_1(s) = c_1(\overline{s}) = -c_1(s) \quad \Rightarrow \quad 2c_1(s) = 0 \quad \Rightarrow \quad s = 0.$$

**Example.** We have yet to compute any examples of involutive Heegaard Floer homology. The easiest example is the 3-sphere.

From earlier examples, we know that

$$CF^-(\mathbb{S}^3) = \mathbb{F}[U],$$

where we take $\mathbb{F}$ to be the field of size 2. (That is, we're working in mod 2 coefficients.) The boundary map $\partial$ is trivial, since the terms in $\mathbb{F}[U]$ with a fixed degree in $U$ all lie in the same grading. (That is, the chain complex comes from a Heegaard diagram with one intersection.) Recall that we conclude from here that

$$HF^-(\mathbb{S}^3) = \mathbb{F}[U]$$

and so on.

For involutive Heegaard Floer homology, we now wish to understand

$$CFI^-(\mathbb{S}^3) = (\mathbb{F}[U] \otimes_{\mathbb{F}} \mathbb{F}[Q]/Q^2, Q(1 + \iota)).$$

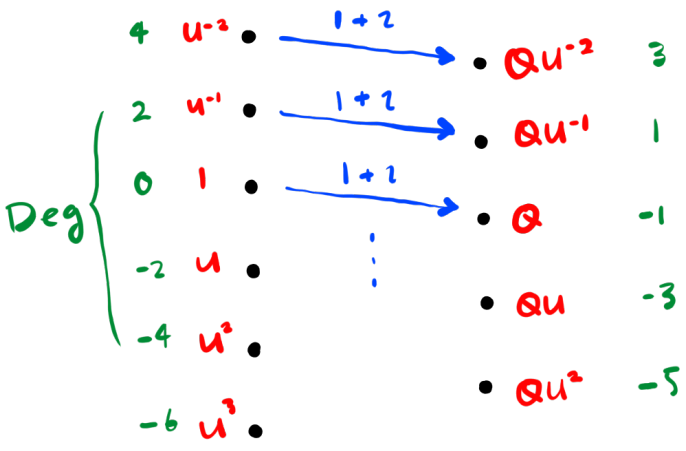


Figure 9.1: $CFI^-(\mathbb{S}^3)$.

Pictorially, this complex is as shown in figure 9.1.

What is the map $\iota$? Since this is a chain map, in particular it is a homomorphism $\mathbb{F}[U] \to \mathbb{F}[U]$, and is determined by the image of 1 which is either 0 or 1. In the first case, $\iota$ is the zero map, and in the second case, $\iota$ is the identity. However, we also know that $\iota$ is a homotopy involution! This forces $\iota = 1$. But now $1 + \iota$ is the 0 map (since we're working in mod 2 coefficients). It follows that the maps shown in 9.1 are trivial, and

$$HFI^-(\mathbb{S}^3) = \mathbb{F}[U, Q]/Q^2$$

with the grading shown in the figure.

In the above example, we're really just using properties of how involutive Heegaard Floer homology relate to Heegaard Floer homology and not doing anything with the sphere. The property we made use of is formalised in the following proposition.

**Proposition 9.2.3.** There is a long exact sequence

$$\cdots HF^\circ(Y, s) \xrightarrow{1+\iota} HF^\circ(Y, s) \to HFI^\circ(Y, s) \to \cdots .$$

*Proof.* The long exact sequence comes from the short exact sequence of complexes

$$0 \to CF^\circ \to CFI^\circ \to CF^\circ \to 0$$

from the fact that $CFI^\circ$ is the cone of $1 + \iota$. □

In the above example, we can conclude that $1 + \iota = 0$ from the Heegaard homology alone, from which we have that $HFI^-(\mathbb{S}^3) = \mathbb{F}[U, Q]/Q^2$.

**Corollary 9.2.4.** *More generally, it follows that if $Y$ is an $L$-space, then*

$$HFI^-(Y,s) \cong \mathbb{F}[U,Q]/Q^2,$$

*possibly with a degree shift.*

## 9.3 A non-trivial example of $HFI$

Are there examples where involutive Heegaard Floer homology isn't determined by just Heegaard Floer homology? Can we learn something new from Heegaard Floer homology? Such an example is the Brieskorn sphere

$$\Sigma(2,3,7).$$

**Definition 9.3.1.** Let $p,q,r > 1$ be pairwise coprime integers. The *Brieskorn sphere* $\Sigma(p,q,r)$ is defined to be

$$\Sigma(p,q,r) = \{x^p + y^q + z^r = 0\} \cap S(\mathbb{C}^3) \subset \mathbb{C}^3.$$

Brieskorn spheres are so-called because they are examples of integral homology 3-spheres. In particular, $\Sigma(2,3,5)$ is the Poincaré homology sphere.

The fundamental group of a Brieskorn sphere can be expressed as a degree 2 extension of the von Dyck group $V(p,q,r)$, and these are finite (spherical) or infinite (Euclidean or hyperbolic) depending on the size of $1/p+1/q+1/r$. The Poincaré homology sphere is the unique Brieskorn sphere with $1/p+1/q+1/r > 1$, and hence the unique Brieskorn sphere with finite fundamental group! This is why the Poincaré homology sphere is something that appears so often in topology.

**What is the involutive Heegaard Floer homology of $\Sigma(2,3,7)$?**

We first inspect its Heegaard Floer homology. Using the surgery exact triangle and studying how cobordism maps interact with $\iota$, one can show that

$$HF^-(\Sigma(2,3,7)) \cong \mathbb{F}[U] \oplus \mathbb{F},$$

where the $\mathbb{F}$ summand is $HF_{\mathrm{red}}$. The grading is given by $d = 0$: pictorially, $HF^-$ is as shown in figure 9.2.

To compute $HFI^-$, we change coordinates from $a, b$ to $a, c = a + b$. Now $Ua = Uc$, giving a diagram shaped like a "Y" instead of the one shown in 9.2. Moreover, we claim that

$$CF^-(\Sigma(2,3,7)) = \mathbb{F}[U]\langle a,c,z\rangle / \partial a = \partial c = 0, \partial z = U(a+c),$$

and that

$$\iota_* a = c, \iota_* c = a, \quad \iota_* z = z.$$

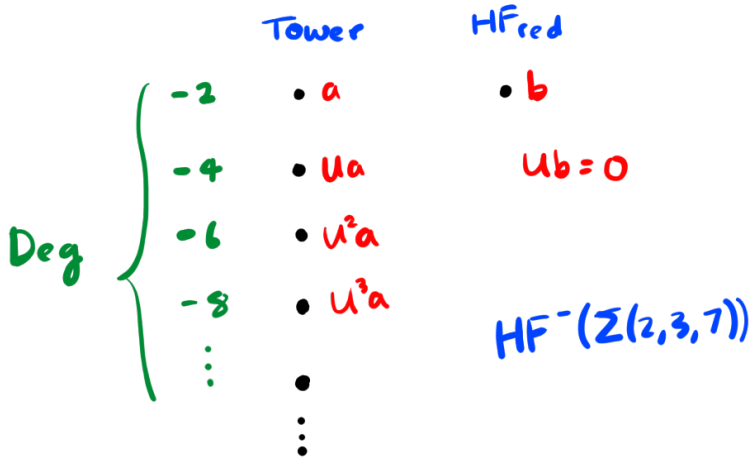


Figure 9.2: $HF^-(\Sigma(2,3,7))$.

The latter calculation comes from cobordism maps, considering $\Sigma(2,3,7)$ as the boundary of a 4-manifold. From the above, we can draw the chain complex and its homology as in figure 9.3: Using the chain complex $CF^-(\Sigma(2,3,7))$ with generators $a, c, z$ as in figure 9.3, we can further deduce $CFI^-(\Sigma(2,3,7))$ and $HFI^-(\Sigma(2,3,7))$, which are shown in figure 9.4.

On the left of figure 9.4, we have $CFI^-(\Sigma(2,3,7))$ which is obtained from $CF^-(\Sigma(2,3,7))$ as the cone over $Q(1+\iota)$. This results in two copies of $CF^-$ side by side, by shifted by degree $-1$ (which is the degree of $Q$), and with additional pieces added to the boundary map.

On the right, we have the homology.

- In degree $-2$, there are two generators: $a$ and $c$. These both map to the same image, namely $Qa + Qc$. Working over $\mathbb{F} = \mathbb{F}_2$, it follows that the kernel of the boundary map in degree $-2$ is generated by $[a + c]$. (That is, the homology in degree $-2$ is generated by $[a + c]$).

- In degree $-3$, $Qa$ and $Qc$ both map to zero under the boundary map. However, they represent the same class in homology, so the degree $-3$ homology is generated by $[Qa]$.

- In degree $-4$, we again have that $Ua+Uc = U(a+c)$ maps to zero. However, this also lies in the image of the boundary map - it's the image of $z$ in degree $-3$. Therefore this term vanishes in homology. However, we also have a kernel term coming from

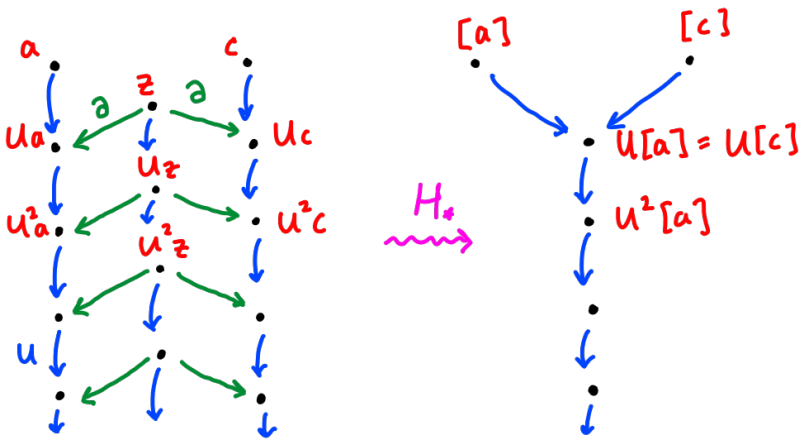


Figure 9.3: $CF^-(\Sigma(2,3,7))$ and $HF^-(\Sigma(2,3,7))$, new generators.

$Qz$ - the term $Ua + Qz$ maps to 0. Nothing maps to these terms, so $[Ua + Qz]$ freely generates the homology in degree $-4$.

- In degree $-5$, we're back to a familiar situation - everything is the same as degree $-3$, just with an extra factor of $U$. That is, the homology is generated by $U[Qa]$.
- This continues, with even degrees generated by $U^i[Ua + Qz]$ and odd degrees by $U^i[Qa]$.

What about maps between homology?

- In degree $-2$, the homology is generated by $[a + c]$. This maps to 0 under both $Q$ and $U$.
- In degree $-3$, we have $[Qa]$ which maps to 0 under $Q$ since $Q^2 = 0$, but $U[Qa]$ is non-zero! There's a non-trivial map between degree $-3$ and $-5$ homology. This holds for all odd degrees.
- Finally in degree $-4$, both $U$ and $Q$ are non-trivial. This holds for all even degrees.

In summary, we have the homology shown on the right side of figure 9.4. Alternatively, see the left imagine in figure 9.5.

In figure 9.5, we also show $HF^-(\Sigma(2,3,7)) \otimes \mathbb{F}[Q]/Q^2$ on the right. This has been computed by using the form of $HF^-(\Sigma(2,3,7))$ computed right at the start of this example. We see that $HFI^-$ is not just the tensor product of $HF^-$ with $\mathbb{F}[Q]/Q^2$. (This was the

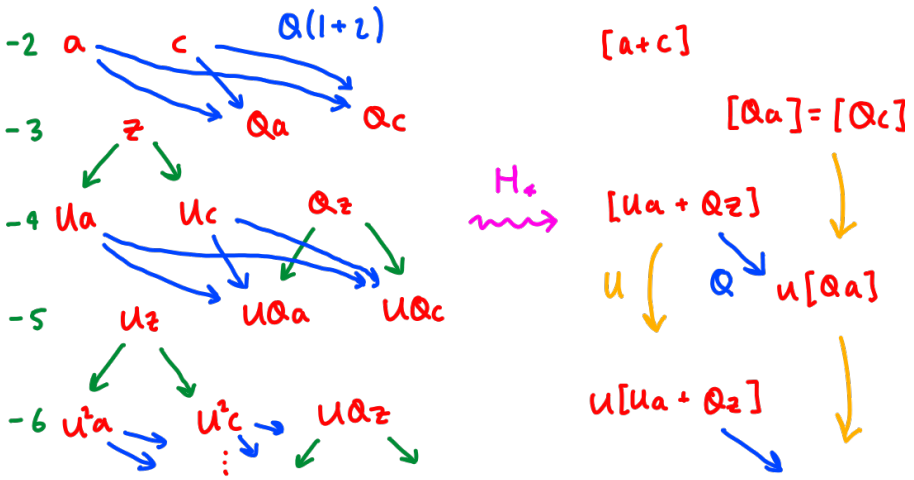


Figure 9.4: $CFI^-(\Sigma(2,3,7))$ and $HFI^-(\Sigma(2,3,7))$.

case in the trivial case of the 3-sphere, and more generally $L$-spaces.) This is perhaps to be expected, because the involution $\iota$ is not the identity map for $\Sigma(2,3,7)$.

**What is the involutive Heegaard Floer homology of $-\Sigma(2,3,7)$?**

This is an even more interesting case to study! When reversing the orientation, the homology turns out to be dual in some sense:

$$HF^-_*(-\Sigma(2,3,7)) = HF^+_{-*+2}(\Sigma(2,3,7)).$$

Computing $HF^+_{-*+2}$, we have what is shown in figure 9.6. Notice that we again have an infinite tower with the same copy of $HF_{\text{red}}$ showing up. However, this time $HF_{\text{red}}$ is in a different degree to the maximum degree of the tail of $HF^-$. This is because of the degree shift which appears in the connecting homomorphism of the long exact sequence $\cdots \to CF^- \to CF^\infty \to CF^+ \to \cdots$. Notice that $HF^-(-\Sigma(2,3,7))$ has at most one copy of $\mathbb{F}$ in each degree! Since $\iota_*$ is an involution, in particular it is an isomorphism on homology. But with a single copy of $\mathbb{F}$ in each degree, there is a unique isomorphism! $\iota_*$ must be the identity map on $HF^-$.

Despite this, we will see that the involutive Heegaard Floer homology of $-\Sigma(2,3,7)$ is non-trivial! At the chain complex level, $CF^-(-\Sigma(2,3,7))$ is "dual" to $CF^+(\Sigma(2,3,7))$, and is the complex shown on the left of figure 9.7.

Proceeding as in the above example, using $CF^-(-\Sigma(2,3,7))$ as shown in figure 9.7, we can explicitly write down $CFI^-(-\Sigma(2,3,7))$. For this, we note that

$$\iota a = c, \iota c = a, \iota z = z$$

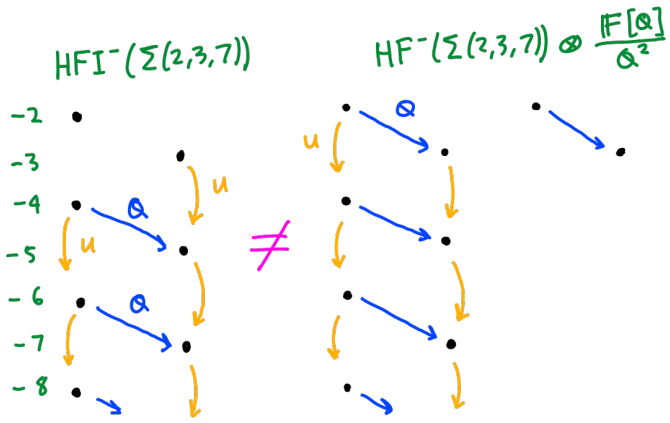


Figure 9.5: $HFI^-$ vs $HF^- \otimes \mathbb{F}[Q]/Q^2$.

as in the previous example. This is interesting because $\iota$ is a non-trivial isomorphism at the chain complex level, but the identity map on the level of $HF^-$. Computing the homology of this complex, we obtain the right side of figure 9.7.

We once again notice that the resulting complex is not determined from $HF^-$! That is,

$$HFI^-(-\Sigma(2,3,7)) \ncong HF^-(-\Sigma(2,3,7)) \otimes \mathbb{F}[Q]/Q^2.$$

This time the result is even more interesting, because the involution $\iota$ was the identity map on $HF^-$.

## 9.4 New maps on the homology cobordism group

Now that we've looked at some non-trivial examples of involutive Heegaard Floer homology, it's time for a more general application. Recall from earlier that an application of $HF^-$ was to construct a homomorphism

$$d/2 : \Theta^3_{\mathbb{Z}} \to \mathbb{Z}.$$

By showing that $d(P) = 2$ where $P$ is the Poincaré homology sphere, we observed that $\Theta^3_{\mathbb{Z}}$ has a $\mathbb{Z}$ summand.

More precisely, we recall the following definitions:

**Definition 9.4.1.** The *homology cobordism group* $\Theta^3_{\mathbb{Z}}$ consists of integral homology 3-spheres, modulo homology cobordism. That is, $Y_0 \sim Y_1$ if and only if there is a smooth 4-manifold $W$ which is a cobordism from $Y_0$ to $Y_1$, and such that $H_*(W, Y_i) = 0$ for each $i$.

Note that $[Y] = 0 \in \Theta^3_{\mathbb{Z}}$ if and only if $Y$ bounds an integral homology 4-ball.

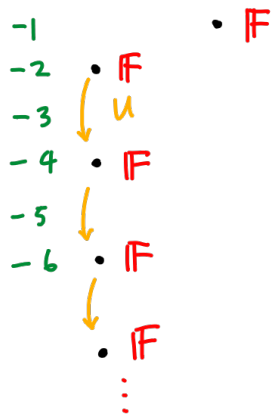


Figure 9.6: $HF^-(-\Sigma(2,3,7))$.

**Definition 9.4.2.** The map $d/2 : \Theta^3_{\mathbb{Z}} \to \mathbb{Z}$ comes from the invariant $d$, where $d(Y)$ is the minimum degree of the $U$-tower in $HF^+$, or equivalently the maximum degree of the $U$-tail in $HF^-$, plus 2.

Note that $d(\mathbb{S}^3) = 0$, $d(P) = 2$.

We now introduce the analogous invariants from involutive Heegaard Floer homology, which also determine maps on the homology cobordism group. Observe that there's a long exact sequence of the form

$$\cdots \to QHF^-(Y,s) \to HFI^-(Y,s) \to HF^-(Y,s) \xrightarrow{1+\iota_*} \cdots .$$

But the map $1 + \iota_*$ is trivial on the $U$-tail of $HF^-$ in degrees $\ll 0$! Therefore we end up with two infinite tails of $HFI^-(Y,s)$ as $\mathbb{F}[U]$-modules!

For a rational homology sphere, notice that the "first tail" doesn't have $Q$, while the "second tail" has $Q$.

**Definition 9.4.3.**

$$\underline{d}(Y,s) = \text{max deg. of first } U\text{-tail in } HFI^- + 2$$
$$\overline{d}(Y,s) = \text{max deg. of second } U\text{-tail in } HFI^- + 3.$$

**Example.** We computed the involutive Heegaard Floer homologies of $\Sigma(2,3,7)$ and $-\Sigma(2,3,7)$ earlier. From these, we find that

| | $\Sigma(2,3,7)$ | $-\Sigma(2,3,7)$ |
|---|---|---|
| $d$ | 0 | 0 |
| $\underline{d}$ | -2 | 0 |
| $\overline{d}$ | 0 | 2. |

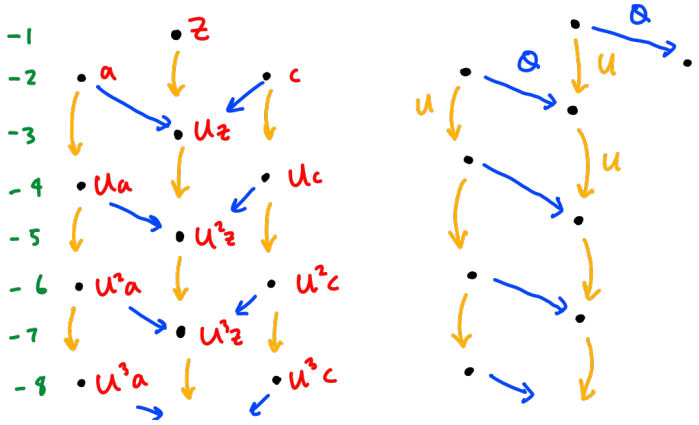


Figure 9.7: Computing $HFI^-(-\Sigma(2,3,7))$.

More generally, it turns out

$$d(-Y) = -d(Y), \quad \overline{d}(-Y) = -\underline{d}(Y).$$

There are some additional properties too:

1. $d(\mathbb{S}^3) = \overline{d}(\mathbb{S}^3) = \underline{d}(\mathbb{S}^3) = 0$.
2. $\underline{d}, \overline{d}$ induce maps $\Theta^3_{\mathbb{Z}} \to \mathbb{Z}$ (not homomorphisms).
3. $\underline{d} \equiv \overline{d} \equiv d \mod 2$.
4. $\underline{d} \leqslant d \leqslant \overline{d}$ from the $\mathbb{F}[U,Q]/Q^2$-module structure.
5. $\underline{d} = d = \overline{d}$ if $Y$ is an $L$-space, for fixed spin$^c$ structures (from the fact that $HFI^- \cong HF^- \otimes \mathbb{F}[Q]/Q^2$).

An application of this is that $\Sigma(2,3,7)$ is non-trivial in $\Theta^3_{\mathbb{Z}}$. Equivalently, $\Sigma(2,3,7)$ does *not* bound a homology ball. (This can also be shown using the Rokhlin invariant.) However, a new result is that $\Sigma(2,3,7)$ is not homology cobordant to any $L$-space.

## 9.5 Connected sum formula (lecture 16)

At the end of the previous lecture, we mentioned that

$$\overline{d}, \underline{d} : \Theta^3_{\mathbb{Z}} \to \mathbb{Z}$$

are not homomorphisms. The fact that these are *not* homomorphisms can be seen using a *connected sum formula*.

In ordinary Heegaard Floer homology we have the following result:

**Theorem 9.5.1** (Ozsváth, Szabó)**.**

$$\widehat{HF}(Y_1\#Y_2, s_1\#s_2) \cong \widehat{HF}(Y_1, s_1) \otimes_{\mathbb{Z}} \widehat{HF}(Y_2, s_2)$$
$$HF^-(Y_1\#Y_2, s_1\#s_2) \cong HF^-(Y_1, s_1) \otimes_{\mathbb{Z}[U]} HF^-(Y_2, s_2)[-2].$$

*In the second equation, the* $[-2]$ *denotes that there is a grading shift up by 2. Notice that there is no analogous formula for* $HF^+$*, since* $HF^+(\mathbb{S}^3) = \mathbb{Z}[U^{-1}]$*, but* $\otimes_{\mathbb{Z}[U]}\mathbb{Z}[U^{-1}] \neq \mathrm{id}$*.*

There is an analogue for involutive Heegaard Floer homology as well.

**Theorem 9.5.2** (Hendricks, Manolescu, Zemke)**.** *There is a chain homotopy equivalence*

$$CF^-(Y_1\#Y_2, s_1\#s_2) \cong CF^-(Y_1, s_1) \otimes_{\mathbb{F}[U]} CF^-(Y_2, s_2)[-2]$$

*such that the involution* $\iota$ *on* $CF^-$ *corresponds to* $\iota_1 \otimes \iota_2$ *up to chain homotopy.*

**Example.** An algebra exercise: from $(CF^-(\Sigma(2,3,7), \iota)$, compute $(CF^-(\Sigma(2,3,7)\#\Sigma(2,3,7), \iota)$. This gives $HFI^-(\Sigma(2,3,7)\#\Sigma(2,3,7))$.

Earlier we computed the Heegaard Floer homology of $\Sigma(2,3,7)$, and established that

$$\underline{d} = -2, d = \overline{d} = 0.$$

On the other hand, it turns out that for $\Sigma(2,3,7)\#\Sigma(2,3,7)$, we also have

$$\underline{d} = -2, d = \overline{d} = 0.$$

Therefore we see that

$$\underline{d}(\Sigma(2,3,7)\#\Sigma(2,3,7)) \neq \underline{d}(\Sigma(2,3,7)) + \underline{d}(\Sigma(2,3,7)).$$

This establishes that $\underline{d}$ is not additive, and hence not a homomorphism on $\Theta^3_{\mathbb{Z}}$. Moreover, because $\overline{d}(-Y) = -\underline{d}(Y)$, we also have that $\overline{d}$ is not a homomorphism.

Is there a more conceptual reason that $\underline{d}, \overline{d}$ are not homomorphisms? Yes - this comes from the module structure.

- $d$ is defined from $\mathbb{F}[U]$-modules, and $\mathbb{F}[U]$ is a PID. It follows (as we will soon see) that the module has a sufficiently rigid structure ensuring that $d$ is additive.
- $\underline{d}, \overline{d}$ come from $\mathbb{F}[U,Q]/Q^2$ modules, and the latter ring is not a PID. The tails then interact with other nonsense resulting in non-additivity.

What do we mean by this? In the case of $HF^-$, we note that $d$ comes from a $\mathbb{F}[U]$-module. However, a finitely generated homogeneous module over $\mathbb{F}[U]$ (or more generally a PID) is a direct sum of copies of $\mathbb{F}[U]$ and $\mathbb{F}[U]/U^k$ by the structure theorem for finitely generated modules over a PID.

For $Y$ an integral homology sphere, we have $HF^-(Y) = \mathbb{F}[U] \oplus HF_{\text{red}}$ where $HF_{\text{red}}$ consists of the torsion part. But now $HF^-(Y_1) \otimes HF^-(Y_2)$ is also of the same form, so it must be the case that the tails are tensored together and the torsion parts are tensored together (without mixing together)! Therefore it follows that

$$d(Y_1 \# Y_2) = d(Y_1) + d(Y_2).$$

For involutive Heegaard Floer homology, the lack of a "structure theorem" results in the above reasoning breaking down. In general, we have

$$HFI^-(Y_1 \# Y_2, s_1 \# s_2) \neq HFI^-(Y_1, s_1) \otimes HFI^-(Y_2, s_2).$$

Recall that the homomorphism $d : \Theta^3_{\mathbb{Z}} \to \mathbb{Z}$ was used to establish the existence of a $d$ summand in $\Theta^3_{\mathbb{Z}}$. The natural question now is whether or not we can use involutive Heegaard Floer homology to construct more homomorphisms (instead of just functions). This is resolved by using *$\iota$-complexes*.

## 9.6 $\iota$-complexes

As the previous section suggests, there is some structure in $(CF^-, \iota)$ that is lost in $HFI^-$ (as we change from a PID to a more general ring). Therefore to define homomorphisms from involutive Heegaard Floer homology, we will divert our attention to $(CF^-, \iota)$.

**Definition 9.6.1.** An *$\iota$-complex* is a pair $(C, \iota)$ where

- $C$ is a $\mathbb{Z}$-graded finitely generated free chain complex over $\mathbb{F}[U]$, with $U$ having degree $-2$, and $U^{-1}H_*(C) \cong \mathbb{F}[U, U^{-1}]$.
- $\iota : C \to C$ is a grading preserving involution.

**Example.** For $Y$ a $\mathbb{Z}HS^3$, $(CF^-(Y)[-2], \iota)$ is an $\iota$-complex. Notice the pesky grading shift! This is an artefact of $HF^+$ originally being more popular than $HF^-$.

**Definition 9.6.2.** Two $\iota$-complexes $(C, \iota), (C', \iota')$ are called *equivalent* if there are chain homotopy equivalences of complexes of $\mathbb{F}[U]$-modules

$$F : C \to C', \quad G : C' \to C$$

such that $FG \sim \text{id}, GF \sim \text{id}$, and $F$ and $G$ preserve the involution up to homotopy: $F\iota \sim \iota' F, G\iota' \sim \iota G$.

**Example.** If $Y$ is a $\mathbb{Z}HS^3$, then $(CF^-(Y)[-2], \iota)$ is an invariant of $Y$ up to equivalence.

This strong notion of equivalence isn't particularly useful in our case - a weaker but more useful notion is the following:

**Definition 9.6.3.** $(C, \iota), (C', \iota')$ are *locally equivalent* if there are chain maps of complexes of $\mathbb{F}[U]$-modules

$$F : C \to C', \quad G : C' \to C$$

such that $F, G$ induce isomorphisms on $U^{-1}H_*$, and $F$ and $G$ preserve the involution up to homotopy.

**Example.** If $Y$ and $Y'$ are homology cobordant, then $(CF^-(Y_1)[-2], \iota)$ and $(CF^-(Y_2)[-2], \iota)$ are locally equivalent but not necessarily equivalent. The local equivalence comes from the fact that cobordism maps induce isomorphisms on $HF^\infty = \mathbb{F}[U, U^{-1}]$ (since the homology cobordisms are negative definite, and an earlier theorem of Ozsváth and Szabó applies).

**Definition 9.6.4.** The *local equivalence group* is the collection of $\iota$-complexes modulo local equivalence, denoted by $\mathcal{J}$.

**Proposition 9.6.5.** $\mathcal{J}$ is an abelian group, under the operation

$$(C, \iota) \otimes (C', \iota') = (C \otimes_{\mathbb{F}[U]} C', \iota \otimes \iota').$$

*Proof.* The unit is $(\mathcal{F}[U], \mathrm{id})$. The inverses are given by

$$-(C, \iota) = (C^\vee, \iota^\vee), \quad C^\vee = \mathrm{Hom}_{\mathbb{F}[U]}(C, \mathbb{F}[U]).$$

The main thing to check is that the claimed inverse is really an inverse. □

**Remark.** By using local equivalence, we have a group structure, even though inverses wouldn't have existed in general had we used equivalence instead. This is analgous to the homology cobordism group being a group, even though homology spheres up to homeomorphism or diffeomorphism are not groups. Similarly, the knot concordance group is a group, even though knot equivalence doesn't give a group.

The main reason we care about $\mathcal{J}$ is because there is a natural homomorphism

$$h : \Theta^3_{\mathbb{Z}} \to \mathcal{J}, \quad h([Y]) = (CF^-(Y)[-2], \iota).$$

This map is clearly non-trivial, since different homology spheres can have different involutive Heegaard Floer homologies. A more precise measure of non-triviality would be if we could find maps from $\Theta^3_{\mathbb{Z}}$ which factor through $\mathcal{J}$. Indeed,

$$d, \underline{d}, \overline{d} : \Theta^3_{\mathbb{Z}} \xrightarrow{h} \mathcal{J} \to \mathbb{Z}$$

factor through $\mathcal{J}$. If we can understand the structure of $\mathcal{J}$, it will help to understand $\Theta^3_{\mathbb{Z}}$. Currently, the structure of $\mathcal{J}$ is an open question.

## 9.7 Using $\iota$-complexes to study $\Theta^3_{\mathbb{Z}}$

One of the themes of these lecture notes is the study of $\Theta^3_{\mathbb{Z}}$. As an application of cobordism maps, we showed that the invariant $d(Y)$ is a homology cobordism invariant, and used this to prove that $\Theta^3_{\mathbb{Z}}$ has a $\mathbb{Z}$-summand. Using involutive Heegaard Floer homology and $\mathcal{J}$, we can obtain some even better results!

We begin with an overview of results.

**Theorem 9.7.1.** *$\Theta^3_{\mathbb{Z}}$ contains $\mathbb{Z}^\infty$ as a subgroup.*

1. *First proof: Fintushel-Stern, Furuta, circa 1990, using Yang-Mills theory.*
2. *Newer proof: Stoffregen, circa 2015, using Pin(2)-equivariant Seiberg-Witten theory.*
3. *Newer proof: Dai and Manolescu, using involutive Heegaard Floer homology and $\mathcal{J}$.*

*Moreover, in 2018, the result was strengthened further:*

4. *Dai, Hom, Stoffregen, and Truong, showed that $\Theta^3_{\mathbb{Z}}$ has a $\mathbb{Z}^\infty$ summand by again using $\mathcal{J}$.*

In this section, we will first describe the result of Dai and Manolescu, and later explore the more recent result of Dai, Hom, Stoffregen, and Truong.

**Theorem 9.7.2.** *$\Theta^3_{\mathbb{Z}}$ has a $\mathbb{Z}^\infty$ subgroup.*

*Proof.* The idea is to compute

$$(CF^-(\Sigma(p, 2p-1, 2p+1)), \iota)$$

up to local equivalence, where $p \geqslant 3$ is odd.

Figure 9.8 shows a representative of the local equivalence class for each $p$:

By algebra, the $\iota$-complexes can be shown to be linearly independent in $\mathcal{J}$ for each $p$. □

Next we give a proof outline for an improved result.

**Theorem 9.7.3** (Dai, Hom, Stoffregen, Truong 2018)**.** *$\Theta^3_{\mathbb{Z}}$ has a $\mathbb{Z}^\infty$ summand.*

**Remark.** It might not be clear that this is any strong! Notice that $\mathbb{Z}^\infty$ is a subgroup of $\mathbb{Q}^\infty$, but not a summand.

*Proof.* We wish to construct homomorphisms $f_i : \mathcal{J} \to \mathbb{Z}$ such that

$$\Theta^3_{\mathbb{Z}} \xrightarrow{h} \mathcal{J} \xrightarrow{f} \mathbb{Z}^\infty$$

is *surjective*, where $f$ is the direct sum of the $f_i$.

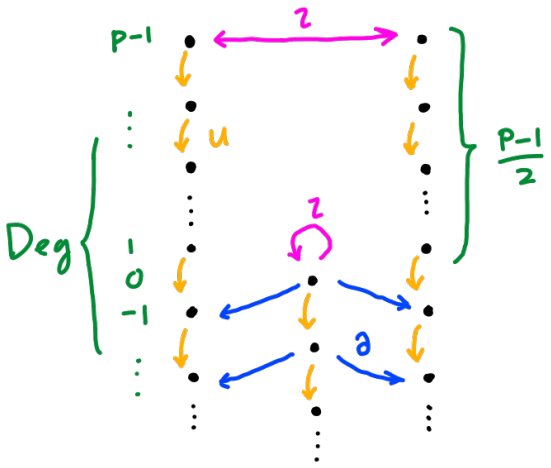


Figure 9.8: The local equivalence class of $(CF^-(\Sigma(p, 2p-1, 2p+1)), \iota)$.

Concretely, define $Y_i = \Sigma(2i+1, 4i+1, 4i+3)$, and suppose $f_i(h(Y_i)) = \delta_{ij}$. Then $f \circ h$ would indeed be surjective. It follows that

$$\Theta^3_{\mathbb{Z}} \cong \langle Y_i \rangle \oplus \ker(f \circ h) = \mathbb{Z}^\infty \oplus \text{mystery summand}.$$

In this proof, we will construct such maps $f_i$.

The main difficulty is that chain complexes over $\mathbb{F}[U, Q]/Q^2$ are difficult to understand. Instead, it is easier to consider complexes over $\mathbb{F}[U, Q]/(Q^2, QU)$. This is also not a PID, but it's closer!

**Definition 9.7.4.** A *almost $\iota$-complex* is a pair $(C, \iota)$ such that

1. $C$ is a finitely generated free $\mathbb{Z}$-graded complex over $\mathbb{F}[U]$, with degree $U = -2$, and $U^{-1}H_*(C) \cong \mathbb{F}[U, U^{-1}]$.
2. $\iota : C \to C$ is a grading preserving $\mathbb{F}[U]$-module homomorphism such that $\iota\partial + \partial\iota \in \operatorname{im} U, \iota^2 + \mathrm{id} \in \operatorname{im} U$. That is, $\iota$ is a chain map modulo $U$, and a homotopy involution modulo $U$.

**Definition 9.7.5.** Two almost $\iota$-complexes $(C, \iota), (C', \iota')$ are *locally equivalent* if there is a grading preserving homomorphism of $\mathbb{F}[U]$-chain complexes

$$f : C \to C', \quad g : C' \to C$$

such that $f, g$ induce isomorphisms on $U^{-1}H_*$, and $f\iota \sim \iota' f \mod U, g\iota' \sim \iota g \mod U$.

Almost $\iota$-complexes also give rise to an abelian group!

**Definition 9.7.6.** The abelian group of almost $\iota$-complexes up to local equivalence is denoted by $\widehat{\mathcal{J}}$.

Notice that there is a natural homomorphism

$$\mathcal{J} \to \widehat{\mathcal{J}},$$

simply the forgetful map. The proof of DHST proceeds by classifying the elements of $\widehat{\mathcal{J}}$, and using it to define relevant desired maps mentioned at the start of this proof.

**Theorem 9.7.7.** *Every almost $\iota$-complex is locally equivalent to a chain complex of the form $C(a_1, b_2, a_3, \ldots, a_{2n-1}, b_{2n})$, where $a_i \in \{\pm\}$ and $b_i \in \mathbb{Z} - \{0\}$, freely generated by elements $T_0, \ldots, T_{2n}$ with*

$$\begin{aligned} a_i = - \quad &\Rightarrow \quad (1+\iota)T_{i-1} = T_i \\ a_i = + \quad &\Rightarrow \quad (1+\iota)T_i = T_{i-1} \\ b_i < 0 \quad &\Rightarrow \quad \partial T_i = U^{|b_i|}T_i \\ b_i > 0 \quad &\Rightarrow \quad \partial T_i = U^{|b_i|}T_{i-1} \end{aligned}$$

*and $\partial = 0$ otherwise. Note that the first two conditions together with $\iota^2 \sim \mathrm{id} \mod U$ determine $\iota$ up to local equivalence.*

**Example.** To unobfuscate the above theorem, figure 9.9 shows $C(-, -3, -, 4, +, -2)$.

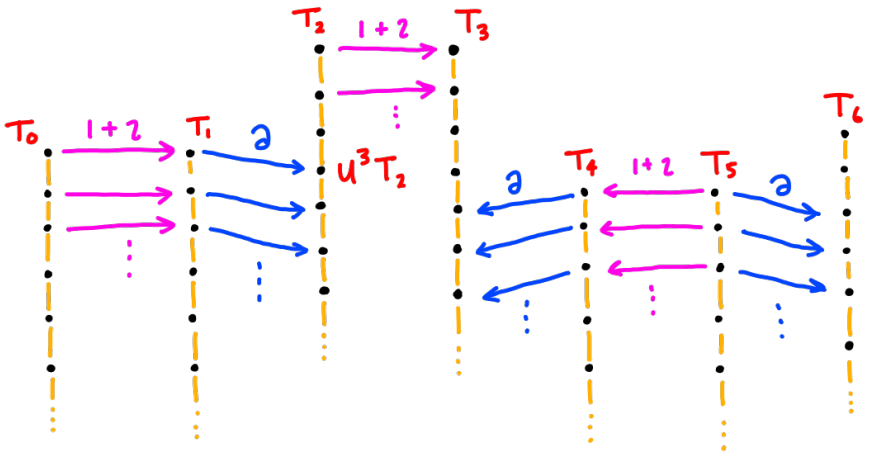


Figure 9.9: $C(-, -3, -, 4, +, -2)$; an example of the structure theorem for $\widehat{\mathcal{J}}$.

The above result is analogous to the structure theorem for finitely generated modules over a PID. Overall, this classifies $\widehat{\mathcal{J}}$ as a set. However, it should be noted that the group structure is still mysterious!

Define $\varphi_n : \widehat{\mathcal{J}} \to \mathbb{Z}$ by

$$\varphi_n(C(a_1, \ldots, b_{2n})) = \#(\text{parameters with } b_i = n) - \#(\text{parameters with } b_i = -n).$$

This is really a signed count of towers of length $n$ in $H_*$. The remainder of the proof is to show that the $\varphi_n$ are *homomorphisms*, and if we consider the composition

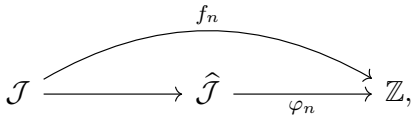


then we have $f_n(h(Y_i)) = \delta_{ij}$ as required. □

# Chapter 10

# Knot Floer homology introduction

The last big topic of the course is knot Floer homology. In 3 and 4 dimensional topology, we find that knots are an invaluable tool, as they are a lot easier to study and understand than 3 and 4 manifolds, but also contribute many non-trivial examples (and in the case of 3-manifolds, even a classification of oriented closed 3-manifolds in terms of knots). In subsequent sections and chapters we will introduce knot Floer homology. The two main applications we consider are to the structure of the knot concordance group, but also the existence of an algorithm to compute all the different versions of Heegaard Floer homology four 3 manifolds (beyond just the hat version). A good survery on knot Floer homology is Manolescu's *introduction to knot Floer homology.*

## 10.1 Alexander-Conway polynomial (lecture 17)

**Definition 10.1.1.** A *knot* is a smooth oriented embedding of $\mathbb{S}^1$ in $\mathbb{S}^3$. We consider knots up to isotopy. A *link* is a disjoint union of knots.

**Definition 10.1.2.** The *Alexander-Conway polynomial*, also just called the Alexander polynomial, is the unique polynomial $\Delta_L(q) = \Delta(L) \in \mathbb{Z}[q^{1/2}, q^{-1/2}]$ satisfying

1. $\Delta(\text{unknot}) = 1$ (normalisation)
2. $\Delta\left(\right) - \Delta\left(\right) = (q^{1/2} - q^{-1/2})\Delta\left(\right)$ (skein relation).

If $L$ is a knot, then $\Delta(L) \in \mathbb{Z}[q, q^{-1}]$.

**Example.** What is the Alexander polynomial of the unlink? Using the definition, we have

$$0 = 1 - 1 = \Delta\left(\right) - \Delta\left(\right) = (q^{1/2} - q^{-1/2})\Delta\left(\right),$$

so that

$$\Delta\left(\right) = 0.$$

What is the Alexander polynomial of the Hopf link? Again we use the definition and find that

$$\Delta\left(\text{ 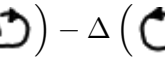 }\right) - \Delta\left(\text{ 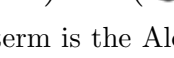 }\right) = (q^{1/2} - q^{-1/2})\Delta\left(\text{  }\right).$$

The second Alexander term is the Alexander polynomial of the unlink, and the last term is of the unknot. This gives

$$\Delta\left(\text{  }\right) = q^{1/2} - q^{-1/2}.$$

What about the trefoil knot?

$$\Delta\left(\text{ 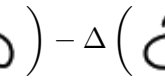 }\right) - \Delta\left(\text{}\right) = (q^{1/2} - q^{-1/2})\Delta\left(\text{}\right).$$

This time the second term is the unknot and the last term the Hopf link, giving

$$\Delta\left(\text{ 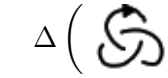 }\right) - 1 = (q^{1/2} - q^{-1/2})^2.$$

Therefore the Alexander polynomial of the trefoil is

$$\Delta\left(\text{ 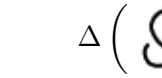 }\right) = q - 1 + q^{-1}.$$

**Remark.** It is straight forward to show that a polynomial satisfying the definition of the Alexander polynomial is a knot invariant. However, the work is in showing that such a polynomial exists (and is unique). To prove this, loosely speaking, one inducts on $n$, considering the space $D_n$ of all diagrams with $n$ crossings. The proof formalises the fact that for any link, we can compute its Alexandedr polynomial as we did above, and the choice of path of crossing resolutions doesn't affect the outcome.

**Proposition 10.1.3.** Here are several elementary properties of the Alexander polynomial.

- $\Delta_K(1) = 1$ whenever $K$ is a knot.
- $\Delta_K(q) = \Delta_K(q^{-1})$.
- $\Delta_K(q) = \Delta_{m(K)}(q)$, where $m(K)$ denotes the *mirror* of $K$. (Change all crossings.)
- $\Delta_K(q) = \Delta_{K^r}(q)$, where $K^r$ denotes the *reverse* of $K$. (Change orientation of $K$.)

Note that typically $K, m(K), K^r$, and $m(K^r)$ are all distinct. We also denote the mirror of a knot by $\overline{K}$.

## 10.2 Heegaard diagrams for knots

Our goal is to develop Heegaard Floer homology for knots. This will require some type of Heegaard diagram for a knot, which we introduce in this section.

**Definition 10.2.1.** Let $K \subset \mathbb{S}^3$ be a knot. The data

$$(\Sigma, \alpha_1, \dots, \alpha_g, \beta_1, \dots, \beta_g, w, z)$$

is a *Heegaard diagram for* $K$ if it satisfies the following:

- $(\Sigma, \alpha_i, \beta_i)$ is a Heegaard diagram for $\mathbb{S}^3$.
- $w, z$ lie in $\Sigma - \cup_i \alpha_i - \cup_i \beta_i$.
- There exist curves $\gamma_\alpha, \gamma_\beta$ so that $K = \gamma_\alpha \cup \gamma_\beta$, and $\gamma_\alpha$ is a path lying in $U_\alpha - \cup_i D_{\alpha_i}$, while $\gamma_\beta$ is a path lying in $U_\beta - \cup_i D_{\beta_i}$. Here we write $U_\alpha$ to denote the handlebody determined by the $\alpha$ curves and $D_{\alpha_i}$ to denote the disk in $U_\alpha$ determined by $\alpha_i$, and similarly for $\beta$.

Of course, we've established that every oriented closed 3-manifold admits a Heegaard diagram. Does every knot admit a Heegaard diagram? Yes!

**Proposition 10.2.2.** Every $K \subset \mathbb{S}^3$ admits a Heegaard diagram.

*Proof.* Write $Y = \mathbb{S}^3 - \text{nbhd}(K)$. Then $\partial Y = T^2$. We can choose a Heegaard diagram $(\Sigma, \alpha_1, \dots, \alpha_g, \beta_1, \dots, \beta_{g-1})$ of $Y$, i.e. $Y$ is a union of a genus $g$ handlebody with $g-1$ neighbourhoods of $\beta$ disks. Now adding the meridian $\beta_g$ of the knot gives a Heegaard diagram $(\Sigma, \alpha_1, \dots, \alpha_g, \beta_1, \dots, \beta_g)$ of $\mathbb{S}^3$.

Fix $w, z$ to be points close to $\beta_g$, on either side. I claim that

$$(\Sigma, \alpha_1, \dots, \alpha_g, \beta_1, \dots, \beta_g, w, z)$$

is a Heegaard diagram for $K$. Define $\gamma_\alpha$ to be the small arc directly joining $w$ and $z$ by crossing $\beta_g$. On the other hand, we define $\gamma_\beta$ to be the arc following the longitude of $K$ in $U_\beta$. This avoids all of the $\beta$ curves, because by construction the longitude of $K$ does not intersect $\beta_1, \dots, \beta_{g-1}$ (by considering the Heegaard diagram of $Y$). But now it is clear that $K = \gamma_\alpha \cup \gamma_\beta$, and we have indeed constructed a Heegaard diagram of $K$. □

**Proposition 10.2.3.** Any two Heegaard diagrams for $K$ are related by a sequence of moves:

- isotopies away from $w, z$,
- handleslides away from $w, z$,

- stabilisation/destabilisation.

Recall from earlier chapters that $\widehat{HF}(Y,s)$ is $\mathbb{Z}/N\mathbb{Z}$-graded where $N\mathbb{Z}$ is the image of the Maslov-grading map $\mu : \hat{\pi}_2(x,x) \to \mathbb{Z}$, where $x$ represents the equivalence class $s$ of intersection points $\mathbb{T}_\alpha \cap \mathbb{T}_\beta$. (Alternatively, $s$ can be considered to be a spin$^c$-structure.) But we also know that the Maslov map has trivial image if $Y$ is a rational homology sphere, giving an integral grading. We now recall the Maslov grading for the 3-sphere, which will give us a grading for knot Floer homology.

Let $(\Sigma, \alpha_i, \beta_i)$ be a Heegaard diagram for $\mathbb{S}^3$. Recall that $\text{Spin}^c(\mathbb{S}^3) = H_1(\mathbb{S}^3) = 0$. In other words, for *any* $x, y \in \mathbb{T}_\alpha \cap \mathbb{T}_\beta$, there exists some $\varphi \in \pi_2(x,y)$, and the relative grading between $x$ and $y$ is given by $\varphi$. More precisely, $CF^\circ(\Sigma, \alpha, \beta) = CF^\circ(\mathbb{S}^3)$ admits a $\mathbb{Z}$-grading $M : \mathbb{T}_\alpha \cap \mathbb{T}_\beta \to \mathbb{Z}$ given by the Maslov index $\mu$, satisfying

$$M(x) - M(y) = \mu(\varphi), \quad \varphi \in \pi_2(x,y), n_w(\varphi) = 0.$$

Recall that the second condition on $\varphi$ is specifying that $\varphi$ must stay away from $w$; we declare that $w$ is the basepoint of the Heegaard diagram. For general $\varphi$, we can actually just decree that

$$M(x) - M(y) = \mu(\varphi) - 2n_w(\varphi).$$

Finally this grading is made absolute by noting that $\widehat{HF}(\mathbb{S}^3) = \mathbb{Z}$ is concentrated in degree 0.

**Example.** Consider the standard genus 1 Heegaard diagram for $\mathbb{S}^3$, with basepoint $w$, as shown in figure 10.1.

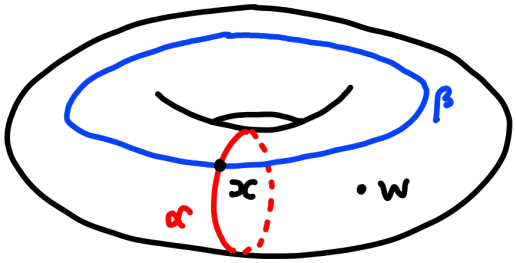


Figure 10.1: Example of the Maslov grading formula for $\mathbb{S}^3$.

Cutting along the $\alpha$ and $\beta$ curve gives a single rectangular region $R$, with $\mu(R) = 2$. This follows from the Lipshitz formula, since $R$ is a region from $x$ to itself, and

$$\mu(R) = e(R) + n_x(R) + n_x(R) = 0 + 1 + 1 = 2.$$

On the other hand, we see that $R$ passes over the point $w$ once, giving $n_w(R) = 1$. But now

$$\mu(R) - 2n_w(R) = 0.$$

This agrees with the general theory, from which we require that

$$M(x) - M(x) = \mu(R).$$

In particular, $M(x) = 0$ because the Heegaard Floer homology of $\mathbb{S}^3$ is concentrated in degree 0.

## 10.3 Knot Floer homology: definition and properties

We're now ready to define knot Floer homology. In the 4-manifolds class in Spring 2020, we finished with Khovanov homology. We saw that this was a categorification of the Jones polynomial. More precisely, Khovanov homology was bigraded - by the *homological grading* $i$ and the *Jones grading* $j$. The Euler characteristic

$$\chi(\mathrm{Kh}(K)) = \sum_{i,j}(-1)^i q^j \operatorname{rk} \mathrm{Kh}^{i,j}(K)$$

is equal to $(q + q^{-1})J_K(q)$, where $J_K(q)$ is the *Jones polynomial* of $K$.

Knot Floer homology, which we now define, is analogously a categorification of the Alexander polynomial. Writing $i$ for the *Maslov grading* and $s$ for the *Alexander grading*, we will see that

$$\Delta_K(q) = \sum_{i,s}(-1)^i q^s \operatorname{rk}(\widehat{HFK}_i(K, s)).$$

A good place to learn about knot Floer homology is Ciprian's 2016 expository article *An introduction to knot Floer homology.*

**Definition 10.3.1.** Let $K \subset \mathbb{S}^3$ be a knot. Let $(\Sigma, \alpha_i, \beta_i, w, z)$ be a Heegaard diagram for $K$. Then the *knot Floer homology* of $K$ is

$$\widehat{HFK}(K) = HF(\mathbb{T}_\alpha, \mathbb{T}_\beta \text{ in } \mathrm{Sym}^g(\Sigma - w - z)).$$

Recall that the restriction to $\mathrm{Sym}^g(\Sigma - w - z)$ means that we only count $J$-holomorphic curves in $\pi_2(x, y)$ with $n_w = n_z = 0$.

**Proposition 10.3.2.** Knot Floer homology is integrally bigraded:

$$\widehat{HFK}(K) = \bigoplus_{i,s\in\mathbb{Z}} \widehat{HFK}_i(K, s).$$

Here $i$ is the *Maslov* or *homological* grading, and $s$ is the *Alexander grading.*

We already described the Maslov grading at the end of the previous section, and observed that it was integral. It remains to describe the Alexander grading.

We declare that $x \sim y$ if and only if there exists $\varphi \in \pi_2(x, y)$ such that $n_w(\varphi) = n_z(\varphi) = 0$. Then the set of equivalence classes is in bijective correspondence with spin$^c$-structures on the knot complement, so that

$$\{ \text{ equivalence classes } \} \cong \text{Spin}^c(\mathbb{S}^3 - K) \cong H_1(\mathbb{S}^3 - K) = \mathbb{Z}.$$

Partitioning the knot Floer homology by these equivalence classes then gives an integral grading, which we call the *Alexander grading*.

As promised earlier, the bigrading gives rise to the Alexander polynomial!

**Proposition 10.3.3.**

$$\chi(\widehat{HFK}(K)) = \sum_{i,s \in \mathbb{Z}} (-1)^i q^s \operatorname{rk}(\widehat{HFK}_i(K, s)) \in \mathbb{Z}[q, q^{-1}]$$

is the Alexander polynomial, $\Delta_K(q)$.

*Proof.* It suffices to verify that the Euler characteristic satisfies the defining relations of the Alexander polynomial - normalisation and the skein relation. Specifically, for the skein relation, one can show that

all fit in a long exact sequence! (Notice that we technically cannot prove this yet! Resolving crossings typically doesn't preserve the number of components - we first need a notion of knot Floer homology for links.) □

**Example.** Adding an extra marked point to the Heegaard diagram of $\mathbb{S}^3$ shown in the previous section gives a Heegaard diagram of the unknot, as shown in figure 10.2. From this

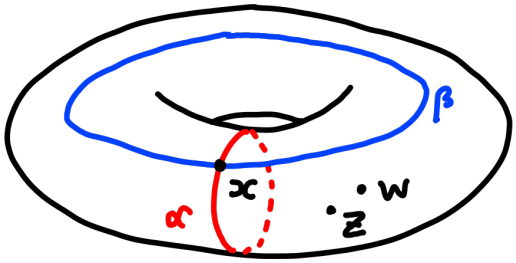


Figure 10.2: Heegaard diagram of the unknot.

Heegaard diagram, we immediately deduce that $\widehat{HFK}(\text{unknot}) = \mathbb{Z}$, and this is concentrated in bidegree $(0, 0)$. The Euler characteristic is then 1, which is indeed the Alexander polynomial of the unknot.

**Proposition 10.3.4.** Knot Floer homology enjoys various symmetries, which can be thought of as generalisations of the symmetries at the level of the Alexander polynomial.

1. $\widehat{HFK}_i(K,s) = \widehat{HFK}_i(K^r,s)$.
2. $\widehat{HFK}_i(K,s) = \widehat{HFK}_{-i}(\overline{K},-s)$. In fact, this gives
$$\widehat{HFK}(LHT) \neq \widehat{HFK}(RHT),$$
which we know is *not* the case for the Alexander polynomial. Therefore knot Floer homology contains more information than the Alexander polynomial!
3. $\widehat{HFK}_i(K,s) = \widehat{HFK}_{i-2s}(K,-s)$. This is conjugation symmetry, corresponding to the symmetry $\Delta_K(q) = \Delta_K(q^{-1})$ of the Alexander polynomial.

We do not prove these symmetries.

One of the dankest applications of knot Floer homology is that it solves the genus problem for knots!

**Definition 10.3.5.** Given a knot $K \subset \mathbb{S}^3$, a *Seifert surface* of $K$ is an oriented properly smoothly embedded surface $\Sigma \subset \mathbb{S}^3$ with $\partial\Sigma = K$. The *genus* $g(K)$ of the knot $K$ is the minimum of the genera of Seifert surfaces of $K$.

**Example.** The genus of the unknot is 0, since it bounds an embedded disk. Conversely, the boundary of any embedded disk is always an unknot, so
$$g(K) = 0 \quad \Leftrightarrow \quad K \text{ is an unknot.}$$

The trefoil knot is knot the unknot, so it must have $g(K) \geqslant 1$. On the other hand, there exists a Seifert surface with genus 1 (by using the diagram with three crossings with rotational symmetry of order 2). Therefore $g(\text{trefoil}) = 1$.

A classical result bounds the genus of a knot from below: if
$$\Delta_K(q) = a_s q^s + a_{s-1}q^{s-1} + \cdots + a_s q^{-s}, a_s \neq 0,$$
then $g(K) \geqslant s$. Ozsváth and Szabó improved this result, giving an equality.

**Theorem 10.3.6** (Ozsváth, Szabó)**.**
$$g(K) = \max\{s : \widehat{HFK}(K,s) \neq 0\}.$$

**Corollary 10.3.7.** *$\widehat{HFK}$ detects the unknot. That is, if $\widehat{HFK}$ of a knot is trivial, then its genus must be 0, so the knot is the unknot.*

This result can actually be combined with the next property we describe to detect even more knots!

**Definition 10.3.8.** A knot $K$ is *fibred* if there exists a fibre bundle

$$\Sigma \to \mathbb{S}^3 - \text{nbhd}(K) \to \mathbb{S}^1,$$

where $\Sigma$ is some surface with boundary.

**Example.** The unknot is fibred, because the knot complement of the unknot is topologically $\mathbb{S}^1 \times D^2$. This is the total space of a bundle over $\mathbb{S}^1$ with fibre $D^2$.

Other examples of fibred knots include the trefoil and figure 8 knots.

A classical result is that if $K$ is fibred, then $\Delta_K(q)$ is monic. (That is, $a_s = \pm 1$). This can be strengthened by knot Floer homology.

**Theorem 10.3.9.** *A knot $K$ is fibred* if and only if $\widehat{HFK}(K, g(K)) = \mathbb{Z}$.

Using this result, we now show that knot Floer homology detects the trefoil and figure 8 knots.

**Corollary 10.3.10.** *$\widehat{HFK}$ detects the trefoil and figure 8 knots.*

*Proof.* We use the following fact: the *only* fibred knots of genus 1 are the two trefoils (left and right handed trefoils) and the figure 8 knot (which is amphichiral). As an example, we show that knot Floer homology detects the right handed trefoil, as the same argument carries through.

1. Compute $\widehat{HFK}(K)$. Suppose it's equal to the knot Floer homology of the right handed trefoil.

2. Since the trefoil has genus 1, by the genus theorem of Ozsváth and Szabó, we know that

   $$1 = g(RHT) = \max\{s : \widehat{HFK}(RHT, s)\} = \max\{s : \widehat{HFK}(K, s)\} = g(K),$$

   so $K$ has genus 1.

3. Since the trefoil is fibred, we also know that

   $$\widehat{HFK}(K, g(K)) = \widehat{HFK}(K, 1) = \widehat{HFK}(RHT, g(RHT)) = \mathbb{Z}.$$

   Therefore $K$ is fibred. In summary, $K$ is a fibred knot with genus 1.

4. The only such knots are the left and right handed trefoils and figure 8 knot. These three knots each have distinct knot Floer homologies, so $K$ cannot be the left handed trefoil or the figure 8 knot. This leaves only the right handed trefoil, so $K = RHT$.

□

**Remark.** Finally we remark that knot Floer homology is knot a complete invariant: there exist knots $K_1, K_2$ which are not equivalent, but such that their knot Floer homologies are equal. One can take $7_4$ and $9_2$, for example.

## 10.4 Heegaard diagrams from bridge presentations

We have yet to describe how to actually compute knot Floer homology, since we don't know how to obtain a Heegaard diagram of a knot! This turns out to be very straight forward, using knot diagrams.

**Definition 10.4.1.** A *b-bridge presentation* of a knot $K$ is a knot diagram of $K$ consisting of $2b$ arcs, which alternate between $b$ arcs which strictly underpass other arcs, and $b$ arcs which strictly overpass.

**Example.** The trefoil admits a 2-bridge presentation. Specifically, figure 10.3 is a 2-bridge presentation of the right handed trefoil knot.

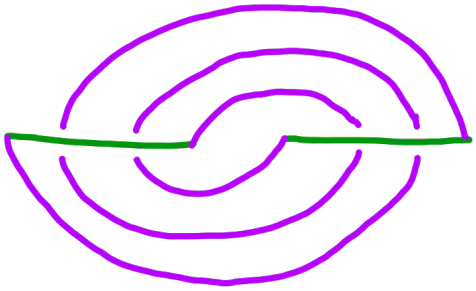

Figure 10.3: A 2-bridge presentation of RHT

It turns out that every knot has a $b$-bridge presentation for some $b$! This is easy to see because given any diagram of a knot with $b$ crossings, one can simply convert each overpass to a small arc which is declared an overpassing arc for the bridge presentation. In summary, we have:

**Proposition 10.4.2.** Every knot admits a $b$-bridge presentation for some $b$.

**Definition 10.4.3.** The *bridge number* $b(K)$ of a knot $K$ is the minimum $b$ such that $K$ admits a $b$-bridge presentation.

It turns out that given a $b$-bridge presentation of a knot $K$, we can describe a Heegaard diagram of genus $b-1$ for $K$! We describe the process using words here, but it is best understood through examples.

**Proposition 10.4.4.** Let $K$ be a knot with a $b$-bridge diagram. The following process defines a Heegaard diagram of $K$ with genus $b-1$.

1. Replace $b-1$ underpassing arcs with $\alpha$-curves: the endpoints become circles in the Heegaard diagram which are identified to give genus.
2. Replace the last underpass with the symbols $w$ and $z$ at its endpoints.
3. Remove the bridge (overpassing arc) incident to $z$.
4. Replace all other bridges with $\beta$-curves: visually, this is taken to be the boundary of a regular neighbourhood of the arc.

**Example.** Figure 10.4 shows two examples of the above procedure, one for the unknot, and one for the left handed trefoil.

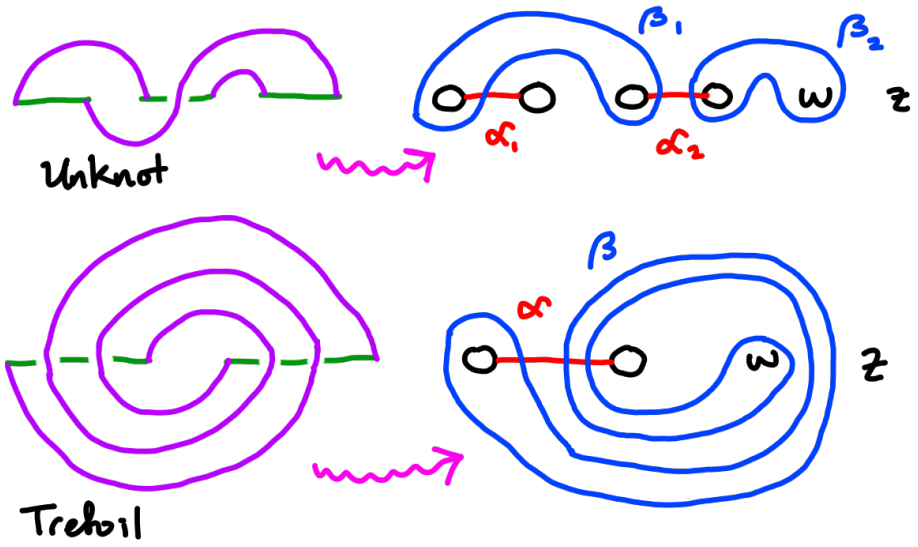


Figure 10.4: Examples of obtaining a Heegaard diagram from a bridge presentation.

Why is this really a Heegaard diagram of the given knot? The idea is that a bridge presentation corresponds to an embedding of a surface $\Sigma$ in $\mathbb{S}^3$, so that $\Sigma \cap K$ are all of the points in the bridge presentation where a bridge meets an underpass. $\Sigma$ cuts $\mathbb{S}^3$ into two nadlebodies - the "top handlebody" contains the bridges, and the "bottom handlebody" contains underpasses. These are the handlebodies of the Heegaard diagram. Finally, specifying the $\alpha$ and $\beta$ curves as above allow us to reconstruct the knot as a union of two arcs (as in the definition of a Heegaard diagram of a knot) in a canonical way.

This is difficult to convey in words, so instead an example is provided in figure 10.5.

Recall that $(\Sigma, \alpha_i, \beta_i, w, z)$ is a Heegaard diagram of $K$ if it's a Heegaard diagram for $\mathbb{S}^3$ with curves $\gamma_\alpha$ and $\gamma_\beta$, lying in $U_\alpha - \cup_i \alpha_i$ and $U_\beta - \cup_i \beta_i$ respectively, so that $K = \gamma_\alpha \cup \gamma_\beta$.

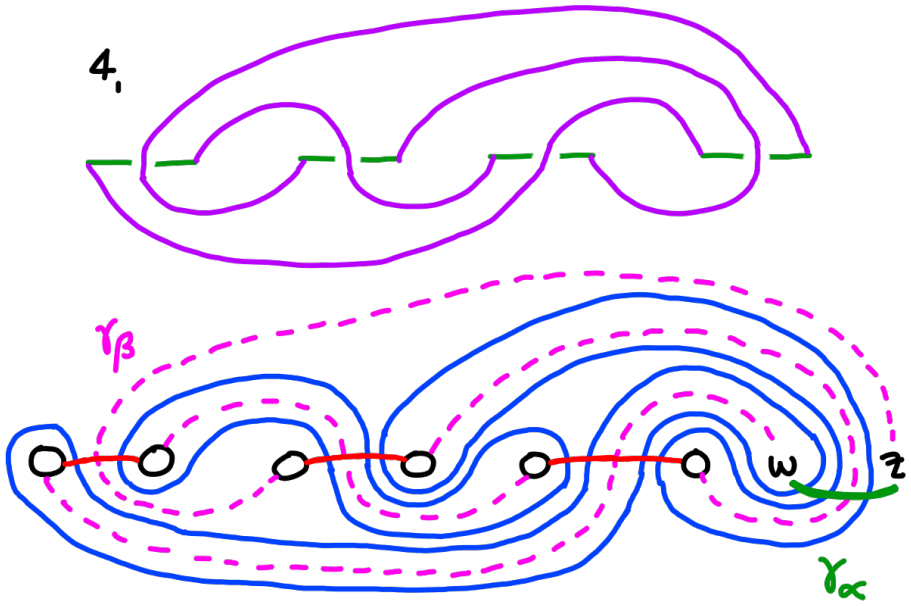


Figure 10.5: Example to verify that the Heegaard diagrams obtained above are really Heegaard diagrams of the knot.

In our case, we see that $\gamma_\alpha$ can be taken to be the bridge which was deleted (in the conversion of our bridge presentation to the Heegaard diagram), and $\gamma_\beta$ can be taken to be the union of all of the other arcs from the bridge presentation.

## 10.5 Example calculations of knot Floer homology (lecture 18)

In this section, we'll compute the knot Floer homologies of some 2-bridge knots. These knots canonically admit genus 1 Heegaard diagrams by the process described in the previous lecture, so the calculations are reasonably easy. To be more precise, if a Heegaard diagram has genus 1, then we consider

$$\mathrm{Sym}^1(\Sigma - w - z) = \Sigma - w - z,$$

in which domains end up being exactly bigons. From earlier, we know that bigons admit exactly one $J$-holomorphic strip, so we can easily describe the boundary map in the Floer chain complex.

**Definition 10.5.1.** A knot admitting a 2-bridge presentation is called a *2-bridge knot*. These are classified by the rationals! Examples include the trefoil and figure 8 knots.

Formally, our method for computing knot Floer homologies is as follows:

1. Find $\mathbb{T}_\alpha \cap \mathbb{T}_\beta$. Let $\varphi \in \pi_2(x, y)$. We know that the Maslov grading is given relatively by
$$M(x) - M(y) = \mu(\varphi) - 2n_w(\varphi).$$
On the other hand, the Alexander grading is given relatively by
$$A(x) - A(y) = n_z(\varphi) - n_w(\varphi).$$

2. $M$ is upgraded from a relative grading to an absolute grading since we require $\widehat{HF}(\mathbb{S}^3) \cong \mathbb{Z}$ to be concentrated in degree 0. Recall that $\widehat{HF}(\mathbb{S}^3)$ is the Lagrangian Floer homology of $\mathbb{T}_\alpha, \mathbb{T}_\beta$ in $\mathrm{Sym}^g(\Sigma - w)$ as opposed to $\widehat{HFK}(K)$ which is the homology in $\mathrm{Sym}^g(\Sigma - w - z)$. We track where $\widehat{HF}(\mathbb{S}^3)$ lifts to $\widehat{HFK}(K)$.

3. $A$ is upgraded from a relative grading to an absolute grading by the requirement that the Euler characteristic (Alexander polynomial) is symmetric.

**Example.** For our first example, we will compute
$$\widehat{HFK}(LHT)$$
using the Heegaard diagram shown in figure 10.6. Notice that we can isotope a $\beta$ curve "over infinity" in the diagram on the left to arrive at the much simpler diagram on the right.

Using this Heegaard diagram, we're ready to calculate! First, we see that there are three intersection points, $a, b, c$. Therefore
$$\widehat{CFK} = \langle a, b, c \rangle.$$
What's the boundary map? There are exactly two bigons in the Heegaard diagram, one containing $w$ and one containing $z$. Therefore there are no bigons *away* from $w$ or $z$. Therefore all of the moduli spaces of $J$-holomorphic strips are empty, and the boundary map is trivial! We have
$$\widehat{HFK}(LHT) = \langle a, b, c \rangle = \mathbb{Z}^3.$$
Next we determine the relative grading differences between the points $a, b, c$ which generate the homology. For the Maslov grading, we have
$$M(a) - M(b) = \mu(D_z) - 2n_w(D_z) = 1 - 2 \cdot 0 = 1$$
where $D_z$ is the bigon containing $z$. We also have
$$M(c) - M(b) = \mu(D_w) - 2n_w(D_w) = 1 - 2 \cdot 1 = -1$$

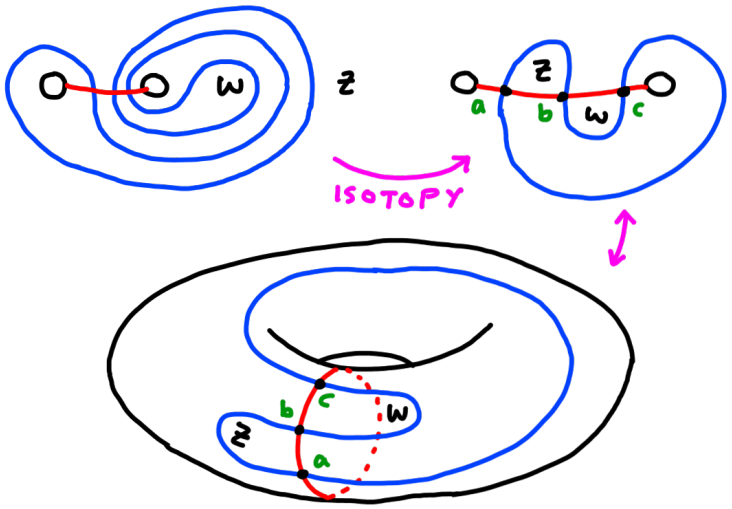


Figure 10.6: Heegaard diagram of a left handed trefoil.

where $D_w$ is the bigon containing $w$. Therefore

$$M(c) + 2 = M(b) + 1 = M(a).$$

To make this an absolute grading, we determine $\widehat{HF}(\mathbb{S}^3)$ in terms of $a, b, c$. This time we *can* consider regions that cover $z$, so in particular the bigon containing $z$ contributes to a non-trivial term in the boundary map: we have

$$\partial a = b, \partial b = \partial c = 0.$$

Therefore $\widehat{HF}(\mathbb{S}^3) = \langle c \rangle$. Since this is concentrated in degree 0, it must be the case that

$$M(c) = 0, M(b) = 1, M(a) = 2.$$

Finally we determine the Alexander grading. We have

$$A(a) - A(b) = n_z(D_z) - n_w(D_z) = 1 - 0 = 1, \quad A(c) - A(b) = n_z(D_w) - n_w(D_w) = 0 - 1 = -1.$$

Therefore

$$A(c) + 2 = A(b) + 1 = A(a).$$

We want the Alexander polynomial to be symmetric (in the sense of $\Delta(q) = \Delta(q^{-1})$, so this forces the middle term $b$ to lie in grading 0, with $c$ in grading $-1$ and $a$ in grading 1. This concludes our calculation of the bidegrees of the non-vanishing terms in $\widehat{HFK}(LHT)$: the homology is as in the following table.

Knot Floer homology of LHT

| $A$ \ $M$ | -3 | -2 | -1 | 0 | 1 | 2 | 3 |
|---|---|---|---|---|---|---|---|
| 3 | | | | | | | |
| 2 | | | | | | | |
| 1 | | | | | | $\mathbb{Z}$ | |
| 0 | | | | | $\mathbb{Z}$ | | |
| -1 | | | | $\mathbb{Z}$ | | | |
| -2 | | | | | | | |
| -3 | | | | | | | |

We can also compute the Alexander polynomial readily from this table:

$$\Delta_{LHT}(q) = q - 1 + q^{-1}.$$

To compute the knot Floer hpomology of the right handed trefoil, we rewind back to the very first step where we draw a Heegaard diagram. Here the diagram is "reflected", corresponding to reversing orientations. Then almost all of the calculations carry out in the same way, except with $a, b, c$ labelled the same way, the non-trivial part of the $\widehat{HF}(\mathbb{S}^3)$ boundary map becomes $\partial b = c$. Therefore the homology is generated by $a$, and the Maslov grading shifts by 2:

Knot Floer homology of RHT

| $A$ \ $M$ | -3 | -2 | -1 | 0 | 1 | 2 | 3 |
|---|---|---|---|---|---|---|---|
| 3 | | | | | | | |
| 2 | | | | | | | |
| 1 | | | | $\mathbb{Z}$ | | | |
| 0 | | | $\mathbb{Z}$ | | | | |
| -1 | | $\mathbb{Z}$ | | | | | |
| -2 | | | | | | | |
| -3 | | | | | | | |

This shows that knot Floer homology distinguishes the chirality of trefoils! On the other hand, we see that the right handed trefoil also has Alexander polynomial $q - 1 + q^{-1}$.

**Remark.** Recall that one of the basic properties of knot Floer homology described in the introductory section was that

$$\widehat{HFK}_i(K, s) = \widehat{HFK}_{-i}(\overline{K}, -s).$$

This says that the table of the knot Floer homology of RHT should be the 180 degree rotation of the LHT knot Floer homology, about $(0, 0)$. We see that this is indeed the case.

**Example.** For our next example, we will determine the knot Floer homology of a figure-8 knot. The 2-bridge diagram and associated Heegaard diagram (shown in figure 10.7 are quite a bit funkier than the previous example!

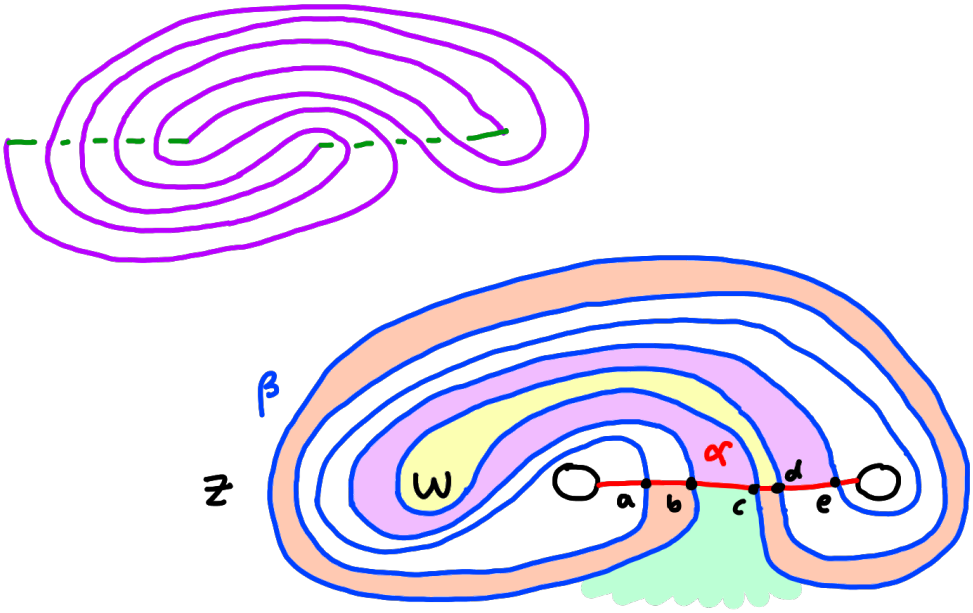


Figure 10.7: Heegaard diagram of the figure 8 knot.

This time we see that the Floer chain complex has five generators. Again, there are no bigons away from $z$ or $w$, so the boundary map is trivial, giving

$$\widehat{HFK}(4_1) = \langle a, b, c, d, e \rangle = \mathbb{Z}^5.$$

It remains to determine the gradings. To this end, we have added some colour to regions in the Heegaard diagram in figure 10.7 to aid in the calculations.

Consider the intersections $c$ and $d$. There is a bigon from $c$ to $d$ (shown in yellow). This bigon meets $w$ but not $z$. Therefore

$$M(c) - M(d) = 1\mu - 2n_w = -1.$$

Next we consider $a$ and $c$. There is no immediate bigon, but we can combine the bigon from $c$ to $d$ with the rectangular region shown in orange (with vertices $a, b, c, d$)! This rectangle has $\mu - 2n_w = 0 - 0 = 0$. Therefore

$$M(b) - M(a) = M(c) - M(d) = -1.$$

Next we notice that there is a bigon from $c$ to $b$, which wraps around infinity. This does not meet $w$ (as it meetz $z$ instead). We have

$$M(c) - M(b) = 1 - 2 \cdot 0 = 1.$$

Finally combining this with the purple rectangle, we have

$$M(d) - M(e) = 1.$$

This determines the relative Maslov grading completely: we have

$$M(d) - 1 = M(a) = M(c) = M(e) = M(b) + 1.$$

As for the Alexander grading, we use the same regions as above. For example,

$$A(c) - A(d) = n_z - n_w = -1$$

since the yellow bigon contains $w$ but not $z$. In fact, we end up with the same relative grading as the Maslov index!

$$A(d) - 1 = A(a) = A(c) = A(e) = A(b) + 1.$$

Since the Alexander grading must be symmetric, for the absolute grading we end up with

$$A(b) = -1, \quad A(a) = A(c) = A(e) = 0, \quad A(d) = 1.$$

For the absolute Maslov grading, notice that the bigons from $c$ to $b$ and $d$ to $e$ do not contain $w$, so the boundary map in $\widehat{CF}(\mathbb{S}^3)$ obtained from the above Heegaard diagram is defined by

$$\partial d = e, \quad \partial c = b, \quad \partial a = 0.$$

That is, $\widehat{HF}(\mathbb{S}^3) = \langle a \rangle$. Therefore the absolute Maslov grading is fixed by $M(a) = 0$. This gives

$$M(b) = -1, \quad M(a) = M(c) = M(e) = 0, \quad M(d) = 1.$$

In summary, the knot Floer homology of the figure-8 knot is as in the following table.

Knot Floer homology of $4_1$

| $A$ \ $M$ | -3 | -2 | -1 | 0 | 1 | 2 | 3 |
|---|---|---|---|---|---|---|---|
| 3 | | | | | | | |
| 2 | | | | | | | |
| 1 | | | | | $\mathbb{Z}$ | | |
| 0 | | | | $\mathbb{Z}^3$ | | | |
| -1 | | | $\mathbb{Z}$ | | | | |
| -2 | | | | | | | |
| -3 | | | | | | | |

Reading off the Euler characteristic, we have

$$\Delta_{4_1}(q) = -q + 3 - q^{-1}.$$

We see that the knot Floer homology is preserved by a 180 degree rotation of the table about $(0, 0)$, agreeing with the fact that $4_1$ is amphichiral.

## 10.6 The relationship between Maslov and Alexander gradings

In the examples in the previous sections, all of the knot Floer homologies were non-trivial along a gradient 1 line. That is to say, $A - M$ was constant. This is a general property: for 2-bridge knots, all generators can be related by bigons which pass through either $w$ or $z$ exactly once, from which one can show that $A - M$ is constant. In fact, we can calculate this constant.

**Theorem 10.6.1** (Rasmussen)**.** *If $K$ is a 2-bridge knot, then $A - M = \sigma(K)/2$, where $\sigma(K)$ is the signature of $K$. Moreover,*

$$\widehat{HFK}_i(K, s) = \begin{cases} \mathbb{Z}^{|a_s|} & i = s + \sigma/2 \text{ where } \Delta_K = \sum a_s q^s \\ 0 & \text{otherwise.} \end{cases}$$

For Heegaard Floer homology, we introduced *L-spaces* as being the manifolds which are homologically simplest. The analogue in knot Floer homology is precisely those knots with homology as above.

**Definition 10.6.2.** If $\widehat{HFK}(K)$ satisfies the above formula, $K$ is called *perfect* or *Floer $\sigma$-thin.*

In this terminology, Rasmussen showed that 2-bridge knots are Floer $\sigma$-thin.

**Remark.** Considering knots of up to 9 crossings, only two are *not* Floer $\sigma$-thin, namely $8_{19}, 9_{42}$.

Rasmussen's result can be improved, and this improved version is the result we will give a proof outline for.

**Theorem 10.6.3** (Ozsváth, Szabó)**.** *Alternating knots are Floer $\sigma$-thin.*

This gives a hierarchy of knot-structure as follows:

$$\text{knots} \supset \text{Floer } \sigma\text{-thin} \supset \text{alternating} \supset \text{2-bridge}.$$

It's not immediately clear from our definition of 2-bridge knots that they are alternating: the idea is to instead consider the projection "from above".

How did Ozsváth and Szabó prove their result? The key idea is to consider a new method for obtaining a Heegaard diagram of a knot. This method will typically give a higher genus than the bridge-method, but it highlights the fact that different forms of diagrams can be more useful at different times.

**Proposition 10.6.4.** Let $K$ be a knot with a planar diagram with $c$ crossings. The following process defines a Heegaard diagram of $K$ with genus $c+1$.

1. Consider the planar diagram as sitting in the $(x, y)$-plane in $\mathbb{R}^3$. Let $\Sigma$ be the boundary of a regular neighbourhood of the diagram in $\mathbb{R}^3$. (Then $\Sigma$ immediately has genus $c+1$.)

2. Place $\alpha$ curves around each of the $c+1$ holes of $\Sigma$. (These are canonical, as we will see in a subsequent example.)

3. Fix a basepoint of the knot. Add a $\beta$ curve as a meridian at the corresponding part of $\Sigma$.

4. Add the $w$ and $z$ points on $\Sigma$ to lie on either side of the previously defined $\beta$ curve.

5. The remaining $c$ $\beta$ curves are added to each of the crossings of the diagram, respecting the over/underpass data.

**Example.** Following the above steps is basically impossible without an example! We carry out the process for a figure-8 knot and determine the corresponding Heegaard diagram. Next we verify that it really is a Heegaard diagram of the knot. Figure 10.8 shows the Heegaard diagram obtained from the standard diagram of the figure-8 knot.

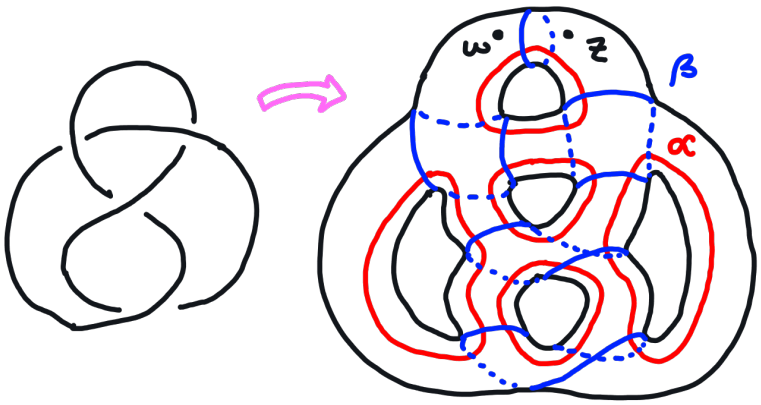


Figure 10.8: Heegaard diagram of a figure-8 knot obtained by the alternative method.

It is easy to see that the diagram on the right is really what we obtain, by following the rules described in the preceding proposition.

Now we verify that this is a Heegaard diagram of the figure-8 knot. The first step is verifying that this is a Heegaard diagram of $\mathbb{S}^3$. To see this, define $U$ to be the volume outside of $\Sigma$, and $V$ the volume inside $\Sigma$. For each $\alpha$ curve, we glue a disk $D_\alpha$ into $U$ with boundary the $\alpha$ curve. Then $U - \cup_i D_{\alpha_i}$ is topologically a 3-ball! Therefore we can take $U$ to be the handlebody $U_\alpha$. Conversely, we can also glue in a disk $D_\beta$ inside $V$ for every $\beta$ curve. Following the path of knot from $z$ to $w$, we find that the complement of these disks in $V$ is again a 3-ball. Therefore we've described a Heegaard diagram of $U \cup V = \mathbb{S}^3$.

Next we must verify that there are curves $\gamma_\alpha$ and $\gamma_\beta$ so that $K = \gamma_\alpha \cup \gamma_\beta$, and each curve lives in $U_\alpha - \cup_i D_{\alpha_i}$ and $U_\beta - \cup_i D_{\beta_i}$ respectively. This is best explained with a diagram: see figure 10.9. The idea is similar to the above, where $\gamma_\beta$ is really just obtained by following the path of the knot. (This is actually the same argument that the volume $V$ earlier is the $U_\beta$ handelbody.)

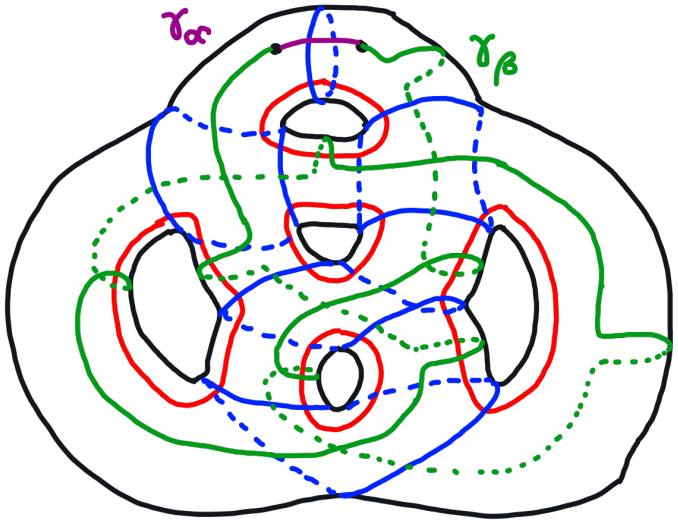


Figure 10.9: The diagram is truly a Heegaard diagram of the figure-8 knot.

At each crossing we were given two choices for how to "orient" the $\beta$ curves. We see from figure 10.9 that our choices really guarantee that we can follow the diagram along the knot to define $\gamma_\beta$ as required. (The crossings at each intersection over/underpass correctly.) This completes the example-proof, which generalises to arbitrary planar diagrams.

Next we'll compute the knot Floer homology from such a Heegaard diagram. Things get a bit messy with the figure-8 knot, as genus 5 is already getting quite large for human means. Instead we'll consider the trefoil.

**Example.** Starting with the standard diagram of the trefoil, we obtain a genus 4 Heegaard diagram as shown in figure 10.10.

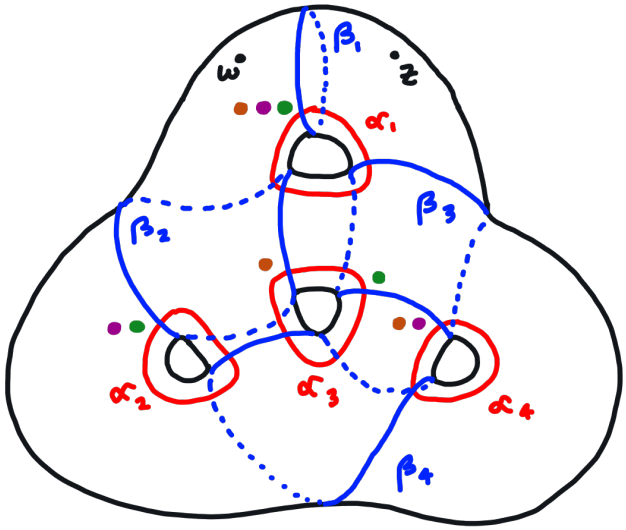


Figure 10.10: Heegaard diagram of a trefoil knot obtained by the alternative method.

Since the Heegaard diagram has genus 4, the intersection points $x \in \mathbb{T}_\alpha \cap \mathbb{T}_\beta$ are unordered tuples $\{x_1, \ldots, x_4\}$, where each $x_i$ comes from an honest intersection of $\alpha$ and $\beta$ curves. More formally, they are of the form $x = \{x_1, \ldots, x_4\}$ where

$$x_i \in \alpha_{\sigma(i)} \cap \beta_i, \quad \sigma \in S_4.$$

Using this rule, we can readily enumerate the points in $\mathbb{T}_\alpha \cap \mathbb{T}_\beta$ by inspecting the figure. Firstly, $\beta_1$ only intersects $\alpha_1$, so we can take $x_1$ to be the intersection denoted by a green dot at the top of the diagram. Next, $\beta_2$ intersects $\alpha_1, \alpha_2$, and $\alpha_3$. Since $\alpha_1$ has already been taken, we can choose between $\alpha_2$ or $\alpha_3$. Let's choose $\alpha_2 \cap \beta_2$. This is the green dot on the left of the figure. Similarly we have two choices for $\beta_3$. Finally, we're left with only one choice for $\beta_4$.

Repeating this process with each of the choices, we end up with exactly three possibilities, as shown in green, purple, and orange. Therefore $\mathbb{T}_\alpha \cap \mathbb{T}_\beta$ consists of 3 points, $a, b, c$. In fact, one can show that $\partial = 0$ so that

$$\widehat{CFK} = \widehat{HFK} = \langle a, b, c \rangle = \mathbb{Z}^3.$$

It remains to determine the gradings.

*Proof outline of the Ozsváth-Szabó Floer $\sigma$-thin theorem.* Ozsváth and Szabó used these diagrams to show that for alternating knots, the generators satisfy

$$A - M = \sigma/2.$$

In this case, for a fixed $A$, all generators lie in the same Maslov grading, which implies that $\partial = 0$. Therefore $\widehat{HFK}_i(K, s) = \mathbb{Z}^{|a_s|}$ in degree $i = s - \sigma/2$. □

The next immediate goal is to extend knot Floer homology to links. This was alluded to in the previous lecture, where we remarked that any proofs involving crossing resolutions really requires the notion of knot Floer homology to be extended to links. The idea is to consider Heegaard diagrams with even more base points, since we should need two basepoints for every component of the link.

**Question from class.** Naively, Khovanov homology looks very different from knot Floer homology. However, the Jones and Alexander polynomials are related by being special cases of the HOMFLY polynomial. Are these two homology theories related? Is there perhaps a triply graded homology theory, with Euler characteristic the HOMFLY polynomial?

*Answer.* Yes! This is formalised by spectral sequences! A recent result established that there is a spectral sequence induced by knot Floer homology. The second page (and higher) are knot invariants. In particular, the second page is triply graded, and its graded Euler characteristic is the HOMFLY polynomial. By construction, the spectral sequence converges to knot Floer homology.

Alternatively, there is an older notion - Khovanov-Rozansky homology (which is an $\mathfrak{sl}(N)$-knot homology generalising Khovanov homology) which induces a spectral sequence converging to Khovanov homology, and conjecturally also to knot Floer homology. □

# Chapter 11

# Combinatorial knot Floer homology

We established in an earlier chapter that $\widehat{HF}(Y)$ was combinatorial (for mod 2 coefficients) by using "nice diagrams". These are diagrams in which all of the badness is moved into the region containing the basepoint, since we don't consider $J$-holomorphic strips over the basepoint. However, it wasn't clear how to generalise to other versions of Heegaard Floer homology in which we consider strips over the basepoint as well.

In knot Floer homology, we'll actually prove that all the versions are combinatorial! This is because we'll soon see that all Heegaard diagrams for knots can be taken to have low genus by trading them off with additional basepoints. With genus 0 or 1, *every* region can be taken to be a bigon or rectangle. In fact, this will imply that the other versions of Heegaard Floer homology for 3-manifolds are also combinatorial, since 3-manifolds can be described in terms of knots by the Lickorish-Wallace theorem and the Heegaard Floer homology is then expressed in terms of the knot Floer homology.

## 11.1 Heegaard Floer homology with multiple basepoints (lecture 19)

The main prerequisite for showing that knot Floer homology is combinatorial is the concept of Heegaard diagrams with multiple basepoints.

**Definition 11.1.1.** Let $Y^3$ be closed and oriented. A *Heegaard diagram for $Y$ with multiple basepoints* is the data

$$(\Sigma_g, \alpha_1, \dots, \alpha_{g+k}, \beta_1, \dots, \beta_{g+k}, z_1, \dots, z_{k+1})$$

where $k \geqslant 0$. Each set of $\alpha$ and $\beta$ curves must consist of disjoint simple closed curves that span a half dimensional subspace of $H^1(\Sigma_g; \mathbb{Z}) = \mathbb{Z}^{2g}$, and each component of $\Sigma - \bigcup \alpha_i$,

$\Sigma - \bigcup \beta_i$ must contain *exactly one* basepoint.

**Example.** Figure 11.1 shows the $\alpha$ curves of a Heegaard diagram for a 3-manifold with genus 3 and 4 basepoints (i.e. $k = 3$).

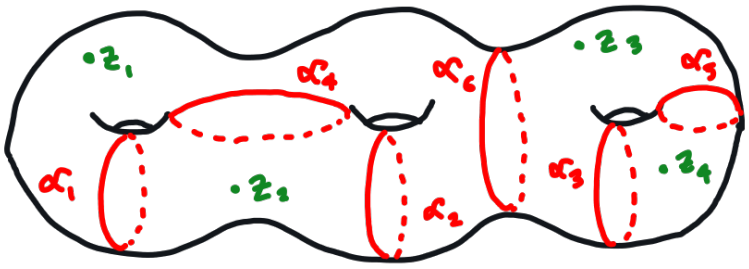


Figure 11.1: Multiple basepoint Heegaard diagram example.

We find that the 6 simple closed curves in the diagram do indeed span a half-dimensional subspace of $H_1(\Sigma; \mathbb{Z}) = \mathbb{Z}^{2g} = \mathbb{Z}^6$, since

$$[\alpha_4] = [\alpha_1] + [\alpha_2], \quad [\alpha_5] = [\alpha_3], \quad [\alpha_6] = 0.$$

Therefore the space is generated by $[\alpha_1], [\alpha_2]$, and $[\alpha_3]$. It is also clear from the figure that each cut component indeed has exactly one basepoint.

In the setting of Heegaard diagrams with multiple basepoints, we consider the tori

$$\mathbb{T}_\alpha = \alpha_1 \times \cdots \times \alpha_{g+k}, \mathbb{T}_\beta = \beta_1 \times \cdots \times \beta_{g+k} \subset \mathrm{Sym}^{g+k}(\Sigma_g - \{z_1, \ldots, z_k\}) \subset \mathrm{Sym}^{g+k}(\Sigma_g).$$

**Proposition 11.1.2.** $HF(\mathbb{T}_\alpha, \mathbb{T}_\beta \text{ in } \mathrm{Sym}^{g+k}(\Sigma_g - \{z_i\})) = \widehat{HF}(Y) \otimes (H_*(\mathbb{S}^1))^{\otimes k}$. Intuitively, $HF(\mathbb{T}_\alpha, \mathbb{T}_\beta)$ is comprised of $2^k$ copies of $\widehat{HF}(Y)$.

*Proof sketch.* Any two Heegaard diagrams with multiple basepoints, for the same $Y$, are related by the usual moves (isotopies, handleslides, and stabilisation and destabilisation) together with a new type of stabilisation which consists of adding a new basepoint and an $\alpha/\beta$ curve pair as in figure 11.2.

If the original complex is $C_*$, then upon the new stabilisation the complex is updated to $C_* \oplus C_{*-1}$, where the first factor contains the $x$ intersection point, and the second $y$. The degree shift is because $x$ lives in one degree higher than $y$. It turns out that $\partial x = 0$ in the new complex, because there are two $J$-holomorphic curves from $x$ to $y$ - as shown in the highlighted parts of the figure. To verify that there is an "outer" curve (instead of just the inner one, which is clear), formally we neck-stretch along the outermost dashed curve and do some analysis. It follows that $H_*$ is updated to $H_* \oplus H_{*-1}$ upon stabilisation, as required. □

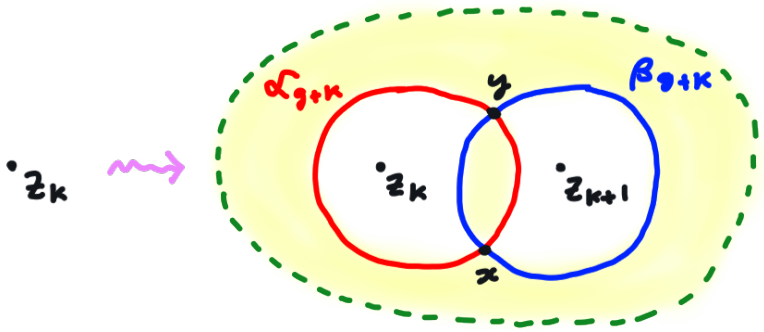


Figure 11.2: New type of stabilisation.

**Example.** This is best seen by an example. Figure 11.3 shows a Heegaard diagram of $\mathbb{S}^3$ with genus 0 and $k = 1$ (two base points).

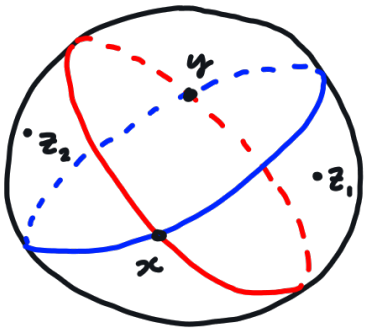


Figure 11.3: Heegaard diagram of a sphere with two basepoints.

There are two intersections, $x$ and $y$. It is clear that there are two bigons from $x$ to $y$ which do not pass over the basepoints, and the $J$-holomorphic curves cancel in pairs so that $\partial = 0$. It follows that the homology of the Heegaard diagram is

$$\langle x, y \rangle = H_*(\mathbb{S}^1)$$

by noting that $x$ is in degree one higher than $y$. Notice that this is equal to $\widehat{HF}(\mathbb{S}^3) \otimes H_*(\mathbb{S}^1)$ since the former is literally just $\mathbb{Z}$ in degree 0.

We've established some properties of the "hat version" of Heegaard Floer homology with multiple basepoints. By allowing $J$-holomorphic curves to pass over basepoints, we also obtain other types of homology. In particular, we next define a version of "minus" homology:

**Definition 11.1.3.** Consider $\mathbb{T}_\alpha, \mathbb{T}_\beta \subset \mathrm{Sym}^{g+k}(\Sigma_g)$. We define $CF^-$ to be freely generated by intersection points $x \in \mathbb{T}_\alpha \cap \mathbb{T}_\beta$, over $\mathbb{Z}[U_1, \ldots, U_{k+1}]$. The boundary map is defined by

$$\partial x = \sum_y \sum_{\varphi \in \pi_2(x,y), \mu(\varphi)=1} \#(\mathcal{M}(\varphi)/\mathbb{R}) U_1^{n_{z_1}(\varphi)} \cdots U_{k+1}^{n_{z_{k+1}}(\varphi)} y.$$

We define $HF^-$ to be the homology of this complex.

As with the hatted version, this is also closely related to more familiar versions of Heegaard Floer homology.

**Proposition 11.1.4.** As a $\mathbb{Z}[U]$-module, $HF^-(\mathbb{T}_\alpha, \mathbb{T}_\beta)$ is isomorphic to $HF^-(Y)$. (To view the former as a $\mathbb{Z}[U]$-module, all the $U_i$ are identified with $U$.)

*Proof sketch.* Under the new stabilisations, a complex $C_*$ is sent to

$$C_*[U_{k+1}] \xrightarrow{U_k - U_{k+1}} C_*[U_{k+1}],$$

with homology $H(C_*)[U_{k+1}]/U_k = U_{k+1}$. This is evidently isomorphic to $H(C_*)$ as required. □

**Remark.** We can also set all of the $U_i = 0$ to obtain a homology theory over $\mathbb{Z}$, in which case the homology is isomorphic to $\widehat{HF}(Y)$.

## 11.2 Knot Floer homology for links

We're now ready to define knot Floer homology for links, by using Heegaard diagrams with multiple basepoints.

**Definition 11.2.1.** Let $L \subset \mathbb{S}^3$ be a link with $\ell$ components. A *Heegaard diagram for $L$* is the data

$$(\Sigma_g, \alpha_1, \ldots, \alpha_{g+\ell-1}, \beta_1, \ldots, \beta_{g+\ell-1}, z_1, \ldots, z_\ell, w_1, \ldots, w_\ell)$$

where

$$(\Sigma, \alpha_i, \beta_i, z_i), (\Sigma, \alpha_i, \beta_i, w_i)$$

are both Heegaard diagrams for $\mathbb{S}^3$ (with multiple basepoints), and there exist arcs $\gamma_{\alpha_i}, \gamma_{\beta_i}$ connecting $w_i$ to $z_i$, the former in $U_\alpha - \bigcup_i D_{\alpha_i}$, the latter in $U_\beta - \bigcup_i D_{\beta_i}$, so that the union of all the arcs in $\mathbb{S}^3$ is the link $L$.

**Definition 11.2.2.** Let $L \subset \mathbb{S}^3$ be a link with $\ell$ components, and $(\Sigma, \alpha_i, \beta_i, z_i, w_i)$ be a Heegaard diagram of $L$. Then the *knot Floer homology of $L$* is defined by

$$\widehat{HFK}(L) = HF(\mathbb{T}_\alpha, \mathbb{T}_\beta \text{ away from } w_i, z_i),$$

i.e. the Lagrangian Floer homology of the tori in $\mathrm{Sym}^{g+\ell-1}(\Sigma - \{w_i, z_i\})$. This decomposes as

$$\widehat{HFK}(L) = \bigoplus_{i,s\in\mathbb{Z}} \widehat{HFK}_i(L,s),$$

where $i$ is the homological grading and $s$ is the Alexander grading.

**Proposition 11.2.3.** Given a link $L$, the Euler characteristic of it's knot Floer homology is a scaled Alexander polynomial:

$$\chi(\widehat{HFK}(L)) = (1-q^{-1})^{\ell-1}\Delta_L(q).$$

**Remark.** In fact, there are $\ell$ Alexander gradings $s_1, \ldots, s_\ell$, and $s = \sum_i s_i$. The Euler characteristic of the $s$-graded knot Floer homology is the Alexander polynomial, but the Euler characteristic of $s_i$-graded knot Floer homology is the *multivariable Alexander polynomial*. The $s_i$-graded theory is sometimes called *link Floer homology*.

**Example.** As an example, we begin with the unlink of two components. An example Heegaard diagram is shown in figure 11.4.

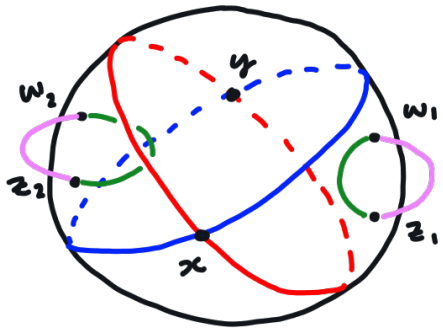


Figure 11.4: Knot Floer homology of the unlink.

In the figure we've drawn green arcs to represent $\gamma_{\alpha_i}$ and pink arcs for $\gamma_{\beta_i}$. Indeed, these verify that our Heegaard diagram is really a Heegaard diagram of the unlink with two components.

We know from earlier that $\partial x = y - y = 0$, so that $\widehat{HFK}(L) = \langle x, y\rangle = \mathbb{Z}^2$. It remains to compute the gradings. We consider a bigon from $x$ to $y$ that does not meet any basepoints, and choose $\varphi \in \pi_2(x,y)$ mapping into the bigon. This establishes that

$$M(x) - M(y) = 1, \quad A(x) - A(y) = 0.$$

Upon deletion of the $z$ points to obtain asbolute gradings, the knot Floer homology of the unlink is as in the following table:

Knot Floer homology of the unlink

| $A$ \ $M$ | -3 | -2 | -1 | 0 | 1 | 2 | 3 |
|---|---|---|---|---|---|---|---|
| 3 | | | | | | | |
| 2 | | | | | | | |
| 1 | | | | | | | |
| 0 | | | $\mathbb{Z}$ | $\mathbb{Z}$ | | | |
| -1 | | | | | | | |
| -2 | | | | | | | |
| -3 | | | | | | | |

Notice that this uses the convention that

$$\widehat{HF}(\mathbb{S}^3) \otimes H(\mathbb{S}^1) = \mathbb{Z}^2$$

is in degrees $-1$ and 0.

Reading off the Euler characteristic, $\Delta_L(q) = (1-q^{-1})^{-1}(1-1) = 0$ as required.

**Example.** For our next example, we consider the Hopf link, which we again denote by $L$. This time $\Delta_L(q) = q^{1/2} - q^{-1/2}$, so we expect

$$\chi(\widehat{HFK}(L)) = (1-q^{-1})(q^{1/2}-q^{-1/2}) = q^{1/2} - 2q^{-1/2} + q^{-3/2}.$$

In figure 11.5, we show a genus 1 Heegaard diagram with on the right.

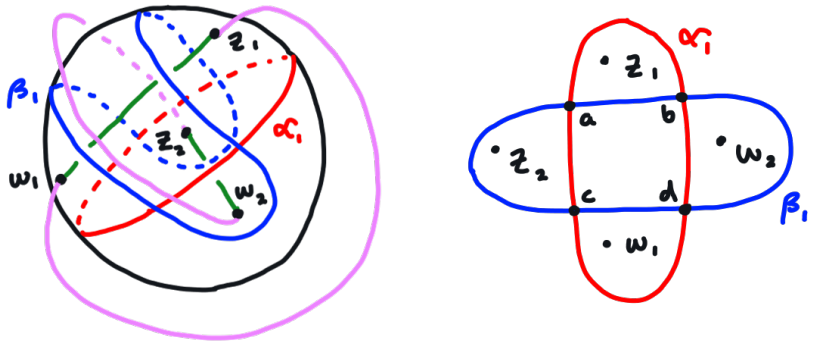


Figure 11.5: Knot Floer homology of the Hopf link.

To see why this is a Heegaard diagram of the Hopf link, consider the image on the left. Again the boundary maps are trivial, so that

$$\widehat{HFK} = \mathbb{Z}^4.$$

This time they are trivial because there are no bigons that don't contain a $z$ or $w$ point. As for the relative gradings, we can compute them using the four bigons wrapping around the right-side figure. For example, $M(b)-M(a) = 1-2n_w = 1-0 = 1$, and $A(b)-A(a) = \sum n_{z_i} - \sum n_{w_i} = 1-0 = 1$. Overall, we find that the relative gradings are

$$M(d) = M(b)+1 = M(c)+1 = M(a)+2, \quad A(d) = A(b)+1 = A(c)+1 = A(a)+2.$$

The Alexander grading is made absolute by inspecting the Euler characteristic (Alexander polynomial). We find that it is half-integral!

$$A(d) = 1/2, \quad A(b) = A(c) = -1/2, \quad A(a) = -3/2.$$

On the other hand, to make the Maslov index absolute, we allow holomorphic curves over $z$ basepoints. Then $\partial b = a$, $\partial c = a$, so that

$$\widehat{HF}(\mathbb{S}^3) \otimes H(\mathbb{S}^1) = \langle b-c, d\rangle.$$

Using the convention that the above is in degrees $-1$ and $0$, we have

$$M(a) = -2, \quad M(b) = M(c) = -1, \quad M(d) = 0.$$

In summary the knot Floer homology of the Hopf link is as in the following table:

Knot Floer homology of the unlink

| $A$ \ $M$ | -3 | -2 | -1 | 0 | 1 | 2 | 3 |
|---|---|---|---|---|---|---|---|
| 5/2 | | | | | | | |
| 3/2 | | | | | | | |
| 1/2 | | | | $\mathbb{Z}$ | | | |
| -1/2 | | | $\mathbb{Z}^2$ | | | | |
| -3/2 | | $\mathbb{Z}$ | | | | | |
| -5/2 | | | | | | | |

## 11.3 Knot Floer homology with multiple basepoints

The reason Heegaard diagrams with multiple basepoints is required for combinatorial knot Floer homology is that we will use it to trade genus with basepoints. For this to make sense, we must introduce a notion of knot Floer homology with more basepoints (than just twice the number of link components).

**Definition 11.3.1.** Let $L \subset \mathbb{S}^3$ be a link with $\ell$ components. Let $k \geqslant \ell$. A Heegaard diagram

$$(\Sigma_g, \alpha_1, \dots, \alpha_{g+k-1}, \beta_1, \dots, \beta_{g+k-1}, z_1, \dots, z_k, w_1, \dots, w_k)$$

is a Heegaard diagram of $L$ (with multiple basepoints) if each of $(\Sigma, \alpha_i, \beta_i, z_i)$ and $(\Sigma, \alpha_i, \beta_i, w_i)$ is a Heegaard diagram (with multiple basepoints) of $\mathbb{S}^3$, and there exist arcs $\gamma_{\alpha_i}, \gamma_{\beta_i}$ in $U_\alpha - \bigcup_i D_{\alpha_i}$ and $U_\beta - \bigcup_i D_{\beta_i}$ respectively, with one endpoint on a $z$ basepoint and one on $w$ basepoint, so that their union is the link $L$. (Note that each component of $L$ is allowed to be comprised of more than two arcs!)

**Example.** Figure 11.6 shows possible arcs comprising an unlink in a Heegaard diagram with additional basepoints. This diagram has $g = 3$ and $\ell = 2$, but $k = 4$.

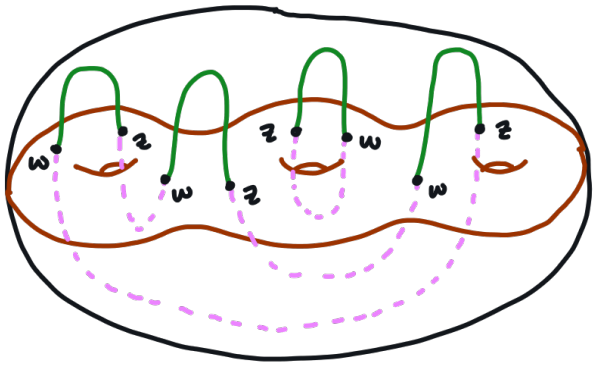


Figure 11.6: Example of arcs in a Heegaard diagram for the unlink with extra basepoints.

**Proposition 11.3.2.** $HF(\mathbb{T}_\alpha, \mathbb{T}_\beta$ away from all the $w_i, z_i)$ is isomorphic to $\widehat{HFK}(L) \otimes V^{\otimes(k-\ell)}$, where $V = \mathbb{Z}^2 = H(\mathbb{S}^1)$ has generators in bidegrees $(-1,-1)$ and $(0,0)$. Intuitively, it says that $HF$ is $2^{k-\ell}$ copies of $\widehat{HFK}$.

*Proof sketch.* Again, any two diagrams of $L$ are related by the usual moves along with "new stabilisations". To verify that the new stabilisation (addition of basepoints and curves, but not genus) really gives a Heegaard diagram of the same link, we inspect figure 11.7.

In the bottom part of the figure, we see how the new stabilisation genuinely gives a Heegaard diagram of the link by declaring what the appropriate new $\gamma_\alpha, \gamma_\beta$ arcs are.

We see that $\widehat{CFK}$ is sent to $\widehat{CFK} \oplus \widehat{CFK}$, with the first component being generated by $x$ and the second by $y$. This inductively gives the first part of the proposition, but we still need to determine gradings. Inspecting the Heegaard diagram on the top right of the figure, we see from the right-most-bigon (from $x$ to $y$) that $A(x) - A(y) = M(x) - M(y) = -1$, giving the desired grading as well. □

We have mentioned on several occasions that the advantage of Heegaard diagrams with extra basepoints is that genus can be traded for basepoints.

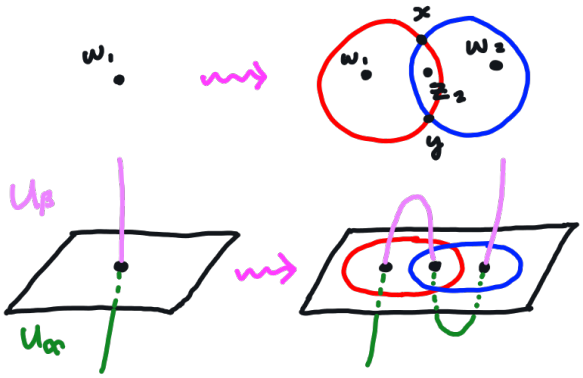


Figure 11.7: New stabilisation for Heegaard diagram of a link.

**Proposition 11.3.3.** Every link admits a genus 0 Heegaard diagram of some number of base points.

*Proof.* We don't give a full proof - instead, we will walk through an example for the construction of such a Heegaard diagram.

The general algorithm to produce a genus 0 Heegaard diagram is as follows:

1. Start with a bride diagram of the link. Delete one bridge and one underpass.
2. Replace all other bridges with blue sausages, and replace its end points with $w$ and $z$ basepoints. Similarly, replace all underpasses with red sausages.

As an example, we consider figure 11.8.

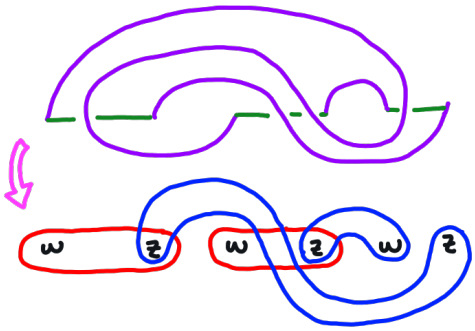


Figure 11.8: Genus 0 Heegaard diagram example.

To verify that this is indeed a Heegaard diagram for the link, simply re-draw the bridges and underpasses from the bridge diagram. These are exactly the arcs that verify that the

Heegaard diagram represents the given link: the underpasses are the $\gamma_\alpha$ arcs, and the bridges are the $\gamma_\beta$ arcs. □

## 11.4 Grid diagrams

Recall that Sarkar and Wang showed the existence of an algorithm for computing $\mathbb{F}_2$ hat Heegaard Floer homology for 3-manifolds. This made use of *nice diagrams* in which all regions were bigons or rectangles, except for the one including the basepoint. This means we can count $J$-holomorphic disks without analysis.

Suppose a surface admits a Heegaard diagram in which all regions are bigons or rectangles. Then we have

$$2 - 2g = \chi(\Sigma_g) = \sum(\text{Euler measures of regions}) \geqslant 0,$$

because the Euler measure of a bigon is $1/2$ and that of a rectangle is 0. This forces $g = 0, 1$, which is why we cannot in general force all regions to be bigons and rectangles.

However, for knots and links, we're in luck! We can simply add more basepoints and guarantee that the surface has genus 0 or 1! Moreover, this means that potentially every region can be a bigon or rectangle, so we can even compute other versions of knot Floer homology (rather than just the hatted version). Indeed this turns out to be the case - we use so-called *grid diagrams*.

**Definition 11.4.1.** Let $L \subset \mathbb{S}^3$ be a link. A *grid diagram* of $L$ is an $n \times n$ grid with $2n$ markings of two types, $w$ and $z$, such that

- each row has exactly one $z$ and one $w$,
- each column has exactly one $z$ and one $w$,
- Joining $w$ to $z$ by vertical and horizontal arcs, with vertical arcs always overpassing, we obtain a diagram for $L$.

Moreover, a grid diagram defines a Heegaard diagram of genus 1 by declaring that all horizontal lines (between the rows of the grid) are $\alpha$-curves, the vertical lines are $\beta$-curves, and the outermost opposite edges are identified to make a torus.

**Example.** Figure 11.9 shows a grid diagram for the trefoil knot.

The light pink lines show that the marked points do indeed give a grid diagram for the trefoil knot.

**Remark.** All regions in a grid diagram are rectangles! This means that given a grid diagram, we can combinatorially/algorithmically compute the knot Floer homology! If all links admit grid diagrams, then knot Floer homology itself is combinatorial.

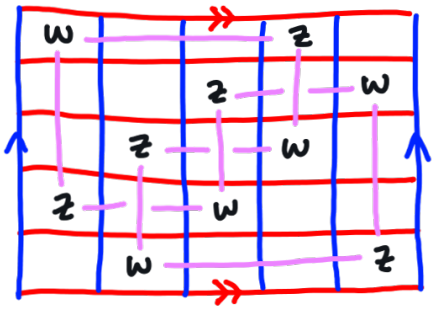


Figure 11.9: Grid diagram for the trefoil knot.

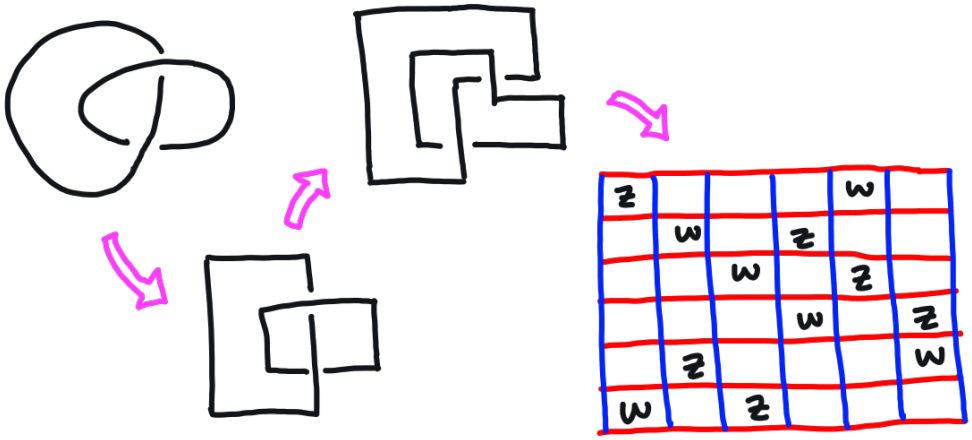


Figure 11.10: Existence of grid diagrams.

**Proposition 11.4.2.** Every link admits a grid diagram.

*Proof.* We do not give a general proof, but instead use an example: figure 11.10.

First we take any link diagram for the given link. Then we make it rigid, replacing the components with vertical and horizontal edges. Then we locally rotate any of the crossings that don't overpass vertically. Finally writing $w$ and $z$ at the vertices, we have a grid diagram! □

In summary, all links admit grid diagrams, and all grid diagrams allow for knot Floer homology to be computed combintaorially! Nice!

Some references on combinatorial knot Floer homology (which will be explored a little more in the final lecture) are:

1. Manolescu, Ozsváth, Sarkar - 2006. *A combinatorial description of knot Floer homology.*

2. Manolescu, Oszváth, Szabó, Thurston. *On combinatorial link Floer homology.*

3. Book by Ozsváth, Stipsicz, Szabó.

## 11.5 Combinatorial knot Floer homology (lecture 20)

In the previous lecture we introduced *grid diagrams* with a view to proving that knot Floer homology is combinatorial. In this lecture we show how to obtain the combinatorial *grid complex* given a grid diagram. As an example, we will use the grid diagram $\Gamma$ of a Hopf link as in figure 11.11.

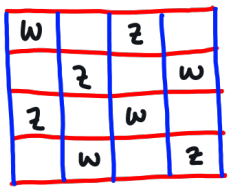


Figure 11.11: Grid diagram $\Gamma$ of Hopf link.

We must do four things:

1. Describe the underlying module of the Floer complex induced by the grid diagram.

2. Describe relative Maslov gradings between generators.

3. Describe the boundary map of the Floer complex.

4. Describe relative Alexander gradings between generators. (The Maslov grading can be made absolute by computing the gradings of surviving generators in the homology of the torus - this is combinatorial by Sarkar-Wang. The Alexander grading can be made absolute by computing the Alexander polynomial, which is also combinatorial.)

1. Given a Heegaard diagram with $n$ $\alpha$ curves and $\beta$ curves, the generator of the corresponding Heegaard complex has generators the intersection $\mathbb{T}_\alpha \cap \mathbb{T}_\beta$ in $\mathrm{Sym}^n(\Sigma)$. In our Hopf link example, we have a $4 \times 4$ grid $\Gamma$ induced by 4 $\alpha$ and $\beta$ curves. Therefore the generators are

$$x = \{x_{1\sigma(1)}, \ldots, x_{4\sigma(4)}\}, \sigma \in S_4, \quad x_{ij} = \alpha_i \cap \beta_j.$$

Enumerating these, there are exactly $4! = 24$ choices. Our grid complex is the free $\mathbb{Z}$-module generated by 24 symbols. Yeouch!

$$CG(\Gamma) = \mathbb{Z}\langle a_1, \ldots, a_{24}\rangle.$$

In general, an $n \times n$ grid diagram gives a grid complex with $n!$ generators.

2. Next we must describe the Maslov grading, with a view to defining the boundary map. For this we can use the *Lipshitz formula*. Any $J$-holomorphic strip $\varphi$ mapping into the torus maps into some polygon in the grid diagram, bound by segments of $\alpha$ and $\beta$ curves. We have

$$\mu(\varphi) = e(\varphi) + \sum n_{v_i}(\varphi),$$

where $e(\varphi)$ is the Euler measure of $\varphi$, and $n_{v_i}$ is the average vertex multiplicity. The image of a strip is of the form $D(\varphi) = \sum a_i R_i$ where $a_i \geqslant 0$ and $R_i$ are the *regions* of the grid, i.e. squares of size 1. Now $e(D(\varphi)) = \sum a_i e(R_i) = 0$. The average vertex multiplicity can similarly be computed, and is given by

$$\sum n_{v_i}(\varphi) = -1 + \#\text{edges of } \varphi/2.$$

Therefore

$$\mu(\varphi) = e(\varphi) + \sum n_{v_i}(\varphi) = -1 + \#\text{edges of } \varphi/2.$$

The above is a purely combinatorial description of the Maslov index of a strip. Now to define the Maslov grading, we recall that

$$M(x) - M(y) = \mu(\varphi) - n_w(\varphi),$$

where $n_w(\varphi)$ is the number of times a strip $\varphi$ from $x$ to $y$ passes over a $w$ point.

**Example.** In figure 11.12, we show two generators of $\mathbb{T}_\alpha \cap \mathbb{T}_\beta$: green intersection points represent the generator $x$, and pink $y$.

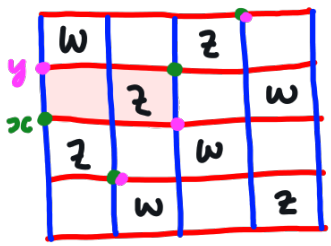


Figure 11.12: Maslov grading example

These differ by a single rectangle, which is represented by a $J$-holomorphic curve $\varphi$, giving

$$M(x) - M(y) = \mu(\varphi) = -1 + 4/2 - 2 \cdot 0 = 1$$

from the above identity.

3. To define the boundary map, we must count index 1 $J$-holomorphic strips which do not pass over $w$ or $z$. Inspecting the above identity, such a strip must have image an *empty rectangle*. We've established a bijective correspondence

$$\{J\text{-holomorphic strips of index 1 away from } w\} \leftrightarrow \{\text{empty rectangles in } \Gamma\}.$$

Formally, an *empty rectangle* is a rectangle as shown in the above example, but one which does not contain any $z$ or $w$ points. The boundary map is given by

$$\partial x = \sum_y \pm n_{xy} y, \quad n_{xy} = \#\text{empty rectangles from } x \text{ to } y \in \{0, 1, 2\}.$$

To see why the number of empty rectangles is an element of $\{0, 1, 2\}$, we simply notice that given any two generators which differ on exactly two $\alpha$ and $\beta$ curves, the number of rectangles between them is exactly 2. It remains to see whether or not these rectangles contain $w$ or $z$ points. (See figure 11.13.)

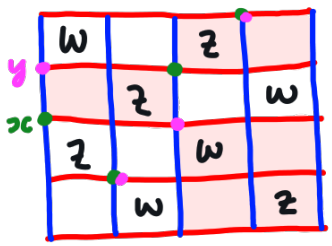


Figure 11.13: The two rectangles from $x$ to $y$.

**Example.** The two generators $x$ and $y$ in figure 11.13 were shown to differ my Maslov grading 1. However, $n_{xy} = 0$, since neither of the two rectangles from $x$ to $y$ are empty.

In summary, we have defined the *grid complex*

$$(CG(\Gamma), \partial).$$

Finally it remains to determine the relative Alexander grading. This can be combinatorially achieved easily by recalling that

$$A(x) - A(y) = n_z(\varphi) - n_w(\varphi).$$

**Example.** In figure 11.12, we show two generators of $\mathbb{T}_\alpha \cap \mathbb{T}_\beta$ whose relative Alexander grading we'll compute. These differ by a single rectangle, which is represented by a $J$-holomorphic curve $\varphi$, giving

$$A(x) - A(y) = n_z(\varphi) - n_w(\varphi) = 1 - 0 = 1.$$

This completes the description of combinatorial knot Floer homology. By construction, we have the following result:

**Proposition 11.5.1.** Let $\widehat{HG}(L)$ denote the homology of the grid complex $(CG(\Gamma), \partial)$, where $\Gamma$ is a grid diagram of $L$. then

$$\widehat{HG}(L) = \widehat{HFK}(L) \otimes V^{\otimes(n-\ell)}$$

where $V \cong \mathbb{Z} \oplus \mathbb{Z}$ has generators in degrees $(-1,-1)$ and $(0,0)$.

By the above proposition, since we know how large our grid is, we have

**Theorem 11.5.2.** *Knot Floer homology is combinatorial.*

In fact, combinatorial knot Floer homology also solves the genus problem!

**Theorem 11.5.3.** *There is an algorithm to compute the genus of a knot.*

*Proof.* We have established that

1. there is an algorithm to compute knot Floer homology; $\widehat{HFK}_i(K,s)$,
2. knot Floer homology detects genus:

$$g(K) = \max\{s : \widehat{HFK}(K,s) \neq 0\}.$$

Recall that the *genus* of a knot is the minimum genus of a Seifert surface of the knot.

The result follows by combining these. □

**Corollary 11.5.4.** *There is an algorithm to determine whether or not a given knot diagram represents the unknot.*

**Remark.** Kronheimer and Mrowka showed that Khovanov homology also detects the unknot, and Khovanov homology is inherently combinatorial.

Finally, one of the grand applications is that combinatorial knot Floer homology extends to a "combinatorialisation" of all the versions of Heegaard Floer homology of a 3-manifold!

**Theorem 11.5.5** (Manolescu, Ozsváth, Thurston (2009))**.** *There is an algorithm to compute $HF^\pm$ for 3 manifolds (as well as the mixed invariants $\varphi_{X,s}$ of 4-manifolds, mod 2).*

*Proof idea.* The important observation is that the above combinatorial knot FLoer homology also works for other types of knot Floer homology, that is, we have a combinatorial algorithm to compute $HFK^{\pm}$ and so on. To this, we apply two results:

1. The Lickorish-Wallace theorem: all closed 3-manifolds are obtained by surgery on a link $L \subset \mathbb{S}^3$.

2. The link surgery formula: Ozsváth and Szabó proved a *knot surgery formula* which computes the Heegaard Floer homology of a surgery on $K$ in terms of the knot Floer homology of $K$. This was generalised to links by Manolescu and Ozsváth, in which the Heegaard Floer homology of the surgery on $L$ is determined by the knot Floer homology of $L$ and all of its sublinks.

Combining these two results and adding a bit more work, the result follows. □

**Remark.** This is really a theoretical result rather than a practical result. For example, a K3 surface is obtained by surgery on a knot with a $44 \times 44$ grid diagram. The corresponding grid complex has 44! generators, which is far too many for our computers to handle.

This completes one of the big themes of this course - Heegaard Floer homology is not only useful, but also combinatorially computable!

# Chapter 12

# Other versions of knot Floer homology

In the final chapter of these notes, we explore a few other versions of knot Floer homology. We'll finish with an application to the *knot concordance group*, which is the knot theoretic analogue of the *homology cobordism group* for 3-manifolds.

## 12.1 Full knot Floer homology

Let $K \subset \mathbb{S}^3$ be a knot, and

$$\mathcal{H} = (\Sigma, \alpha_1, \dots, \alpha_{g+k-1}, \beta_1, \dots, \beta_{g+k-1}, w_1, \dots, w_k, z_1, \dots, z_k)$$

a Heegaard diagram. So far we've only defined $\widehat{HFK}(K)$ for a Heegaard diagram with exactly 2 basepoints, and described the homology theories arising from additing more basepoints in terms of $\widehat{HFK}(K)$. Additional versions of knot Floer homology are defined as follows.

**Definition 12.1.1.** $\widetilde{HFK}(K)$ is the Lagrangian Floer homology of $\mathbb{T}_\alpha, \mathbb{T}_\beta$ in $\mathrm{Sym}^{g+k-1}(\Sigma - \{z_i, w_i\})$. That is, the only valid $J$-holomorphic strips are those that do not pass over any $z$ or $w$ points.

We observe that

$$\widetilde{HFK}(K) \cong \widehat{HFK}(K) \otimes V^{\otimes(k-1)},$$

and in particular when $k = 1$ the two homologies are the same.

**Definition 12.1.2.** $HFK^-(K)$ is the homology of $\mathbb{T}_\alpha, \mathbb{T}_\beta$ in $\mathrm{Sym}^{g+k-1}(\Sigma - \{z_i\})$. That is, we do not allow $J$-holomorphic curves to pass over $z$ points, and we keep track of how

they pass over $w_i$ with a variable $U_i$. Formally, the boundary map is

$$\partial x = \sum_y \sum_{\mu(\varphi)=1, n_{z_i}(\varphi)=0} (\#\mathcal{M}(\varphi)/\mathbb{R})\, U_1^{n_{w_1}(\varphi)} \cdots U_k^{n_{w_k}(\varphi)} y.$$

The correspondong homology is an invariant of $K$, which is a module over $\mathbb{Z}[U_1, \ldots, U_k]$.

The above can be taken to be a module over $\mathbb{Z}[U]$ by setting all the $U_i \coloneqq U$.

**Definition 12.1.3.** A more general definition of $\widehat{HFK}(K)$ is to define it in terms of $HFK^-$ with multiple basepoints: we simply set one of the $U_i = 0$. (That is, we consider $J$-holomorphic strips which are not allowed to meet $z_1, \ldots, z_k, w_i$.)

Finally we define the *full version* of knot Floer homology. The first version $\widetilde{HFK}$ contains the least information, as we're heavily restricting the $J$-holomorphic strips we consider. Then $\widehat{HFK}$ allows us to pass over $i-1$ of the $w$ points, and $HFK^-$ considers strips passing over all of the $w$ points. In the full version, we extend it further by considering $J$-holomorphic strips that also pass over the $z$ points.

**Definition 12.1.4.** $\mathcal{CFK}$ denotes the *full knot Floer complex* in which $J$-holomorphic curves are permitted to pass over all basepoints. We keep track of $w_i$ by $U_i$ and $z_i$ by $V_i$, and consider the complex over $\mathbb{Z}[U_1, \ldots, U_k, V_1, \ldots, V_k]$. The boundary map is given by

$$\partial x = \sum_y \sum_{\mu(\varphi)=1, n_{z_i}(\varphi)=0} (\#\mathcal{M}(\varphi)/\mathbb{R})\, U_1^{n_{w_1}(\varphi)} \cdots U_k^{n_{w_k}(\varphi)} V_1^{n_{z_1}(\varphi)} \cdots V_k^{n_{z_k}(\varphi)} y.$$

**Example.** In figure 12.1, we show a Heegaard diagram of the unknot with $k = 2$.

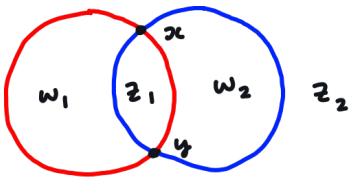


Figure 12.1: Unknot Heegaard diagram.

We see that $\partial x = (U_1 - U_2)y$, but also $\partial y = (V_1 - V_2)x$. Therefore

$$\partial^2 = (U_1 - U_2)(V_1 - V_2) \neq 0.$$

This example demonstrates that the *full knot Floer complex* as defined isn't actually a complex! In general,

$$\partial^2 = (U_1V_1 - V_1U_2 + U_2V_2 - V_2U_3 + \cdots + U_kV_k - V_kU_1).$$

Such an object is called a *matrix factorisation*. This is similar but gives a more complicated version of homological algebra. Notice that kernel mod image nolonger makes sense, but there are homotopical alternatives.

Two common ways of dealing with the full knot Floer complex are as follows.

1. Work over $\mathbb{Z}[U_i, V_i]/(U_1V_1 - V_1U_2 + \cdots - V_kU_1)$. Then the boundary map satisfies $\partial^2 = 0$ and homological algebra works.
2. Ensure that $k = 1$ in the original diagram. Then the boundary map is automatically that of a chain complex. This is denoted by $\mathcal{HFK}$, and is a homology theory over $\mathbb{Z}[U, V]$.

**Question from class.** What are the Euler characteristics of the various versions of knot Floer homology?

*Answer.* They're all various multiples of Alexander polynomials. □

**Example.** Figure 12.2 shows a Heegaard diagram of the left handed trefoil LHT, along with its hatted knot Floer homology $\widehat{HFK}(LHT) = \mathbb{Z}^3$. The boundary map is easily seen to be trivial, since the only two bigons both contain basepoints. Below the diagram, we also compute some other versions of knot Floer homology for the trefoil.

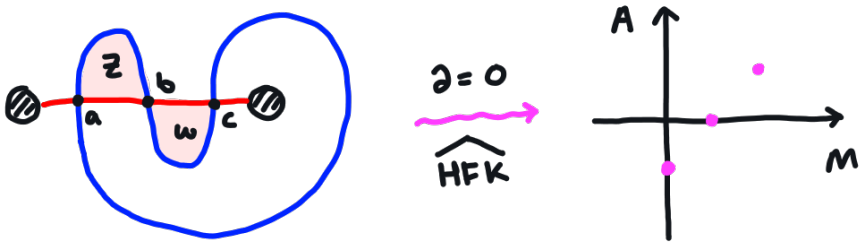


Figure 12.2: Left handed trefoil Heegaard diagram and $\widehat{HFK}$.

Next, what is $HFK^-(LHT)$? Over $\mathbb{Z}[U]$ we have $\partial c = Ub$ and $\partial a = \partial b = 0$. Therefore

$$HFK^- = \ker \partial / \operatorname{im} \partial = \langle a, b \rangle / \langle Ub \rangle.$$

Therefore $HFK^- = \mathbb{Z}[U] \oplus \mathbb{Z}$, where the first summand is generated by $a$ and the latter is $\langle b : Ub = 0 \rangle$.

As for $\mathcal{HFK}$, we have $\partial a = Vb$, $\partial c = Ub$, and $\partial b = 0$. Therefore

$$\mathcal{HFK}(LHT) = \langle b, Ua - Vc \rangle / \langle Ub, Vb \rangle \cong \mathbb{Z}[U, V] \oplus \mathbb{Z}$$

where the first summand is $\langle Ua - Vb \rangle$ and the latter is $\langle b : Ub = Vb = 0 \rangle$.

## 12.2 Applications to the knot concordance group

As mentioned earlier, the knot concordance group is an analogue of the homology cobordism group.

**Definition 12.2.1.** Two knots $K_1, K_2 \subset \mathbb{S}^3$ are *concordant* if there is a smoothly properly embedded annulus $A \subset \mathbb{S}^3 \times [0,1]$, with $\partial A = (-K_1) \cup K_2$, where $K_1 \subset \mathbb{S}^1 \times \{0\}$ and $K_2 \subset \mathbb{S}^3 \times \{1\}$.

Is the collection of equivalence classes non-trivial? That is, do there exist knots that are not concordant? yes, this is indeed the case: a knot is concordant to the unknot if and only if it bounds a smooth disk $D$ in $B^4$, i.e. if and only if the knot is slice. This is demonstrated by figure 12.3. The majority of knots seem not to be slice - for example, Rasmussen's $s$-invariant gives a lower bound for the slice genus, and this can be computed to be non-trivial for most small knots.

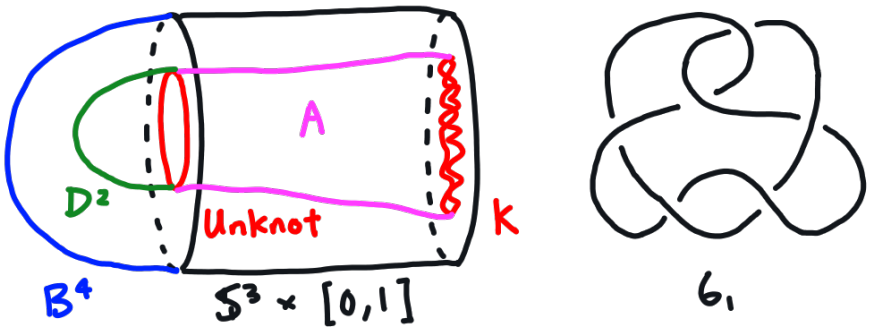


Figure 12.3: Slice $\Leftrightarrow$ null-concordant, $6_1$ is slice.

The knot $6_1$, also shown in figure 12.3, is the smallest slice knot.

**Open question.** Find and algorithm to determine sliceness of knots.

Since we've developed combinatorial knot invariants that detect the unknot, perhaps we can one day detect sliceness too!

**Definition 12.2.2.** The *knot concordance group*, denoted $\mathcal{C}$, consists of all oriented knots up to concordance. This is an abelian group under

$$0 = [\text{unknot}], \quad [K_1] + [K_2] = [K_1 \# K_2], \quad -[K] = [m(K^r)].$$

(By $m(K^r)$, we mean the mirror of the opposite orientation knot.)

**Remark.** We mentioned that the knot concordance group is analogous to the homology cobordism group. To strengthen this, we mention that there are various homomorphisms

$$\mathcal{C} \to \Theta^3_{\mathbb{Z}}, \Theta^3_{\mathbb{Q}}.$$

Examples include: mapping a knot to the surgery on the sphere along the knot, or mapping a knot to double covers branched over the knot. Therefore understanding the structure of $\mathcal{C}$ can help understand $\Theta^3$ and vice versa.

**Open question.** What is $\mathcal{C}$? We don't know what its isomorphism class as an abelian group is, although more is known about it than $\Theta^3_{\mathbb{Z}}$. This reflects the fact that knots are easier than 3-manifolds.

Recall that for the homology cobordism group $\Theta^3_{\mathbb{Z}}$, Heegaard Floer homology provided a surjective homomorphism

$$d : \Theta^3_{\mathbb{Z}} \to \mathbb{Z},$$

where $d([Y])$ is the maximum grading of an element in the infinite tail of $HF^-(Y)$, plus 2. Similarly we can consider

$$\tau(K) = -\max\{s : \exists x \in HFK^-(K,s), U^j x \neq 0 \, \forall j \geqslant 0\}.$$

In other words $\tau(K)$ measures the largest $s$ for which $HFK^-(K,s)$ contains an element belonging to an infinite tail.

**Remark.** The invariant $\tau$ measures the Alexander grading rather than the Maslov (homological) grading! In this manner it is distinct from $d$.

**Proposition 12.2.3.** The invariant $\tau$ defines a homomorphism

$$\tau : \mathcal{C} \to \mathbb{Z}.$$

**Example.** Let $K = LHT$ be the left handed trefoil. Then

$$HFK^-(T) = \mathbb{Z}[U] \oplus \mathbb{Z} = \langle a \rangle \oplus \langle b : Ub = 0 \rangle.$$

The Alexander grading of $a$ is 1, and the Alexander grading of $b$ is 0. $U$ decreases the Alexander grading by 1. Therefore the maximum $s$ for which $HFK^-(K,s)$ contains an element belonging to an infinite tail is $s = 1$, and we can take the element to be $a$. It follows that

$$\tau(K) = -1.$$

Therefore the trefoil is not slice!

There are more concordance invariants arising from knot Floer homology. Examples include

$$\nu, \nu^+, \varepsilon, \dots$$

In particular, Ozsváth, Stipsicz, and Szabó introduced the invariants $\Upsilon_t$ for $t \in [0,1]$. These invariants are defined for a variant of $\mathcal{HFK}$ over $\mathbb{Z}[U]$, where $w$ is kept track of by $U^{tn_w(\varphi)}$ and $z$ by $U^{(1-t)n_z(\varphi)}$ in the boundary map. Otherwise the definition of $\Upsilon_t$ imitates that of $\tau$. These give rise to infinitely many distinct homomorphisms

$$\Upsilon_t : \mathcal{C} \to \mathbb{Z}.$$

From these, we find that

**Proposition 12.2.4.** $\mathcal{C}$ has a $\mathbb{Z}^\infty$ summand.

This result was already known. However, a more impressive application is that the homomorphisms restricted to

$$\Upsilon_t : \mathcal{C}_{TS} \to \mathbb{Z}$$

also shows that $\mathcal{C}_{TS}$ has a $\mathbb{Z}^\infty$ summand! The space $\mathcal{C}_{TS}$ consists of *topologically slice knots up to smooth concordance*. A knot is said to be topologically slice if there is an embedded disk in $B^4$ whose boundary is the knot, but the embedding is only required to be *locally flat* rather than smooth. This is crazy! It shows that there are very many knots which are topologically slice but not smoothly slice.

This concludes Maths 283A of Fall quarter 2020. Thank you again Ciprian for a fantastic course! It was a lot of fun.